

**A THREE PHASE ELECTRONIC LOAD GOVERNOR  
FOR MICRO HYDRO GENERATION.**

Thesis submitted by

**DOUGLAS STUART HENDERSON, B.Sc., C.Eng., MIEE.**

for the degree of  
**DOCTOR OF PHILOSOPHY.**

to

The University of Edinburgh,  
Faculty of Science and Engineering.

JUNE 1992.



## ABSTRACT

The need for an economic alternative to the traditional speed governor for micro hydro applications is discussed and the Electronic Load Governor (ELG) is identified as the solution. The international market for the ELG is seen to vary in accordance with the development and traditions of those countries with micro hydro resources. Technical and economic design parameters for a novel, prototype ELG are developed in relation to previous work in the field. The need for a reliable unit based on digital electronic circuits and capable of three phase balancing is identified.

The significance of the "droop" is introduced, along with the concepts of "deadband", "wait delay" and the "coefficient of stability". A technique for prediction of the droop, and hence the deadband, using the turbine runaway speed is presented. The predictions are confirmed as a result of empirical tests. The voltage-speed characteristics are also determined empirically.

A mathematical expression is derived which represents the frequency variation with time of the system, when subjected to a load rejection, and controlled by the ELG. The transfer function of the control system is derived as far as is practicable given the non-linear nature of the ELG control action. A computer model is developed which predicts the frequency transient for any Pelton installation under the control of the ELG. The model is modified to predict the performance of the ELG subject to proportional-derivative control actions.

## LIST OF CONTENTS

	<u>Page</u>
Abstract	2
List of Contents	3
List of Illustrations	9
List of Tables	15
Acknowledgements	17
Declaration	18
Definitions	19
Dedication	20
<b>CHAPTER 1        INTRODUCTION</b>	<b>21</b>
1.1    Micro Hydro Generation	21
1.1.1.    Micro Hydro Potential	22
1.1.2.    Components of a Micro Hydro Installation	24
1.2    Speed Governing Techniques	31
1.3    Electronic Load Governing	35
1.3.1.    Phase Angle Control	36
1.3.2.    Binary Loads	37
1.4    Electronic Load Controller	39
1.5    Market Survey	40
1.5.1.    Demand for Electronic Load Governors	40
1.5.2.    Existing Electronic Load Governors	44
1.5.3.    Relation to Previous Work	45
 <b>CHAPTER 2        ELG DESIGN PARAMETERS</b>	 <b>47</b>
2.1    Technical Considerations	47
2.1.1    Problems with Existing Designs	47
2.1.2    Proposed Design Features	53

	<u>Page</u>
2.1.2.1. Load Governing Aspects	54
2.1.2.2. Electronic Circuit Aspects	61
2.1.2.3. Application Aspects	62
2.1.2.4. Manufacture Aspects	63
2.2 Economic Design Considerations	64
<b>CHAPTER 3 ELG DESIGN</b>	<b>68</b>
3.1 Microcomputer Choice	68
3.2 Essex FORTH Microcard	71
3.3 Input/Output Board Design	73
3.3.1. Digital Switched Input Circuit	74
3.3.2. Digital Output Circuits	75
3.3.3. Frequency Measurement Circuit	75
3.3.4. Analogue Input Circuit	77
3.3.5. Power Supply Circuit	80
3.4 Printed Circuit Board	81
<b>CHAPTER 4 PROGRAM DEVELOPMENT</b>	<b>85</b>
4.1 The Software Development System	85
4.1.1. Computer System	85
4.1.2. Operating Modes	86
4.2 The FORTH Language	86
4.3 The Load Governing Program	87
4.3.1. Main Program	88
4.3.2. Frequency Detection	89
4.3.3. Main Program Description	93
4.4 EPROM Preparation	104

	<u>Page</u>
<b>CHAPTER 5      TEST EQUIPMENT</b>	106
5.1    Peripheral Equipment	107
5.1.1.    Consumer Load	108
5.1.2.    Solid State Relays	108
5.1.3.    Ballast Load	109
5.1.4.    Current Transformers	111
5.1.5.    Metering	112
5.2    Motor-Generator Set	113
5.2.1.    Rating Details	113
5.2.2.    Speed / Load Characteristic - Theory	115
5.2.3.    Speed Control	116
5.2.4.    Speed / Load Characteristic - Measured	117
5.2.5.    D.C. Motor Model	119
5.3    Turbine-Generator Sets	122
5.3.1.    Boving Turbine and Three Phase Generator	124
5.3.1.1.      Rating Details	124
5.3.1.2.      Speed / Load Characteristic - Theory	126
5.3.1.3.      Speed / Load Characteristic - Predictions	133
5.3.1.4.      Speed / Load Characteristic - Measurements	136
5.3.2.    Gilkes Turbine and Single Phase Generator	139
5.3.2.1.      Rating Details	139
5.3.2.2.      Speed / Load Characteristic - Measurements	140
5.3.3.    Francis Turbine	142
5.3.3.1.      Rating Details	142
5.3.3.2.      Speed / Load Characteristic	142
5.4    Digital Storage Oscilloscope	143
5.5.    Data Acquisition System	147

	<u>Page</u>
<b>CHAPTER 6        THE ELG IN OPERATION</b>	<b>149</b>
6.1    Comparison with Proposed Design	149
6.1.1.    Technical Compliance	149
6.1.2.    Economic Compliance	150
6.2    Functional Testing of the ELG	152
6.2.1.    Running In	152
6.2.2.    Parameters for Steady-State Operation of the Boving Turbine	155
6.2.3.    Parameters for Steady-State Operation of the Gilkes Turbine	162
6.2.4.    Parameters for Steady-State Operation of the Francis Turbine	163
6.2.5.    Summary	163
6.2.6.    Parameters for Steady-State Operation of Other Turbines	164
6.3    Interaction with the Generator Excitation	165
6.4    Operation with Uniform Ballast Load	166
<b>CHAPTER 7        TRANSIENT PERFORMANCE STUDIES</b>	<b>167</b>
7.1    Theoretical Considerations	168
7.1.1.    Torque Balance	168
7.1.2.    The Ungoverned Frequency Transient	170
7.1.3.    Inertia Estimation	172
7.1.4.    The Load Governed Frequency Transient	173
7.1.5.    Resume	175
7.2    Measured Transient Performance	178
7.2.1.    Frequency Transient	178
7.2.2.    Voltage Transient	184

	<b><u>Page</u></b>	
7.3	Transfer Function	186
7.3.1.	The Rotating System Transfer Function	187
7.3.2.	The Turbine Transfer Function	188
7.3.3.	The ELG Transfer Function	189
7.3.4.	Simplified Overall Block Diagram	192
7.4	Computer Model	193
7.4.1.	STTURB4	193
7.4.2.	STTURB3	196
7.4.3.	Model Validity	196
7.4.4.	Model Use on Alternative Installations	202
7.4.5.	Model Applications	205
7.5	Improving the Performance	206
<b>CHAPTER 8</b>	<b>CONCLUSIONS AND SUGGESTIONS FOR FURTHER WORK</b>	<b>211</b>
8.1	Conclusions and Outcomes	211
8.1.1.	The ELG Market	211
8.1.2.	The Requirements of an ELG	212
8.1.3.	The Development of a Functional ELG	213
8.1.4.	The Establishment of Test Facilities	216
8.1.5.	Prediction of Deadband Selection for Steady-State Operation	217
8.1.6.	Prediction of Transient Operation	218
8.2	Further Work	219
8.2.1.	Reactive Power Control	221
8.2.2.	Protection Functions	223
8.2.3.	Data Logging / Condition Monitoring	225

	<u>Page</u>
8.2.4. Additional Control Functions	227
8.2.5. Market Penetration	228
8.3 Postscript	228
Appendix 1 Printed Circuit Board Detail	229
Appendix 2 The FORTH Load Governing Program	231
A2.1 LG9	231
A2.2 Standard RSC-FORTH Words in LG9	236
A2.3 User Defined Words in LG9	236
Appendix 3 D.C. Motor Model	237
Appendix 4 Model Program Listings	240
A4.1 Program STTURB4.BAS	240
A4.2 Program STTURB3.BAS	244
A4.3 Program PDCONT1.BAS	248
Appendix 5 Publications List	252
List of References	254
Bibliography	262



## LIST OF ILLUSTRATIONS

		<u>Page</u>
 <b>CHAPTER 1</b>		
Figure 1	Breakdown of the mini/micro hydro potential	23
Figure 2	Components of a micro hydro installation	24
Figure 3	Turbine application diagram	26
Figure 4	Unit cost curve	29
Figure 5	Mechanical/hydraulic governor	33
Figure 6	Electro/hydraulic governor	34
Figure 7	Load governing principle	35
Figure 8	Phase angle control - voltage waveforms	37
Figure 9	Ballast load characteristic	38
 <b>CHAPTER 2</b>		
Figure 10	Typical phase angle control circuit	48
Figure 11a	Load voltage waveform, low firing angle	48
Figure 11b	Load voltage waveform, high firing angle	49
Figure 12	Supply voltage waveform compared with load voltage waveform	49
Figure 13	Harmonics produced by phase angle control	50
Figure 14	Schematic diagram for three phase load governing	55
Figure 15	Power variations of ideal operation	56
Figure 16	Typical droop characteristic, frequency vs power	57
Figure 17a	Calculated deadband centred on 50 Hz	59
Figure 17b	Deadband value on both sides of 50 Hz	59

**CHAPTER 3****Page**

Figure 18	Switched input circuit	74
Figure 19	Ballast load switching output circuit	75
Figure 20a	Frequency measurement circuit	76
Figure 20b	Schmitt Trigger output in relation to a.c. waveform	77
Figure 21	Current measurement circuit	78
Figure 22	Analogue-to-Digital conversion circuit - block diagram	79
Figure 23	Power supply circuit	81
Figure 24	The I/O printed circuit board	83
Figure 25	The ELG in its enclosure	84

**CHAPTER 4**

Figure 26	A block diagram of the computer system	85
Figure 27	Flowchart of the main load governing program	88
Figure 28	Flowchart of the initialisation routine	95
Figure 29	Flowchart of the frequency comparison routine	98
Figure 30	Flowchart for increasing the ballast load	99

**CHAPTER 5**

Figure 31	Control system block diagram	106
Figure 32	Schematic diagram for three phase load governing	107
Figure 33	Speed - torque characteristics	113
Figure 34a	Circuit diagram of d.c. motor	114
Figure 34b	Circuit diagram of a.c. generator	115
Figure 35	Effect of field resistance on droop	117

	<u>Page</u>	
Figure 36	Effect of armature resistance on droop	118
Figure 37	Model predictions of motor/generator droop	120
Figure 38	Screen display of MODEL4 output	121
Figure 39a	The Boving turbine and its three phase generator	123
Figure 39b	The Gilkes turbine and the single phase generator	123
Figure 39c	The Francis turbine and the single phase generator	124
Figure 40	Excitation diagram of the three phase generator	125
Figure 41	Water flow from a conical nozzle	126
Figure 42	Turbine output power vs peripheral velocity coefficient	130
Figure 43	Turbine droop - frequency vs p.u. load	134
Figure 44	Variation of runaway frequency with head	135
Figure 45a	Plot of frequency vs output power (Boving)	136
Figure 45b	Plot of frequency vs phase impedance (Boving)	137
Figure 46	Plot of frequency vs phase admittance (Boving)	137
Figure 47	Plot of frequency vs p.u. load (Boving)	138
Figure 48	Plot of frequency vs power (Gilkes)	141
Figure 49	Plot of frequency vs p.u. load (Gilkes)	141
Figure 50a	DSO trace of section 1 of ballast load in one phase	144
Figure 50b	DSO trace of the toggle output line	145
Figure 50c	DSO trace of the Schmitt Trigger output	146
Figure 50d	DSO trace of the a.c. waveform	146
Figure 51	Typical plot from the data acquisition system	148

## CHAPTER 6

Figure 52	Frequency transient for small-scale load rejection	158
Figure 53a	Demonstration of instability	159

	<u>Page</u>
Figure 53b Stable operation with added wait delay	159
Figure 54 Plot of voltage variation with frequency	166

## CHAPTER 7

Figure 55a Turbine torque components	169
Figure 55b Turbine output torque	169
Figure 56 Torque vs frequency relationship	171
Figure 57 Typical frequency transient	174
Figure 58a Measured frequency transient for 27m head and 31l/s flow	179
Figure 58b Measured frequency transient for 29m head and 31l/s flow	180
Figure 58c Measured frequency transient for 31m head and 31l/s flow	180
Figure 58d Measured frequency transient for 33m head and 31l/s flow	180
Figure 59a Measured frequency transient for 30m head and 27l/s flow	181
Figure 59b Measured frequency transient for 30m head and 29l/s flow	181
Figure 59c Measured frequency transient for 30m head and 31l/s flow	182
Figure 59d Measured frequency transient for 30m head and 33l/s flow	182
Figure 60a Measured frequency transient for zero wait delay	183
Figure 60b Measured frequency transient for 4ms wait delay	183

	<u>Page</u>
Figure 60c Measured frequency transient for 8ms wait delay	183
Figure 60d Measured frequency transient for 12ms wait delay	184
Figure 61 Voltage transient at 27m head	185
Figure 62 Voltage transient at 33m head	186
Figure 63 Control system block diagram	187
Figure 64 Rotating system block diagram	187
Figure 65 Typical torque vs frequency curve	188
Figure 66 Turbine block diagram	188
Figure 67 ELG block diagram	189
Figure 68 Time varying application of ballast load	190
Figure 69 Equivalent circuit of synchronous generator	191
Figure 70 Final block diagram of the control system	192
Figure 71 Typical screen output of the STTURB4 model	195
Figure 72 Comparison of the measured and model frequency transients for the nominal operating conditions	197
Figure 73 Comparison of the measured and model frequency transients at 27m head and 31l/s flow	199
Figure 74 Comparison of the measured and model frequency transients at 33m head and 31l/s flow	200
Figure 75 Comparison of the measured and model frequency transients at 30m head and 27l/s flow	201
Figure 76 Comparison of the measured and model frequency transients at 30m head and 33l/s flow	202
Figure 77 Measured frequency transient for Gilkes turbine	204
Figure 78 Predicted frequency transient for Gilkes turbine	204
Figure 79 Predicted frequency transient with added inertia	205
Figure 80a Frequency transient for original control method	207

	<u>Page</u>
Figure 80b Frequency transient with proportional-derivative actions	208
Figure 81 Effect of increased constant of proportionality	208
Figure 82a Part load rejection transient with constant = 8	209
Figure 82b Part load rejection transient with constant = 4	209
Figure 82c Part load rejection transient with constant = 2	210

### **APPENDIX 1**

Figure A1.1 Essex FORTH Microcard PCB layout	229
Figure A1.2 Essex FORTH Microcard circuit diagram	229
Figure A1.3 I/O PCB layout	230
Figure A1.4 I/O PCB circuit diagram	230a

### **APPENDIX 3**

Figure A3.1 D.C. motor circuit diagram for model	237
--	-----

**LIST OF TABLES**

	<u>Page</u>
<b>CHAPTER 1</b>	
Table 1     Hydro-electric Categories	21
<b>CHAPTER 2</b>	
Table 2     Capital Purchase Costs of Control Equipment	66
<b>CHAPTER 3</b>	
Table 3     Suitable Microprocessor Systems	70
<b>CHAPTER 4</b>	
Table 4     Deadband Settings	93
<b>CHAPTER 5</b>	
Table 5     CT Primary Turns	111
Table 6     Digital : Line Current Resolution	112
Table 7     Predicted Droop Values for a Range of Operating Heads	135
Table 8     Measured Droop Values and Associated Deadband Selection	138

**CHAPTER 6****Page**

Table 9	Deadband Settings (+-Hz) for Varying Head and Wait Delay	161
Table 10	Comparison of Deadband Selections	162
Table 11	Predicted Deadbands for Other Turbine Types	164



## ACKNOWLEDGEMENTS

I would like to thank the many people who have assisted and encouraged me in the course of this work.

My supervisors, Dr D. E. Macpherson and Dr H. W. Whittington of the University of Edinburgh are thanked for their advice and guidance throughout the project.

Thankyou to Napier University for their indulgence in making the project possible and through the provision of resources and facilities in the Department of Electrical, Electronic & Computer Engineering and the Department of Mechanical, Manufacture & Software Engineering. Particular thanks go to John Daly, John Dorner and John Mumford for their time and considerable effort in providing me with assistance.

Thankyou to Robin Wallace, the original "prime mover", for his support, advice and for his assistance with "Atari" matters.

Last, but by no means least, thankyou to Karen, Scott and Kerry for foregoing the pleasure of my company over the last few years when they might otherwise reasonably have expected it.

## DECLARATION

I declare that;

- a. this thesis has been composed by myself, and
- b. the work is my own, except where indicated otherwise.  
and as summarised below;

Signed :

Douglas Stuart Henderson.

1. The Input/output PCB artwork and manufacture, Section 3.4.
2. The Francis turbine testing, Section 5.3.3.
3. The data acquisition system programming, Section 5.5.

## DEFINITIONS

The following terms are defined as being specific to this thesis.

1. **Electronic Load Governor (ELG)** - an electronic unit which performs the single function of load governing.
2. **Electronic Load Controller (ELC)** - an electronic unit which performs control and monitoring functions in addition to load governing.
3. **Droop** - the relationship between the speed ( or frequency ) and the 'load' of a turbine-generator set. The measure and unit of 'load' is developed as part of this work.
4. **Coefficient of Stability** - A measure of the probability of the frequency leaving preset limits as a result of small-scale disturbances to the torque balance.
5. **Specific Speed** - The speed at which a geometrically similar turbine would rotate developing 1 metric horse power when operating under a net head of 1 metre.

**DEDICATION**

To Scott and to Kerry, the future.

---

## CHAPTER 1 INTRODUCTION

### 1.1. MICRO HYDRO GENERATION

The use of water as a source of energy is by no means a new concept. Energy is available in water in two forms, potential and kinetic, and for centuries mankind has converted this energy into a mechanical form and used it for a variety of purposes, most notably milling. Typically, the rating of these early water mills would be in the order of 2 kW<sup>1</sup>. The first hydro-electric installation, rated at 12.5 kW, was completed in 1882 at Wisconsin USA<sup>2</sup>. The rated output of hydro-electric generating units increased rapidly with time, the largest single unit of any type currently installed being rated at 825MVA at Grand Coulee, also in the USA<sup>3</sup>.

<u>Rating</u>	<u>Category</u>
> 10 MW	Large
1 to 10 MW	Small
0.1 to 1 MW	Mini
< 100 kW	Micro

**Table 1 - Hydro-electric Categories**

Hydro-electric generation is usually categorised using rated output power, see Table 1. Unfortunately there is not industry-wide agreement on the use of these categories and thus many different sets of categories exist. For example there is dispute as to whether 'power' refers to unit rating or power station rating and alternative boundaries are often to be found. For the purposes of this thesis, the definition

---

for **micro hydro** generation given in Table 1 will be used, i.e. a unit rating of less than 100 kW.

### 1.1.1. **Micro Hydro Potential**

A major disadvantage of the non uniformity of the various categories is that as surveys are done to assess the extent of the potential for hydro-electric generation, different results tend to appear; however, the **total** hydraulic potential remaining to be developed amounts to at least 1,630,000 MW<sup>3,4</sup> worldwide.

The countries who are actively developing their hydro resources naturally favour the development of the most economically attractive schemes first. The unit cost of hydro-electric installations decreases with increasing output power, and hence it is the larger schemes which are usually considered when resources are being studied.

These factors combine to make accurate survey and estimation of the true potential for **micro hydro** development extremely difficult - a few hundred kW is overshadowed by the total worldwide hydro potential and micro hydro sites are often completely overlooked in national surveys. The recent survey of small hydro potential in the United Kingdom, carried out on behalf of the Energy Technology Support Unit<sup>5</sup>, excluded all possible sites with an output of less than 25 kW, with the result that many possible micro hydro installations were excluded from the survey.

---

Accepting that the data is by no means accurate, the potential for micro hydro generation is summarised as follows;

The total worldwide hydraulic potential has an output capacity of 2,200,000 MW<sup>4</sup> and the corresponding total energy production is estimated as 15,000,000 GWh per annum<sup>3</sup>, of which the mini/micro energy production is estimated to be 560,000 GWh per annum<sup>6</sup> - 3.7% of the total. Using this percentage, the mini/micro output capacity is 81,400 MW of which 31,030 MW is already constructed, is under construction or is planned<sup>6</sup>, leaving 50,370 MW yet to be considered. If it is assumed that half of this total falls into the micro hydro category then, as shown in figure 1, the remaining potential for micro hydro is 25,185 MW, which at a maximum of 100 kW per unit, represents a minimum of over 250,000 units.

**Remaining potential for micro hydro**  
100% is 81,400 MW

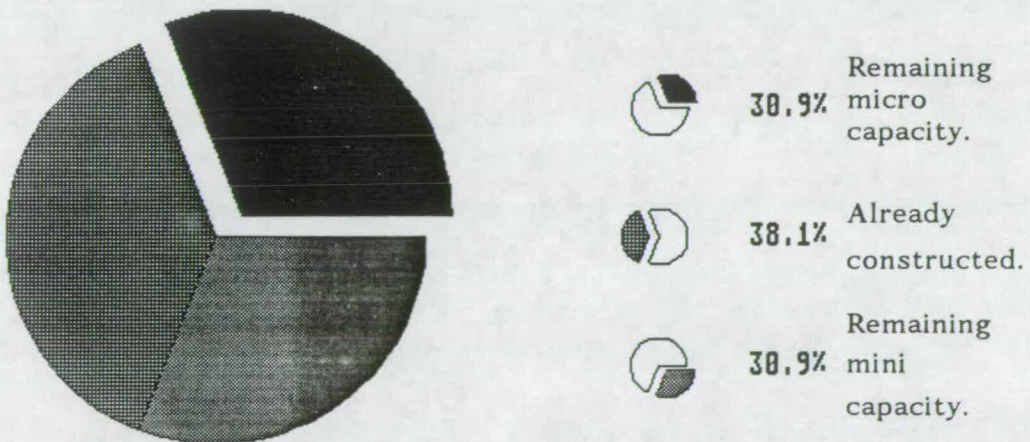


**Figure 1 - Breakdown of the mini/micro hydro potential**

### 1.1.2. Components of a Micro Hydro Installation

The components of a micro hydro scheme vary from installation to installation. However, typically they are as shown in figure 2. Generally they are 'run-of-river' schemes where a fraction of the flow of the river is diverted via the intake pipework through the water turbine and then returned from the tailrace to the river. Often a small weir or dam structure is employed to maintain the water level at the intake - rather than for long term water storage.

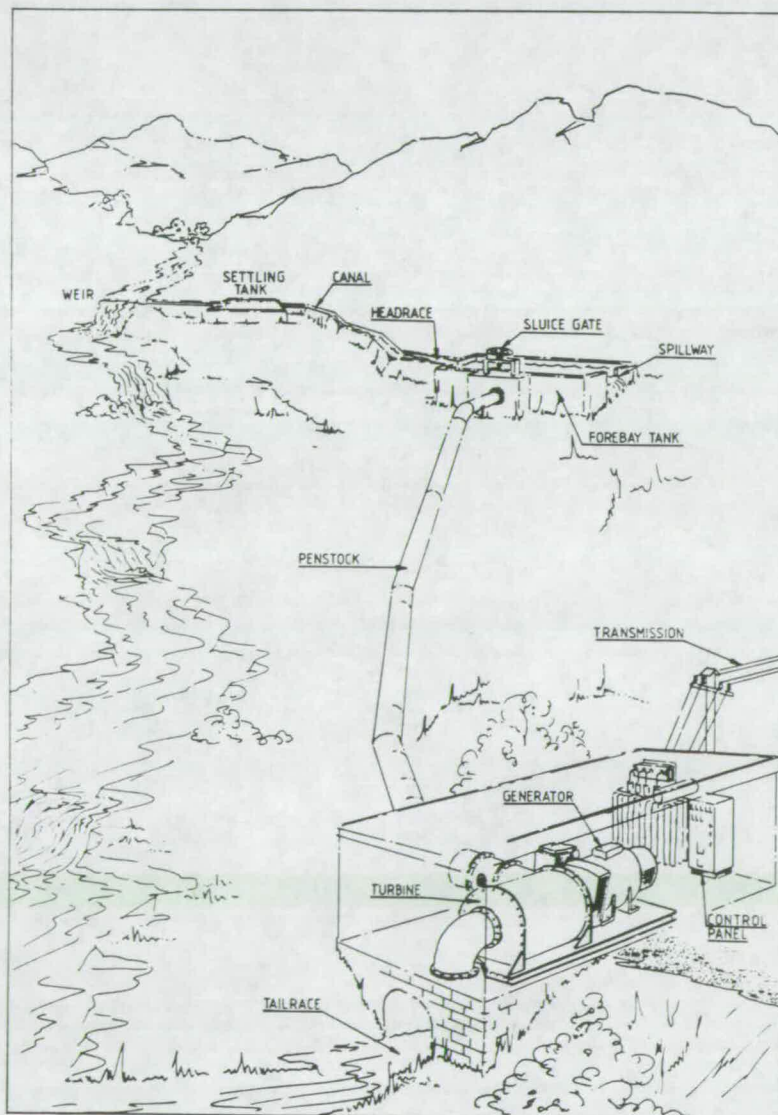


Figure 2 - Components of a micro hydro installation



Traditionally, the electro-mechanical package of any hydro-electric generating unit would consist of a high efficiency water turbine, a speed governor and an a.c. generator complete with an automatic voltage regulator.

### ***Water Turbines***

The selection of a water turbine for a given application depends on the head<sup>7</sup>. Turbine designs are classified by their specific speed and the actual rotational speed is directly proportional to the specific speed. It is usually the practice to arrange the running speed of a turbine at the highest speed possible, to facilitate the use of high speed generators and so minimise the cost of the generator. The choice of turbine which is to produce a given output at a given head can be made from an application diagram which the turbine manufacturers publish to demonstrate their range of machines. A typical application diagram is shown in figure 3.

Water turbines fall into two main categories, the reaction type ( Francis and Kaplan ) and the impulse type ( Pelton and Turgo ). There are many traditional and modern variations on these turbines. To enable speed governing they all require one common feature - high performance water regulating equipment. For the reaction type turbines this takes the form of guide vanes which control the flow of water onto the turbine runner in response to the output of the speed governor. Kaplan type turbines may also have adjustable runner blades - so called 'double regulation'. Impulse type turbines usually have one or more spear valves which control the flow of water in response to the governor output.

---

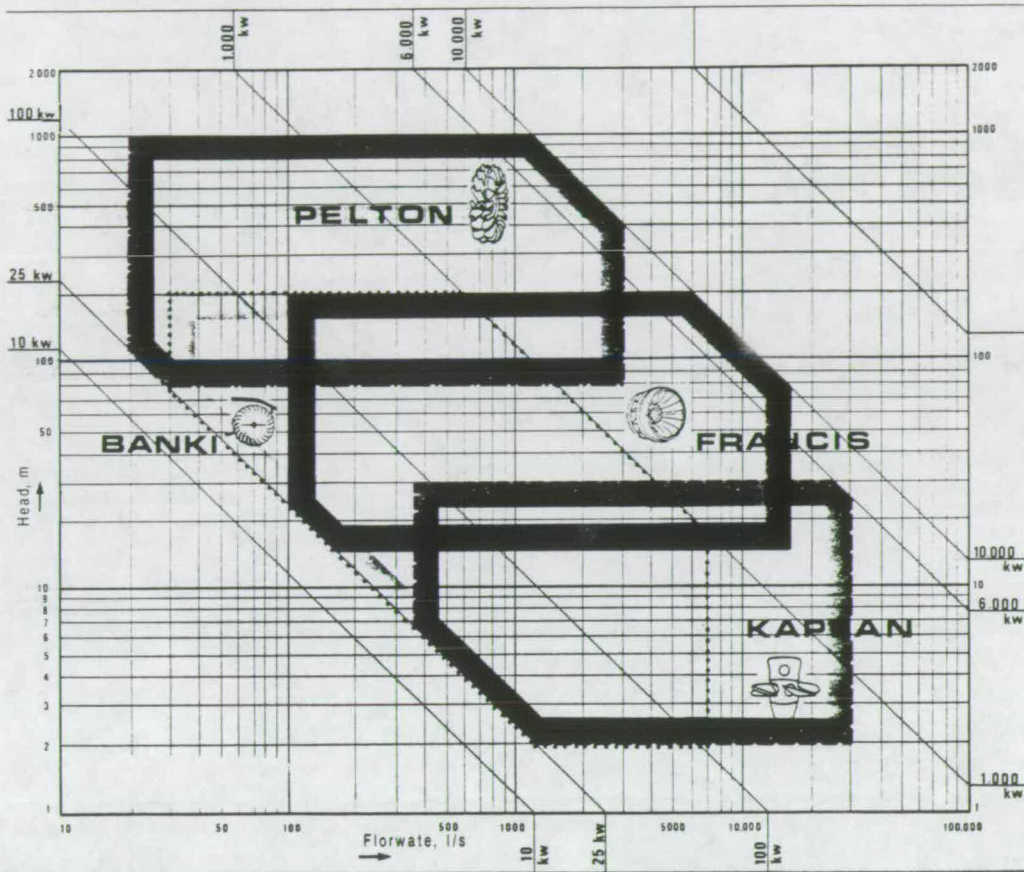


Figure 3 - Turbine application diagram

Impulse turbines operate through the action of a jet of water striking a turbine runner which causes the runner to rotate. The water jet is at atmospheric pressure as it leaves its nozzle and the kinetic energy which it has due to the head is removed by changing the direction of the water in buckets on the runner. The water then falls into the tailrace below. The turbine casing therefore can be designed simply to retain the water as it is redirected by the buckets.

Reaction turbines do not have a free jet of water, rather the water supplied to the turbine acts on the runner under pressure, maintaining

the turbine full of water. A draft tube is required to discharge the water and maintain the so called suction head. As a consequence, the turbine casing is effectively a pressure vessel, and a more complicated discharge arrangement is required. One major advantage of the reaction turbine over the impulse type are that they have a higher specific speed and therefore will rotate faster for a given output and head; another advantage is that they can utilise the suction head in addition to the pressure head above the turbine.

Crossflow, or "Banki", turbines do not strictly reside in either of the above categories as theoretically they can have a specific speed which varies from that associated with Pelton wheels to those of Francis turbines, all within the one design.

Setting aside the governor itself, the high quality engineering design and manufacture required of the water flow components such as the guide vanes and spear valves contributes to the relatively high cost of the water turbine, and consequently the complete installation.

### ***Generators***

Almost exclusively, generation is performed using a.c. machines, and either induction or synchronous type machines are available<sup>8</sup>. The induction generator has to be driven at a speed greater than synchronous speed and requires a source of magnetising current for its operation. Traditionally this latter requirement meant that they could only be used where they could be connected to a strong enough grid, implying their application as grid-supplementation rather than for

---

isolated operation. Capacitors can provide an alternative source for the magnetising current and on this basis it is possible to operate an induction generator in an isolated situation<sup>9,10</sup>.

Whilst induction generators are lower in capital cost per kVA than synchronous machines, the addition of excitation capacitors begins to erode that cost advantage and also begins to reduce the reliability of the unit. The synchronous machine is designed to operate as an isolated generator as it has the ability to provide its own magnetisation ( or 'field' ). The source of the field can be derived in a number of different ways, self excitation being the best suited to isolated micro hydro applications<sup>11</sup>.

### ***Engineering***

Micro hydro installations usually require a very different engineering approach than that used for small and large hydro practice, not a *lower* engineering standard, more an *appropriate* engineering standard. This occurs as a result of the trend of the unit cost of hydro-electric installations which rises dramatically as the rated output power is reduced below 100 kW<sup>12</sup>, refer figure 4. Moreover, in many of the Lesser Developed Countries ( LDC's ), the engineering of the installation is only one of the aspects which needs considered. Operator training and appropriate tariffing are equally important if a micro hydro installation is to be successful<sup>13</sup>.

---

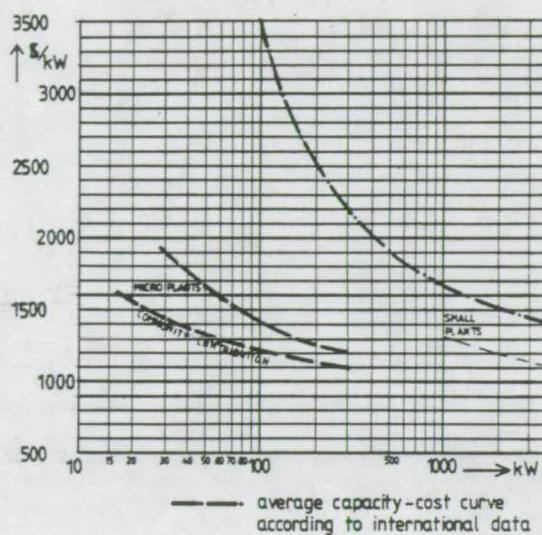


Figure 4 - Unit cost curve

### *Plant Selection*

Appropriate selection of the water turbine for a micro hydro installation requires an acceptance that efficiency is not of paramount importance, and that a turbine may be selected primarily on economic grounds. The design of the traditional Francis and Pelton turbines can be simplified<sup>13</sup> or standardised. Alternatively, other turbine designs may be used such as the crossflow type<sup>14</sup>. In addition, turbines may be selected slightly away from their normal point on the application diagram<sup>15</sup>, again with a reduction in efficiency, but nevertheless able to produce electrical energy where the 'traditional' choice of turbine may have proved uneconomical.

The optimum turbine running speed is often relatively low. If the generator were to be directly connected to the turbine shaft this would require a slow speed machine. These are rarely available at such low

power ratings; economically they would be very costly if they were custom designed and built, and therefore standard 4 or 6 pole generators are employed. The normal application for these standard machines is to be driven by diesel engines which have a limited overspeed of around 20 - 40 % above rated speed. Because of this they require to have additional bracing for the higher runaway speeds which can occur with water turbines, typically 80 - 120 % above rated speed.

As a consequence, there is often the requirement for a speed increaser on a micro hydro installation. This may take the form of a belt drive, either V-belts or a flat belt, which gives a degree of flexibility in respect of the relative shaft alignments of the turbine and generator. Many micro hydro schemes operate at mill sites where the water power is used for mechanical power during working hours, and is used for electrical generation purposes at other times. Belt drives provide a simple means of connection of the appropriate machine and are normally used in these mixed drive situations. For single power usage applications, higher transmission efficiency can be obtained using a gearbox, which is an acceptable item of plant for micro hydro sites *provided* that adequate maintenance facilities are available.

The use of an electronic load governor is now widely accepted for micro hydro installations<sup>16</sup>, bringing with it economic benefits, not only in the cost of the governor, but also in the turbine. The following Section outlines the various governor options that are available.

---

## 1.2. SPEED GOVERNING TECHNIQUES

The frequency of the electrical output voltage waveform from an a.c. generator is directly proportional to the speed of the generator shaft. The majority of small and large hydro generators are grid connected and consequently, their running speed is held nearly constant by the grid frequency. On the other hand, the majority of micro hydro generators operate in isolation from a grid system and, thus, accurate control of the rotating components is required, in order to hold the generated frequency close to 50 or 60 Hz. It is implicit herein that the application of the governor is on systems which are operating in isolation from a grid network.

The mechanical output power from a water turbine is proportional to the product of nett head and volume flow rate. If it is assumed that the head is constant, control of the power output is by control of the water flow rate. Speed governing involves the alteration of the **turbine output** in response to changes of load on the electrical system. If the speed of the set is to be maintained nearly constant, then the control of the water flow must be relatively fast to meet the changing load conditions. This control is normally effected by adjustment of a water regulating device such as the spear valve or the guide vanes. Somewhat more crude control can also be achieved by control of the inlet valve to the turbine.

Mechanical/hydraulic governors sense changes in speed either by direct belt drive onto a speed sensing head with flyballs, or the head is motor

---

driven, proportional power being supplied from a generator PMG or voltage transformers. Mechanical movement of the flyballs is transferred to movement of a pilot valve which ports oil to one or other side of a servo motor which operates the turbine flow control system. An example of this type of governor is the Woodward UG type which is shown in figure 5.

Design of a conventional mechanical/hydraulic governor for a micro hydro installation must take into consideration the compromise between the maximum speed rise of the turbine-generator set on full load rejection and the maximum resultant pressure rise in the penstock<sup>17</sup>. These can be optimised by careful specification and design of the inertia of the rotating components and the closing time of the water regulating device.

The drawbacks inherent in the application of a conventional speed governor to a micro hydro scheme are as follows;

- they are precision devices which need regular, skilled maintenance if they are to operate successfully for any significant period.
  - they are expensive, often dearer than the cost of the generator.
  - a precision water regulating device on the turbine is necessary.
  - the governing system is site specific.
-





Whilst many mechanical/hydraulic governors are in use today, many new installations now employ the electronic equivalent, the electro/hydraulic governor, see figure 6. In this type of governor, the flyball arrangement is replaced with an electric or electronic speed sensing system. They provide greater flexibility as the site-specific variables can readily be adjusted. They are adaptable to all types of water turbines and may also be used for other functions such as water-level control, unit automation and monitoring<sup>18</sup>. This type of governor is now the first choice for many new installations, especially on small and mini hydro schemes. It is also possible to convert or upgrade the mechanical type to the electro type<sup>19</sup> because many of the components are common to both systems. Not suprisingly, the electro/hydraulic governor has many of the same drawbacks as the mechanical type where micro hydro installations are concerned.

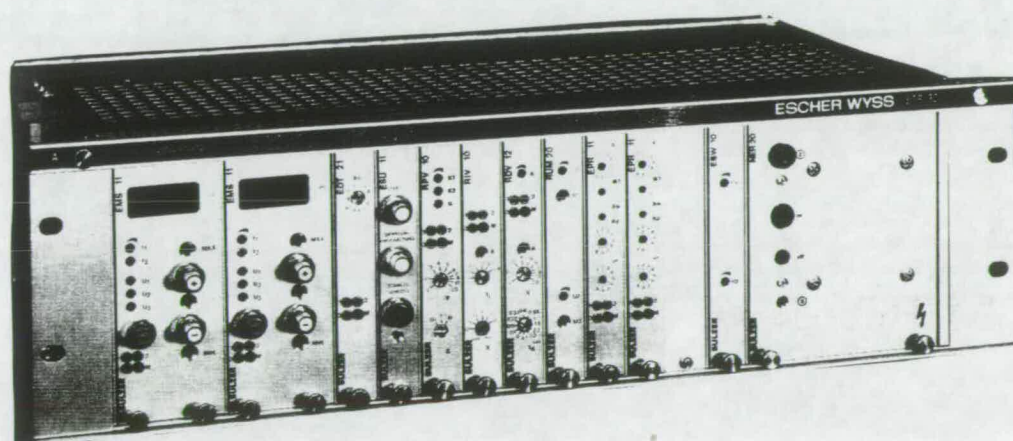


Figure 6 - Electro/hydraulic governor

With neither of the above governing systems suited for micro hydro schemes with outputs below approximately 50 kW, an alternative is required, the *Electronic Load Governor* ( ELG ).

---

### 1.3. ELECTRONIC LOAD GOVERNING

With **load governing**, speed equilibrium is attained, not by adjustment of the water turbine output to match a varying electrical load, but by controlling the total load such that at all times it is equal to the turbine output. Since the total load includes a varying *consumer* component, there must be a third compensatory load component, the *ballast load*, refer figure 7. At any instant, the consumer load and the ballast load will equal the turbine-generator set output, and the electrical frequency is held constant.

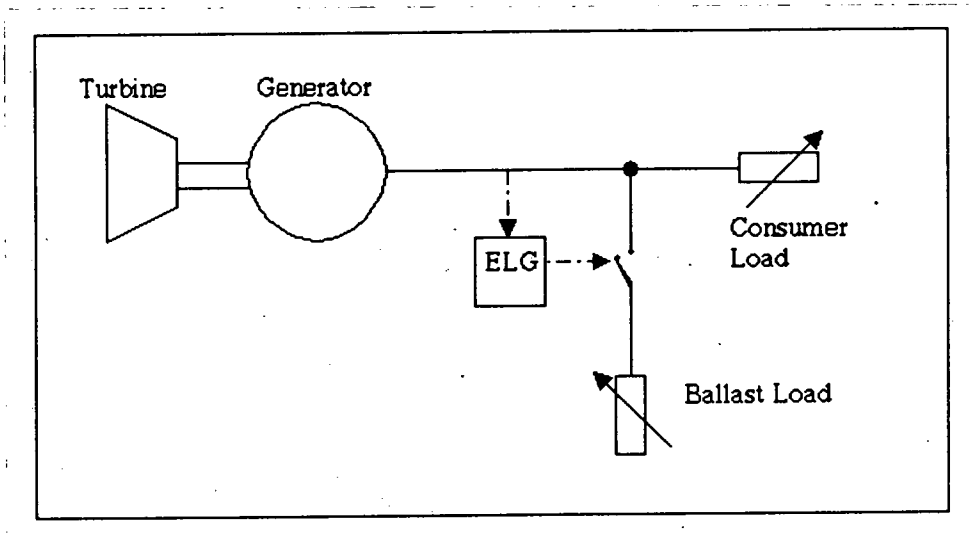


Figure 7 - Load governing principle

Water control is achieved manually at the inlet valve: operation of the generating unit occurs with the valve fully opened; shut-down is achieved by closing the valve. Hence, there is no requirement for the sophisticated water regulating equipment on the turbine such as the spear valve or guide vanes. This significantly affects the turbine design and reduces the cost. In addition, as this system does not rely on the adjustment of the water flow, there is no possibility of a pressure rise

in the penstock and the consequential risk of damage is eliminated.

The load governing function is almost always done by an electronic circuit, hence the term Electronic Load Governor. The ballast load is usually resistive and the power dissipated is preferably used for space or water heating, avoiding energy wastage. For synchronous generating systems, the change of consumer load is detected by sensing the frequency of the electrical system: for induction generator systems, the voltage is monitored.

The two most commonly adopted systems for Electronic Load Governing differ by the means of control of the ballast load power. These are now described in detail.

### 1.3.1. Phase Angle Control

The ballast load comprises a permanently connected, single resistive load circuit of magnitude equal to ( or slightly larger than ) the full load rated output of the generator. As a result of the detection of a change in the consumer load, the firing angle of a power electronic switching device, such as a triac, is adjusted, thus altering the level of the voltage fed to, and hence the power dissipated by, the ballast load<sup>20</sup>.

As with all power electronic switching of this nature this technique introduces unwelcome harmonics onto the electrical system. The shape of the voltage waveform of the ballast load is given in figure 8. It should be noted that these chopped-sine waveforms are *continuously*

---

*present* for all phase angle control apart from full ballast load. The presence of the harmonics may cause overheating of electrical equipment connected to the system and of the generator, usually counteracted by the derating of the plant<sup>21</sup>. In certain cases, high neutral currents may be produced due to the triacs switching at uneven times in response to unbalanced loads<sup>20</sup>.

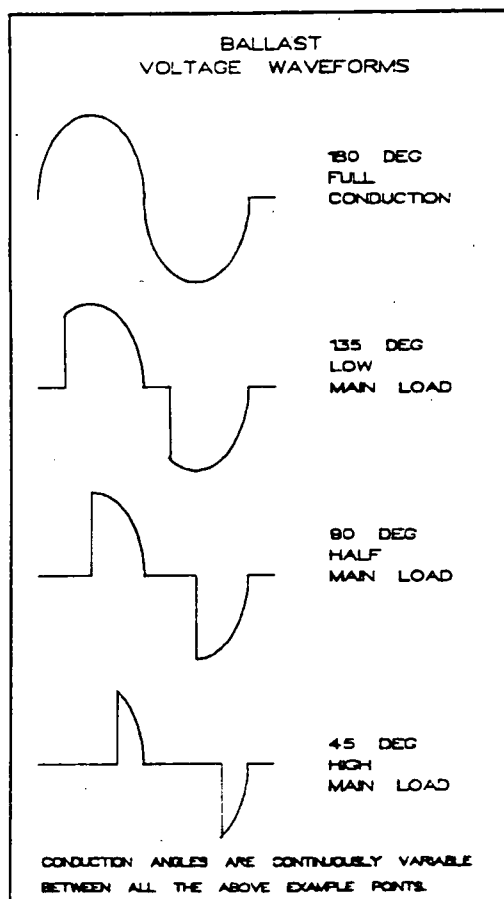


**Figure 8 - Phase angle control - voltage waveforms**

### 1.3.2. Binary Loads

In this method, the ballast load is made up from a switched combination of a binary arrangement of separate resistive circuits. The

load proportion carried by each of the steps is in the ratio 1 : 2 : 4 : 8 and when switched in sequence, the ballast load exhibits a stepped characteristic, see figure 9. The summation of all of the ballast load steps is equal to ( or slightly greater than ) the rated output of the generator.

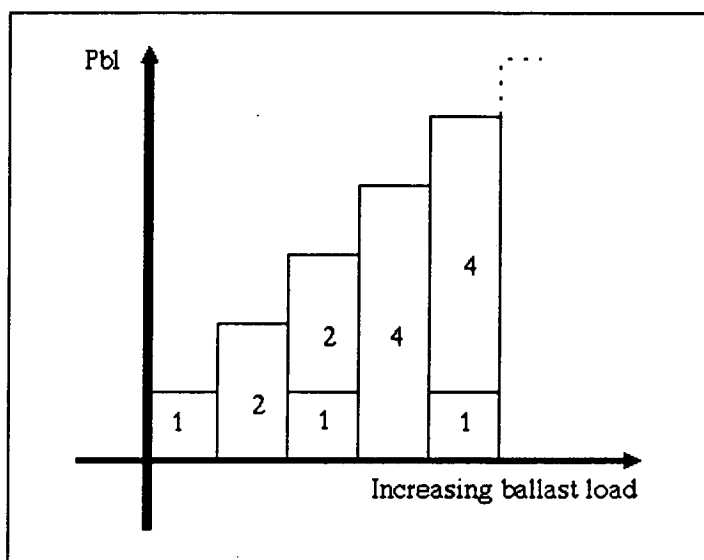


Figure 9 - Ballast load characteristic

In response to a decision to alter the level of the ballast load a switching sequence is performed to select a new combination of the load steps. The switching operation is for a transient period only, thereafter full system voltage is applied to the new fraction of the ballast load and hence *harmonics are not produced at all* in the steady state condition. In addition, it is usually the practice to adopt solid state relays which include a zero-voltage switching circuit that reduces the harmonic distortion associated with the transient switching period.

#### 1.4. ELECTRONIC LOAD CONTROLLER

For the purposes of this thesis, the distinction is now made between the Electronic Load Governor ( ELG ) and the Electronic Load Controller ( ELC ). The former is used to describe an electronic unit which performs the single function of load governing, that is to say the control of the speed of the turbine generator unit by adjustment of the load. The latter is used to describe an electronic unit which is a multi-function unit and will perform other tasks as well as load governing.

These other tasks could be load management, synchronising, water economy, generating unit protection, reactive power control, data logging, and condition monitoring. As will be discussed in Chapter 2, two of the design parameters of the ELG whose development is described herein are simplicity of operation and financial economy. Hence, the addition of any other functions to the basic ELG requires careful consideration to ensure that the possible disadvantages of their implementation do not outweigh the advantages. The electro-hydraulic governors described in Section 1.2 are multi-function units but, as a result, are not economically viable for micro hydro installations. If any additional functions are to be performed by the ELC then a compromise has to be reached; this is discussed further in Chapter 8.

---

## 1.5. MARKET SURVEY

### 1.5.1. Demand for Electronic Load Governors

Almost every nation has micro hydro potential but its future development will vary from country to country for many reasons such as legislative acts, bureaucracy, national policies, traditions, economics and natural resources. The following examples highlight some of these variants. Three countries with quite different characteristics have been chosen to illustrate the range of application of micro hydro technology.

#### *United Kingdom*

A developed country such as the UK appears at first glance to offer no further opportunity for micro hydro development. Historically the UK has been an industrial nation and the electrification of the country is nearly at 100%, only very remote communities in the North of Scotland remaining isolated from the extensive grid network. The UK has evolved a generation mix which includes fossil fuel plant ( coal, oil and gas ), nuclear plant and hydro-electric plant. The majority of the potential for hydro-electric generation falls within Scotland and that is where the majority of the hydro-electric installations are located in the UK. The major thrust of this development took place between 1945 and 1965<sup>22</sup>. Since then the UK has installed large fossil fuelled or nuclear fuelled plants with ever increasing unit ratings of up to 660 MW.

---



Nevertheless, the UK today has a requirement for new generating plant, either to meet increases in demand or to replace old plant which is being taken out of service. Installation policy is influenced by geography, technology and legislation. The demand for electrical energy is largely from the South East of England but the location of 88.7% of the UK's economic hydro potential is in Scotland<sup>5</sup>, mostly at sites with a capacity of 10 MW or less. However, Scotland has an over capacity of generation of approximately twice its own demand, and consequently the electricity companies in Scotland have no incentive to exploit the Scottish hydro potential.

The means by which electrical energy is transferred from Scotland to England is via the interconnecting transmission network, which is currently loaded to its maximum operational capacity. There are, however, plans in hand to upgrade this interconnector by 1994.

In September 1990 the first Order for setting a Non-Fossil Fuel Obligation ( NFFO ) for renewable sources of electricity was laid before Parliament<sup>23</sup>. This Order specifies initial levels of renewable-sourced generating capacity. Of the first block for which Contracts were concluded, hydro-electric generation accounted for 11.6 MW from the total of 168 MW, ie 6.9%. It should be noted that this Order applied only to the Twelve Regional Electricity Companies in England and Wales and did not apply in Scotland. In the second Order, issued in November 1991<sup>24</sup>, 12 hydro projects with a capacity of 10.36MW were let. This amounted to only 2.2% of the total capacity of that Order, and again none of the sites was in Scotland.

---

In May 1991, the Government reached an agreement with the two Scottish Electricity companies where they will pay up to 5.3p per unit to independent power producers instead of the 1.8p they had offered before. This agreement will operate only until the end of 1998.

Other factors, such as the economic aspects and environmental barriers, serve to increase the complexity of the situation. As a result of the NFFO and the agreement in Scotland, the development of the UK's hydro-electric resources is expected to increase probably through private development. It is reasonable to assume that some of these private installations will fall into the micro hydro category and that they may be in locations where either a) there is no local grid, or b) there is a grid but either it is subject to frequent interruption or a back up is required, or c) there is no intention to run in parallel with the local grid. Hence, there will be a small demand for Electronic Load Governors in the UK, as evidenced by an installation at Laurieston Hall near Dumfries in South-West Scotland<sup>15</sup>.

### ***Malaysia***

Malaysia is recognised as a Less Developed Country and is geographically split between Peninsular Malaysia and the States of Sabah and Sarawak in North Borneo ( East Malaysia ). A National Energy Policy exists which includes amongst its aims the diversification of its energy resources and the increased coverage of the rural electricity supply<sup>25</sup>, which aimed to have achieved 77% coverage by 1990. The rural electrification programme is making rapid progress in Peninsular Malaysia where hydro generation accounts for 27.6% of the total

---

generation, however in East Malaysia progress has not been so rapid.

Malaysia has an indigenous source of oil and gas therefore in Peninsular Malaysia, where the rural electrification is often simply an extension of the grid network, hydro-electric generation is not likely to make a major contribution to the increased output. In the remote areas, however, where grid extensions would be uneconomic, renewable energy sources, in particular mini and micro hydro, will be more appropriate. At present there are very few mini or micro hydro installations in East Malaysia but those that do exist, whilst relatively young, are seen as demonstration plants. It is likely that there will be further development of isolated, micro hydro installations in this region and that there will be an associated demand for Electronic Load Governors.

### *Nepal*

Like Malaysia, Nepal is also classified as a Less Developed Country, but the profile of its energy supply is far removed from that of Malaysia. Nepal has no fossil-fuel resources and 87% of the country's energy needs are met by fuelwood<sup>26</sup>. The country has an abundance of hydro potential and has a tradition of using water power for milling. Nepal is situated on the southern slopes of the mid-Himalaya range and the mountain and hill regions account for 77% of the land area. In such circumstances, grid connection is virtually impossible in most localities and isolated stand-alone power plants are installed as a matter of routine.

---

The modern development of micro hydro in Nepal began in the 1960's when local companies began manufacturing and installing turbines on many of the original mill sites. These either produce mechanical energy alone or are multi-purpose, producing mechanical and electrical energy. To date there are over 530 turbine mills in operation<sup>27</sup> and there are at least 9 local manufacturing companies producing water turbines<sup>28</sup>. Approximately 10% of these turbines have associated electrical generators, the majority of which are controlled by Electronic Load Governors. With the continued implementation of such micro hydro schemes in Nepal, there is a constant demand for ELG's for these installations.

### **1.5.2. Existing Electronic Load Governors**

The examples given in Section 1.5.1 highlight the varied demand for ELG's. The concept of the ELG was developed in the early 1970's when the emerging electronics industry coincided with the resurgence of interest in micro hydro generation. At the outset of this research project, in 1987, a survey was done of the ELG's publicised at that time. Although 16 developers/manufacturers/suppliers publicised that they had electronic governors suitable for micro hydro applications, only 6 provided appropriate information to the author.

The data gathered showed that three of these units used the binary load technique, two used the phase delay technique and one used a hybrid combination of binary load and phase delay. Significantly, four of these units used analogue electronic circuits and only two used digital electronic circuits.

---

A fresh survey in 1991 produced valid responses from four additional ELG suppliers, located in Austria, France and Italy. A similar mix of load governing techniques was identified, one based on binary switching, one based on phase delay and two hybrid models. Of the four, three used digital circuitry, the other used analogue circuits. Significantly it was determined that in the preceding 12 months, these four suppliers had sold 110 ELG units, confirming the existence of the market.

### **1.5.3. Relation to Previous Work**

One of the units included in the above survey results was a microprocessor based ELG which utilised the binary load technique. A single phase unit had been developed and tested on a micro hydro installation at Baindoang, Papua New Guinea. The ELG worked satisfactorily but was later removed because the load on the generator became constant and in this event there is no requirement for a governor at all. The unit was developed by staff working at the University of Technology at Lae in Papua New Guinea, who subsequently took employment elsewhere, resulting in the cessation of the development work of the ELG.

The potential of the design concept was recognised by staff at the University of Edinburgh, Electrical Engineering Department and, from 1985 to 1987, two successive final year Honours projects were mounted to investigate variations on the theme<sup>30,31</sup>. That work aimed to produce three phase, microcomputer based ELG's, but the outcome of these studies was limited by time constraints such that neither achieved successful three phase operation.

---

It was against this background that the research study described in this thesis was undertaken. There appeared to be scope for the research and development of a microcomputer based ELG utilising the binary load technique which would operate on a three phase electrical system. It was evident that the program for load governing alone would be relatively short and that there would be sufficient processing and memory capacity for additional subroutines, converting the unit from an Electronic Load Governor to an Electronic Load Controller. The experiences of the previous work were well recorded and the lessons learnt were recognised at the outset of this project.

---

---

## CHAPTER 2 ELG DESIGN PARAMETERS

### 2.1 TECHNICAL CONSIDERATIONS

The alternative techniques of Electronic Load Governing have been outlined in Chapter 1 and the use of different types of electronic circuitry was mentioned. This Chapter highlights the problems with existing ELG units and describes the overriding design principles which were chosen at the outset of the development of the prototype ELG unit.

#### 2.1.1. Problems With Existing Designs

##### *Phase Angle Control*

The phase angle control technique produces harmonics and to demonstrate this, a phase angle controlled light dimmer circuit was built, refer figure 10, and the voltage waveforms examined with an oscilloscope. As the firing angle,  $\alpha$ , of the triac is increased, the portion of the supply waveform which is applied to the load is reduced, refer figures 11a and 11b. The disturbance that the rapid switching of the triac causes to the supply voltage waveform is seen on the CH1 trace in figure 12, where the position of the "glitch" occurs at the firing angle of the trace below, REF1.

---

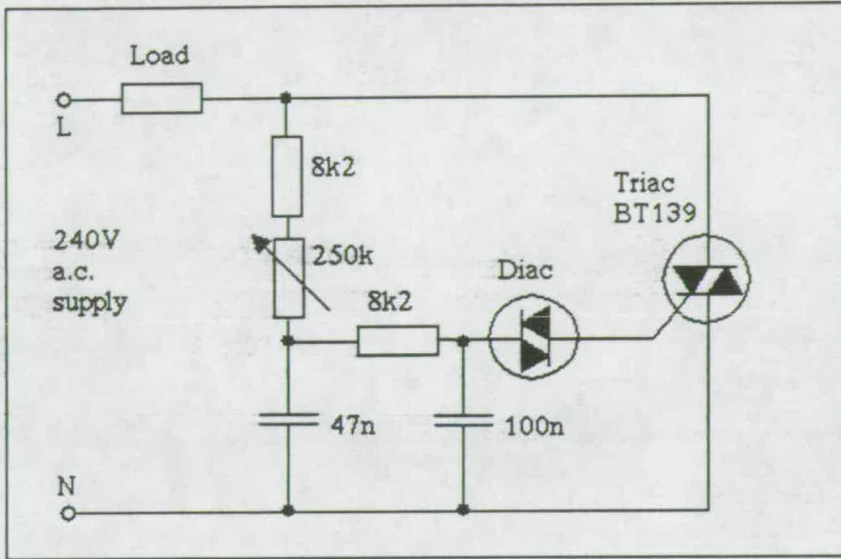


Figure 10 - Typical phase angle control circuit

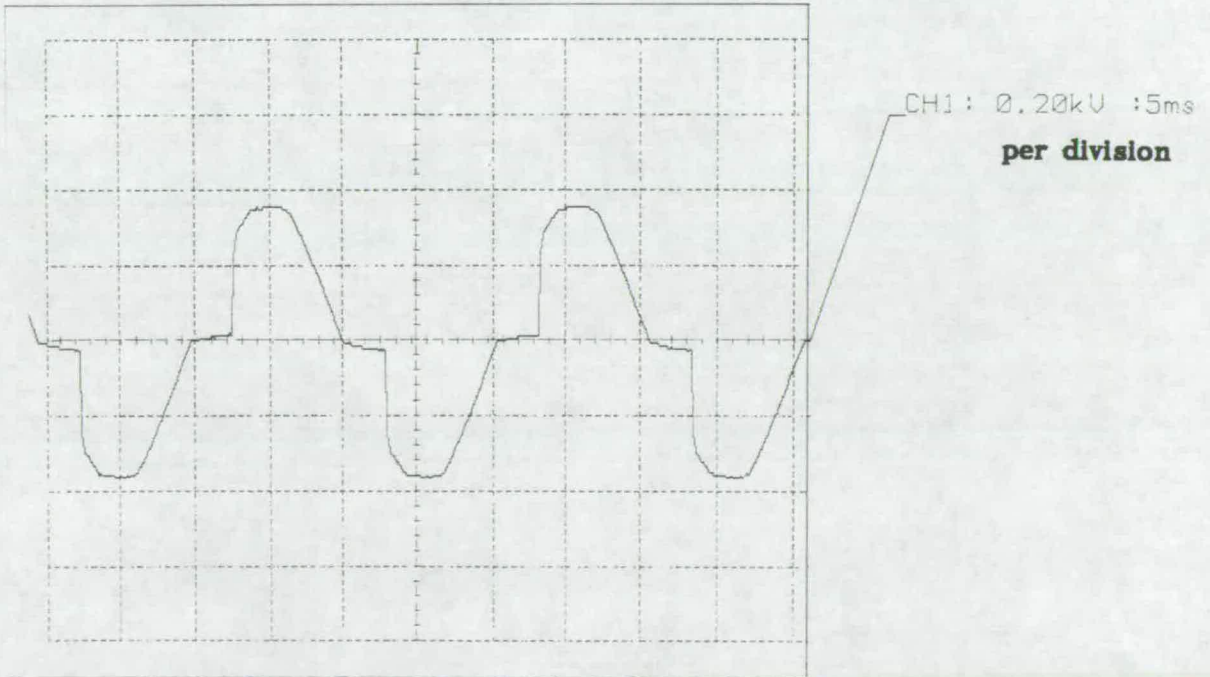
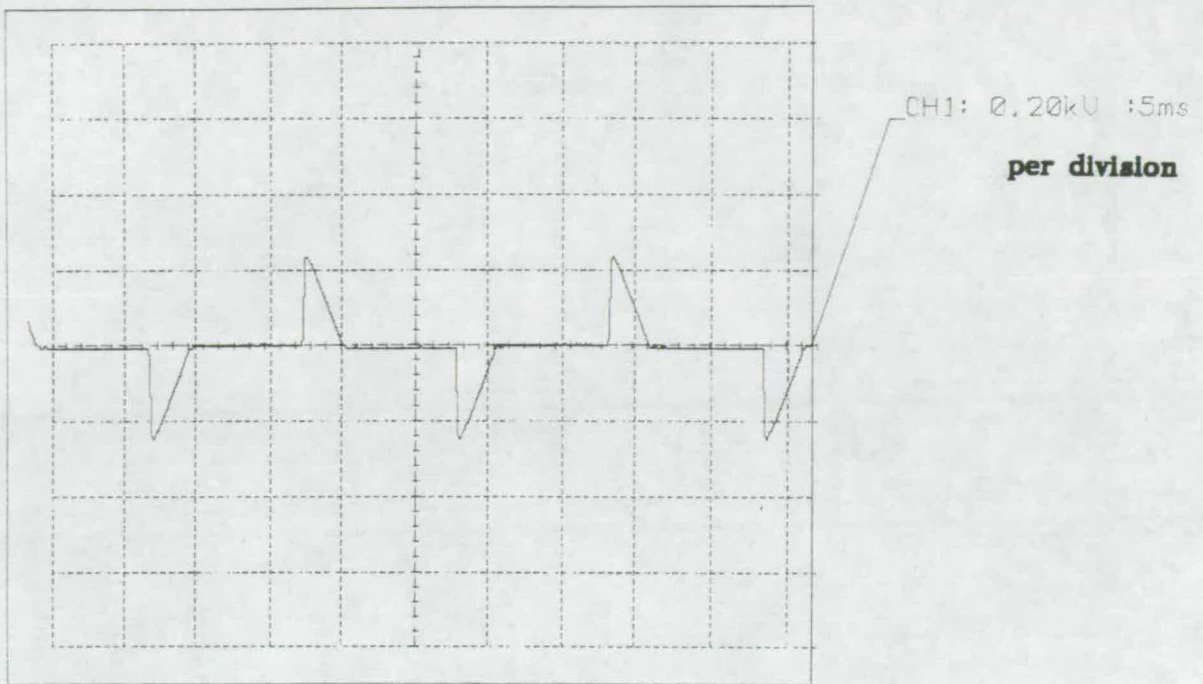
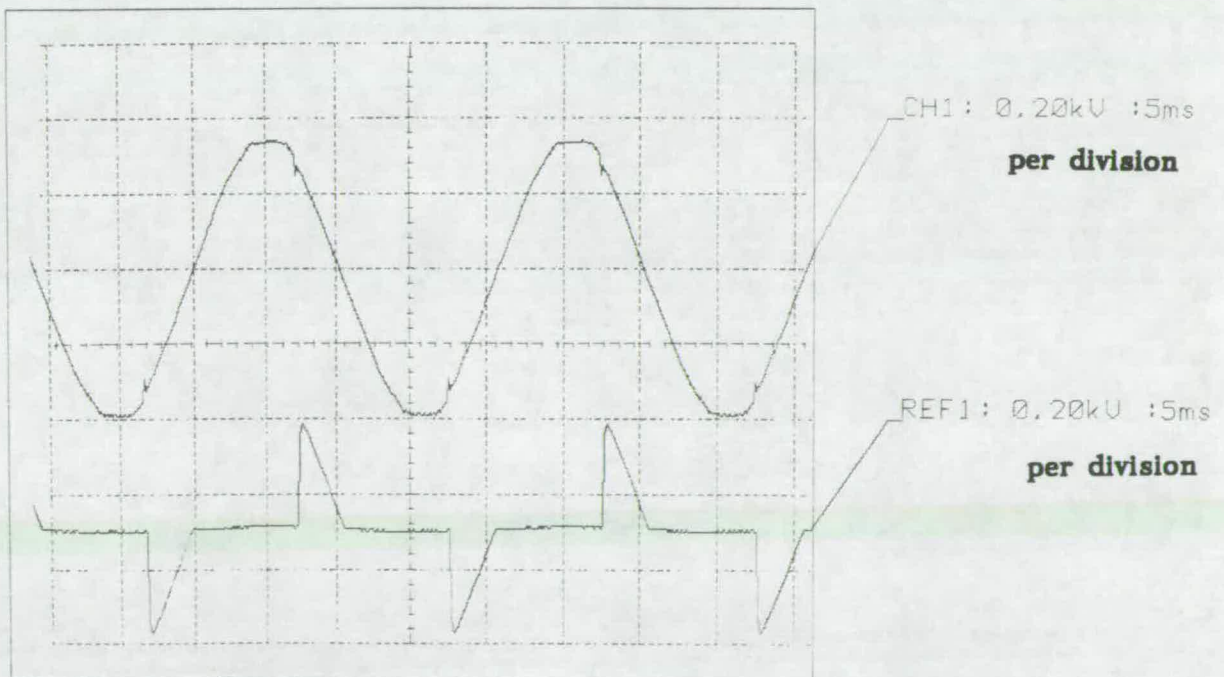


Figure 11a - Load voltage waveform, low firing angle





**Figure 11b - Load voltage waveform, high firing angle**



**Figure 12 - Supply voltage waveform compared with  
load voltage waveform**

---

As the negative half cycle is a reflection of the positive half cycle, there are no even harmonics present. The expression for the harmonic content of this circuit is given by Lander<sup>32</sup>, and the percentage values up to the 9th harmonic are shown plotted against  $\alpha$  in figure 13. It is possible to add electronic filters to the circuit to suppress the harmonic distortion but the distortion increases with the magnitude of the load current and suppression becomes more difficult and expensive. In addition, the harmonic distortion is increased when the load has a longer time constant, such as an electric heating element, a common type of ballast load.

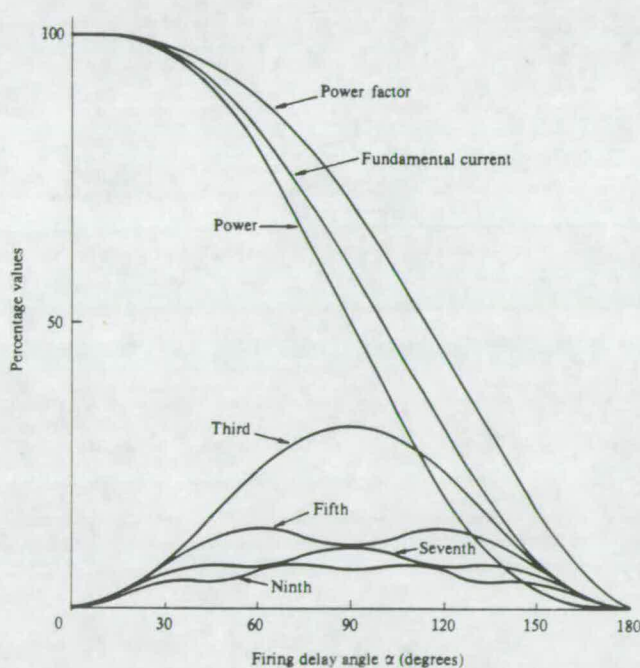


Figure 13 - Harmonics produced by phase angle control

### *Integral Cycle Control*

Integral cycle control is the term used to describe the action of many Electronic Load Governors where increments of load are switched on each cycle of the a.c. waveform. Accurate frequency control requires

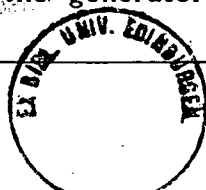
accurate measurement of the period of the voltage waveform, but it was found<sup>33</sup> that the transient reactance of the generator ( whether of the synchronous or induction type ) causes a phase shift in the generator terminal voltage whenever a step change in the connected load occurs. This results in an incorrect measurement of the frequency and could lead to instability occurring. Part of the solution to this problem is the requirement for the inertia of the rotating elements of the turbine/generator set to be greater than or equal to a specified minimum value. If this specified inertia is not inherent in the design of the turbine/generator, additional inertia has to be provided by a flywheel<sup>34</sup>. This clearly incurs additional penalties in respect of the size, the weight and the cost of the installation.

### ***Induction Generator Systems***

The use of induction type machines has received widespread promotion for use in micro hydro installations, largely because of the availability of relatively cheap induction motors. These machines are driven at super-synchronous speed to operate as generators, but are not designed for use as generators. When operated in an isolated situation there are the disadvantages of excitation and voltage control to be overcome, problems which have been studied and solutions proposed<sup>10</sup>.

From an Electronic Load Control viewpoint there is a further disadvantage to the use of induction generators. The ELG's developed respond to changes in voltage rather than frequency<sup>9</sup>, but the voltage level on an electrical system can vary widely, especially when there are lengthy cable runs from the generator to the load(s). The location of

---



the ELG therefore becomes critical for accurate control of the output of the generator, and could lead to additional cabling between the controller and the ballast load, which in a village scheme could be several kilometers distant.

### *Analogue Electronic Circuits*

The characteristics of an individual micro hydro site are unique and the experience of Robinson<sup>35</sup> was that the on-site tuning of ELG's employing analogue electronic components became difficult due to the critical timing nature of the ELG design. A digital circuit design which was easy to adjust on-site was proposed by Robinson as a solution to this problem.

Additional disadvantages in the use of analogue electronic circuits are the inability to store data for any length of time and the requirement for additional circuits to perform additional functions. These two aspects clearly limit the conversion of a basic ELG to an ELC.

### *Microcomputer Choice*

Assuming that it is accepted that the digital electronic route offers advantages over the analogue route, the choice of the microcomputer is important. The work of Watson<sup>30</sup> was hampered by his choice of the Sinclair QL Microcomputer. This computer is based on a 16 bit, 68008 microprocessor and all tasks performed by the computer are controlled by the QDOS operating system. The specific problem encountered was related to the software interface between the ELG program and the

---

QDOS software for interrupt handling. There were also problems due to the complexities of the QDOS operating system. Amongst Watson's recommendations was the adoption of a simpler microprocessor system, preferably through the use of a single card microcomputer.

### ***Unbalanced Loading***

Some ELG designs for control of three phase generation make no attempt to balance the load currents: indeed operation often involves adding the ballast load on one phase only, thus creating a severe unbalance of the currents on the generator. The effects of this unbalance on the generator would be;

- to create unbalanced magnetic forces, causing undue strain on the bearings of the system;
- to produce circulating currents within the generator which would result in increased heating of the machine; and,
- to create unbalanced terminal voltages due to the different currents in each phase of the generator.

### **2.1.2. Proposed Design Features**

A design philosophy was established to provide solutions to avoid the disadvantages of existing ELG's. The design covered four different aspects; those of *a)* the Load Governing technique, *b)* the electronic circuits, *c)* the application and *d)* the manufacture and assembly.

---

During the course of this study a laboratory prototype ELG was assembled for testing purposes. The prototype unit incorporated as many of these design features as was practicable, although certain aspects such as the manufacture and assembly of a production stage unit were not addressed. It was considered that these should be attended to at a more appropriate stage, and not during the initial development of the unit.

#### 2.1.2.1. Load Governing Aspects

The ELG was designed for applications in electrical generating systems which are isolated from grid networks and which are fed by three phase, synchronous a.c. generators. It was recognised that there may also be applications with single phase generators and an alternative version was prepared for single phase use. Although changes in the consumer load are monitored essentially through frequency measurement, *frequency* is not in fact calculated by the ELG. Instead it measures and compares the *period* of the a.c. voltage waveform. The prototype is designed for 50 Hz systems, but 60 Hz systems would be readily achievable by software modification.

The load governing technique adopted is that of binary load switching. As the design is for a three phase system, the ballast load in each phase is sectioned into a 1, 2, 4 format and a current balancing feature is implemented. This requires knowledge of the relative levels of the current in each of the generator lines, achieved through the use of current transformers ( CT's ). The relays used to effect the switching of the ballast load are solid state devices incorporating a zero-voltage

---

circuit. A schematic diagram of the electrical system is given in figure 14.

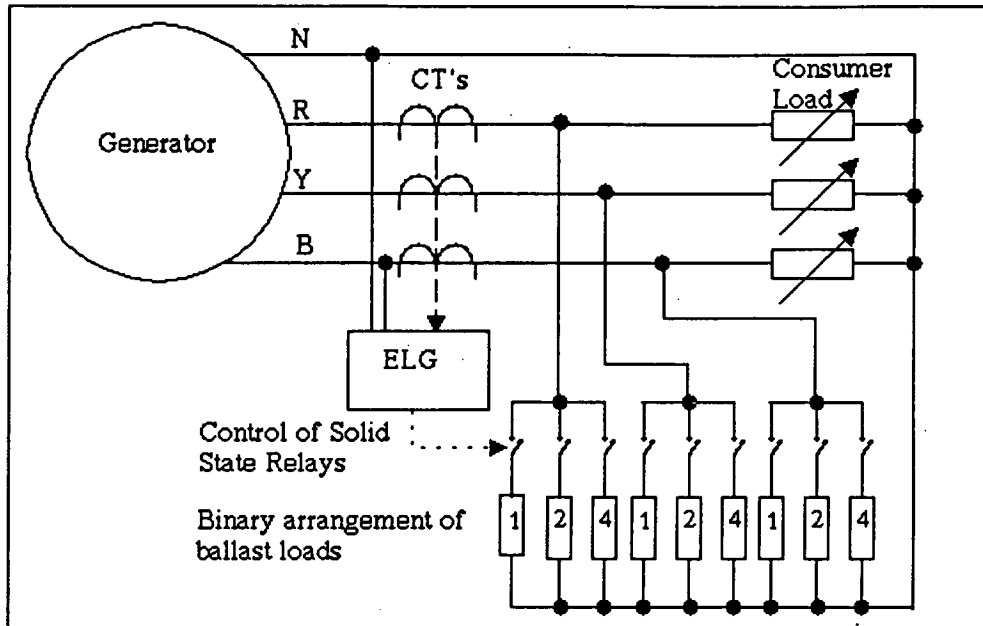


Figure 14 - Schematic diagram for three phase load governing

### *Ideal ELG Operation*

An explanation of the method of operation of the ELG is useful at this stage. For the purposes of this explanation, the assumption is made here that the total ballast load rating,  $P_B$ , is equal to the generator output power,  $P_G$ . The power-in to the shaft system,  $P_{IN}$ , is assumed to be constant, the efficiency is assumed to be 100% and the generated voltage is assumed to be constant. The true operational characteristics of turbine-generator sets are given in Chapter 5.

On detection of a frequency which is outside of pre-set limits, the ELG *reacts* by adding, or subtracting, **one** step of ballast load in each *cycle* of its operation. As the ballast load is arranged in a binary format, the

resolution of one ballast load step is 0.143 p.u. of the phase load, which, with three phase balancing, becomes a resolution of 0.0476 p.u. of the total three phase load. This means, for instance, that for a generator with a full load output of 30 kW, when a single step of ballast load,  $P_S$ , is added, 1.43 kW is switched in. It is further assumed that suitable ballast loads will be available, or could be contrived, which will be approximately equal to the step size required. If this were not the case, the per unit magnitude of each step will be determined by whatever loads are available, and this in turn will dictate the steady-state frequency variation that will occur.

The consumer load,  $P_C$ , is assumed to be infinitely variable up to the generator rated output and this technique demands that there is normally a variation of the sum of the total connected load. The ideal situation is shown in figure 15 where the ballast load is reduced from one step to the next by the ELG as the consumer load rises linearly from zero to the rated generator output. The maximum variation in the total connected load will be equal to  $P_S$ .

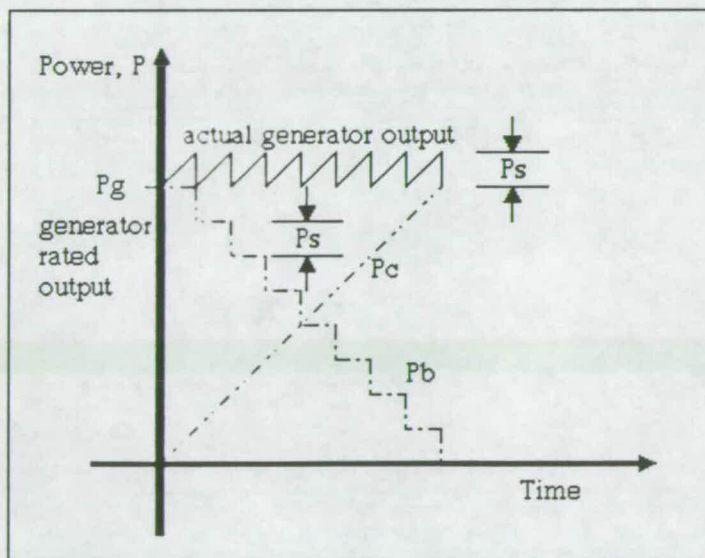


Figure 15 - Power variations of ideal operation



It is the effect that this variation has on the speed of the set, and therefore the frequency, that is important to the operation of the ELG. Any difference between the shaft input torque and the connected electrical load torque will cause the shaft system to speed up or slow down until the torque balance has been restored. Ignoring the transient behaviour at present, the extent of the frequency variation depends on the ungoverned **droop** of the turbine generator set. The droop is a measure of the change in frequency for a change in connected load, refer figure 16. Expressing "load" in terms of power (kW), then,

$$\text{Droop} = \frac{\Delta f}{\Delta P} \quad (\text{ Hz/kW } ) \quad ( 2.1 )$$

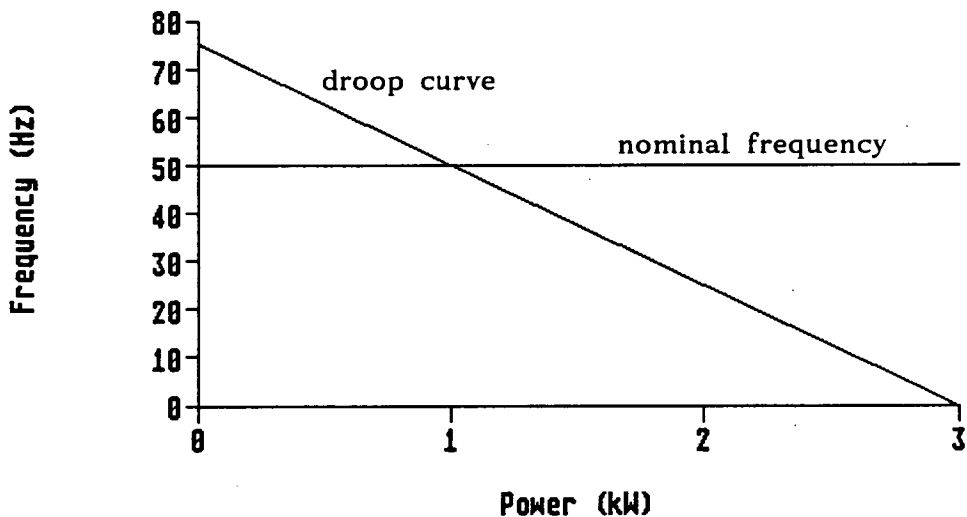


Figure 16 - Typical droop characteristic, frequency vs power

Hence it is to be expected that in steady-state operation the frequency will not be maintained strictly at 50 Hz; rather it will vary within a predetermined **deadband**. The deadband is the tolerated variation in frequency which results from a change of load of magnitude equal to one step of ballast load, ie

$$\text{Deadband} = \text{Droop} \times P_S \quad (\text{ Hz } ) \quad ( 2.2 )$$

It should be stressed that it is an inherent feature of the method of operation of the ELG that, in the steady-state situation, the frequency will vary within limits around 50 Hz and will not be maintained exactly at 50 Hz. The extent of the frequency deviation depends on the magnitude of the droop and the aim is to limit the variation to within  $\pm 2.5$  Hz from 50 Hz. Whilst these variations would be outside the strict frequency limits imposed on the UK generating companies, they are considered acceptable in applications where the installation is either an economic alternative to a grid supply or makes possible a supply of electricity where there is no grid present. The specification for a rural electricity supply is suggested by Woodward<sup>36</sup> as  $\pm 5\%$  variation on the voltage and  $\pm 2\%$  on the frequency.

The majority of the loads which would be connected to remote, isolated generating systems in rural networks would not be sensitive to such small frequency variations, e.g. light bulbs and heaters, although equipment such as motors, radio and television are not uncommon. Tests were done to determine the effect of a varying frequency supply to a television set. A deviation of greater than 0.25 Hz gave rise to moving bands on the screen which increased their rate of travel as the frequency deviation from 50Hz increased.

The ELG is programmed to react only when the measured frequency values fall outside of the deadband limits. If the deadband value calculated by equation 2.2 was centred on 50 Hz then there would be little or no margin in respect of stability. Referring to figure 17a, if the calculated deadband value was, say, 1 Hz, then the upper and lower limits would be 50.5 and 49.5 Hz respectively. When a frequency value

---

just above the deadband is measured and a single step of ballast load added, the steady-state frequency would fall to just inside the lower deadband limit, therefore giving rise to a high probability of further switching. This probability could be measured as a 'coefficient of stability'.

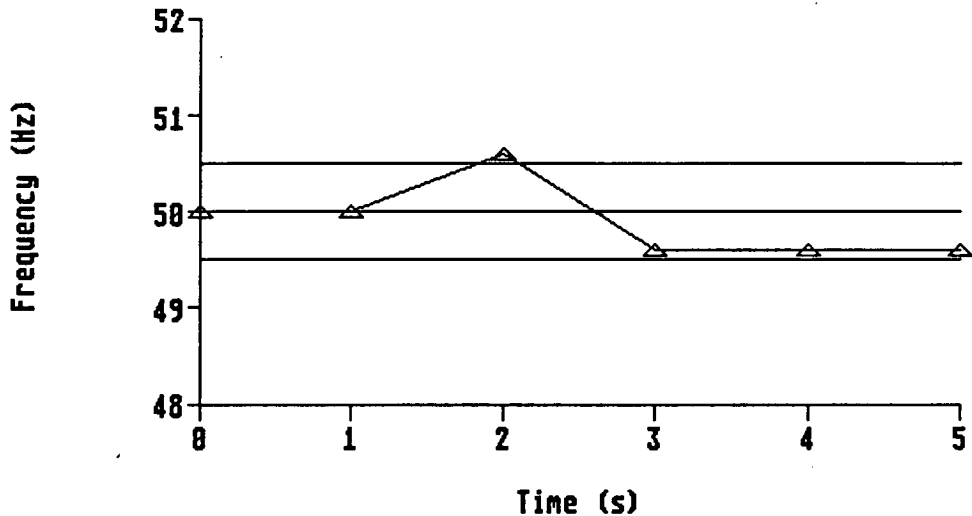


Figure 17a - Calculated deadband centred on 50 Hz

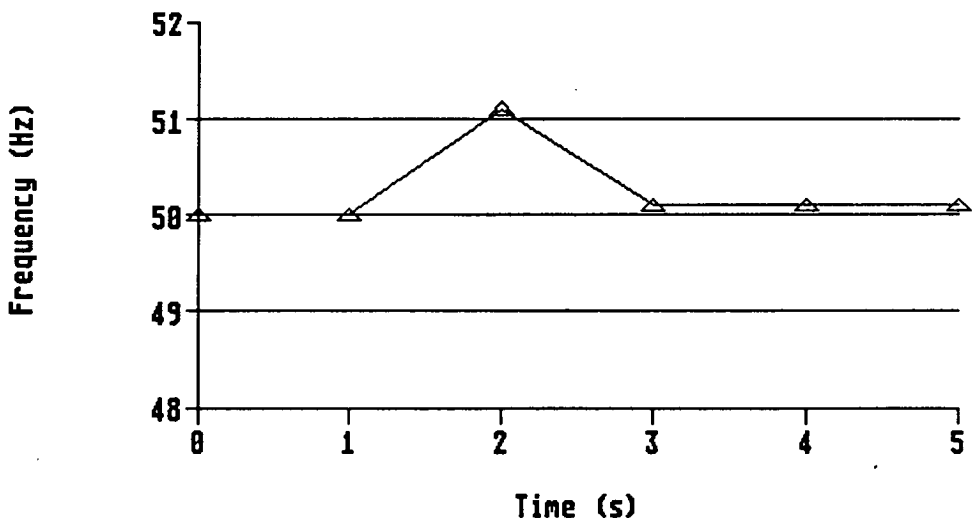


Figure 17b - Deadband value on both sides of 50 Hz

The solution to this is to create a stability margin, by arranging that the selected deadband value is equivalent to the full calculated value on either side of 50 Hz, as shown on figure 17b. In this case, when the

ELG responds to a frequency value just above the upper limit, the addition of the single step of ballast load will return the frequency *to the centre of the deadband*, ie close to 50 Hz. This results in a high value for the coefficient of stability and is considered to be the *preferred or ideal* deadband selection.

The coefficient of stability can thus be determined by;

$$\frac{\text{Selected deadband width} - \text{Calculated width}}{\text{Calculated width}} \quad ( 2.3 )$$

For example, if the deadband is calculated as 1.6 Hz, and the ideal deadband of  $\pm 1.6$  Hz is selected, then the coefficient of stability would have a value of unity. Alternatively, if the calculated deadband value is 1.4 Hz, and the same deadband is used, then the coefficient of stability would be 1.28. Finally, if the calculated deadband value is 1.85 Hz, and the selected value remains as  $\pm 1.6$  Hz, then the coefficient of stability is 0.73. The coefficient of stability is thus a measure of the probability of the frequency leaving the deadband limits due to small-scale disturbances to the torque balance. A value approaching zero implies a high risk of further ballast load switching, and a negative value infers that the system will be unstable.

The magnitude of the droop and of the ballast load steps may not be known until the site characteristics are determined during the installation and commissioning of the set. Therefore it is essential that the deadband limit is adjustable on-site. This facility will also permit a compromise to be reached, if required, between the preferred deadband selection, as described above, and the setting necessary as a result of on-site testing.

---

A feature considered necessary by Robinson<sup>35</sup> was the ability to introduce a delay period into the ELG's operation to permit transients to settle before further frequency measurements were taken, thus avoiding the problems associated with integral cycle control experienced by Elder *et al*<sup>33</sup>. Again this facility, known as the *wait delay*, is adjustable on-site to take account of unique site characteristics that occur. The effects of the addition of wait delay are discussed in Section 6.2.2.

### 2.1.2.2. Electronic Circuit Aspects

The design is based on digital electronic circuitry and centres around a microcomputer. The operation of the ELG is controlled by a program which is stored in a digital memory device such as an EPROM or a PROM. Hence the design included both hardware and software elements. In order to overcome the problems experienced by Watson, a single card microcomputer is used which simplifies the operation of the microcomputer and reduces the total number of components, pins and component interfaces. It is expected that this will have a positive effect on the reliability of the unit.

The ability to prepare different ELG units applicable to different system frequencies ( 50 or 60 Hz ) and for either single or 3 phase generators simply by modifying the software means that, except for the replacement of the memory device, the hardware can be otherwise identical. The flexibility of the software permits solutions to stability such as variable deadband and wait delays without the addition of filters and flywheels.

---

Deliberately, the hardware has built-in spare capacity, so that the unit can easily be extended to perform additional functions such as unit protection and data logging through software changes, rather than through the introduction of additional electronic circuitry.

### **2.1.2.3. Application Aspects**

The design minimises the degree of on-site adjustment that is required during the commissioning phase of the installation. It is anticipated that commissioning may not always be performed by engineers trained to Western standards, if trained at all, so it is essential that any on-site adjustment is minimal and simple.

Once installed, it would be preferable that the ELG thereafter requires no operator intervention during normal operation. This implies that it should have an integral power supply, that there are no devices external to the ELG case which could be (mal-)controlled by an operator, and that the unit automatically caters for run-up and shut-down of the generating set. By definition, an isolated system must be capable of starting without the presence of a grid, and as battery supplies may be non-existent, the ELG must derive its power supply from the generator it controls.

Maintenance and repair will be as simple as possible. All components used are standard and readily available, at least to the manufacturers of the unit. Thereafter, such spares that are considered feasible for operator replacement can be made available to the operator. The extent of spares supplied will depend very much on the location of the site

---

and the skills that the operators are known to possess. Given that the likely market for the ELG is in Less Developed Countries, a general philosophy of repair by replacement will apply. It would be preferable that unskilled operators are not involved with individual chip replacement ( assuming that they had the skill to identify a problem related to a specific chip ), rather that they replaced a complete printed circuit board, or even the complete electronic unit if the costs were low enough.

#### **2.1.2.4. Manufacture Aspects**

The design should be robust and suitable for the intended environments in which it might operate. The transportation of the unit to the site may be by a variety of means which could include hand carriage or transport by animals, and therefore the unit must be physically strong enough to withstand vibration and shocks during transport. The unit may not be mounted within a larger control cubicle, so it should be environmentally secure against temperature ( high and low ), humidity, dust and vermin. The unit would not normally be handled or moved during operation, however contingency against accidental movement or damage should be considered. The unit should be designed to guard against unwelcome interference by personnel, authorised or otherwise.

Reliability is of vital importance but most of the measures to ensure reliability of the unit would be implemented at the production phase, not the research and development phase. Such measures would include catering for the environmental aspects mentioned above, quality control during the manufacture and assembly of the hardware, and adequate test

---

procedures. The measures taken at the initial design stage were the use of standard, well proven components and the minimising of the total pin count through the use of digital electronics and printed circuit board assemblies.

A design aspect concerning the manufacture of the unit which would impinge on the on-site design considerations is the use of a modular construction for the unit. This would allow simple pull-out, plug-in replacement of faulty circuit boards and would simplify the maintenance of the unit.

During the prototype assembly of the ELG, the design focus was on the aspects listed in foregoing sections. The manufacturing aspects of the design will be tackled at a later stage.

## **2.2. ECONOMIC DESIGN CONSIDERATIONS**

As many micro hydro units are installed by remote communities, often in Developing Countries, the initial capital cost of a micro hydro installation is critical. The efficiency of the installation is important, but not critical, and there is a compromise to be met between efficiency and capital cost. Generally the running costs of micro hydro plants are low and therefore the characteristic is one of being capital intensive which results in a high sensitivity to interest rate fluctuations ( if applicable ).

---



Scaling down equipment and using *large hydro* practice on micro hydro installations results in conventional micro hydro equipment being disproportionately expensive. The installed unit costs are found<sup>12</sup> to vary inversely with both turbine output power and nett head. As the energy available per unit volume of water rises with head, the physical size, and thus costs, of higher head installations tend to reduce for constant power. Selection of impulse turbines for higher heads enables the construction of less complex civil works. The traditional lower head limit to which these turbines are applied can be stretched using speed increasers and multi-jet machines.

Accurate historical cost data for successful micro hydro installations is scarce and varied. In addition, the site specific nature of all hydro installations results in a wide range of costs for a given output power. As a proportion of the total purchase cost of a micro hydro installation, the electro-mechanical plant is approximately 40%<sup>37,38</sup>, excluding transmission and distribution costs. A typical target total system purchase cost is £1600/kW - plus or minus 30% - which suggests a target electro-mechanical unit purchase cost of £640/kW. This portion of the total cost will include the turbine, the control equipment, and the generator. In the micro hydro power range, the turbine tends to predominate the cost of the electro-mechanical plant, the proportion of costs being 80 : 10 : 10 respectively.

For a range of site outputs, this suggests the capital purchase costs (i.e. the selling price from the suppliers viewpoint) for the control equipment given in Table 2 below;

---

---

<u>Site Output ( kW )</u>	<u>Purchase Cost of Control Equipment ( £ )</u>
15	960
30	1920
50	3200

**Table 2 - Capital Purchase Costs of Control Equipment**

The extent of equipment included in the term "control" will clearly vary from one installation to another but it is assumed that typically this will include an element of metering, control switches, and indicators, in addition to the main electrical power switches and the ELG. The cost of the main power switch will vary proportionally with output power. The ELG will include a fixed cost component ( the electronic circuits ) and a variable cost component ( the ballast load switches ), all other control costs will be largely independent of site output power. It is assumed that the cost of the loads, both consumer and ballast, are excluded from this analysis.

As a part of the survey of ELG suppliers undertaken in 1991, ( refer Section 1.5.2. ), budget prices for the ELG units were obtained. These ranged from £600 for a 2 kW unit through to £3,000 (rating unspecified).

The foregoing suggests a target selling price for the ELG design of between £500 and £2000, depending on the site output power. Irrespective of power rating, there will be a minimum price for the electronic circuits and the power independent components, thereafter the

---

price will rise as a function of the output power of the site. In any event, it was necessary to be aware of the target selling price for the ELG during its design.

Recent experience of the author with mini hydro installations is that the price of mechanical/hydraulic type governors is a factor of 10 higher than the above target price for the ELG.

---

---

## CHAPTER 3 ELG DESIGN

With the design overview established, the implementation of the concept in electronic circuit hardware was carried out in parallel with the development of the software for the microprocessor. The software development is described in Chapter 4; this Chapter details the hardware design. A step-by-step approach was adopted, tackling each function in turn from initial design through to testing. In this way, fault finding was limited to the most recently built circuit.

At the core of the hardware is the microcomputer, a fully operational computer system built around a microprocessor. The microprocessor works as a control unit executing a predetermined set of instructions stored in a memory. In its target application, the microcomputer operates in a stand alone mode, and is complete with a microprocessor, ROM, RAM and a clock. Initially, the microcomputer was connected to additional equipment to assist with the program development and testing.

### 3.1 MICROCOMPUTER CHOICE

The specification for the microprocessor system was established in order that research could be performed to select the most appropriate system for the application. The following points emerged as those relevant to the microprocessor selection;

- i) The microprocessor should be suited to a control application.
-

- ii) A total of 40 input/output ports would be required.
  - iii) Capacity for future expansion would be required as it was known from the outset that there would be several stages to the development.
  - iv) Interrupt facilities would be required.
  - v) A low pin count would be required, suggesting a single chip microprocessor.
  - vi) A high-level language, software development and edit facility would be of benefit during the development stage. Critical sections of the program should be convertible to assembly language to speed up the operation of these tasks.
  - vii) It was envisaged that the complete circuit would be relatively small and hence power requirements would generally be of low order. Nevertheless, in order to simplify the design of the power supply for the target application, the number of different voltage levels required for the electronic circuits should be minimised.
  - viii) The greater the bit length, the more complex are the tasks that the microprocessor can perform and the faster the speed of operation of the processor, at the expense of a greater number of memory chips. This application did not demand complex operations or particularly high speed but did require as low a component count as possible, thus a bit width of 8 would be adequate.
-

---

Research into the different microprocessor systems commonly available was conducted and a summary of those identified as generally meeting the above specification is given in Table 3.

<u>Series</u>	<u>Comments</u>
Intel 8080.	Good for control applications but a three chip device.
Intel 8085.	A single chip version of the 8080.
Z80.	A single chip system, good for control applications and with good interrupt and input/output facilities.
M6800.	Good for control, particularly real-time applications. A multi chip system.
M6502.	A direct descendant of the M6800.

**Table 3 - Suitable Microprocessor Systems**

Clearly each of these has advantages and disadvantages, and factors such as reliability, economics and availability were also taken into account.

Apart from the performance of the microprocessor itself, the software development was also important, in a number of ways;

---

- A high level language was preferred.
- A modular programming structure was recommended<sup>39</sup> to ease the testing and growth of the program.
- Good editing facilities were required, involving the use of a host microcomputer.
- Disc storage of the software was essential during its development.
- Transfer facilities to EPROM were necessary.

It was decided to use a proprietary microcomputer since effort could quickly be directed to the *application* of the microcomputer rather than its design and construction. Several single card microcomputers were considered and the one adopted for use is the Essex FORTH Microcard. The salient details of this microcomputer are given in the following Section.

### **3.2. ESSEX FORTH MICROCARD**

The Essex FORTH Microcard is based on the Rockwell R65F12 8-bit, NMOS single chip microprocessor which contains an enhanced R6502 CPU, an internal clock oscillator ( 2MHz ), 3K bytes of ROM, 192 bytes of RAM and interface circuitry. The interface circuitry includes two programmable timer/counters; five, 8-bit input/output ports ( resulting in a total of 40 input/output lines ); a serial input/output channel and ten interrupt lines.

---

The processor chip includes a FORTH software *Kernel* contained within ROM which allows a single chip system for target applications and a two chip set for software development - through the addition of the R65FR1 RSC-FORTH Development ROM. The Microcard packages the microprocessor chip along with two memory sockets for up to 16K bytes of RAM/EPROM, RS232 compatible serial interface circuitry and interface connectors.

Program development of the Microcard is possible in a number of ways, one of which is the use of a host computer. This method allows the development of programs on virtually any computer which has an RS232 serial interface and mass-storage facilities. Source programs written in the FORTH high level language on the host computer can be downloaded into the Microcard and tested. Completed programs can then be up-loaded into the host computer for EPROM preparation.

The choice of the FORTH microcomputer satisfies the application specification in the following ways;

- it is based on the well proven, 8-bit, microprocessor, the 6502, recommended for use on control applications, refer Table 3.
  - it is a single chip system.
  - it has a high input/output capacity.
  - it has a high memory capacity for program expansion.
  - several different interrupt facilities are available.
  - only a single 5V power supply is required.
  - it allows high level language ( FORTH ) programming via the serial port.
-



- FORTH uses a modular structure.
- program editing and disc storage is possible using a host computer.

Full details of the Microcard can be found in the FORTH Microcard Technical Manual<sup>40</sup>. The Microcard PCB layout and circuit diagram are given in Appendix 1.

### **3.3. INPUT/OUTPUT BOARD DESIGN**

The 40 input/output ( I/O ) lines of the R65F12 microprocessor are organised as five 8-bit ports - referred to as Ports A, B, E, F & G. Port E can be used for output only, the remainder can be used for either input or output and some Port A lines are multifunction. The I/O lines are unbuffered and approximate to a standard TTL load as inputs and can drive a single TTL load as outputs.

To interface between the microprocessor, mounted on the Microcard, and the power system which it is monitoring and controlling, an I/O board was designed and built. There are four different types of circuit required of the interface; a digital switched input circuit; a digital output circuit; a frequency measurement circuit and an analogue input circuit. The design of each of these is described below. A power supply circuit is required to provide all the power consumed by the electronic circuits; the design of this is also described. Positive logic has been used in the digital design where +5V is a digital 1 and 0V is a digital 0.

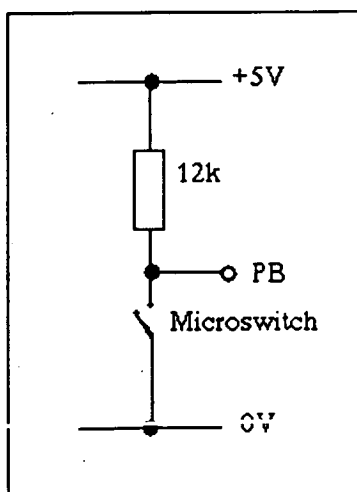
---

### 3.3.1. Digital Switched Input Circuit

Switched inputs allow the provision of variable parameters such as the frequency deadband and the wait delay. These variables will normally be adjusted only during the initial commissioning of the ELG and will affect the stability of the system. Once set, there should be no requirement for operator intervention. Thus, these switches are of the microswitch type, mounted such that they are not accessible during normal operation of the unit.

In a digital circuit, the number of different combinations arising from a sequential group of switches varies as  $2^n$  where  $n$  is the number of switches in the group. Hence, the use to which the information present on the input switches can be put can be varied not only by the software which reads and acts on the information but also by the value of  $n$ .

The design of the input circuits is as shown in figure 18. With the switch open, a digital 1 is presented to the appropriate line of the microprocessor and with the switch closed, a digital 0 is presented to



the input line. A total of eight switched inputs are provided - connected to Port B. Of these eight, three are allocated to deadband selection, two for wait delay variation and three are spare for future use.

Figure 18 - Switched input circuit

### 3.3.2. Digital Output Circuits

All the microprocessor output lines are buffered through a standard inverter gate, as in some instances they are required to drive more than one load. Ports E and G have been designated as output ports. The outputs are used for several different functions; ADC control ( refer Section 3.3.4. ); ballast load switching complete with LED indication; and program status ( LED ). Of these, the ballast load switching circuit is shown in figure 19. A digital 1 on the microprocessor output line is inverted to a digital 0 which switches on the solid state relay and causes the LED to illuminate. A digital 0 on the processor output line switches off the relay and the LED.

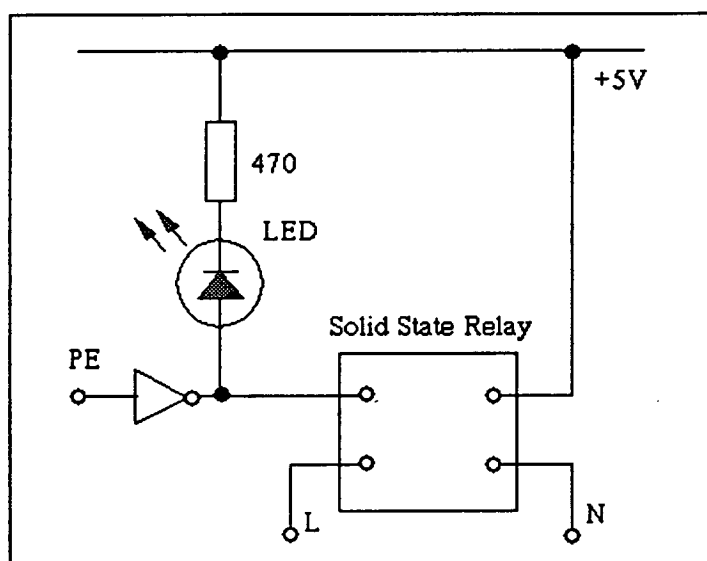


Figure 19 - Ballast load switching output circuit

### 3.3.3. Frequency Measurement Circuit

The ability to determine the period of the a.c. voltage waveform on the power system is critical to the operation of the ELG. The microprocessor normally recognises one of two states, 1 or 0, however

it also has the ability to recognise changes between these two states. This feature, known as *edge detection*, when operated in conjunction with the interrupt and counter/timer facilities of the microprocessor permits timing of intervals between "like" edges to be performed.

Hence, a circuit is necessary which converts the power system a.c. voltage into an alternative form with fast rising/falling edges which corresponded directly to the a.c. waveform. The circuit, as used previously by Kormilo<sup>29</sup>, is shown in figure 20a. The power system voltage is stepped down by a transformer to 12V. This voltage is clipped by a zener diode to the digital circuit level and then passed to the input gate of a Schmitt Trigger IC.

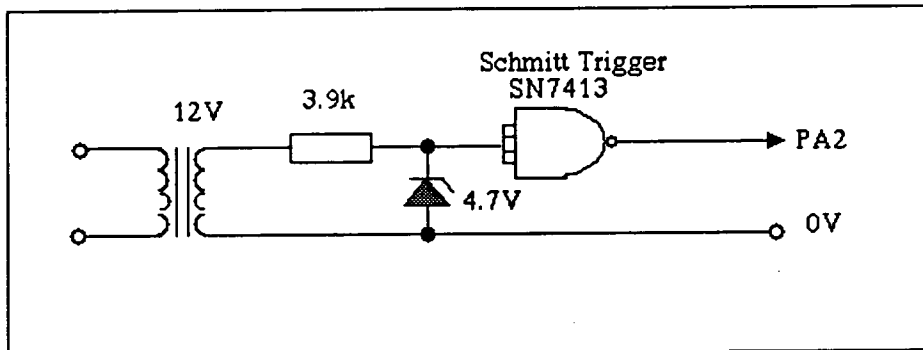


**Figure 20a - Frequency measurement circuit**

The output of the Schmitt Trigger is a rectangular waveform, refer trace CH2 of figure 20b. This signal is fed to an input line of the microprocessor, PA2, which specifically detects the negative going edges, the inverse of the period between these being equivalent to the frequency of the a.c. system. The processing of this signal is discussed in Section 4.3.2.

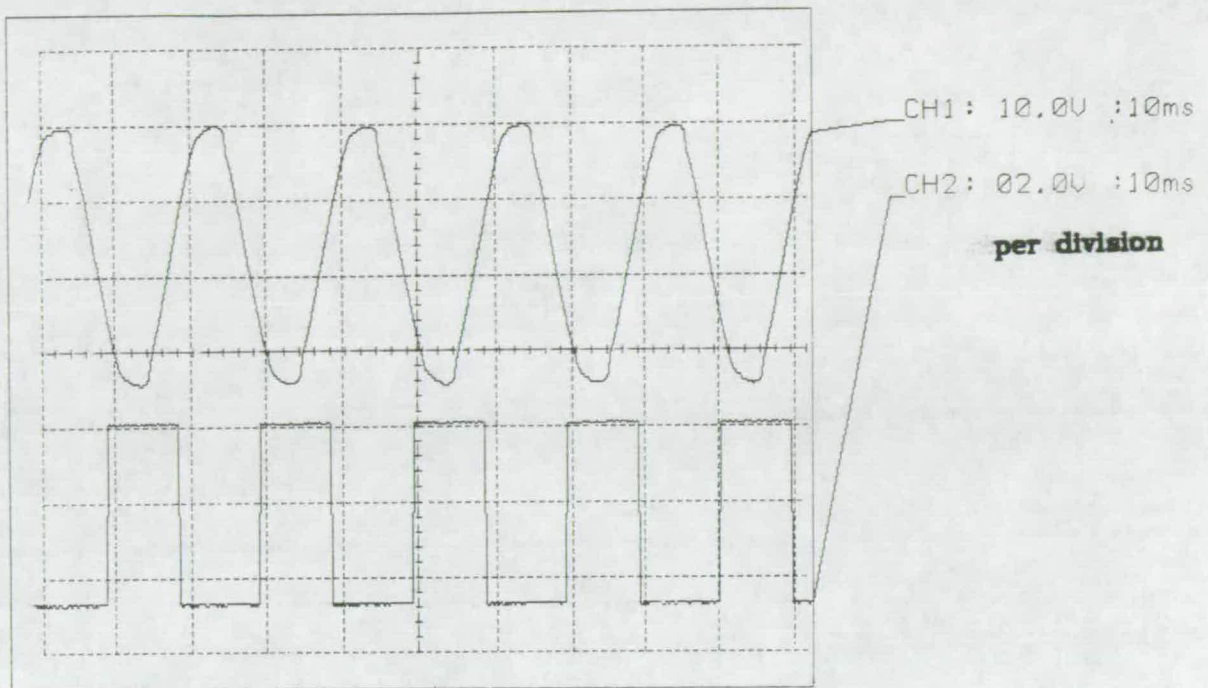


Figure 20b - Schmitt Trigger output in relation to a.c. waveform

#### 3.3.4. Analogue Input Circuit

When a ballast load change is necessary, the ELG decides to add or subtract load, to or from, the phase with the lowest or highest current respectively. To achieve this, the relative value of the current in each phase is obtained, rather than the absolute level of current.

With future developments in mind, particularly the introduction of electrical protection, there remains the possibility that absolute current magnitudes will be required at a later date. In addition, knowledge of the *voltage* magnitude may be required, hence the initial provision is for four analogue inputs.

Two conversions are necessary to alter the a.c. current waveform into a digital value. Firstly the a.c. waveform provided by the output of a current transformer is rectified and smoothed to provide a d.c. signal, the level of which will vary with the magnitude of the current. This is the *analogue* signal and the circuit is shown in figure 21.

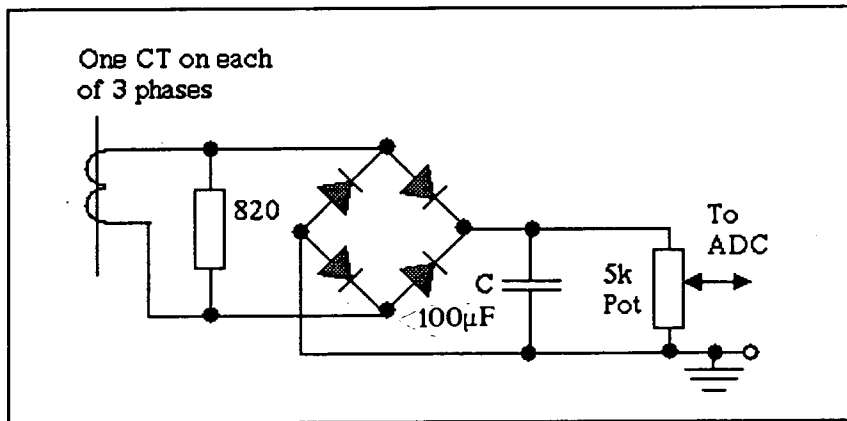


Figure 21 - Current measurement circuit

The CT output is in the range of 0 - 25 mA and is shunted with a resistor to provide a significant a.c. voltage for rectification. The full wave rectifier output is smoothed to attenuate the 100 Hz ripple which it possesses. As the change in the phase current is 14% when a ballast load unit is switched, then smoothing to a ripple of less than 5% is adequate. The need to avoid building in large electrical time constants which would 'slug' the response to current changes was considered, although no problems were experienced in this respect. The ripple measured in practice was 1.6%. The smoothed signal is fed to a potential divider to allow calibration of the analogue level.

Secondly, the analogue signal requires to be converted to an 8-bit digital number which varies in accordance with the d.c. level. This task is performed by an analogue to digital converter ( ADC ) and to avoid

excessive duplication of components, multiplexing of the analogue signals is necessary. The specification for the ADC circuit was prepared and included the following items;

- a single power supply level to maintain the simplicity of the power supply circuit.
- minimal peripheral components to interface to the microprocessor.
- a minimum overall pin count.
- a minimum number of dedicated I/O on the microprocessor.
- readily programmable via the microprocessor.

A study of the available ADC's revealed that a number of suitable devices met the specification, all of which included on-chip multiplexers. The device which *best* satisfied the requirements is the ADC0844 which, when used in conjunction with the SN74LS245 Octal buffer IC, has a single +5V power/reference supply, a total pin count of 40, required only 11 I/O lines of the microprocessor and is designed for microprocessor applications. Port F is used for the data and address lines and 3 lines of Port G are used for the ADC control. A diagram of the circuit is given in figure 22.

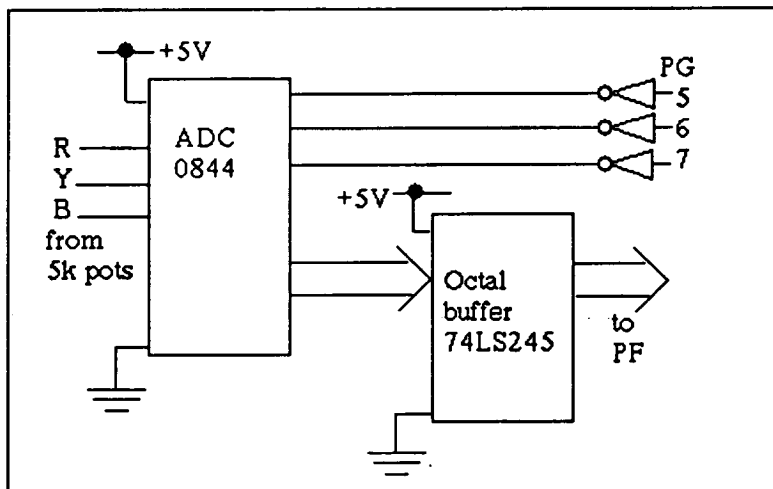


Figure 22 - Analogue-to-Digital conversion circuit - block diagram

### 3.3.5. Power Supply Circuit

During the initial development stage, the power supplies to the electronic circuits were obtained from standard laboratory stabilised Power Supply units. This facility would not be available in a target application, so a power supply circuit was designed which sourced its energy from the generator terminals. This implies that there will be no power available until the turbine-generator set has voltage on its terminals. Depending on the excitation system of the generator, the terminal voltage may build up gradually from zero to rated voltage, or it may appear as a step change on the closure of a field contactor. In addition, there may be occasions when the set is running at overspeed and the terminal voltage is higher than the rated value.

The design of the power supply has to cater for all of these conditions without incurring unsafe operation of the electronic circuits. As a result of the design philosophy aimed at maintaining the simplicity of the power supply, only a single voltage level is required, +5V d.c. relative to 0V. The current demand was measured and indicated a minimum rating of 600mA. The design is based on the 7805, 5V, 1A, fixed voltage linear regulator<sup>41</sup> which accepts a variable input voltage range of 7 - 25 V. This is supplied from a step down transformer with a voltage ratio of 240:12 V and permits operation over a voltage range of 140 - 500 V on the transformer primary.

In order to prevent the electronic circuits receiving any power before a firm 5V d.c. level is available, a thyristor is added in series with the supply, triggered by a zener diode when the regulator input reaches 10V.

---



Hence the power supply energises when the transformer primary voltage exceeds 200V. The complete power supply circuit is as shown in figure 23.

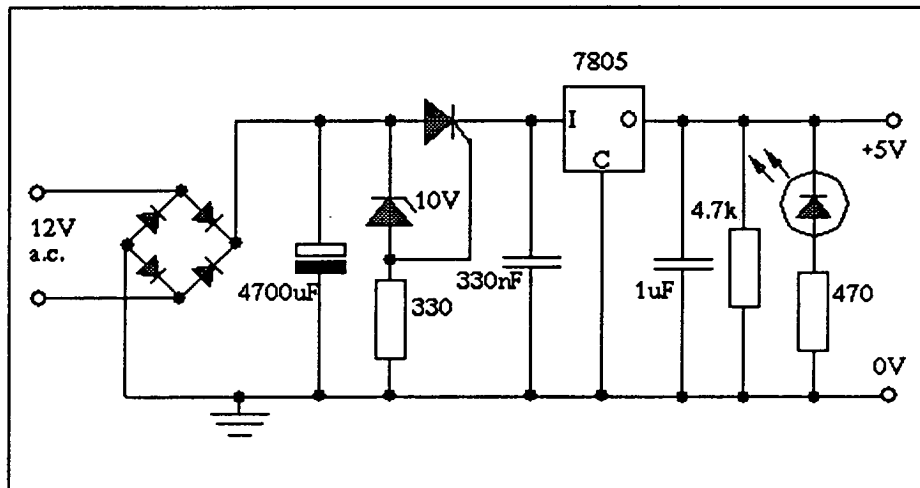


Figure 23 - Power supply circuit

### 3.4. PRINTED CIRCUIT BOARD

Initially the circuits described in Section 3.3. were built on standard Veroboard, which was adequate for the circuit development and general experimentation. Once laboratory testing of the unit had demonstrated satisfactory operation of the circuits, the design of the I/O interface board was committed to a custom built printed circuit board ( PCB ). The design of the component and track layout of the PCB was performed by others, which not only required the circuit diagram and the component list, but also a specification of the layout requirements.

The application of the PCB based hardware is initially limited to further laboratory testing and future development of the ELG. A decision was thus taken not to design the PCB for its *final* on-site application, since this will involve modularisation and ruggedisation. However, the PCB

that resulted is not only suitable for laboratory use but is also suitable for use on hydro sites with a benign environment to locate the ELG.

The ADC circuit described in Section 3.3.4. is necessary for all 3 phase systems. When the unit is applied to a single phase system, the ADC circuits are redundant. Nevertheless, it was decided to design a single PCB, based on the 3 phase application, rather than design two separate PCB's. The same board can be used for either system and in this way the production costs can be minimised.

The ELG hardware essentially comprises three modules, a step down transformer, the Microcard and the I/O PCB. The mounting of these in an enclosure necessitates that various input and output signals pass through the walls of the enclosure. The power system components, such as the CT's and solid state relays, are mounted in separate enclosures. The I/O PCB therefore interfaces to the other modules within the enclosure **and** to the enclosure walls.

Included in the PCB specification are such facets as;

- spare capacity and tracks for future circuit additions.
  - provision of test points for circuit measurements and supervision.
  - access to the card for commissioning of the ELG, but not at other times.
  - provision of intercard connections, their type and position.
  - mounting of components for through-enclosure access, eg LED's and connectors.
  - the relative positions of the modules in the enclosure.
-

Two complete ELG units were assembled for performance testing in the laboratories. Photographs of the I/O PCB and the complete ELG in its enclosure are given in figures 24 and 25 respectively. The layout of the PCB is given in Appendix 1 along with the full circuit diagram.

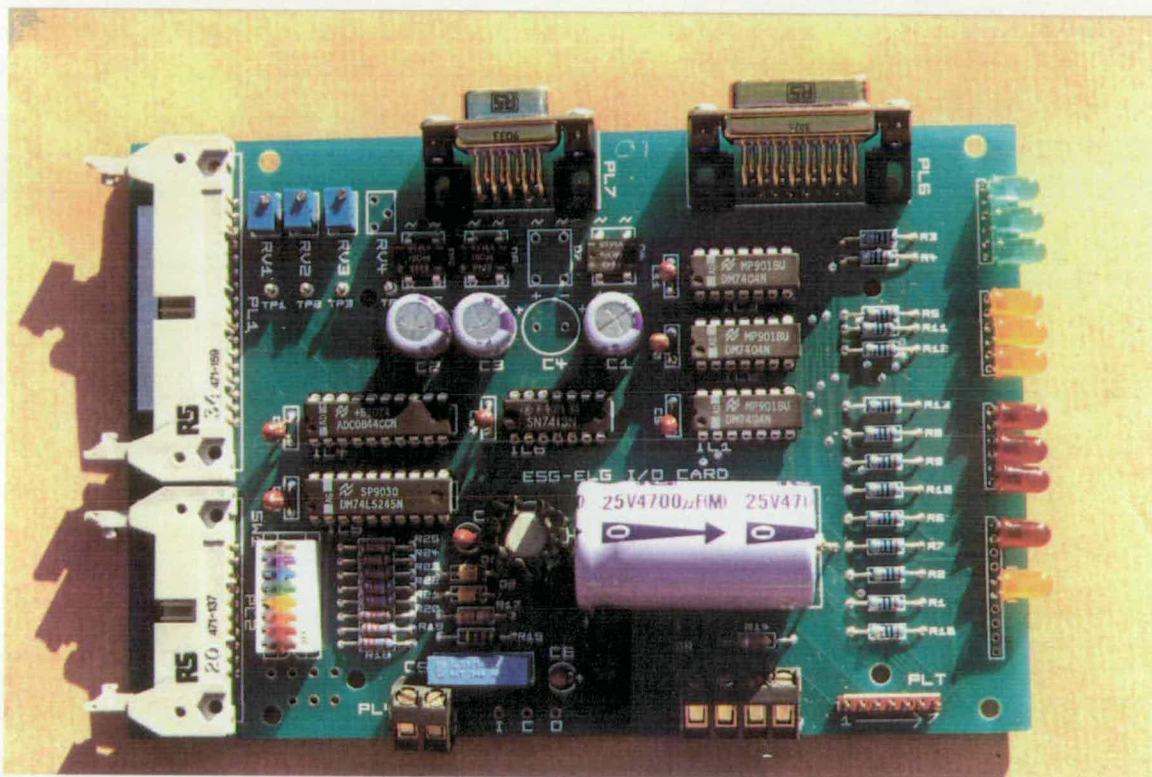


Figure 24 - The I/O printed circuit board

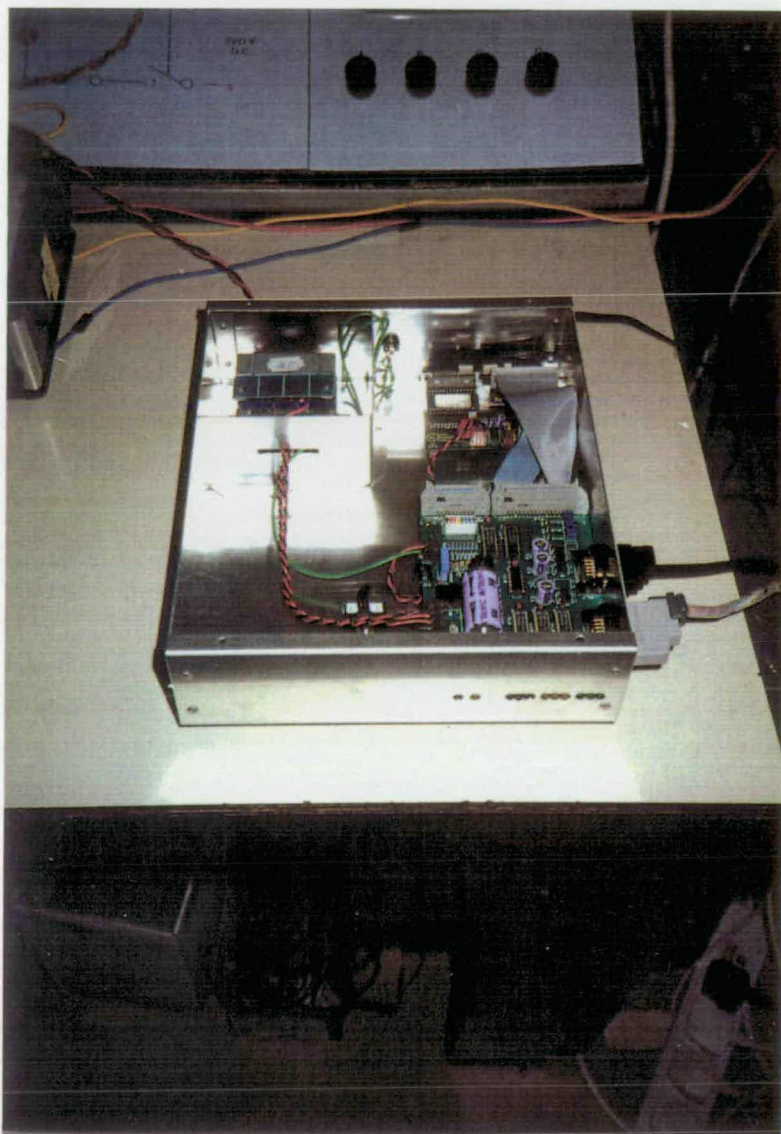


Figure 25 - The ELG in its enclosure

---

---

## CHAPTER 4 PROGRAM DEVELOPMENT

### 4.1. THE SOFTWARE DEVELOPMENT SYSTEM

#### 4.1.1. Computer System

A block diagram of the computer system used for the program development is shown in figure 26. The host computer is a BBC Model B Microcomputer complete with a disc drive, a monitor and a printer. Communication with the FORTH Microcard is via a serial communication line operating at 1200 baud and connected to the RS423 socket of the BBC machine. A software package, FORTHWRITER, was obtained for use on the BBC, enabling it to become a development system for the Microcard. The FORTHWRITER package is menu driven and includes facilities to download FORTH source code to the Microcard from a disc file, and to edit the source files with commercially available wordprocessor systems. This package is described in detail in the Technical Manual<sup>42</sup>.

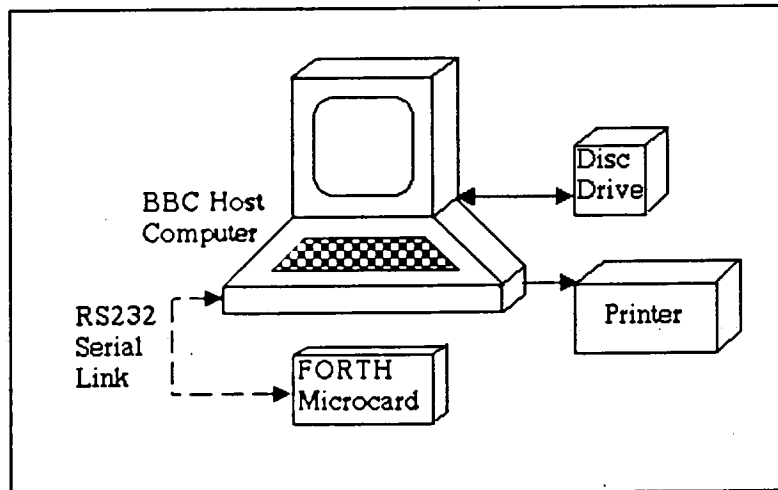


Figure 26 - A block diagram of the computer system

---

#### 4.1.2. Operating Modes

For the ELG program development, the FORTHWRITER facilities most commonly used are the following;

i). **Terminal Emulator.** This allows direct communication between the BBC keyboard and the microprocessor. FORTH code can be entered "live" and the instruction executed immediately. This enables software testing without the need to store and download a program. No permanent record of the entered code is available and this facility, whilst very useful, is limited in application to short sections of code.

ii). **Downloading Source Code.** Larger sections of code, building up into complete programs, require permanent storage on disc. These programs are downloaded into the microprocessor on demand.

iii). **Programme Editor.** The production and the editing of the FORTH source code is performed using the VIEW wordprocessing facility contained within the BBC computer.

#### 4.2. THE FORTH LANGUAGE

FORTH is a high-level language which is extensible, meaning that a user's own operations, called *words*, can be added to the original language. New words are defined in terms of those previously defined, until a single word represents the complete program.

---

The FORTH words are modular, permitting testing of each word as it is developed and limiting de-bugging to that one word at any one time. Once successfully tested, the word then forms the basis of another operation. FORTH uses a *stack* system where data is constantly added to, manipulated round or taken from the stack. A full assembler, based on R6502 code, is included for assembly language programming.

Typical operations which the standard FORTH words perform are; arithmetic ( + .. - ), stack manipulation ( DUP .. SWAP ), memory read/write ( @ .. ! ), logic functions ( AND .. OR ), loops, control structures ( IF .. THEN ), and input/output through the five microprocessor Ports and from/to the keyboard/monitor of the host computer. FORTH also provides software control of the ten interrupts and of the counter/timer advanced microprocessor operations.

A description of the FORTH language is given in the RSC-FORTH User Manual<sup>43</sup> and various text books as listed in the Bibliography.

### 4.3. THE LOAD GOVERNING PROGRAM

During the development of the load governing program, the FORTH source code was stored on disc and downloaded on each separate occasion that it was used. The instruction to start the program was issued via the Terminal Emulator by keying in the final word of the program. In the target situation, the microcomputer stands alone, the host computer and serial link are removed and the program is stored in EPROM. Hence an autostart instruction is added to the program for target mode operation.

---

Following power-up of the Microcard, the R65F12 executes a number of its own initialisation procedures which are independent of the target application. Once these are complete, it examines the external memory space at every 1K boundary for the autostart pattern, ASSA Hex. This pattern indicates the start address of the final FORTH word and the microprocessor begins to execute the instructions stored in the memory.

#### 4.3.1. Main Program

A simplified flowchart of the main load governing program is shown in figure 27. The program begins by performing application specific initialisation procedures. On completion of these, the program enters a continuous loop which reads the deadband setting, compares the frequency against various limits (including the deadband), and changes the ballast load if necessary. At the end of this sequence, one of the output lines is toggled ( 1 to 0 or vice versa ) in order to indicate the completion of the loop and this can be used to measure the duration of

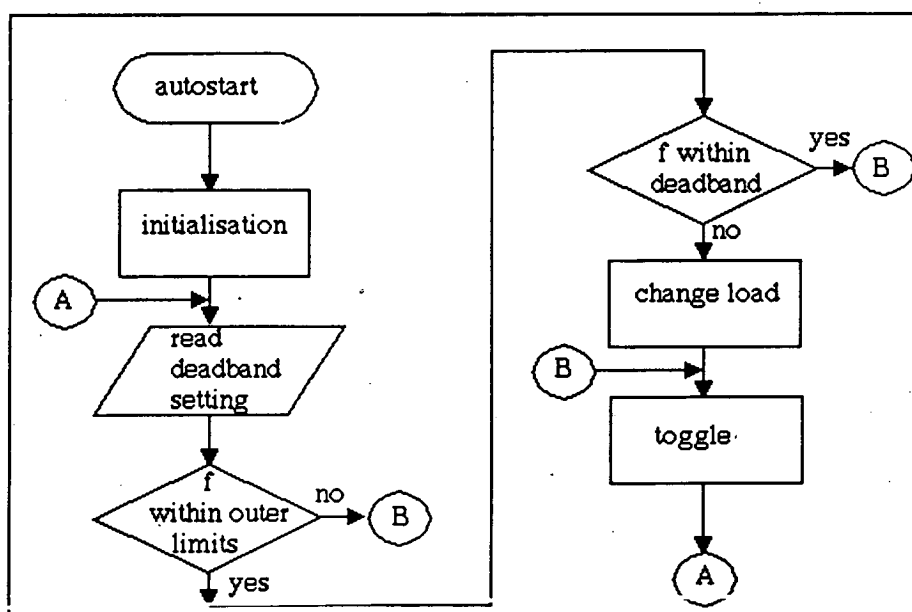


Figure 27 - Flowchart of the main load governing program



the *program cycle*. The sequence then repeats itself indefinitely until the power supply to the Microcard is removed. Detail of the operation of the three phase program is given in Section 4.3.3.

The duration of the three phase program cycle is approximately 4 ms when no ballast load change is required and is approximately 18 ms when ballast load is changed. There are slight variations on these times for program related reasons.

#### 4.3.2. Frequency Detection

The task of the frequency detection is not handled by the main program; instead, it takes the form of an interrupt routine. The initialisation procedure of the main program includes the configuration of Upper Counter B as a timer. On the detection of a negative going edge on PA2 ( refer Section 3.3.3. ) the interrupt vector diverts the microprocessor to execute a series of instructions which are programmed in assembly language. This interrupt service routine simply reads the current value of Upper Counter B, stores it in a RAM memory location for use by the main program and then resets and restarts the timer.

---

The FORTH and assembler code for the interrupt service routine is as follows;

```
CODE SERV
PHA, TYA, PHA,
1D LDA, 200 STA, 11 LDA, 202 STA, FF * LDA, 1E STA,
FB * LDA 10 AND, 10 STA,
PLA, TAY, PLA, RTI,
END-CODE
```

### *Period Timing*

An explanation of the operation of Counter B is necessary as it has a significant bearing on the step size of the frequency deadband. Counter B of the R65F12 is a 16 bit counter, organised as Lower Counter B (LCB) and Upper Counter B (UCB). The counter can be initialised at any value, up to FFFF Hex, and counts down from that value at a rate determined by the microcomputer clock. The clock on the card runs at 2 MHz thus the period of each clock cycle is 0.5  $\mu$ s.

To read the full 16 bit value of the timer, the two components, UCB and LCB have to be read separately whilst the timer continues to run. This operation takes a small but finite number of microprocessor instructions, and hence time - even at assembly language speed. During initial trials, the situation arose where the value of UCB changed from one level to the next before LCB was read, giving significantly spurious measurements for the time period between successive negative going edges.

---

A typical count sequence was ( in Hex );

<u>UCB</u>	<u>LCB</u>	
64	04	
64	03	
<b>64</b>	02	UCB read on this clock cycle.
64	01	
64	00	
63	<b>FF</b>	LCB read on this clock cycle.
63	FE	
63	FD	
63	FC	

Typically the microprocessor requires 3 clock cycles to perform the reading of LCB after it has read UCB, hence the normal error in the reading would be 1.5  $\mu$ s. However, when this occurs at the transition of UCB from 64 to 63, as shown above, then a typical reading would be 64FF, increasing the error by 126.5  $\mu$ s. Unfortunately, this particular transition occurred at a period of 19.96 ms, ie a frequency of 50.08 Hz, and a solution to this problem was necessary to avoid measurement errors of approximately 0.3 Hz.

It was noted that the time period relating to one cycle of LCB counts, ie FF to 00 Hex ( 256 decimal ), was 0.128 ms which equates to a frequency deviation of 0.318 Hz at 50 Hz operation. Due to the inverse relationship between frequency and time, the degree of frequency deviation is not linear, for example the LCB cycle time of 0.128 ms equates to 0.354 Hz for a 19 ms cycle and 0.292 Hz for a 21 ms cycle.

---

### ***Deadband Size Selection***

By simply reading the value of UCB alone, a measure of the frequency within a band of approximately 0.32 Hz results. This value satisfies the aim of Section 2.1.2.1. for the size of the deadband required, 8 steps of  $\pm 0.32$  Hz giving a total maximum deadband variation of  $\pm 2.56$  Hz from 50 Hz.

A deadband of greater than  $\pm 2.56$  Hz could be achieved through an increase in the number of input lines arranged at the microswitch (refer 3.3.1 ), however, unless this later proves necessary for stability reasons, a limit of  $\pm 2.56$  Hz on the frequency variation in steady-state operation is presently considered satisfactory. Table 4 shows the approximate frequency deadbands corresponding to the microswitch selections.

---

---

<u>Deadband</u>	<u>Switch Settings</u>	<u>Approximate Frequency</u>
<u>Number</u>	<u>PB 2 1 0</u>	<u>Variation from 50 Hz</u>
1	0 0 0	+ - 0.32
2	0 0 1	+ - 0.64
3	0 1 0	+ - 0.96
4	0 1 1	+ - 1.28
5	1 0 0	+ - 1.60
6	1 0 1	+ - 1.92
7	1 1 0	+ - 2.24
8	1 1 1	+ - 2.56

**Table 4 - Deadband Settings**

For 60 Hz operation, the deadband step size would be 0.46 Hz resulting in a maximum width of + - 3.68 Hz.

#### **4.3.3 Main Programme Description**

##### ***Initialisation***

The first action of the initialisation section of the program is to store the hex address of the interrupt service routine in the appropriate vector address ( 40 ). On power-up of the Microcard, the output Ports PE and PG have a status of 1, therefore the next action of the program is to put all of the lines in these two Ports to 0. Then the variables are initialised to pre-determined values to ensure that the program starts in a controlled manner. In addition, a *table of deadband limit* values for comparison with UCB readings is stored into a portion of the

---

memory. Counter B is given its initial values and then the interrupt facility is enabled. Finally a delay of 20 ms is added to allow a period of settlement before the continuous loop begins. A flowchart of this is shown in figure 28 and the FORTH code is as follows;

```

: RUN
  081C 40 !
  ZERO INITIALISE SETCB ENABLE WAIT20
  BEGIN SEQU AGAIN ;

```

This word is the product of 6 previously defined words, namely

```

: ZERO
  0 PE C! 0 PG C! ;

```

```

: INITIALISE  which for example contains
  0 RED !      which sets the initial value of the variable RED, and
  6364 220 !  which stores a value in address 220 for deadband
               comparison.

```

```

: SETCB      which selects and initialises counter B.
  E0 MCR C! FF 1C C! FF 1D C! ;

```

```

: ENABLE     which enables counter B.
  4 IER C! ;

```

```

: WAIT20     which is a delay loop of 20 ms.
  140 0 DO LOOP ;

```

and, : SEQU which is the continuous program sequence.

DBCW COMPFP TOG ;

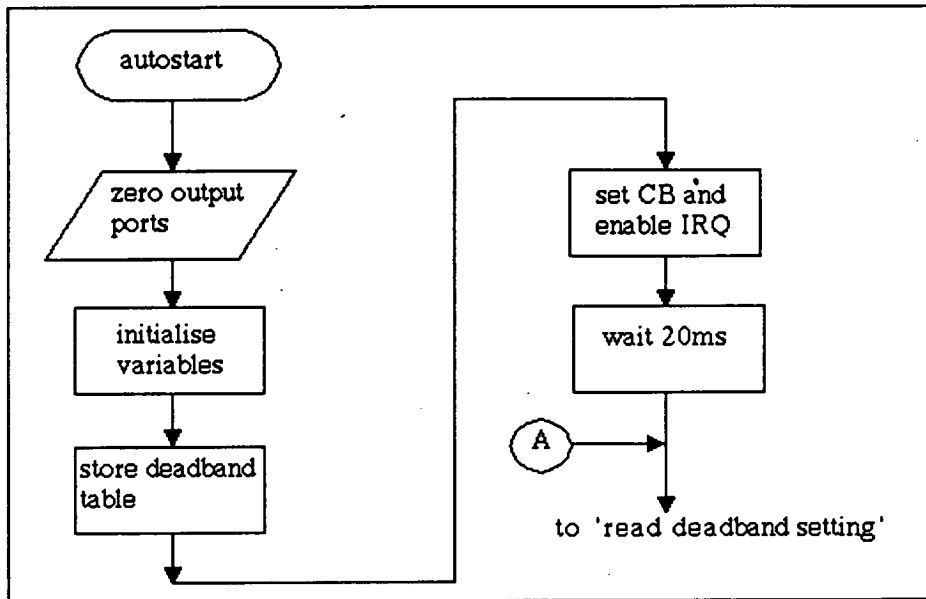


Figure 28 - Flowchart of the initialisation routine

### *Deadband Setting*

During operation of the ELG the deadband selection will not normally be altered and even during commissioning it may be altered only occasionally. Hence, it is not necessary to monitor continuously the deadband selection on the microswitches. The program therefore reads the deadband selection switches once every 256 program cycles. This corresponds to approximately 1 second when the ELG is not changing load.

The hex value of the deadband selection switches is used in conjunction with the table of limits to assign values to *deadband limit variables* for later use by the frequency comparison section of the program. The appropriate section of the FORTH code is;

```

: DBCW
DBC @
FF = IF READFDB 0 DBC ! THEN
DBC @ 1 + DBC ! :

```

which performs the following word only when DBC = FF hex;

```

: READFDB
PB C@ 7 AND
2 * FDBTAB + DUP
C@ FMUPLIM !
1 + C@ FMLOLIM ! :

```

### ***Frequency Comparison***

The measured a.c. cycle period ( and hence the frequency ) most recently stored in memory by the interrupt service routine is compared with up to three sets of limits. The first level of comparison is with wide margins of 40 Hz and 65 Hz. If the frequency is outside these limits then the program takes no action and jumps to the *toggle* section of the program. The reason for this is twofold.

Firstly, an instantaneous change of frequency from 50 Hz is not possible and any such readings under normal operation are treated as spurious. Secondly, whilst at present no action is taken, this comparison could form the basis of a frequency protection routine at a later stage of the ELC's development. Hence the provision for this has been built in to the initial ELG program. The code is as follows;

---



```

: COMPFP
200 C@ DUP
FPLOLIM <
IF 0 ELSE 1 THEN SWAP
FPUPLIM >
IF 0 ELSE 1 THEN AND
IF COMPFM THEN ;

```

The second level of frequency comparison was introduced to counteract a problem which arose at low frequency operation, during initial trials of the unit. On shutdown, for example, as the frequency dropped, so the a.c. cycle period rose until eventually Counter B reached 0000, reset itself and began counting down once more. When the count reached similar values to those relating to 50 Hz then the ELG would begin to function as if controlling to 50 Hz when in fact the frequency was well below 20 Hz.

To avoid this problem, a lower limit of 30 Hz is added to prevent the program completing its normal cycle. In the event that the frequency is below this level, the program diverts to the toggle section via a wait delay. In this way, the load governing action of the program is inhibited below 30 Hz, ie during run-up and shutdown of the generating unit. This is achieved with the following section of the FORTH code.

```

: COMPFM
LOOK NOT
IF CHLOAD ELSE WAIT 1 THEN ;

```

---

which uses the previously defined word, LOOK, to check for very low frequency.

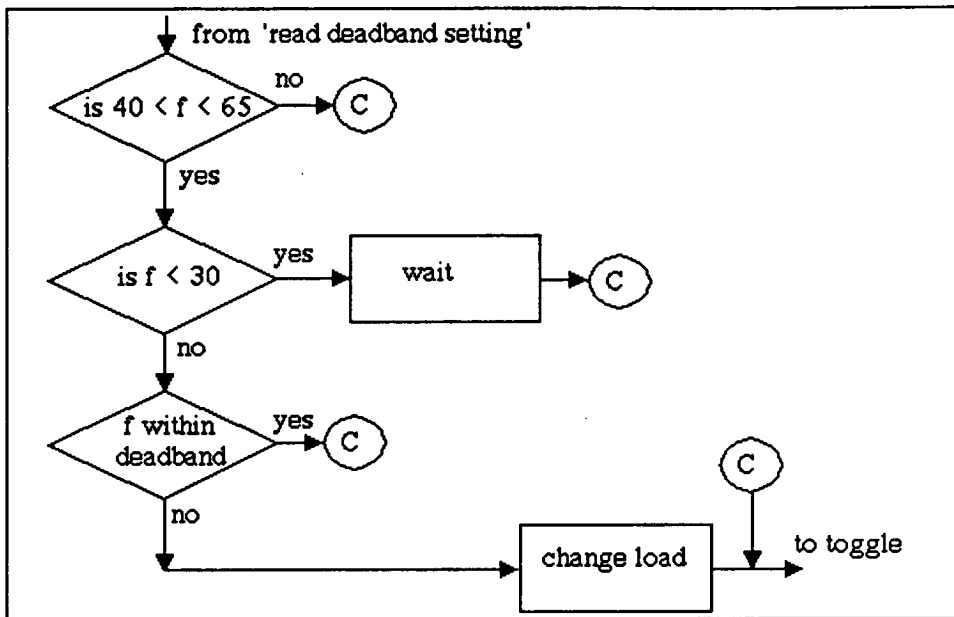


Figure 29 - Flowchart of the frequency comparison routine

The program then proceeds to the final comparison level; the measured frequency compared with the deadband setting. This routine decides if the frequency is below the lower deadband limit or above the upper deadband limit, or if the frequency is within the deadband; in the latter case no action is taken and the program proceeds to the toggle section. The flowchart of the frequency comparisons is given in figure 29 and the FORTH code for the final comparison level is;

```

: CHLOAD
  200 C@ FMLOLIM @ <
  IF DECLOAD ELSE 200 C@ FMUPLIM @ >
  IF INCLOAD THEN
  THEN ;

```

### Change Load

At this point, assuming that the frequency is outwith the deadband, the program follows one of two parallel paths. Either it increases the ballast load due to a high frequency measurement or it decreases the load due to a low frequency measurement. The sequence performed to increase the ballast load is now described and is as shown in figure 30.

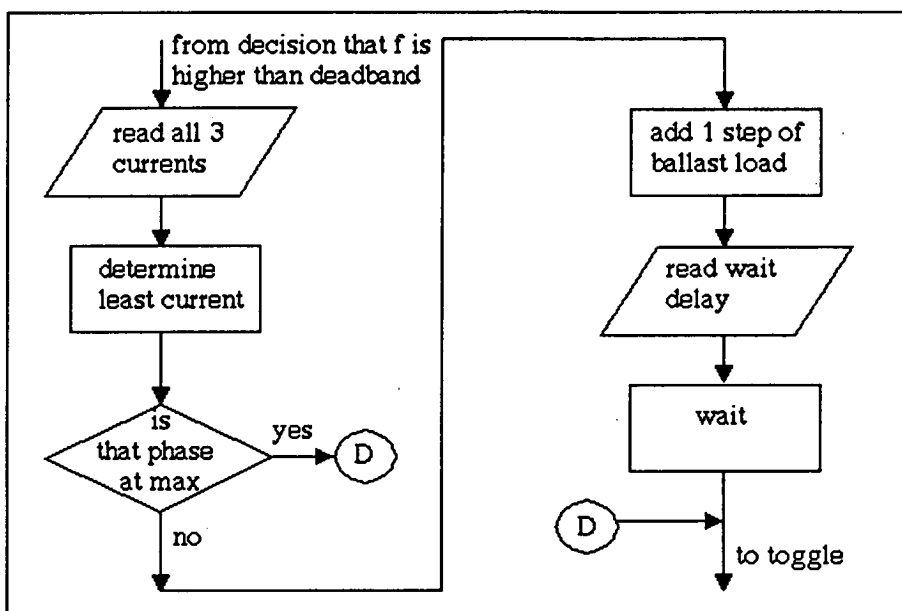


Figure 30 - Flowchart for increasing the ballast load

The object of this routine is to determine which of the three phases has the *least* load on it at this instant and to add a single step of ballast load to that phase. Given that a decision has been made to change the load, it is at this point that knowledge of the relative levels of the three currents is necessary. Hence, the first action of this section of the program is to activate the ADC circuitry ( refer Section 3.3.4. ) to read the red, yellow and blue phase currents and the values obtained are stored as variables, as shown in the following code;

: READI

READIR READIY READIB ;

as the words called by READI perform the same function for the 3 currents, only READIR is now given as an example;

: READIR

4 PF C!

ADCGO

PF C<sub>e</sub> RCUR !

0 OR PG! ;

which selects the multiplex channel and performs an operation of the ADC using ADCGO as follows;

: ADCGO

PG<sub>e</sub> DUP DUP DUP DUP DUP

40 OR PG! C0 OR PG! 40 OR PG! 0 OR PG!

1 0 DO LOOP

60 OR PG! ;

The program executes a comparison routine to identify the phase with the lowest current and then adds one step of load to that phase, if possible. If the ballast load in that phase has already reached its maximum value then no further ballast load can be added. In any event, the final action of this routine is to introduce the wait delay ( refer Section 2.1.2 ) into the sequence. The FORTH code of this routine is as follows;

```

: INCLOAD
READI
RCUR @ YCUR @
< IF RCUR @ LEAST ! ELSE YCUR @ LEAST ! THEN
LEAST @ BCUR @
< IF ELSE BCUR @ LEAST ! THEN
RCUR @ LEAST @ =
IF INCR ELSE BCUR @ LEAST @ =
IF INCB ELSE YCUR @ LEAST @ =
IF INCY THEN
THEN THEN WAIT ;

```

If, say, this routine decides that the red phase current is the least, then it will execute the INCR word to increase the ballast load in the red phase by 1 step.

```

: INCR
RED @ INCTEST RED!
BITSH3L YELLOW @ +
PE C! ;

```

The duration of the wait delay is variable in multiples of 4 ms. Selection via the microswitches permits delays of 0, 4, 8 or 12 ms to be implemented at this point, as shown in the code below, in order to allow the power system to settle. As is the case for the deadband selection, it is intended that the wait delay is adjusted only during the commissioning of the unit.

: WAIT

READWD WD @

1 < NOT IF WD @ WAITVAR THEN ;

which in turn depends on other previously defined words.

### *Toggle*

Initially this feature, which switches one of the output lines on/off at the end of each program cycle, was added to assist monitor the performance of the program during its development. As an LED is connected to this line, a visual indication of the status of the program is available, although the rate of switching of the LED is normally faster than can be detected by the eye. More importantly, with the use of an oscilloscope, accurate timing of the length of the program cycle is possible. It was considered that this feature would continue to be of use in target applications of the ELG and, as it uses up only a very short amount of code, it remains an integral part of the program.

### *General*

The operation of the program as performed by each loop of the continuous sequence can be summarised as follows ( assuming that the power system frequency is within the region of 50 Hz );

- If the period value most recently stored in memory by the interrupt routine corresponds to a frequency which is within the deadband currently selected, then no action is taken.
-

- If the corresponding frequency is outwith the deadband (and within the outer limits) then a single step of ballast load is added to (or subtracted from) the phase with the least (or most) current at that instant.
  
- A wait delay of pre-selected variable length is performed.

The complete FORTH program, filename LG9, is given in Appendix 2, along with separate listings of the standard RSC-FORTH words and the *user* defined words occurring in this program.

### ***The Single Phase Program***

The single phase version of the load governing program essentially follows the same principles of operation. However it differs from the three phase version in two main areas.

- i) the ballast load is arranged in a binary sequence of 4 sections, rather than 3 sections. This gives a resolution of 1/15th for each ballast load step.
  
- ii) there is no requirement for phase balancing. This considerably simplifies and reduces the length of the program as the code concerned with the control of the ADC, the current comparison and phase selection is removed.

As a result. the output port lines used for the ballast load switching and the toggle function are different to that of the three phase version.

---

In addition, the program cycle timings are shorter, 3.5 ms when no load change is performed and 7.5 ms when the ballast load is changed.

#### 4.4. EPROM PREPARATION

On completion of successful trials of the load governing program, the code was transferred onto an EPROM to allow operation of the Microcard in the target mode. Using the FORTHWRITER package on the BBC microcomputer, the *source code* ( FORTH) was downloaded from disc into the memory on the Microcard. Then the *autostart* pattern ASSA was added and the completed *object code* was uploaded from the Microcard into a new file on the disc. This object code file was then transferred to a proprietary EPROM programmer for downloading to the appropriate IC.

Some problems were experienced in the preparation of the EPROMs, namely;

- The new memory map necessary for the target mode of operation required that the starting address of the program be relocated in the memory.
  - The location of the interrupt vector address required to be specified within the program, whereas previously it had been interpreted on downloading directly from the storage disc.
  - Certain FORTH words were unsuitable for useage in the target situation, so alternatives were required.
-



These problems were all identified and solutions found such that target mode operation with the program stored in EPROM was fully successful.

---

## CHAPTER 5 TEST EQUIPMENT

In the course of the development of the ELG tests were performed ranging from simple visual indication of LED's to functional testing of the ELG on water turbine driven generator sets. This Chapter provides the details and characteristics of the major equipment used to perform the tests. The results of the tests are given and discussed in Chapters 6 and 7.

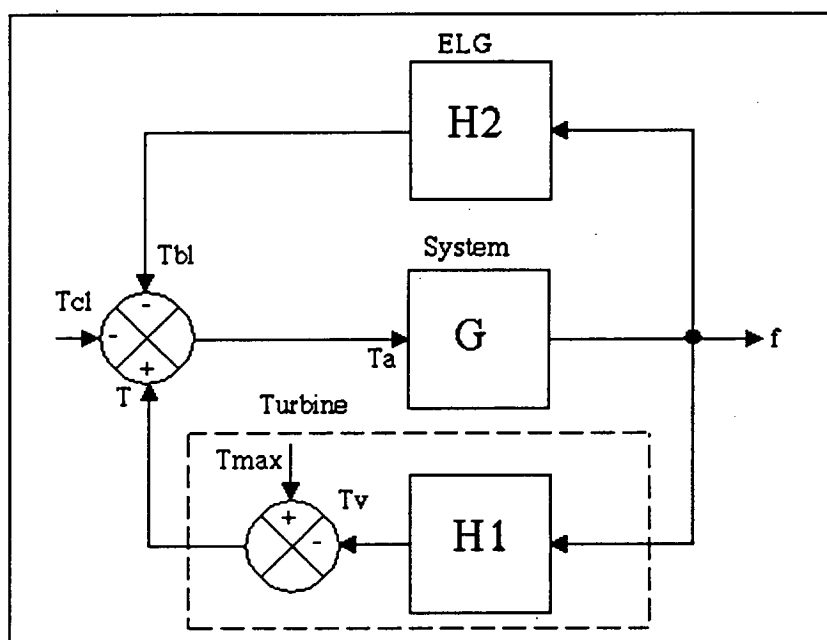


Figure 31 - Control system block diagram \*

The ELG is part of a closed loop system as shown in figure 31. The *input* to the **ELG** is frequency and its *output* is an action on the ballast load connected to the power system, which in turn alters the system frequency. The initial functional testing of the frequency measurement circuit ( refer Section 3.3.3 ) was performed using a signal generator to simulate the a.c. waveform, however, as this was an open loop system, such simulation was very limited in use.

\* Note. The detail of figure 31 is given in Section 7.3.

True closed loop functional testing of the ELG on an isolated 3 phase generator with suitable electrical loads was performed. For the majority of the development phase, this took place on a three phase a.c. generator, driven by a d.c. motor in the Rotating Machines Laboratory at the Craiglockhart Site of Napier University. The details of this test set are given in Section 5.2.

Whilst this permitted convenient functional testing, the torque-speed characteristics of the d.c. motor were not those of a water turbine and so additional functional and performance tests were carried out on two different Pelton turbines and a Francis turbine in the Hydraulics Laboratory at the Merchiston Site of Napier University. This afforded the unique opportunity to assess the performance of the ELG against water turbine torque-speed characteristics, but within a laboratory environment. Details of the turbine-generators are given in Section 5.3.

### 5.1. PERIPHERAL EQUIPMENT

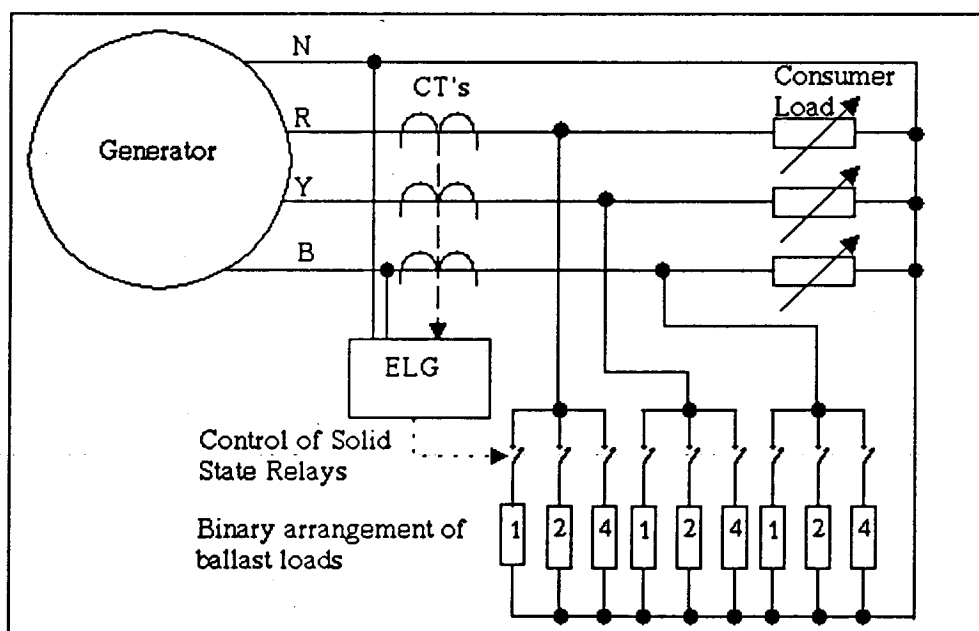


Figure 32 - Schematic diagram for three phase load governing

The electrical system configuration for 3 phase operation is as shown in figure 32. Apart from the generator and the ELG unit, the additional equipment required to complete the system is as described below.

#### **5.1.1. Consumer Load**

The consumer load comprises a Jay-Jay Instruments three phase Loading Resistor<sup>44</sup>. Each phase is capable of carrying 15 A to provide a total load in excess of 10 kW, at a power factor close to unity. The load in each phase of the Loading Resistor can be separately switched through a series of steps and there is a single contactor which can be used to switch all three phases simultaneously. The Loading Resistor is air cooled with fan assistance.

#### **5.1.2. Solid State Relays**

The solid state relays are the main interface between the ELG and the power system. It is the control of these relays, performed by the digital electronic circuits, which adjusts the ballast load on the electrical system in order to maintain the frequency within the selected deadband. It is at this point that the hardware associated with ELG system becomes application specific. The rating, and hence the cost and physical size of these relays, is dependant on the sustained current rating that they will experience in service.

The 3 phase version of the ELG has three ballast-load steps per phase which results in a total of 9 relays ( and heatsinks if necessary ). The maximum steady-state current which any one relay experiences is 0.571

---

p.u. of the line current. The other relays carry 0.286 p.u. and 0.143 p.u. of the line current. For each of the test generators installed in the laboratories, the maximum rated relay current is less than 5A.

The relays selected are 5A flatpack SP type of a sealed construction from RS Components. The 5V d.c. input is optically isolated from the zero voltage switching circuit which, RS claim, produces virtually no radio frequency interference. At this rating, the relays do not require separate heatsinks other than the aluminium trays onto which they are mounted.

### 5.1.3. Ballast Load

The selection of the ballast load circuit is also application specific. The design depends on the system voltage, the maximum output power of the generator and the number of steps per phase. Ideally the total rating of the ballast load will be slightly greater than or equal to the output of the generator with the load in each phase sectioned into the ratio 1 : 2 : 4.

For the d.c. motor driven generator a custom designed ballast loading unit was built. This ballast load consists of 21 individual resistors each rated at 140 V, 120 W, 164  $\Omega$  ( +- 1% ). In each phase, the sections are arranged as follows;

<u>Load Section</u>		<u>Z(<math>\Omega</math>)</u>	<u>Y(mS)</u>
1	1 resistor	164	6.1
2	2 resistors in parallel	82	12.2
4	4 resistors in parallel	41	24.4

The ballast load resistors are housed within an aluminium enclosure and fan assisted air cooling is provided, the supply to the fans being drawn from the generator terminals.

For the turbine driven, three phase generator, the resistive load is provided by an arrangement of fan-cooled, '0.5kW' and '1.0kW' wire-wound, electric-fire, elements as follows;

<u>Load Section</u>		<u>Z(<math>\Omega</math>)</u>	<u>Y(mS)</u>
1	2 - '0.5kW' elements in series	193	5.18
2	1 - '0.5kW' element	101	9.90
4	1 - '1.0kW' element	58	17.24

For the single phase generator, the ballast load has 4 sections provided by combinations of light bulbs providing 40W, 80W, 160W and 320W based on 240 V.

In practice, the availability of suitable loads in precise steps may not be possible, or at least economical, and the next best compromise will have to suffice. From an energy conservation viewpoint, it would be better that the energy dissipated from the ballast load be used to some secondary purpose rather than be lost into the atmosphere. Given that, as an energy (heat) source, the ballast load will be unreliable, in the respect that its output may vary substantially in magnitude, it is difficult to identify industrial use for the ballast energy. Initial useage of such energy has been limited to water heating and crop drying<sup>13</sup> and more recently high-efficiency, low power cookers have been developed<sup>45</sup>.

It would not be economically viable for the ballast load equipment to be customised to suit every individual micro hydro installation. Hence, the use of proprietary loads will result in variations in the performance of the ELG. If necessary, the ballast load steps could all have the same rating<sup>35</sup>, with a reduction in the frequency accuracy as a consequence; Section 6.4 describes a brief trial of such operation. The ballast load should be connected as close to the generator terminals as possible to avoid accidental open-circuits preventing its application on loss of the consumer load<sup>38</sup>.

#### 5.1.4. Current Transformers

The current transformers ( CT's ) are necessary to produce a scaled down current signal which is proportional to the line current for supply to the ADC circuitry at a suitably low current and voltage level. The primary winding is in series with the power circuit, its impedance being negligible compared with that of the power circuit<sup>46</sup>. The CT's used are rated at 20A/25mA which are suitable for both of the three phase test applications - they are not necessary for the single phase generator application. The CT primary is wound a number of times around the transformer body in order to obtain the desired secondary current, as indicated by the selection chart<sup>47</sup>, part of which is shown in Table 5.

<u>Full Load Current (A)</u>	<u>Turns through CT</u>
3.6 to 5.4	5
5.5 to 8.5	4
8.6 to 17.5	2

Table 5 - CT Primary Turns

### ***Current Measurement Calibration***

Calibration of the current measurement circuit is necessary for satisfactory operation of the ELG. The ADC IC has a resolution of 8 bits, i.e. 256 discrete values for input voltages between 0V and the reference voltage, +5 V d.c. Using the potentiometer (refer figure 21) the ADC input voltage is adjusted to 2.5 V when the line current is at full rated value. This permits overcurrents of up to twice full load current to be accurately measured without the ADC saturating. The resolution per digital bit for this arrangement is given in Table 6 for a range of generator outputs, assuming 415 V, unity power factor operation.

<u>Generator</u>	<u>Full Load</u>	<u>Resolution</u>
<u>Output Power</u>	<u>Current</u>	<u>Per Bit</u>
( kW )	( A )	( A )
3.5	5	0.039
25	35	0.273
50	70	0.546

**Table 6 - Digital : Line Current Resolution**

#### **5.1.5. Metering**

Standard laboratory type meters are used for visual indication of the line currents, line voltage, frequency, and power of the electrical output of the generator.



## 5.2 MOTOR-GENERATOR SET

The initial testing of the ELG was performed on a generator driven by a d.c. motor. The speed-torque characteristics of a Pelton wheel turbine are shown in figure 33, along with the characteristics of the different standard d.c. motor field connections. Unfortunately, none of the d.c. motor types matches the characteristic of the Pelton wheel and so the ELG testing on this motor-generator set is limited to experimental and functional testing only. Performance testing is carried out on the water turbine driven generators described in Section 5.3.

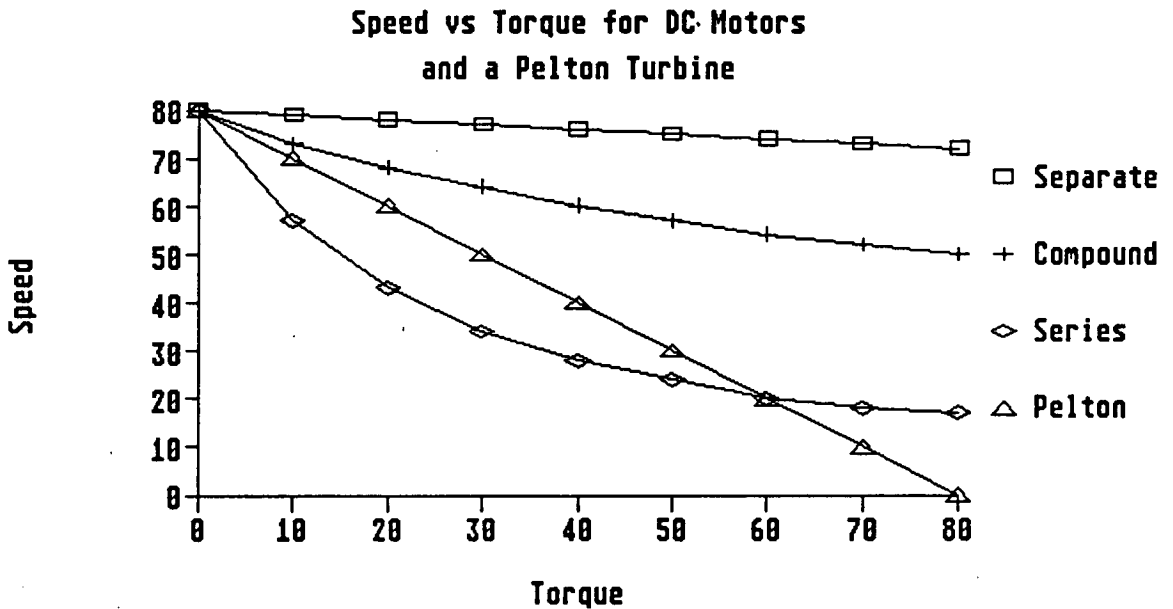


Figure 33 - Speed-torque characteristics

### 5.2.1. Rating Details

The test set used is a Crompton Parkinson bedplate-mounted motor-generator set which has the following rating details.

	<u>D.C. Motor</u>	<u>A.C. Generator</u>
<b>Serial No</b>	F81A10361	FA61A5639
<b>Type</b>	Compound Wound	Synchronous, 4 pole
<b>Rating</b>	2.46 kW	2.5 kVA
<b>Voltage</b>	220 V	240 V, 3 phase,
<b>Current</b>	14.7 A	6 A

The motor is complete with a faceplate starter circuit to reduce the supply current during run-up of the set. The d.c. motor is self excited, connected as a short-shunt, cumulative compound machine. Shunt field regulation provides the primary form of speed control of the motor. The speed range available is 750 to 2250 rev/min and the generator is directly connected to the motor shaft. The circuit diagram of the d.c. motor is given in figure 34a.

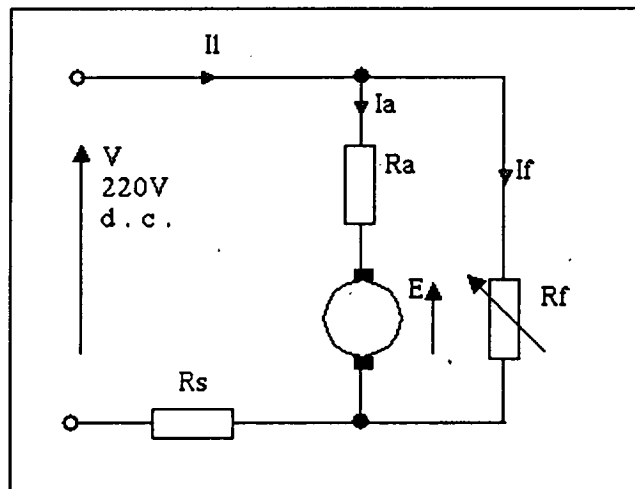


**Figure 34a - Circuit diagram of d.c. motor**

The synchronous a.c. generator is separately excited, its d.c. field supply being derived from the laboratory 220 V d.c. supply. The excitation supply is switched via a contactor and excitation control is achieved by manual adjustment of course and fine potentiometers - there is no

automatic voltage regulation. A circuit diagram of the generator is shown in figure 34b. As the generator is isolated from the grid network, the frequency of the voltage waveform is directly proportional to the speed of the d.c. motor which is driving the generator shaft: a frequency of 50 Hz is obtained at a shaft speed of 1500 rev/min. The rotational speed is indicated on a digital counter which receives a signal from a shaft mounted sensor.

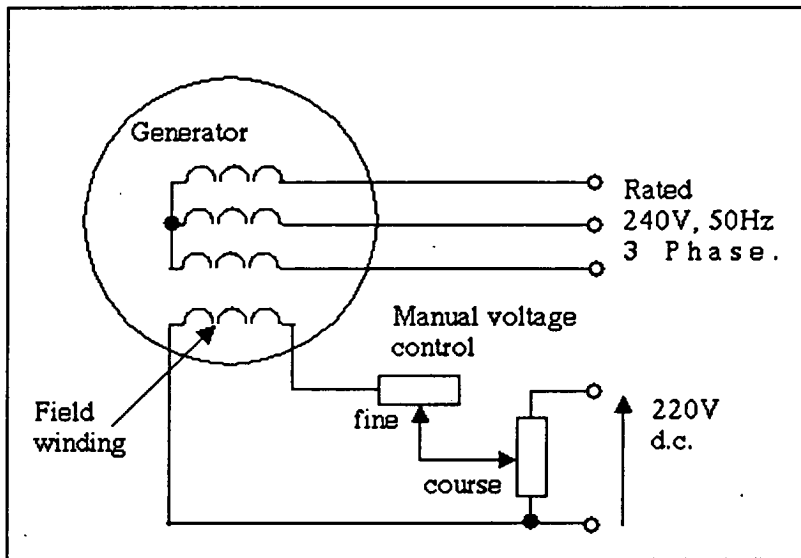


Figure 34b - Circuit diagram of a.c. generator

### 5.2.2. Speed / Load Characteristic - Theory

From the e.m.f. equation for a d.c. machine<sup>48</sup>;

$$E \propto \Phi_M \omega \quad (5.1)$$

and  $\omega \propto N \quad (5.2)$

hence,  $N \propto E/\Phi_M \quad (5.3)$

where  $N$  is the rotational speed in R.P.M.;  $\omega$  is the rotational speed in radians per second;  $E$  is the rotational e.m.f. (V) and  $\Phi_M$  is the magnetic flux per pole (Wb). Neglecting saturation, the flux per pole,

$$\Phi_M \propto I_f, \text{ the field current} \quad (5.4)$$

and in turn,  $I_f \propto 1/R_f$  hence  $\Phi_M \propto 1/R_f$  (5.5)

For the d.c. motor circuit, refer figure 34a,

$$V = E + I_a R_a + I_f R_s \quad (V) \quad (5.6)$$

hence combining equations 5.3, 5.5 and 5.6,

$$N \propto (V - I_a R_a - I_f R_s) \cdot R_f \quad (5.7)$$

From equation 5.7 it can be seen that as the load,  $I_a$ , increases then the speed decreases.

### 5.2.3. Speed Control

Equation 5.7 also shows that, for any given load, the speed of the d.c. motor can be controlled by adjustment of the terminal voltage, the armature resistance, the series field resistance,  $R_s$ , and the shunt field resistance,  $R_f$ . The motor in the laboratory is fitted with fine and course shunt field resistors for manual adjustment of the speed. The voltage supply to the motor is fixed, however the motor terminals are arranged in such a manner as to permit the insertion of additional external resistance in the series field and in the armature windings.

The effect of adding series connected resistance is to reduce not only the e.m.f. but also the voltage across the field winding. This in turn has the effect of reducing the flux and results in a tendency to increase the speed which counteracts the speed reduction produced as a result of reducing the e.m.f. Hence more effective speed control is achieved through the adjustment of added armature resistance.

#### 5.2.4. Speed / Load Characteristic - Measured

As a functional test set for ELG testing, the most important characteristic of the motor-generator set is its droop, ie the variation of speed ( thus frequency ) against electrical load on the generator, (refer Section 2.1.2.1.). Figure 35 shows the measured droop curves for two values of shunt field resistance, with no external resistances added. The curves have similar droop values of 1.7 and 1.8 Hz/kW, the significant difference is that the absolute frequency rises due to the increase in field resistance from 516 $\Omega$  to 540 $\Omega$ . The droop values were calculated over the load range from full load to no-load.

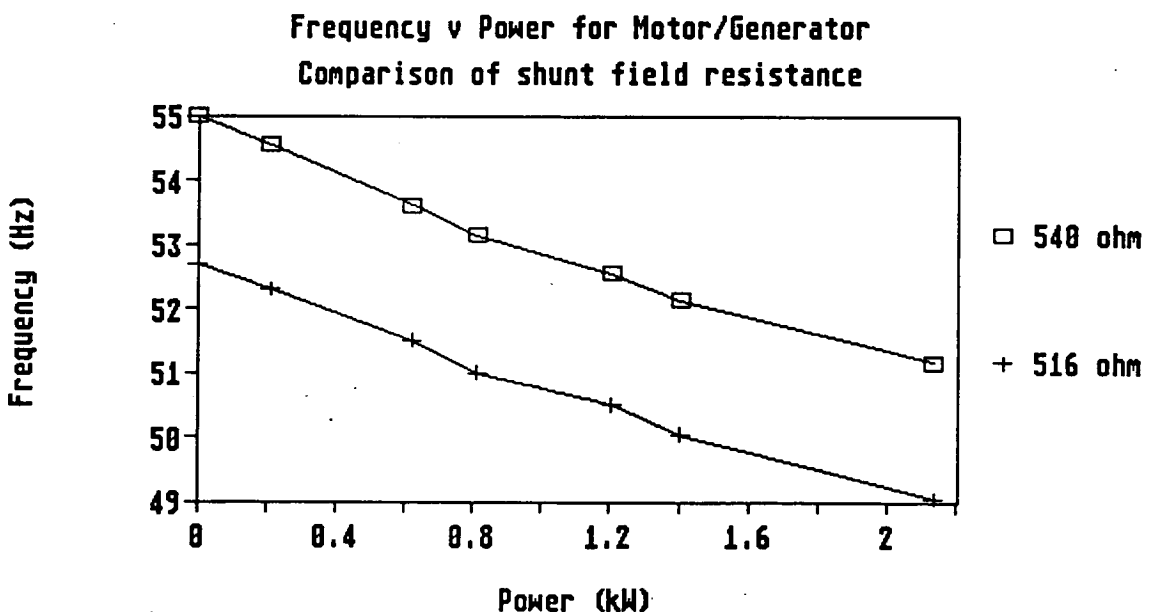
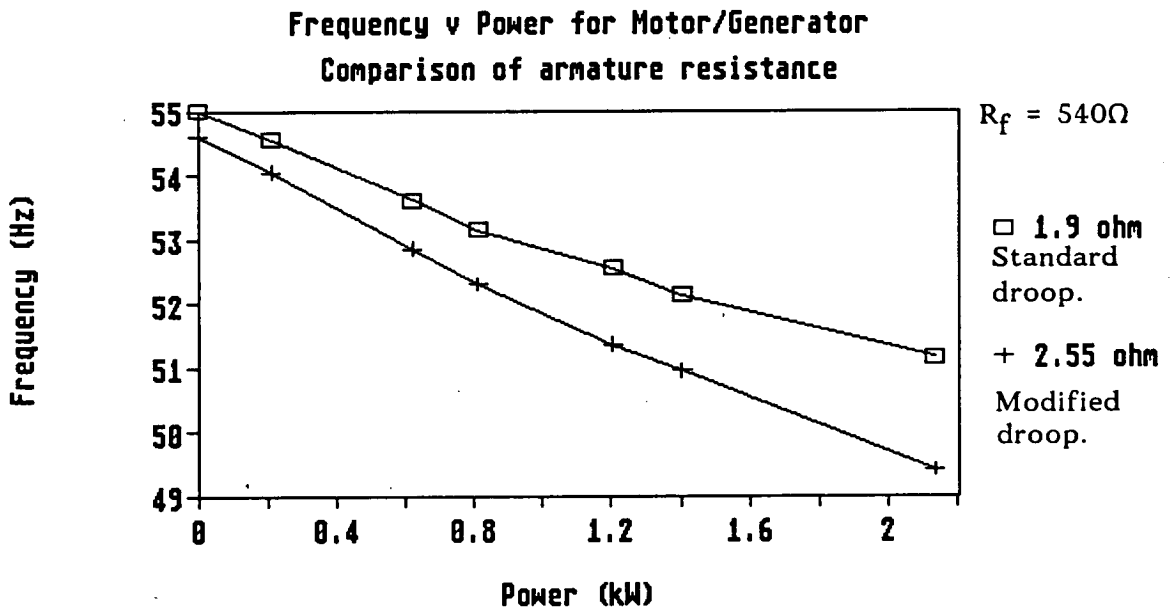


Figure 35 - Effect of field resistance on droop

The "full load" applied to the generator for these tests was 2.13 kW. This value was selected partly due to the resolution of the switch settings of the Jay-Jay Loading Unit and partly to allow an "overload" capability during the experimentation.

Figure 36 shows the effect on the measured droop curve of adding  $0.65\Omega$  to the nominal armature resistance of  $1.9\Omega$ . The no-load frequency is approximately the same but there is a steeper droop characteristic once on load,  $2.42\text{Hz/kW}$  for the modified droop curve compared with  $1.8\text{Hz/kW}$  for the standard droop curve.



**Figure 36 - Effect of armature resistance on droop**

The standard droop was rather shallow compared to the droop of a typical turbine, and hence the modified droop of  $2.42\text{ Hz/kW}$  was used for the majority of the ELG testing on this test set. Before the implementation of the three phase balancing feature, the ballast load steps in each phase were switched together, giving a minimum step value of  $0.36\text{ kW}$ . From equation 2.2, the minimum deadband calculated

for optimum operation was  $\pm 0.87$  Hz and the next setting available (Table 4) was  $\pm 0.96$  Hz. Once the three phase balancing function was operational, then the minimum step value dropped to 0.12 kW and the deadband selection reduced to  $\pm 0.32$  Hz.

Despite the artificial steepening of the droop characteristic of the d.c. motor, its curve was not sufficiently similar to that of a Pelton turbine, particularly as it tends to level out at full load. True performance testing could therefore only be achieved on water turbine driven generators.

#### 5.2.5. D.C. Motor Model

To steepen the droop characteristic for the ELG tests, resistance may be added either in the armature circuit or the series field circuit. A computer model of the steady-state speed-load variation of the d.c. motor was developed as an *engineering tool* to study the effect of adding resistance at these different locations.

The program, MODEL3, was initially written on the BBC Microcomputer in BBC BASIC. This program is menu driven and gives the user options to adjust armature resistance, series field resistance or shunt field resistance. The software determines the variation in speed, and hence generated frequency, from zero to full load.

---

Data for the program was obtained from the d.c. motor using either known values or empirical values. The electrical circuit used was that for the short shunt compound motor. The model was able to produce speed values which were within 2% of the results achieved on test. The model output for varying the shunt field resistance from  $516\Omega$  to  $540\Omega$  is given in figure 37 for comparison with the measured results of figure 35.

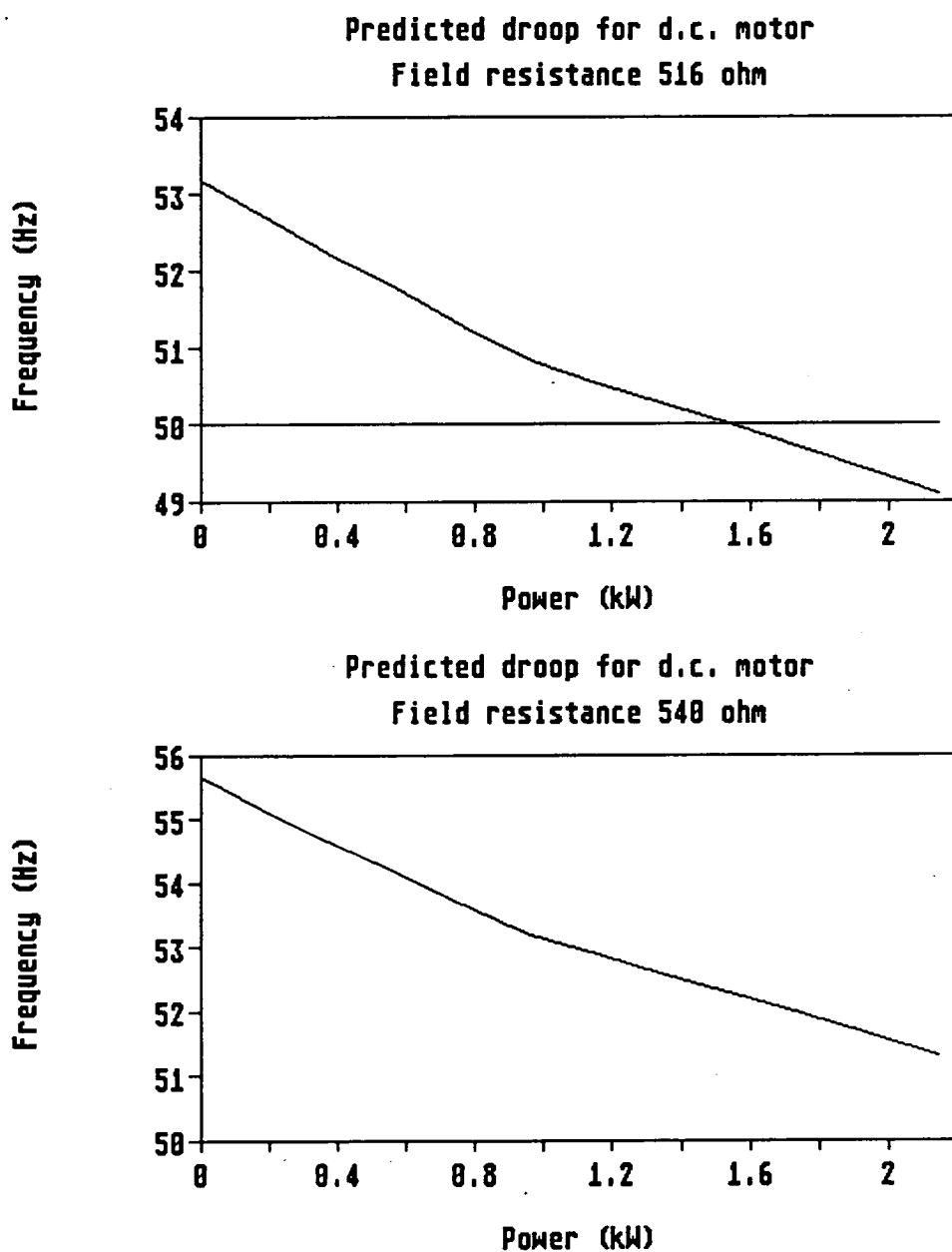


Figure 37 - Model predictions of motor/generator droop



An additional feature of the program was the calculation of the droop and the minimum deadband setting that would apply for the given added resistance. Use of the model confirmed the theory of Section 5.2.3. that the variation of the armature resistance would have a greater effect on the speed variation than that of the series field resistance. In addition, the model was used to assist the final selection of the value of added armature resistance.

The computer model was simplified to determine only the speed-load characteristics for added armature resistance or for variation of the shunt field resistance, using a base field resistance value of  $540\Omega$ . This program is **MODEL4** and a listing thereof, re-written in ST BASIC, is given in Appendix 3 along with the appropriate circuit diagram used for the program. Figure 38 shows the screen output of MODEL4 based on the optimum resistance values used for the testing of the ELG. This curve compares with the modified droop curve shown in figure 36.

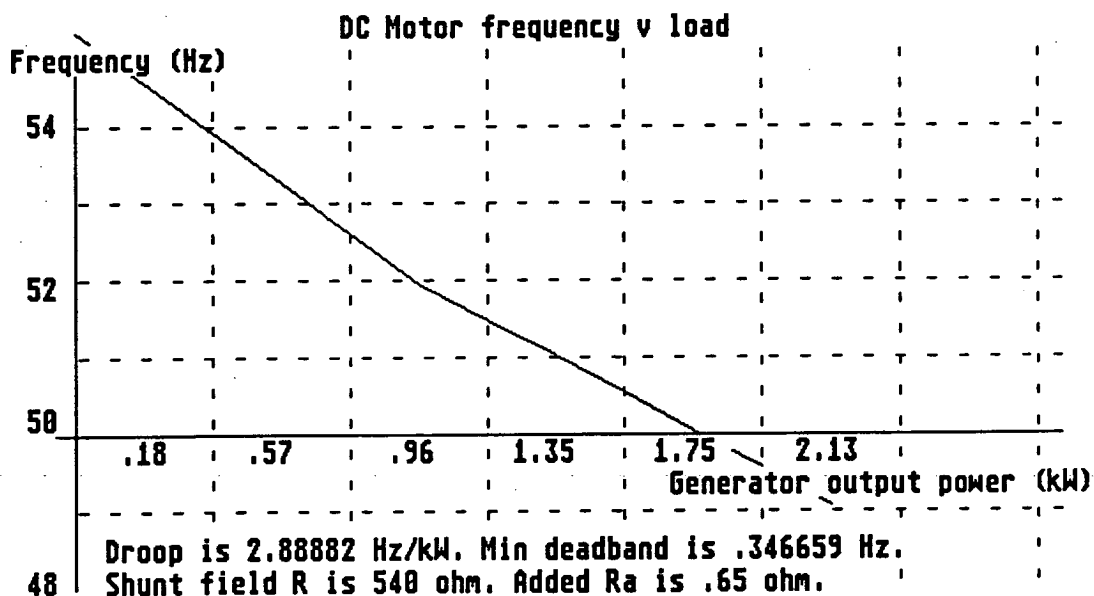


Figure 38 - Screen display of MODEL4 output

### 5.3 TURBINE-GENERATOR SETS

Two different Pelton turbines are available for performance tests of the ELG, both located in the Hydraulics laboratory (A25) at the Merchiston Site of Napier University. The first is a No 15 Pelton wheel Instructional Turbine supplied by Gilkes in the mid 1950's to Napier (the *Gilkes* turbine). As a result of previous undergraduate project work, a single phase synchronous a.c. generator was already installed, connected to the turbine by a belt drive with an on-load speed ratio of 6.17:1 (generator:turbine).

The principal application of the ELG is for three phase systems and hence a three phase generation system was required. As a part of his research work into Small-Scale Hydro Power Generation, Wallace<sup>49</sup> had designed and installed a water turbine test facility in the Napier University Hydraulics laboratory. The turbine installed is a refurbished Pelton wheel which had originally been supplied by Boving to Balruddery Quarry, near Dundee, in 1936 (the *Boving* turbine). During his tests, Wallace loaded the turbine with a two stage centrifugal pump. For the purpose of the ELG tests, a three phase generator was installed, connected to the turbine by a belt drive with an on-load speed ratio of 1.97:1 (generator:turbine).

Tests were also performed on a Francis type turbine, utilising the same single phase generator as for the Gilkes Pelton wheel, suitably re-sited. The water supplied to the inlet pipework of the turbines is pumped from a water sump situated below the floor level of the laboratory. Photographs of the turbine-generator systems are shown in figure 39.

---

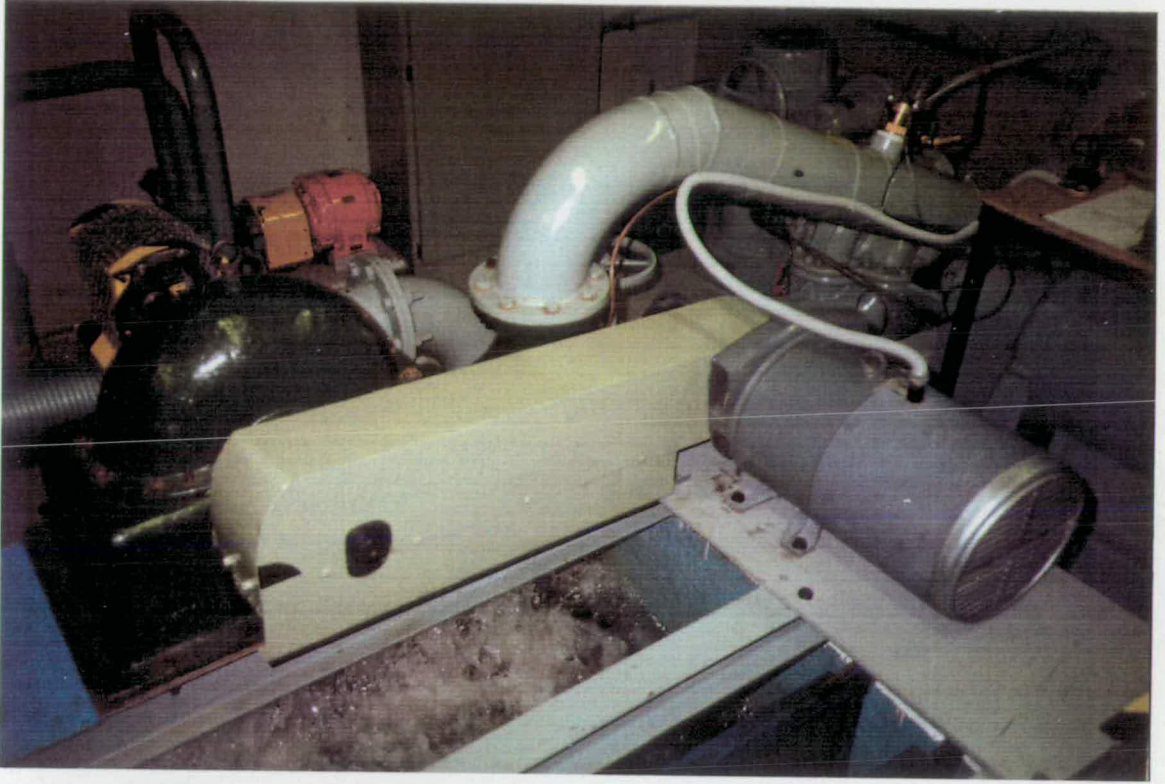


Figure 39a - The Boving turbine and its three phase generator

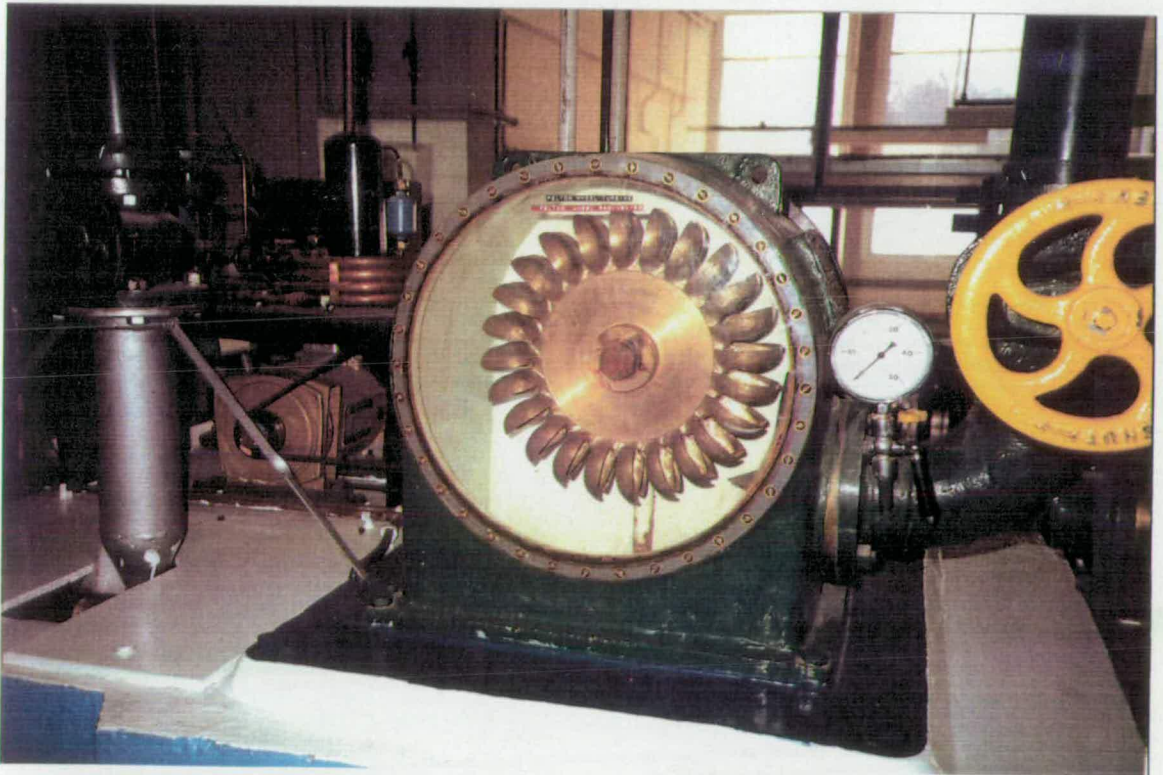


Figure 39b - The Gilkes turbine and the single phase generator

---

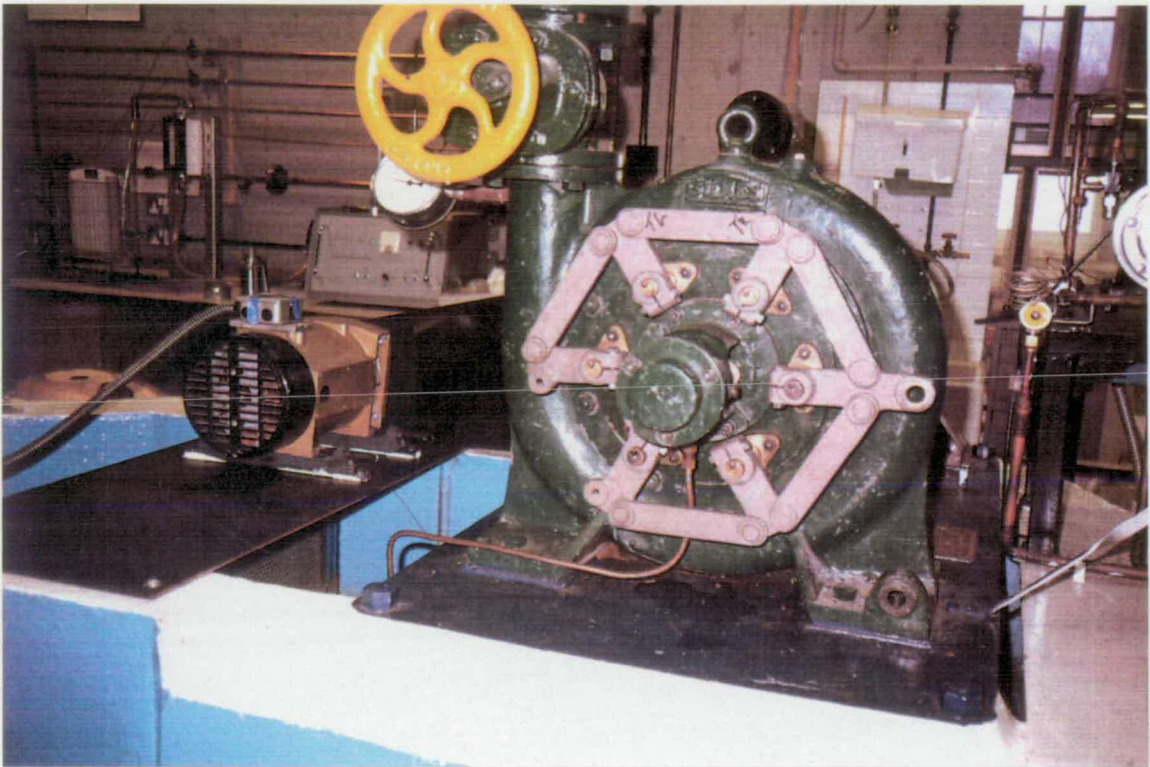


Figure 39c - The Francis turbine and the single phase generator

### 5.3.1. Boving Turbine and Three Phase Generator

#### 5.3.1.1. Rating Details

##### Turbine Data (Boving)

Serial Number	1966
Type	Single jet Pelton wheel
Rated Head	67 m
Rated Output	17 kW
Installed Head	35 m
Installed Flow	35 litres/s
Installed Output	7.6 kW mechanical.

**Generator Data (Markon)**

Serial Number 804219/1  
 Framesize LC28B, 4 pole  
 Type Self Excited, Self Regulating, Revolving Armature,  
 Synchronous A.C. Generator  
 Rating 7.5 kVA  
 Voltage 415/240 V, 3 phase  
 Rated Current 10.4 A

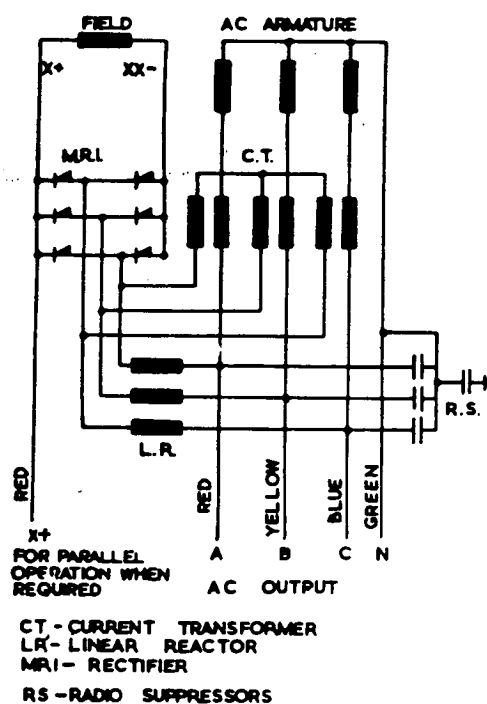


**Figure 40 - Excitation diagram of the three phase generator**

The generator is self excited, incorporating a static, self regulating, power factor compensating control unit. The control gear is split into two parts, one supplying the no-load excitation and the other the additional excitation required under load conditions. Referring to figure 40, on no-load, the field excitation is fed through a linear reactor and is rectified to produce the open circuit voltage. On load, additional field excitation current is obtained from a current transformer. This is added

to the current from the linear reactor and then rectified to give the correct excitation. This generator has an automatic build up of terminal voltage as it accelerates from rest, enabling the ELG to power-up once the generator phase voltage has reached 140 V.

### Nominal Operating Conditions

Head	30 m (+5 and -10 m)
Flow	30 l/s (+5 and -10 l/s)
Line voltage	415 V
Full load output	4.7 kW electrical at 50 Hz. ( 53% overall efficiency )

Selection of these nominal operating points gives a flexibility in the range of head and flow available for the tests.

#### 5.3.1.2. Speed / Load Characteristic - Theory

##### *Ideal Operation*

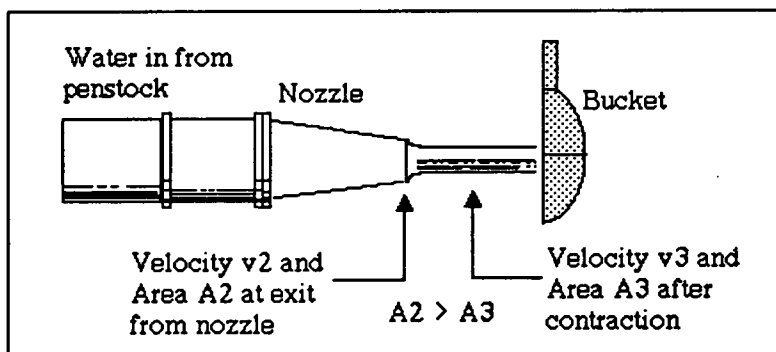


**Figure 41 - Water flow from a conical nozzle**

For the purposes of this study, theoretical examination of the performance of water turbines will be limited to that of the Pelton wheel. This is a reasonable stance on the basis that the majority of

micro hydro installations utilise impulse type turbines. The flow of water through a conical nozzle is shown in figure 41, from entry to the nozzle to the point where it is about to impinge on the buckets on the runner. The jet diameter is reduced on exit from the nozzle due to contraction of the water column, however the continuity equation determines that;

$$Q = A_2 v_2 = A_3 v_3 \quad (\text{m}^3/\text{s}) \quad ( 5.8 )$$

The terms connected with the water velocities, jet areas and jet diameters are as follows;

Q	is the flow	(m <sup>3</sup> /s)
v	is the free jet velocity	(m/s)
v <sub>2</sub>	is the nozzle exit velocity	(m/s)
v <sub>3</sub>	is the contracted jet velocity	(m/s)
A <sub>2</sub>	is the nozzle exit area	(m <sup>2</sup> )
A <sub>3</sub>	is the contracted jet area	(m <sup>2</sup> )

By equating the kinetic and potential energies it is shown that;

$$v = \sqrt{(2gh)} \quad (\text{m/s}) \quad ( 5.9 )$$

where g is the gravitational constant and h is the net head available at the turbine inlet.

The *coefficient of contraction* C<sub>c</sub> relates the nozzle discharge area to the jet area and has a typical value<sup>50</sup> of 0.95.

$$C_c = A_3/A_2 \quad ( 5.10 )$$

The velocity of the water jet arriving at the turbine runner,  $v_3$ , is reduced relative to the free jet velocity,  $v$ , due to head losses within the turbine and nozzle. The *velocity coefficient*,  $C_v$ , relates the two and has a typical value of 0.98 for a conical nozzle<sup>50</sup>.

$$C_v = v_3/v \quad (5.11)$$

Combining equations 5.8 & 5.10 then substituting for  $v_3$  and  $v$  using 5.11 and 5.9 respectively, gives

$$v_2 = C_c v_3 \text{ then,} \quad (\text{m/s})$$

$$v_2 = C_d \sqrt{2gh} \quad (\text{m/s}) \quad (5.12)$$

where  $C_d = C_c C_v$  is the discharge coefficient and has a typical value of 0.93.

The power in the water delivered to the turbine is found from;

$$P_{IN} = \rho ghQ \quad (\text{W}) \quad (5.13)$$

$$\Rightarrow P_{IN} = \rho ghA_2 C_d \sqrt{2gh} \quad (\text{W}) \quad (5.14)$$

In a load governing application, the area of the nozzle exit will be fixed, because there would be no *water* control, and it is assumed that the net head will remain substantially constant. In this case it can be seen from equation 5.14 that the input power to the turbine is constant and will not vary as a function of either load or speed.

The turbine output power,  $P_{OUT}$ , which is transmitted as torque,  $T$ , on the shaft, is found from;



$$P_{\text{OUT}} = T\omega \quad (\text{W}) \quad (5.15)$$

The angular velocity,  $\omega = u/r$  (rad/sec) where  $u$  is the peripheral velocity of the turbine runner (m/s) and  $r$  is the runner radius (m). As the torque is the product of force,  $F$ , (N) and the radius, then,

$$P_{\text{OUT}} = Fu \quad (\text{W}) \quad (5.16)$$

The force on the turbine runner is found from<sup>51</sup>,

$$F = 2\rho Q(v_3 - u) \quad (\text{N}) \quad (5.17)$$

Hence,

$$P_{\text{OUT}} = 2\rho Qu(v_3 - u) \quad (\text{W}) \quad (5.18)$$

In addition, the expression for the torque is,

$$T = 2\rho Qr(v_3 - u) \quad (\text{Nm}) \quad (5.19)$$

Equation 5.18 can be re-written as a quadratic equation;

$$P_{\text{OUT}} = -ku^2 + kv_3u$$

where  $k = 2\rho Q$  and both  $k$  and  $v_3$  are assumed to be constant. This quadratic equation has a parabolic shape and has a maximum turning value which occurs when  $f'(u) = 0$ . Now,

$$f'(u) = -2ku + kv_3$$

hence the maximum output power occurs when  $u/v_3 = 0.5$ . The *peripheral velocity coefficient*,  $\Phi$ , defines the ratio of the runner peripheral velocity and the free jet velocity such that  $\Phi = u/v$ . Hence maximum power is obtained when  $\Phi$  is 0.46 to 0.49 depending on the

value of  $C_V$ . The turbine output power can thus be plotted against  $\Phi$  as shown in figure 42.

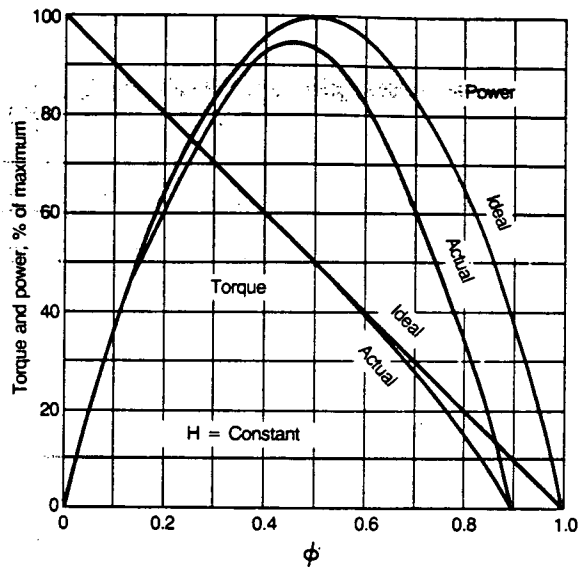


**Figure 42 - Turbine output power vs peripheral velocity coefficient**

From equation 5.19, the turbine torque output is a maximum when  $u=0$  ( or  $\Phi = 0$ , i.e. at standstill ) and is zero when  $u=v_3$  ( or  $\Phi = 1.0$ , i.e. at runaway speed ). This linear relationship is also given in figure 42.

The runner rotational speed,

$$N = 60u/(\pi D) \quad (\text{rev/min})$$

Hence the variation of turbine output power with runner speed can be shown, by direct comparison with figure 42, to be a parabolic function with maximum output power occurring at a little under half of the theoretical runaway speed of the turbine runner. This condition occurs when  $u = v_3$ , and so for a given turbine geometry, the length of the speed axis is dependent on  $\sqrt{h}$ .

### ***Operation in Practice***

A turbine operating in practice would be arranged to run on full load as near to its optimum speed as possible for maximum power transfer. If it were not governed, then as load was removed, the speed of the runner would increase until it eventually reached its runaway speed at no-load. The magnitude of the runaway speed is theoretically twice that of the optimum running speed. However it is limited in practice for a number of reasons, including the hydraulic spoiling effect of water rebounding back off the turbine casing onto the runner.

In the foregoing, the expression for the speed-load droop has been given in terms of Hz/kW and has assumed generator operation at constant voltage. The empirical results given for the d.c. motor driven generator ( Section 5.2.4 ) aligned with this assumption, as the generator excitation current was manually adjusted to achieve constant terminal voltage.

For the two water turbine driven generators, the excitation systems are both self regulating and the voltage control is operative only for a speed variation of 4.5% from full-load to no-load. When the turbine generator set is not governed, the speed variation is approximately 60% over this range, and hence the voltage magnitude varies significantly with load, refer Section 6.3.

---

As a result, it is not valid to use active power, in kW, as a measure of the generator load in the calculation of the droop. Instead, as 'load' changes are made, the electrical quantity which is independent of the voltage is the connected phase *impedance*,  $Z$  ( $\Omega$ ). If there is **no** load on the generator, then the impedance is infinite and the turbine will rotate at its runaway speed. As load is increased, through full load and onwards to an overload situation, then the phase impedance reduces to zero and the speed of the turbine will fall to zero, ie it will stall. The shape of the speed-impedance curve is a rectangular hyperbola.

As the load is connected in parallel with the generator terminals, it is simpler to deal in terms of phase *admittance*,  $Y$ , where  $Y = Z^{-1}$  (S), as admittances in parallel can be added directly. Moreover, the frequency vs admittance curve, refer figure 46, is equivalent to the frequency vs torque relationship of a water turbine, refer figure 42. The advantage of using the admittance is that it can readily be determined from the measurement of voltage and current, neglecting temperature variation. Such calculations of admittance will be used to determine measured p.u. load values in Section 5.3.1.4.

In a given installation, the 'full-load' can be defined in terms of the apparent power,  $S$  (kVA). The magnitude of the full-load apparent power,  $S_{fl}$ , may or may not correspond to the generator *rating* as a result of the generator selection procedure. The admittance per phase value which will correspond to full-load is found from;

$$Y_{fl} = S_{fl} \cdot V^{-2} = 1.0 \text{ p.u. load} \quad (S) \quad (5.20)$$

where  $V$  is the rated line voltage and balanced load changes are assumed. For *unbalanced* load changes, the admittance per phase,  $Y_{fl} = 0.333$  p.u. load. It is further assumed that all the electrical load is purely resistive and hence that  $Y = G$ , the conductance. This is a reasonable assumption at this stage as the electrical loads used on test are largely resistive.

### 5.3.1.3. Speed / load Characteristic - Predictions

It will be a normal function of the design of the installation to arrange that the 1.0 p.u. load point will occur at the design frequency, e.g. 50 Hz. Due to site-specific hydraulic conditions, the power value in kW, equivalent to 1.0 p.u., will differ from site to site. On no-load, when the torque is zero, then the turbine runner will rotate at the runaway speed,  $N_{ra}$ , and the runner peripheral velocity,  $u$ , will be equal to the contracted jet velocity,  $v_3$ . From equations 5.9 and 5.11 it follows that,

$$N_{ra} \propto C_v \sqrt{2gh}$$

Allowing for the appropriate relationship between the runner speed and the frequency of the generator waveform, then,

$$f_{ra} \propto \sqrt{h}$$

where  $f_{ra}$  is the frequency at the runaway speed.

Consequently, two points on the frequency vs p.u. load curve can be determined from basic data pertaining to the installation. Making the assumption that this relationship is linear, then the droop curve can be

plotted from this data, figure 43. For the remainder of this study, "droop" is now redefined as the slope of the frequency vs p.u. load line and has units of Hz/ 1.0 p.u., i.e. Hz. The magnitude of the predicted droop and its associated deadband value can be calculated on a per unit basis, e.g.,

for a three phase, 50Hz system with a runaway speed of 1.5 times the nominal speed, and assuming that the total ballast load is equal in magnitude to 1.0 p.u. load, then,

$$f_{ra} = 75 \text{ Hz, (refer figure 43)}$$

the predicted droop is thus 25 Hz, and as 1 step of ballast load is 0.0476 p.u., then the deadband value found from the droop is,

$$25 \times 0.0476 = 1.19 \text{ Hz.}$$

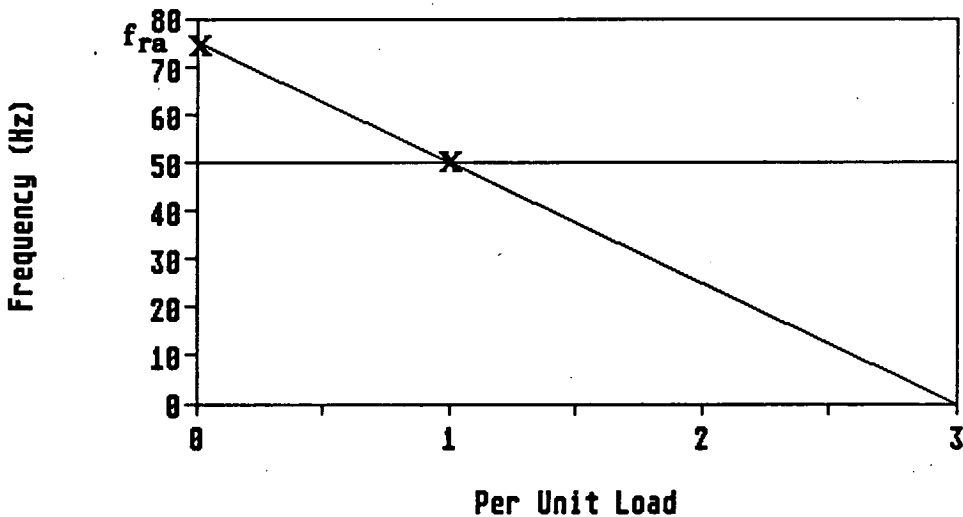
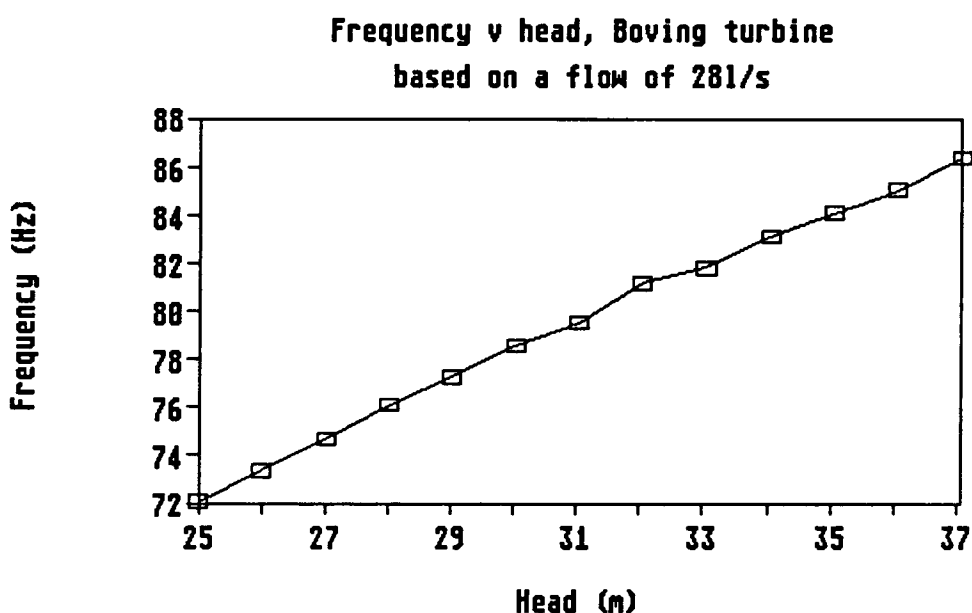


Figure 43 - Turbine droop - frequency vs p.u. load

Tests were done on the Boving turbine to determine the empirical relationship between  $f_{ra}$  and the head. The results of these tests are shown in figure 44. These tests were performed at a flow rate of 28l/s,

as near to the operational flow as was possible. The no-load test flow rate was restricted by the possibility of water turbulence causing the upper-ump, high-level detector to trip the pump drive motor. Changes in the flow rate of  $\pm 5$  l/s produce a variation in the running speed of less than 1% and are thus considered to have a negligible effect on the results. Table 7 below presents the predicted 'droop' and resulting deadband calculations for a range of operating heads.



**Figure 44 - Variation of runaway frequency with head**

<u>Head</u> <u>(m)</u>	<u><math>f_{ra}</math></u> <u>(Hz)</u>	<u>Predicted</u> <u>Droop</u> <u>(Hz)</u>	<u>Preferred</u> <u>Deadband</u> <u>(Hz)</u>	<u>Next</u> <u>Deadband</u> <u>(Hz)</u>
32	81.4	31.4	$\pm 1.5$	$\pm 1.6$
30	78	28	$\pm 1.33$	$\pm 1.6$
28	76	26	$\pm 1.24$	$\pm 1.28$

**Table 7 - Predicted Droop Values for a Range of Operating Heads.**

### 5.3.1.4. Speed / Load Characteristic - Measurements

In order to determine the speed-load characteristics for the Boving turbine, the generator was loaded with a balanced, resistive load, typically over a range from 0.5 to 1.5 per unit, at a variety of head and flow combinations. The following quantities were measured; turbine speed, generator speed, frequency, active power, line voltage and current. The latter two measurements permitted calculation of the phase admittance. Making the approximation that the power factor of the load was unity, then the apparent power corresponding to the full-load ( 50 Hz ) condition was deemed to be equivalent to the active power reading at that point.

For the nominal operating conditions, 30 m head and 30 l/s flow, figure 45a gives the frequency vs active power graph. As predicted in Section 5.3.1.2., the power graph is a parabola, with the maximum output power ( and hence efficiency ) occurring at approximately 46 Hz.

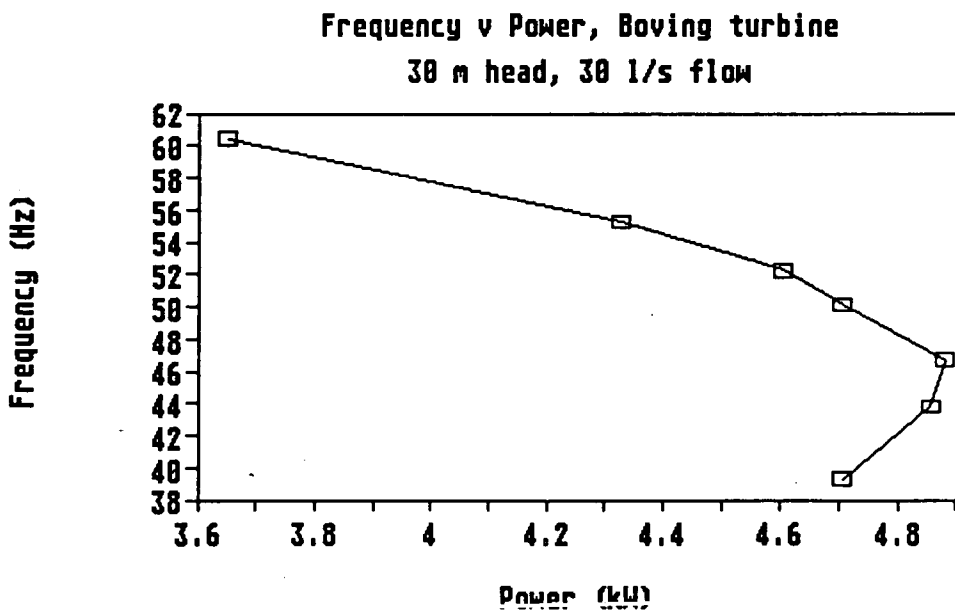


Figure 45a - Plot of frequency vs output power (Boving)



The frequency vs phase impedance curve, figure 45b, is a rectangular hyperbola, also as predicted in Section 5.3.1.2.

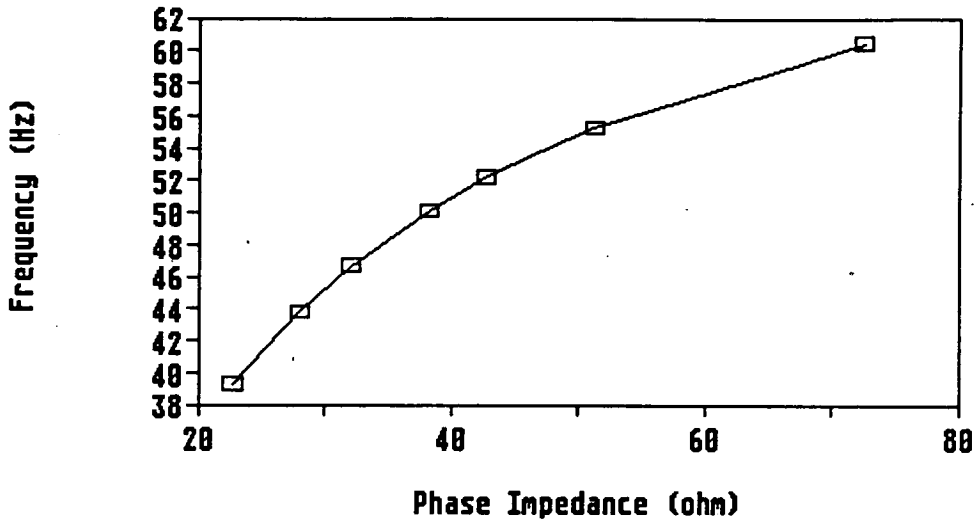


Figure 45b - Plot of frequency vs phase impedance (Boving)

As suggested previously, it is simpler to deal in terms of admittance rather than impedance, and figure 46 shows the plot of frequency against phase admittance for the nominal operating conditions, this curve being an approximation to a straight line. The full load admittance per phase is 0.02728 siemens and hence it is possible to

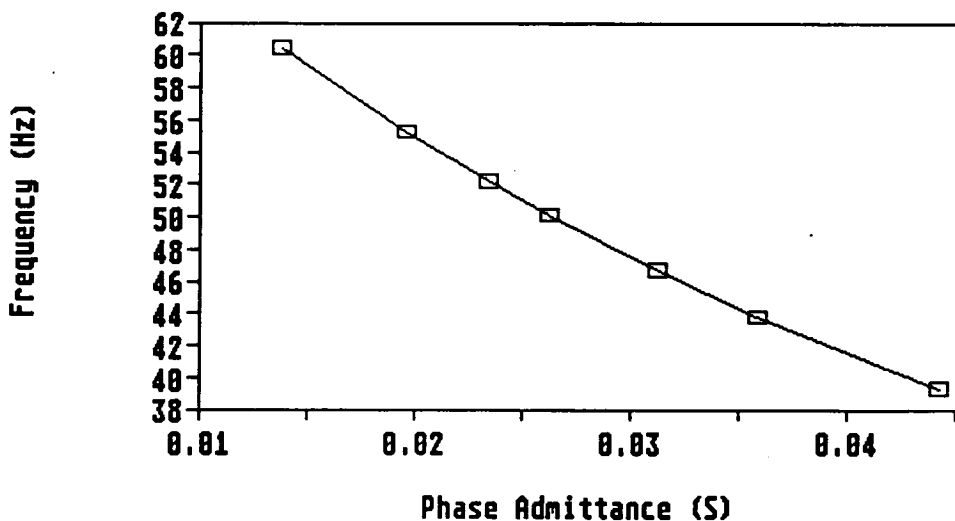


Figure 46 - Plot of frequency vs phase admittance (Boving)

re-plot frequency against p.u. load, refer figure 47. The per unit droop, over the load range of 0.5 to 1.0 p.u., is 22.9 Hz. The load change of the first binary step of one phase of the ballast load is 0.0633 p.u. thus the deadband from the measured data is  $\pm 1.45$  Hz, the next setting available being  $\pm 1.6$  Hz.

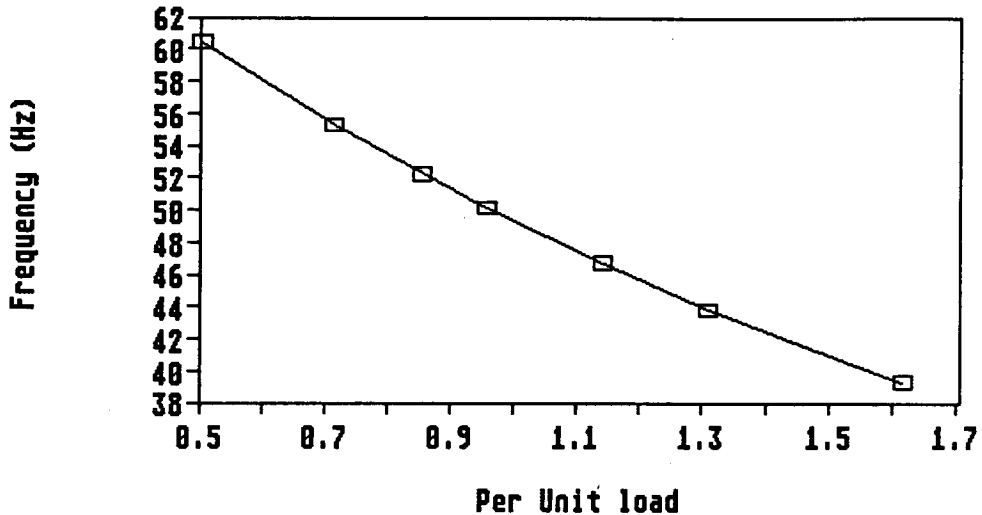


Figure 47 - Plot of frequency vs p.u. load (Boving)

For additional comparison against the predictions of Table 7, the droop values from the measured results at operating heads of 32 m and 28 m were determined and are given in Table 8 below. Whilst the predicted droop values are in the order of 20 - 35 % higher than those calculated from the measured data, this is countered by the fact that the installed ballast load is greater than 1.0 p.u. of the consumer load.

<u>Head</u>	<u>Measured</u>	<u>Preferred</u>	<u>Next</u>
<u>(m)</u>	<u>Droop (Hz)</u>	<u>Deadband (Hz)</u>	<u>Deadband (Hz)</u>
32	25.7	$\pm 1.62$	$\pm 1.92$
30	22.9	$\pm 1.45$	$\pm 1.6$
28	19.5	$\pm 1.23$	$\pm 1.28$

Table 8 - Measured Droop Values and Associated Deadband Selection.

These results suggest that a value of the droop is available, to a first order approximation, without access to installed test data. With this information the load governor deadband setting and the performance of the turbine-generator can be estimated prior to its installation. The success of this in practice is discussed in Section 6.2.5.

### 5.3.2. Gilkes Turbine and Single Phase Generator

#### 5.3.2.1. Rating Details

##### Turbine Data (Gilkes)

Serial Number	5937
Type	Single jet Pelton wheel
Rated Head	15.3 m
Rated Output	1.26 kW
Normal Speed	516 rev/min

##### Generator Data (Markon)

Serial Number	838548
Framesize	SCN21, 2 pole
Type	Self Excited, Self Regulating, Revolving Field Synchronous A.C. Generator.
Rating	1.5 kVA
Voltage	230 V, single phase

The generator excitation system consists of an excitation winding in the stator which supplies current to the rotating field via an impedance choke and a rectifier.

---

**Nominal Operating Conditions**

Head	19.0 m
Flow	11.1 l/s
Line voltage	230 V
Full load output	620 W electrical at 50 Hz.

**5.3.2.2. Speed / Load Characteristic - Measurements**

Absence of accurate data for the runaway speed of this turbine prevents presentation of predicted droop and deadband values. As for the Boving turbine, measurements relating to the speed/load characteristic were taken over a range of head and flow conditions. The graphs of frequency vs power and frequency vs p.u. load are given in figure 48 and figure 49 respectively for the nominal operating conditions. The power curve is part of a parabola which has not reached the maximum output power ( or maximum efficiency ) at the lower end of the frequency axis. The p.u. load curve approximates to a straight line and the measured droop is 17.8 Hz over the range 0.6 to 1.0 p.u. load suggesting a preferred deadband of 1.16 Hz, +- 1.28 Hz being the next available setting.

---

**Frequency v Power, Gilkes turbine  
19 m head, 11.1 l/s flow**

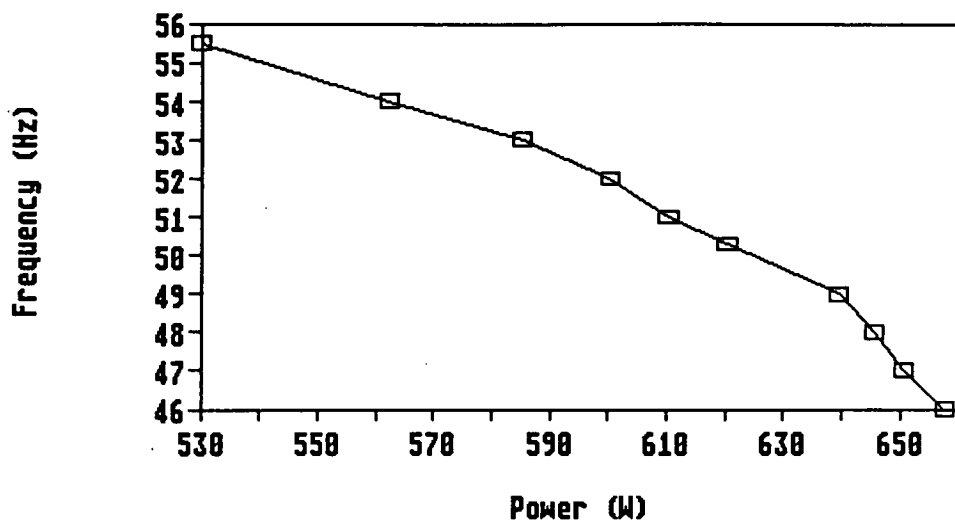


**Figure 48 - Plot of frequency vs power (Gilkes)**

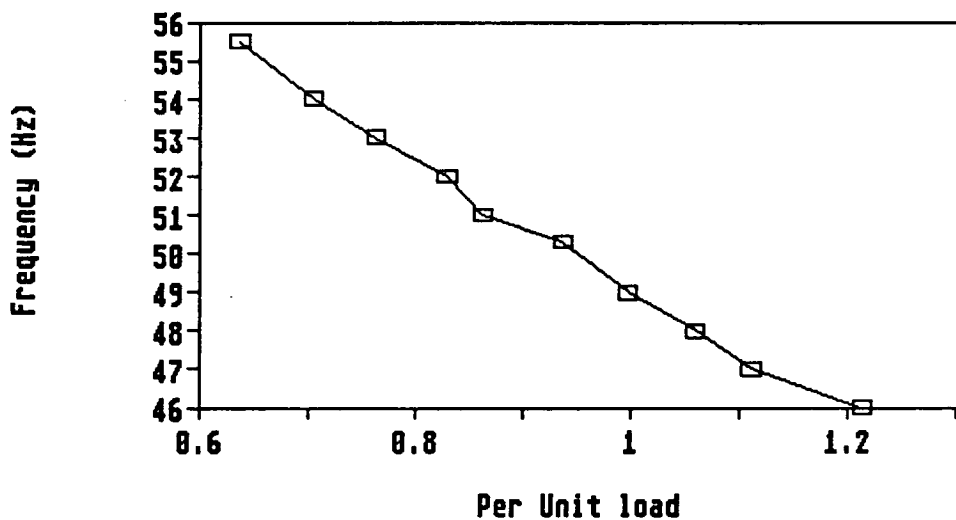


**Figure 49 - Plot of frequency vs p.u. load (Gilkes)**

### 5.3.3. Francis Turbine

#### 5.3.3.1. Rating Details

##### Turbine Data (Francis)

Serial Number	5938
Type	Francis Turbine
Rated Head	15.24 m
Rated Output	1.1 kW
Normal Speed	1270 rev/min

##### Generator Data

Refer Section 5.3.2.1.

##### Nominal Operating Conditions

Head	17 m
Flow	12.3 l/s
Line voltage	230 V
Full load output	600 W electrical at 50 Hz.

#### 5.3.3.2. Speed / Load Characteristic

Under the supervision of the author, a final year project student from the Napier University, B.Eng. Energy Engineering, honours degree course performed the work on the Francis turbine. The detailed results of the tests are contained in Mackintosh's report<sup>52</sup> and the salient points are given below.

---

Predicted droop/deadband	32.1 Hz / +-2.24 Hz
Measured droop/deadband	28.4 Hz / +- 1.92 Hz.

#### 5.4 DIGITAL STORAGE OSCILLOSCOPE

During the testing of the ELG, it is necessary to measure its operation and performance as a function of time, in both steady-state and transient conditions. By analysing a variety of voltage waveforms available from the digital electronic circuits and the power system, information can be obtained about the operation of the unit. Extensive use is made of a Gould 1602 digital storage oscilloscope ( DSO ) for this function. In its storage mode, information can be captured, stored, analysed and transferred to a microcomputer, via an IEEE-488 interface and link, for additional display, analysis and long term storage (refer Section 5.5).

The acquisition memory of the DSO is 10k words per channel for the information displayed on the screen. A typical timebase setting of 100ms/division thus has a sample rate of 10,000 samples per second. The DSO also has an internal screen plotter which produces direct digital screen copies on demand.

The waveforms which are used to monitor the performance of the ELG are as follows;

- the first section of the ballast load in each of the three phases. As the state of this section alters with each successive step change in any phase, the status of the ballast load at any instant
-

can be determined, refer figure 50a. The phase shown is seen to undergo 5 successive changes, followed by a period of inactivity whilst the other phases are active, followed by 2 further changes.

This trace was in response to a full load rejection and the ballast load in the phase shown has changed from zero to maximum.

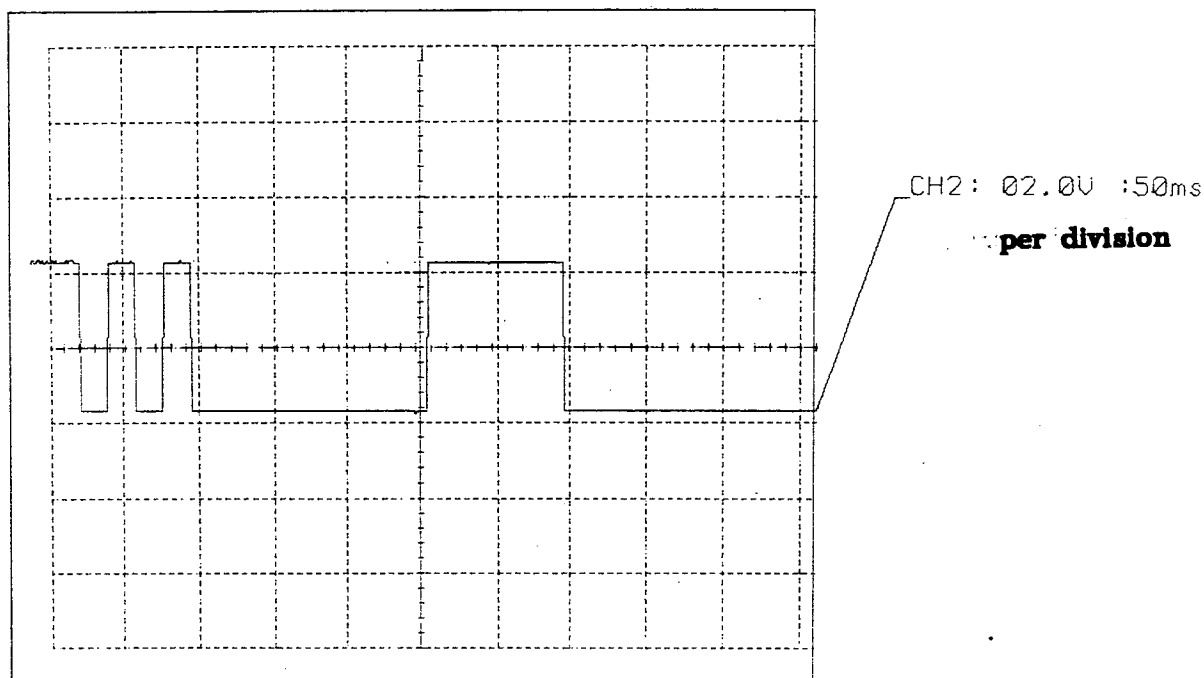


**Figure 50a - DSO trace of section 1 of ballast load in one phase**

- the toggle output line which gives an indication of the program cycle duration. Analysis of the program sequence is possible with this information and program modifications which reduced the cycle time arose from such analysis. Figure 50b shows the difference in the cycle time as the ELG changes from a non-switching mode to a switching mode and back again.



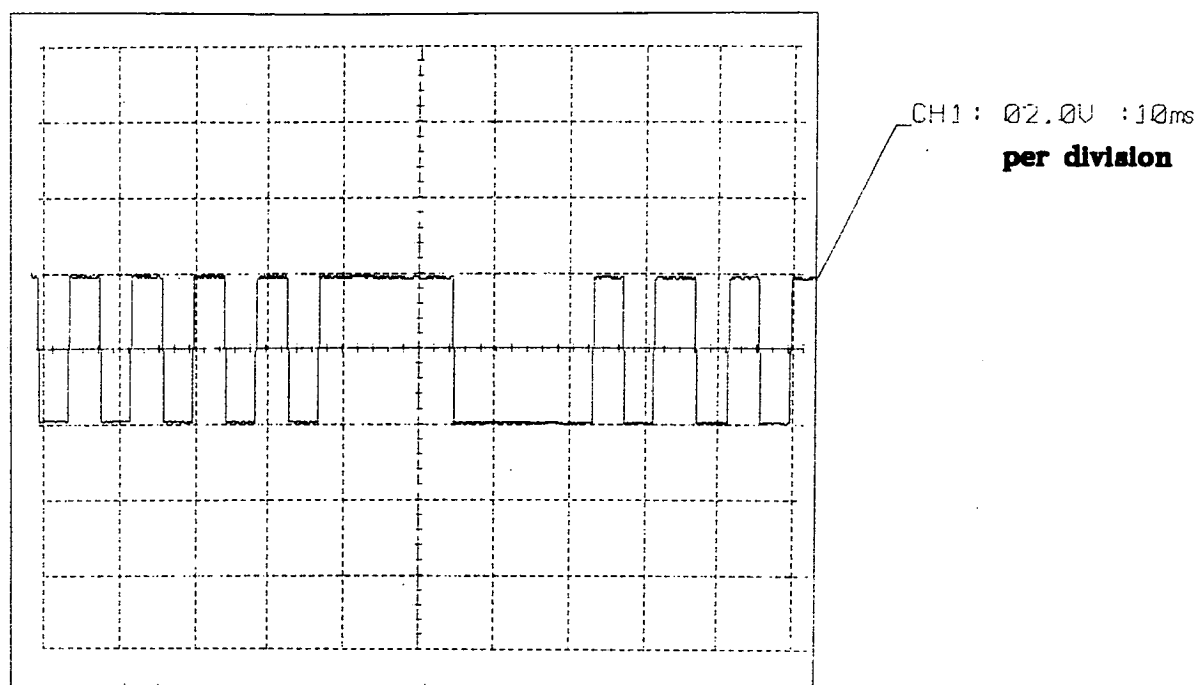


**Figure 50b - DSO trace of the toggle output line**

- the Schmitt Trigger output, which is the signal that the microprocessor uses to determine the a.c. cycle period. This signal, as shown in figure 50c, is used to monitor the transient frequency performance of the ELG, refer Section 5.5.

- the 12 V secondary of the voltage transformer which gives information on the transient voltage performance, refer figure 50d.

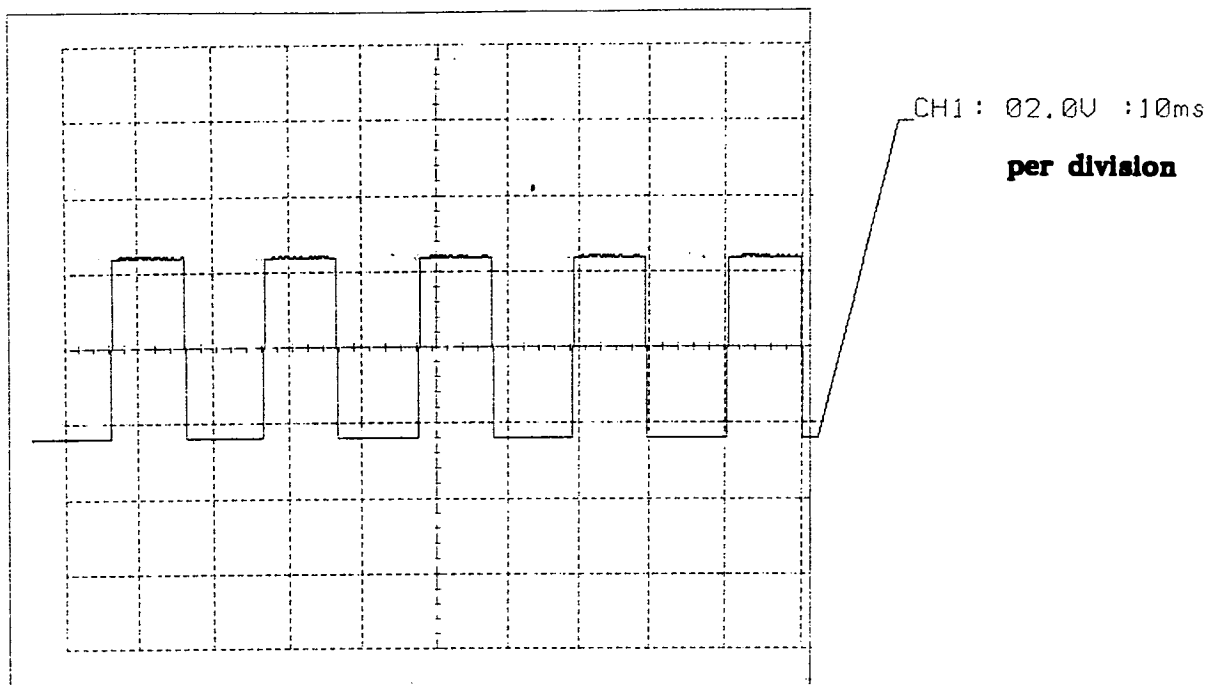


Figure 50c - DSO trace of the Schmitt Trigger output

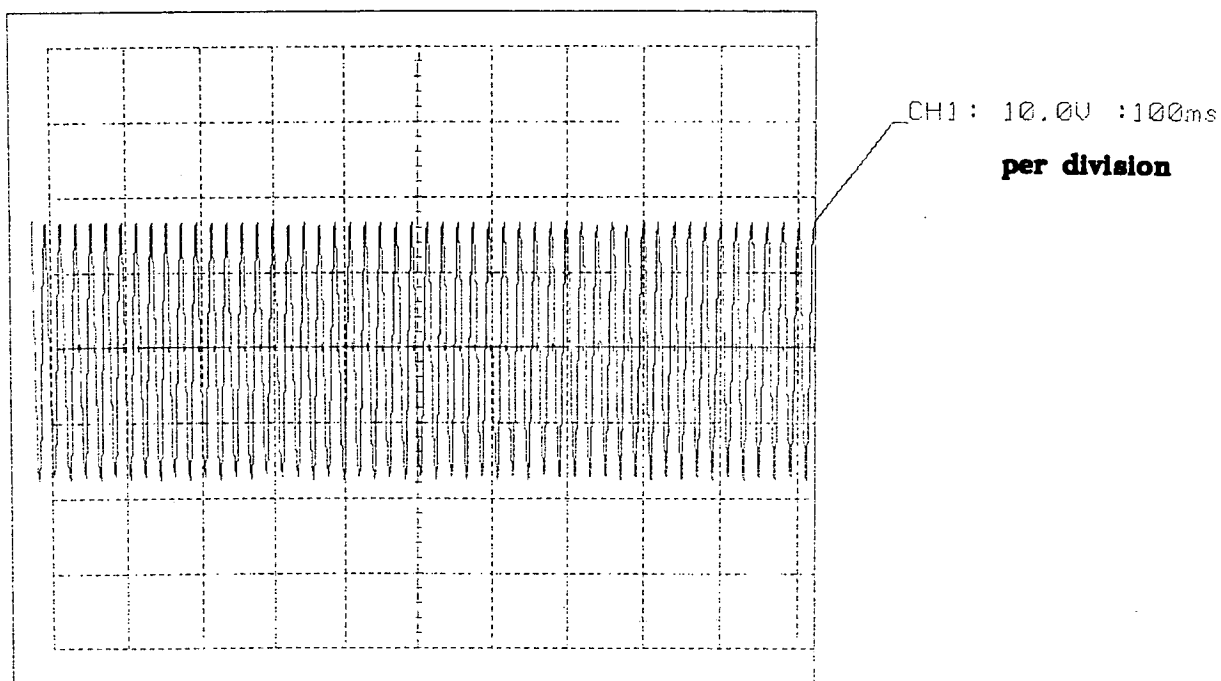


Figure 50d - DSO trace of the a.c. waveform

## 5.5 DATA ACQUISITION SYSTEM

To enable detailed analysis and long term storage of the experimental data, a microcomputer based data acquisition system was established, using the DSO as the initial data capturing instrument. The microcomputer on which the data acquisition software is mounted is an Intel 386, fitted with an IEEE-488, GPIB interface card. A program, *meas.c*, was written to the author's specification by J. Dorner, a technician in the Electrical, Electronic & Computing Department of Napier University. The program was developed using the National Instruments LabWindows(V1.2) data acquisition and instrument control software package. Presently, this program is designed to capture data for the transient frequency analysis, refer Section 7.2.1. It will be possible in the future to expand the functions of the program as necessary.

The event to be analysed is captured on the DSO using a suitable trigger signal on channel 2. For the frequency analysis, the signal PA2 (refer figure 50c) is captured on channel 1 and stored by the DSO. On instruction, the program *meas.c* then interrogates channel 1 for the data relating to the signal PA2. Successive negative going edges are analysed to determine the period and the instantaneous time, and hence a plot of frequency vs time is obtained and displayed on the screen. The frequency and time data is also saved onto disc. Presently this data is used to prepare hard-copy plots of the frequency transient, an example of which is given in figure 51.

---

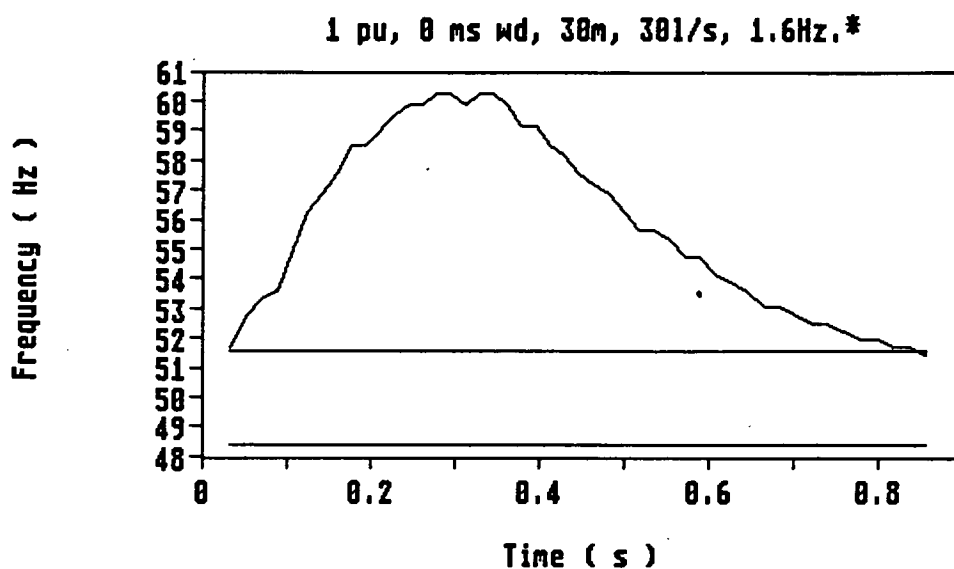


Figure 51 - Typical plot from the data acquisition system

\* The data at the head of this plot and all subsequent, similar, plots in Chapters 6 and 7 gives the following information;

1 pu	advises the per unit value of the load rejection.
0 ms wd	advises the duration of the wait delay in ms.
30m	advises the operating head in m.
30l/s	advises the operating flow in l/s.
1.6Hz	advises the deadband selection, 50Hz +/- the value.

---

## CHAPTER 6. THE ELG IN OPERATION

### 6.1 COMPARISON WITH PROPOSED DESIGN

In Chapter 2, the rationale for the design of the ELG was examined and the proposals made at the outset of this study were given. It is worthwhile at this stage of the thesis to compare briefly the outcome of the design phase with the original objectives.

#### 6.1.1. Technical Compliance

Section 2.1 discussed the technical aspects of the problems with existing ELG units and an alternative design was proposed. The resulting prototype compares favourably with the proposals as follows;

- i) The adoption of the binary load switching technique after a variable wait delay, and in conjunction with zero-voltage solid state relays, overcomes the problems identified with the phase angle control technique and integral cycle control.
  - ii) The use of synchronous generators overcomes the problems associated with excitation of induction generators in isolated operation and the related voltage regulation problems.
  - iii) The deployment of digital circuits and a single chip microprocessor overcomes the problems associated with analogue circuits and multi chip processors.
-

iv) The incorporation of a load balancing routine solves the problems which occur due to unbalanced load operation.

v) The built-in power supply which takes its power from the generator terminals avoids the need for separate power supplies, permits black start operation, and the ELG starts and stops automatically on power-up/power-down.

vi) Once commissioned, no operator intervention is necessary and there are no external control devices which can be tampered with.

All designs are a compromise, and it is recognised that item i) above is achieved at the expense of "tight" frequency control, the frequency is allowed to vary within a deadband rather than be held exactly at 50 Hz. Also, item ii) involves the higher cost of a synchronous generator, however it is the opinion of the author that this is a worthwhile expense, particularly in rural situations where power transmission may be over relatively long distances. It is considered that items iii) to iv) do not significantly compromise the design.

### **6.1.2. Economic Compliance**

The cost figures presented in this Section relate to the component purchase and the assembly/test of an ELG system. These costs specifically exclude the "prototype" costs which would be dominated by the labour cost of the research, design and programming, and would also include an element of component purchase for the original trial circuits. The purpose of this analysis is as a comparison with the

---

market selling price figures presented in Section 2.2. The cost of the ELG unit itself is independent of the rating of the installation, whereas the cost of the solid state relays is current dependent. As a result, it is necessary to determine the cost of each separately.

### ***ELG***

The cost of;

- 1 - FORTH Microcard assembled complete with all necessary components.
- 1 - I/O PCB assembled complete with all necessary components.
- 1 - Transformer, 240:12:12V, 20VA.
- 1 - Sheet steel enclosure.
- 1 - Set of internal wiring and connections.

at 1992 prices is £420 including the preparation of the EPROM, the fabrication of the enclosure, the assembly of the unit and its functional testing. It is estimated that 60% of this cost is the assembly cost which could reduce substantially if local manufacture is adopted.

### ***Solid State Relays***

The cost of;

- 9 - Solid state relays.
- 9 - Heatsinks ( if required ).
- 1 - Enclosure.
- 1 - Set of internal wiring and terminals.

at 1992 prices is £280 for a 10 kW unit and is £480 for a 60 kW unit including the fabrication of the box, assembly and functional testing.

---

The higher cost for the latter is a function of the increased current rating of the relays and the need for heatsinks at this rating.

The total cost for both the ELG and the solid state relays is thus £700 for the 10 kW rating and £900 for 60 kW. These costs exclude the current transformers, the provision of electrical loads, manufacturing overheads, profit margin, taxes, packing and delivery. On the other hand, these costs are based on the assembly, in the Napier University workshop, of a single unit, and thus do not include the expected cost benefits arising from full scale production or local manufacture and assembly.

The costs presented above highlight the problems of dis-economy of scale at the lower power ratings. The total cost per kW is £70 for the 10 kW unit, yet only £15 for the 60 kW unit. In comparison with the target figures of Section 2.2 the above costs compare favourably.

## **6.2. FUNCTIONAL TESTING OF THE ELG**

### **6.2.1. Running In**

The initial testing of the completed ELG took place on the d.c. motor driven generator set. The later availability of the water turbine driven generators presented an opportunity to perform both new tests and repeat some of those previously carried out on the d.c. motor driven set. The results of these tests are described below.

---



### ***Power-up***

For the turbine-generator sets, the terminal voltage of the generator builds up as the set increases in speed. Typically, the run-up time is about 20 - 30 seconds. It is thus possible to monitor visually the voltage rising. Referring to Section 3.3.5., the ELG unit should power-up when the voltage applied to the transformer reaches 200V. In the case of the turbine-driven, three-phase generator, the *phase voltage* is supplied to the transformer, so the expected magnitude of line voltage at which power-up should occur is 346V. In practice, the observed value is 320V.

In the case of the d.c. motor driven generator, the line voltage of 240V is supplied to the transformer and power-up occurs at approximately 200V as expected. As this generator has a switch in its excitation circuit, it is possible to make and break the excitation current rapidly. In this event, the generator terminal voltage rises/falls within a few seconds.

On power-up, the ELG performs its initialisation routines and begins operation, usually before the set has reached full speed. The magnitude of the connected consumer load may vary at the instant of power-up, but the ELG responds as determined by the system frequency. Assuming that the turbine is operating at rated head and flow, if the consumer load is at 0 p.u., then sufficient ballast load is added to match the turbine output power and set the frequency within the deadband. If the consumer load is at 1.0 p.u. then no ballast load is added as the frequency does not exceed the deadband.

---

On power-down, as the turbine-generator set is shut-down, the ELG remains powered-up until a speed corresponding to 40Hz is reached, and thus it inherently removes all connected ballast load as the speed falls. Below 40Hz, the ELG powers-down and ceases operation until the set is re-started. Rapid switching of the generator field, as is possible on the d.c. motor set, causes no adverse effects to the operation of the ELG, it powers-up or down in response to the terminal voltage magnitude.

### *Teething problems*

During the testing of the prototype unit to date, only two significant teething problems have been encountered. The first of these manifested itself as spurious operation of the ELG with output lines switching at random. It was noticed that this problem only arose on one specific ELG unit, the one which had been used for both single phase and three phase operation. Conversion from single to three phase operation necessitates the replacement of the EPROM on the FORTH Microcard, and it is considered that the physical disturbance to the Microcard to effect this operation caused the microprocessor chip to be dislodged slightly from its holder, resulting in this spurious switching as output lines change state.

This problem serves to highlight the danger of encouraging operators to replace individual integrated circuits, even when they are skilled and trained personnel. The less disturbance there is to the printed circuit boards, the less likelihood there is of faults occurring.

---

The second problem was noticed during routine steady-state turbine testing of the three phase ELG unit. Generally speaking, whenever the frequency is less than the lower limit of the deadband, and there is ballast load connected, the ELG should disconnect ballast load until either the frequency rises above the lower deadband limit or the ballast load is fully disconnected. It was observed that under certain unbalanced load situations, the frequency was outside the lower limit and the connected ballast load was not being removed from the circuit.

The reason for this lies in the relative values of the phase currents and in the load balancing algorithm, refer Section 4.3.3. Typically the current magnitudes would be 5.6A, 6.1A and 6.3A for the red, yellow and blue phases respectively - with only red phase ballast load remaining connected. The balancing word, DECLOAD, establishes that the blue phase current is the highest, but is unable to remove any further load from that phase and does not address the other two phases.

#### **6.2.2. Parameters for Steady-State Operation of the Boving Turbine**

Functional testing of the ELG on the Boving turbine driven, three phase generator, essentially comprised witnessing and assessing its operation whilst the consumer load was varied. Initial tests determined that the ELG satisfactorily responded to consumer load changes in either a single phase only or across all three phases, including instantaneous rejection of the full consumer load. Within its programmed operational restraints, and subject to the problem mentioned above, the ELG balances the three phases as expected. The balancing action is performed as part of the load change routine and thus is only

---

operational when the frequency is outwith the deadband. The typical margin of imbalance is  $\pm 1$  ballast load step per phase, i.e.  $\pm 14\%$  of the line current. This is considered to be a significant improvement over the prospect of operation without a balancing routine. The margin could be reduced if the ballast load were split into 4 sections per phase, but this would involve a penalty of additional relays and output lines.

Over a range of operating heads, the remaining tests were concerned primarily with determination of the validity of the deadband predictions given in Section 5.3.1. This involved the removal of a fraction of the consumer load of sufficient magnitude to cause the frequency to leave the upper deadband.

Using standard terminology<sup>53</sup>, the system is said to be;

- asymptotically stable if the frequency returns to the initial value, either directly, or with oscillations, as time approaches infinity.
- marginally stable if the oscillations remain constant.
- unstable if the frequency grows uncontrollably.

If the deadband is made too narrow, either unstable or marginally stable operation will occur. The nature of the oscillation is that as the frequency overshoots, say, the upper deadband limit, the ELG corrects this, and then the frequency overshoots the lower deadband limit. From the system user's viewpoint, oscillatory operation would be unacceptable and the sooner that stability is achieved the better.

The parameters available during commissioning to obtain satisfactory stability are the deadband width and the added wait delay. It is

---

necessary to define the parameters for "steady-state" operation as *the deadband and wait delay settings which will ensure asymptotically stable operation when the system is subject to small-scale disturbances*. It must be accepted that in the "steady-state" the frequency may vary between the lower and upper deadband limits.

A mathematical approach to identifying satisfactory stability would involve the identification of the roots of the characteristic equation of the system, which itself is obtained from the system transfer function. As will be seen in Chapter 7, the solution of the transfer function has not been completely determined and so stability has not been assessed in other than a subjective manner.

Having established which parameters secure asymptotically stable operation, it remains to define an acceptable value for *infinite time*. The object of these tests was to determine the optimum deadband and wait delay settings which would permit a return to a steady-state operation of the system *within a few seconds*. The period during which the ELG performs its initial switching of the ballast load is typically up to 1 second in duration. As the system settles, there is often a further period of ballast load switching activity before absolute stability is reached, typically after 1 - 2 seconds.

The performance of the system during the initial transient period is analysed in Chapter 7: this Section is concerned only with the ability of the ELG to return the system to a stable condition within a reasonable time, say less than 5 seconds - the definition therefore of *infinite time* for this system.

---

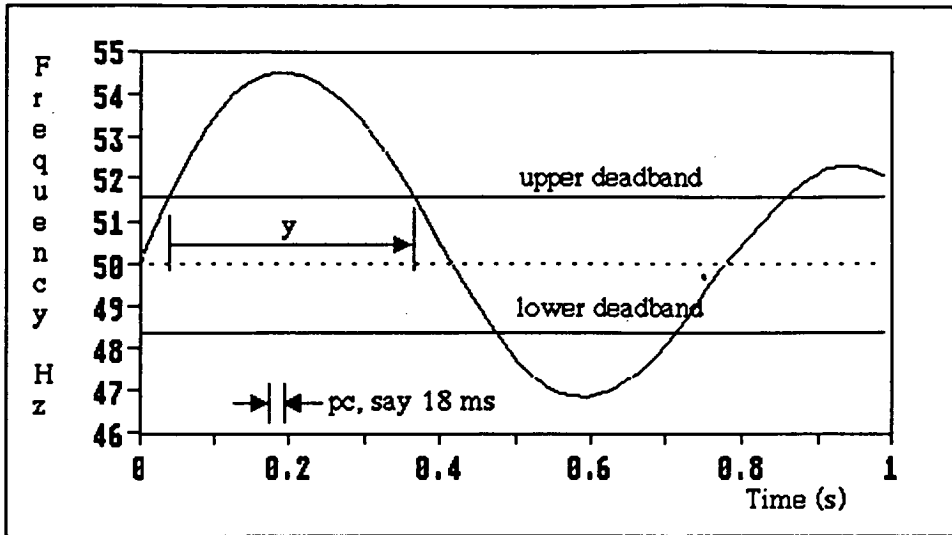


Figure 52 - Frequency transient for small-scale load rejection

The need for added wait delay to the program cycle duration,  $pc$ , is demonstrated in figure 52. This shows the effect of a small-scale (0.5 p.u.) step reduction in the consumer load which has caused the instantaneous frequency to rise above the upper deadband for a significant period of time,  $y$ , where  $y$  is greater than  $2pc$ . As long as the measured frequency remains above the upper deadband level, then an additional step of ballast load will be added every  $pc$  ms. As the load change is less than 1.0 p.u. then the ELG has the opportunity to add more ballast load than is required. Thus it is possible for an excessive number of steps of ballast load to be added with the result that unstable operation occurs.

Figure 53a shows a DSO trace of the first ballast load step in the blue phase switching in response to a small-scale consumer load change on the Boving turbine. The deadband selected is  $\pm 1.28\text{Hz}$  and the trace shows instability over the full 5 seconds of the duration of the trace.

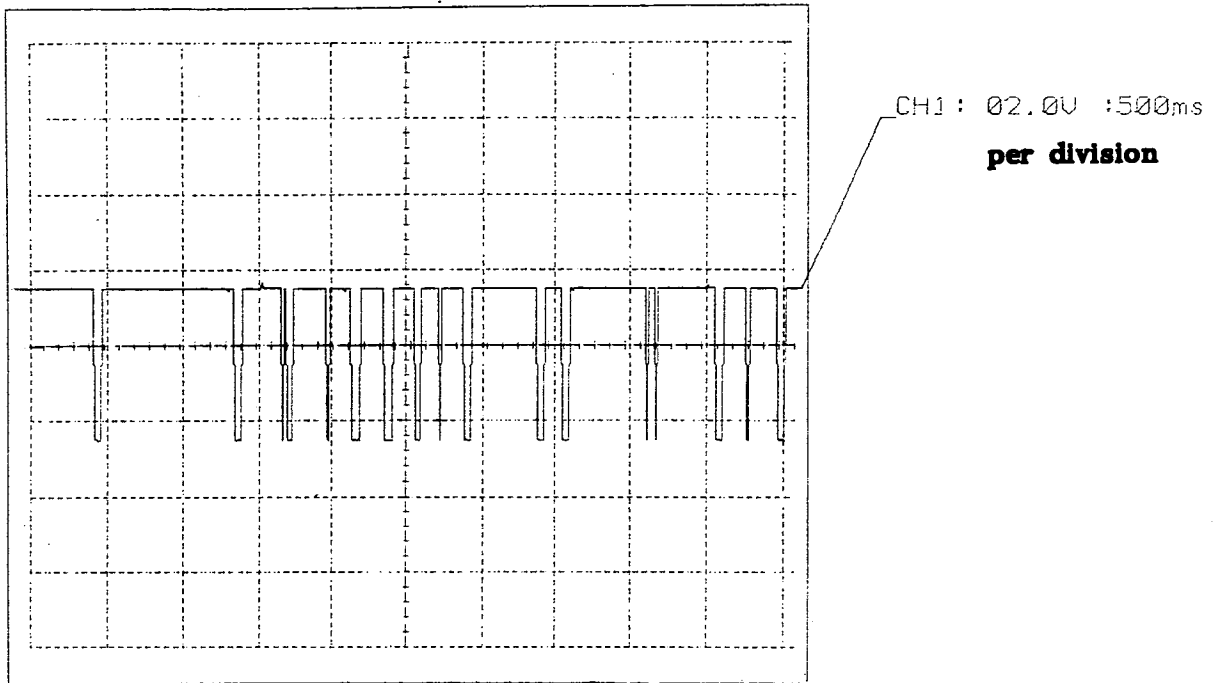


Figure 53a - Demonstration of instability

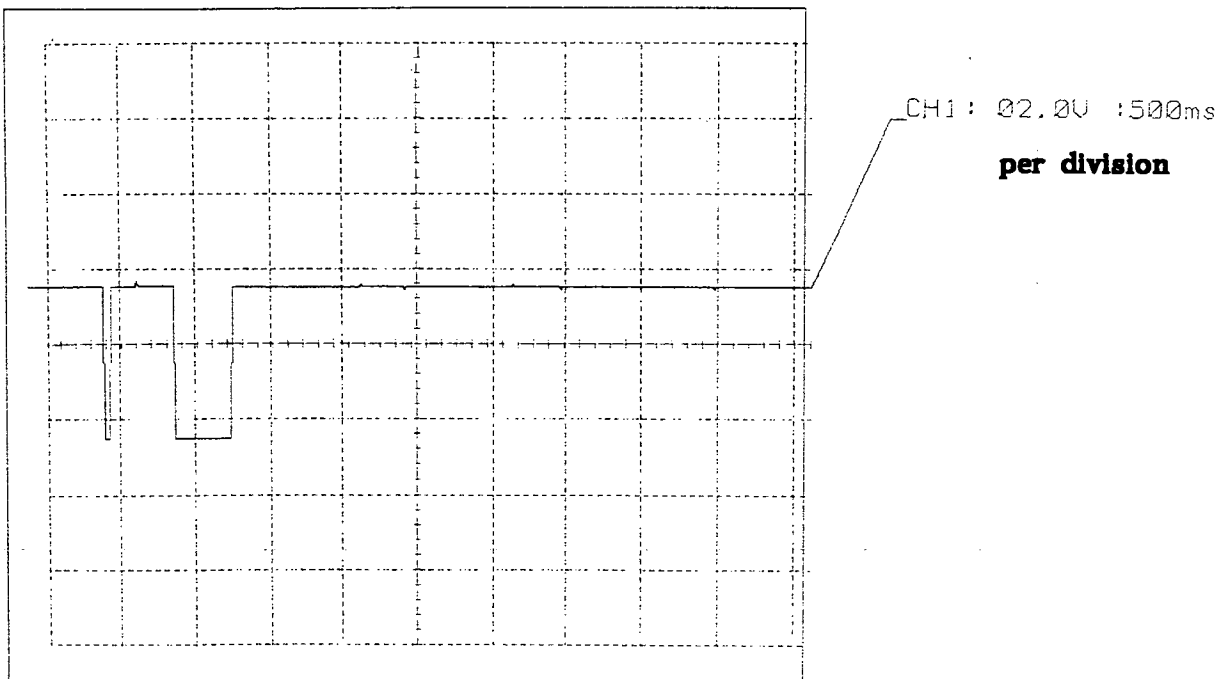


Figure 53b - Stable operation with added wait delay

To limit this effect, either the rate of rise of the frequency can be limited through the addition of inertia to the rotating shaft system<sup>33</sup>, or the program cycle time can be increased by the addition of wait delay. The latter, a simple software option, has the effect of limiting the number of ballast load switching operations which take place during excursions of the frequency outwith the deadband. In this way, addition of wait delay has the same effect as adding inertia to the system.

For a given droop and deadband selection, the coefficient of stability can be determined, refer equation 2.3. If the deadband is subsequently reduced, then the coefficient of stability will reduce and the probability of further switching will be higher. This can be counteracted through the addition of wait delay which can also be considered as compensating for the narrower deadband setting. Figure 53b represents the same conditions as for figure 53a, except that a wait delay of 12ms has been added. This shows that the system has stabilised after approximately 1 second, demonstrating the effect of the wait delay.

The procedure for these tests involved;

1. the selection of the desired deadband and wait delay on the ELG microswitches,
2. the switching out of the consumer load in the order of 0.068 to 0.2p.u.,
3. the visual monitoring of the operation of the ELG and of the frequency meter.

This procedure, along with calibration of the current balance potentiometers, represents the commissioning procedure of the system at a site. The decision as to satisfactory selection of the minimum

---



deadband for stable operation is presently very much a subjective one. Where practicable, the initial frequency and voltage before the instant of switching were the same. For operational reasons it was not possible to guarantee identical test conditions in each case. The results of these tests are given in Table 9 below. Table 10 gives a comparison of these with the deadband settings determined from both the predicted droop curve and the measured droop curve, refer Section 5.3.1.

<u>Head</u> <u>(m)</u>	<u>Wait Delay (ms)</u>				<u>p.u. load</u> <u>change.</u>
	<u>0</u>	<u>4</u>	<u>8</u>	<u>12</u>	
32	1.92	1.60	1.60	1.60	0.123
30	1.92	1.60	1.60	1.60	0.122
28	1.60	1.60	1.28	1.28	0.122
25	1.28	1.28	1.28	1.28	0.068
22	1.60	1.60	1.28	1.28	0.200

**Table 9 - Deadband Settings (+-Hz) for Varying Head and Wait Delay**

The above results display the trends of two separate effects. For a given installation, as head increases then the deadband setting required also increases. In addition, as the wait delay is increased then the deadband setting can reduce, demonstrating how the wait delay compensates for a reduced coefficient of stability caused by a narrower deadband selection. The addition of wait delay has the disadvantage that the overall time for stability to return is increased; a balance requires to be found between the acceptable operating deadband and the duration of the transient period. The effect on the transient period is discussed in more detail in Chapter 7.

<u>Head (m)</u>	<u>Deadband Source</u>		
	<u>Predicted</u>	<u>Measured</u>	<u>Test</u>
	<u>Droop (Hz)</u>	<u>Droop (Hz)</u>	<u>Outcome (Hz) *</u>
32	+ - 1.6	+ - 1.92	+ - 1.6
30	+ - 1.6	+ - 1.6	+ - 1.6
28	+ - 1.28	+ - 1.28	+ - 1.28

\* for wait delays of 8 and 12 ms.

**Table - 10 Comparison of Deadband Selections**

The deadband values in Table 10 are not strictly on a like-for-like basis. The range of load change applicable to each is different; also, the "ideal" minimum ballast load step (0.0476 p.u.) was used in the calculation for the predicted droop, whereas the as-installed value (0.0633 p.u.) was used in the other two instances.

### 6.2.3. Parameters for Steady-State Operation of the Gilkes Turbine

As the generator connected to this turbine is a single phase machine, the emphasis of the functional and performance testing of the ELG has been on the Boving turbine. Nevertheless, the performance of the ELG on a single phase system was of interest; indeed chronologically, this was the *first* turbine which the ELG controlled. The principle function of the steady-state tests was again to determine the deadband and wait delay selections which would give an optimum return to stability in response to small-scale load changes.

The duration of the single phase program cycle,  $pc$ , is 7.5 ms, considerably less than the 20 ms period of a 50 Hz waveform. Switching

of the ballast load at this rate leads to high instability of the system. For the steady-state testing on the Gilkes turbine, a minimum addition of 8 ms wait delay was found necessary, increasing the overall program cycle time to approximately 16 ms, notably still within the 20 ms period of a 50 Hz waveform.

Using the same experimental technique as that used on the Boving turbine, the optimum deadband for the nominal operating head of 19 m is found to be  $\pm 1.28$  Hz, provided a wait delay of 8 ms is added to the program cycle time. This deadband value coincides with the prediction from the measured droop curve in Section 5.3.2.2.

#### **6.2.4. Parameters for Steady-State Operation of the Francis Turbine**

Mackintosh<sup>52</sup> determined that the deadband required for steady-state operation of the Francis turbine was  $\pm 1.6$  Hz, less than either the predicted value or the measured value. In the determination of these values the coefficient of stability will have been greater than, or equal to, 1. In practice, operation with a deadband of  $\pm 1.6$  Hz is possible, but with a reduced coefficient of stability and therefore a greater tendency towards unstable operation.

#### **6.2.5. Summary**

The results of the previous Sections demonstrate that the simple deadband prediction technique derived in Section 5.3.1.3. is an acceptable first order estimation of the deadband value that is required for steady-state operation of the turbine. Further, this prediction can be

---

made with knowledge only of the ratio of the runaway speed to the normal running speed of the turbine. Selection of a narrow deadband is desirable in order to reduce the frequency variation which occurs in "steady-state" operation. However, there is a trade-off between this and the reduction in the coefficient of stability. This can be compensated for by the addition of wait delay, however, this in turn extends the duration of the transient period before steady-state conditions return.

#### 6.2.6. Parameters for Steady-State Operation of Other Turbines

The prediction technique can be used to determine the deadband setting required for any turbine, given knowledge of its runaway speed ratio. Table 11 below presents typical runaway speed ratios and the resultant deadband setting - assuming three phase operation.

<u>Turbine</u> <u>Type</u>	<u>Range of</u> <u>Ratios</u>	<u>Average</u> <u>Ratio</u>	<u>Droop</u> <u>(Hz)</u>	<u>Predicted</u> <u>Deadband (Hz)</u>		<u>Coefficient</u> <u>of Stability*</u>
				<u>Calc</u>	<u>Next</u>	
Pelton	1.5 - 1.8	1.65	32.5	1.55	+1.6	1.06
Francis <sup>54</sup>	1.6 - 1.9	1.75	37.5	1.78	+1.92	1.16
Propellor <sup>54</sup>	2.0 - 2.4	2.2	60	2.85	+2.56	0.8

\* refer equation 2.3

**Table 11 - Predicted Deadbands for Other Turbine Types**

Given the existing limit of deadband selection of  $\pm 2.56$  Hz, when the runaway speed ratio exceeds 2.075, the coefficient of stability drops below 1.0 and "ideal" deadband selection is not possible. Extrapolation determines that the maximum theoretical runaway speed ratio that could

be tolerated is 3.2. This would imply operation at the extreme point of marginal stability. Allowing a 10% margin as a practical stability limit suggests that the maximum tolerated runaway speed ratio will be 2.93. This figure is higher than those associated with most common turbine types and therefore the ELG, as it is presently designed, has a wide application range.

### 6.3 INTERACTION WITH THE GENERATOR EXCITATION

The two turbine driven generators have voltage control systems which cater for speed regulation of +4.5% ( ie +2.25 Hz ) from full load to no-load. Provided that the turbines are governed to this degree of accuracy then it is expected that the terminal voltage will stay within  $\pm 3.5\%$  of the rated value at power factors of 0.8 or better<sup>55,56</sup>.

Without the application of a governor, the high speed-variation obtained from the turbine speed-load characteristic results in a high variation of the terminal voltage also, refer figure 54. As these generators have no automatic voltage regulator (AVR), then the extent of the voltage variation during transient switching operation of the ELG depends on the extent of the speed excursion outside of the range with which the excitation system is designed to operate. It is to be expected that once the speed is outwith the design speed range then the instantaneous terminal voltage will be an approximation to the values plotted in figure 54. The magnitude of the voltage fluctuation during full-load switching transients is studied in Section 7.2.2.

---

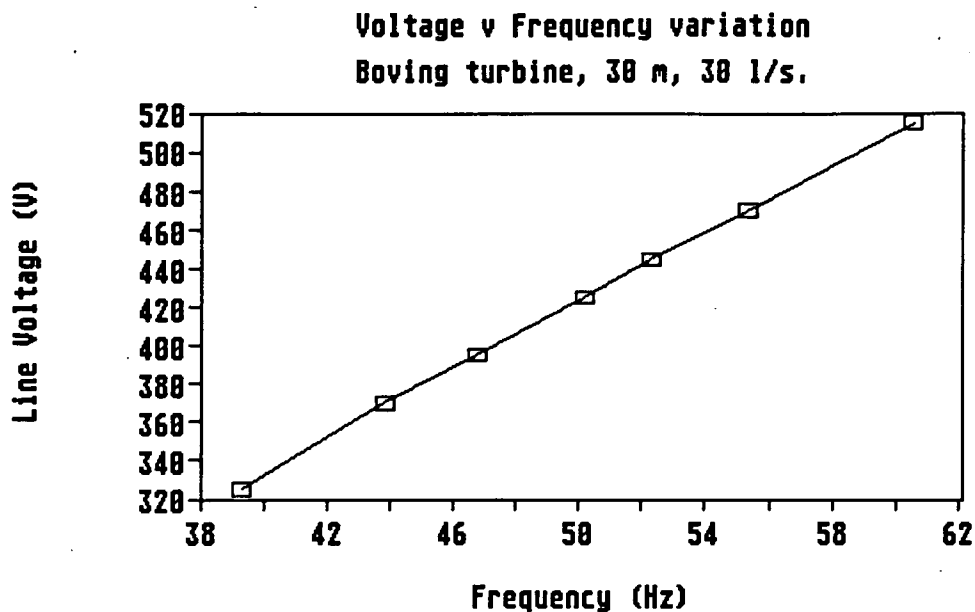


Figure 54 - Plot of voltage variation with frequency

#### 6.4 OPERATION WITH UNIFORM BALLAST LOAD

A test was performed on the single phase version of the ELG where the 4 sections of the ballast load were of equal magnitude. From equation 2.2, it was expected that as the minimum step of ballast load which could be added was now 0.25 p.u. instead of 0.067 p.u. then the deadband would need to be increased pro rata. The resulting calculated deadband value when compared to the upper limit of  $\pm 2.56$  Hz gives a negative value for the coefficient of stability. Hence, the existing design of the ELG would theoretically not be able to effect stable control of this system. With no added wait delay this proved to be the case but with only 4 ms wait delay, stable operation was achieved, again demonstrating the compensation effect of the wait delay.

---

## CHAPTER 7    TRANSIENT PERFORMANCE STUDIES

The measure of the performance of any governor is its reaction to a rejection of the full load, in this case the disconnection of 1.0 p.u. of the consumer load. The performance indicators are the rise in frequency during the transient period and the time taken for the frequency to return to the steady-state condition.

This Chapter is primarily concerned with the study of the frequency transient of the Boving turbine system under the control of the ELG. The period studied is the first second immediately after the instantaneous full load rejection (FLR) and the detailed study is limited to the frequency variation with time. Longer term stability is not included in this study. Provided that the ballast load is approximately equal to the consumer load, then, on loss of the full consumer load, the reaction of the ELG can only be to connect an equal amount of ballast load and, provided there are no other disturbances during this period, the system is bound to return to the initial conditions.

The aim of this study is the production of a model, the main purpose of which is to provide a means whereby the transient frequency performance of the system can be predicted, with a known degree of accuracy, for specified operating limits. In this case *the system* is the ELG controlling the frequency of a hydroelectric installation. It is implicit in the production of a model that it requires validation against reliable empirical data.

---

## 7.1 THEORETICAL CONSIDERATIONS

This Section presents the theory of the frequency transient in response to a full load rejection for a Pelton type water turbine.

### 7.1.1. Torque Balance

Neglecting the elastic and the loss torques<sup>57</sup>, then the instantaneous torque balance on the rotating system is;

$$T_a = T - T_e \quad (\text{Nm}) \quad (7.1)$$

where  $T_a$  is the net accelerating torque,  $T_e$  is the electrical load torque and  $T$  is the turbine output torque, all in Nm. When  $T_e = T$  then the accelerating torque is zero and the rotating system is in the steady state. When there is an imbalance between these torques, such as the electrical load torque reducing, there is an accelerating torque and the angular speed of the system will increase until the torque equilibrium is restored.

The rate of change of the turbine angular speed,  $\omega$ , is<sup>57</sup>;

$$d\omega/dt = T_a/J \quad (\text{rad/s}^2) \quad (7.2)$$

where  $J$  is the total inertia of the rotating elements of the system, with units of  $\text{kgm}^2$  as a  $WR^2$ .

For load governing, the electrical load torque comprises two components;

$$T_e = T_{cl} + T_{bl} \quad (\text{Nm})$$



where  $T_{cl}$  is the consumer load torque and  $T_{bl}$  is the ballast load torque.

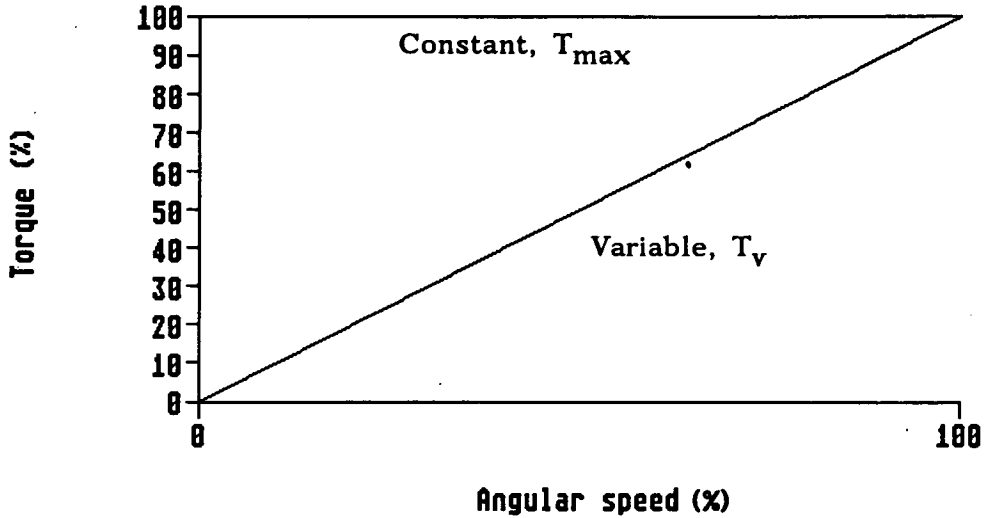


Figure 55a - Turbine torque components

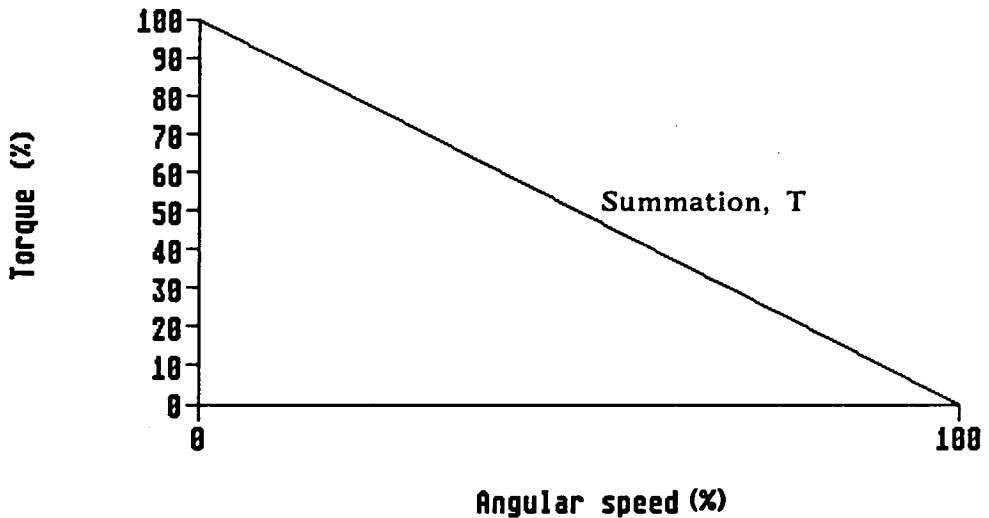


Figure 55b - Turbine output torque

In addition, referring to figure 55, the turbine output torque can be considered as having two components,  $T_{max}$  which is constant and  $T_v$  which varies proportionately with the angular speed ( and hence with the frequency,  $f$ , of the generated waveform ), such that;

$$T = T_{max} - T_v \quad ( Nm )$$

The initial conditions prevailing before the transient period are defined as;

$$T_{bl} = 0 \text{ p.u. ; } T_{cl} = 1.0 \text{ p.u. ; } f = 50 \text{ Hz ; } T = T_e \text{ hence } T_a = 0.$$

and once again the electrical loads are assumed to be purely resistive.

### 7.1.2. The Ungoverned Frequency Transient

With no form of governing present, i.e.  $T_{bl}$  remains at 0 p.u., in the event that  $T_{cl}$  undergoes an instantaneous step change to 0 p.u.,  $T_a = T_{max} - T_v$  and the speed of the system begins to rise. However, as  $T_v$  is proportional to  $f$ , then  $T_a$  reduces to 0 when  $T_v = T_{max}$  and the speed returns to a steady-state condition at a higher level - in this case the runaway speed of the turbine. The angular speed vs time response of such a system has an exponential form<sup>48</sup> such that;

$$\omega(t) = \omega_d [1 - \exp^{-t/\tau}] \quad (7.3)$$

where  $\omega_d$  is the total change in the turbine angular speed from the initial value to the final value and  $\tau$  is the mechanical time constant.

The general rules covering the mechanical transient performance of any similar rotating system are the same and the following derivations are based on the rules relating to a d.c. motor. For such a motor<sup>58</sup>,

$$\omega_d = T_1.k \quad \text{and} \quad \tau = J.k$$

where  $T_1$  is the step change in torque which produces the torque imbalance and  $k$  is a constant, common to both equations. Relating these equations to this application then;

$$\omega_d = T_a \cdot k_1 \quad \text{and} \quad \tau = J \cdot k_1$$

For a given installation, there is a direct relationship between  $\omega$  and  $f$ , and in the case of the Boving turbine,  $f = 0.62\omega$ . The expression for the *frequency change* on loss of electrical load thus becomes,

$$f_d = T_a \cdot k_2 \quad (7.4)$$

where  $k_2 = 0.62 \cdot k_1$

$$\text{and } \tau = J \cdot k_2 \quad (7.5)$$

The change of frequency can be determined simply from knowledge of the ratio of the turbine runaway speed,  $N_{ra}$ , to its normal running speed,  $N$ , ( which would equate to a generated frequency of 50 Hz ). This ratio is available from the turbine manufacturers for a given turbine operating on given hydraulic conditions; thereafter,

$$f_d = (N_{ra}/N - 1) \cdot 50 \quad \text{and} \quad f_{ra} = f_d + 50$$

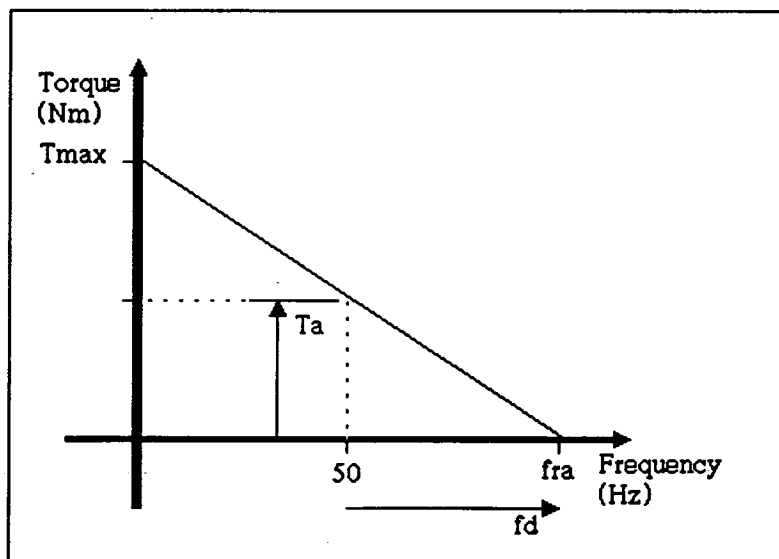


Figure 56 - Torque vs frequency relationship

From equation 7.4,  $k_2 = f_d/T_a$  and is equivalent to the slope of the turbine torque vs frequency plot in figure 56. Assuming that the plot is linear, then

$$|k_2| = f_{ra}/T_{max}$$

where equation 5.19, with  $u=0$ , is combined with equations 5.9 and 5.11 to give,  $T_{max} = 2\rho QrC_v\sqrt{2gh}$  ( Nm ) ( 7.6 )

Hence in equation 7.5,

$$\tau = J.f_{ra}/T_{max} \quad ( 7.7 )$$

and 7.3 can be expressed as the *frequency* transient such that

$$f(t) = f_d[1 - \exp^{-t/\tau}] \quad ( 7.8 )$$

where  $f_d$  and  $\tau$  can be determined from the turbine and hydraulic parameters.

### 7.1.3. Inertia Estimation

Of all the turbine parameters required for the application of equation 7.8 to the Boying turbine, the inertia,  $J$ , was the only one for which the magnitude was unavailable from prior sources. Two separate methods were used to determine the inertia of the rotating system; however, as both depended on either assumptions or experimental data from equipment of uncertain calibration, the outcome of both methods is of questionable accuracy.

Tests were performed to determine the deceleration curve of angular speed vs time for the rotating components. Using equation 7.2 for

no-load conditions then,

$$J.d\omega/dt = P_{out}/\omega$$

An experimental technique was developed to plot  $\omega$  vs  $t$  during deceleration caused by the sudden insertion of the jet deflector, and the no-load turbine output power was determined for specific values of  $\omega$ . This method gave values for  $J$  which ranged from 1.13 - 0.26  $\text{kgm}^2$ .

As an alternative to this experimental method, the turbine was stripped and the runner weighed at 55 kg which, with knowledge of the runner radius, enabled the calculation of the runner inertia using the formula for a solid disc<sup>59</sup>. The inertia of the generator was obtained from the manufacturer<sup>60</sup>, and this was reflected through the belt system by the square of the pulley ratio<sup>61</sup>. A small allowance was made for the additional inertia of the pulleys and belts and the resulting inertia figure was 0.67  $\text{kgm}^2$  as a  $WR^2$ . Accepting that errors were present, the inertia figure used for the remainder of the study was 0.67  $\text{kgm}^2$ .

#### 7.1.4. The Load Governed Frequency Transient

It follows that the frequency transient in response to the *application* of electrical load will also be exponential but that the frequency change will be in the opposite direction to that of load rejection. The manner of operation of the load governor is such that a single ballast load step, nominally of magnitude 0.0467 p.u., is applied on every cycle of the program provided that the frequency is above the pre-set deadband, and that the ballast load is not already at its maximum.

---

The mechanical time constant of each of the step load application components is the same as that for the full load rejection component, and the frequency change associated with each step will be  $0.0467.f_d$ , assuming a linear droop characteristic. Hence the expression for the frequency transient due to the application of ballast load step  $n$  will be,

$$f(t)_n = -0.0467.f_d [1 - \exp^{-(t-nt)/\tau}]$$

where  $t$  is the time interval between the application of each step of the ballast load, i.e.  $t = (wd + pc)$  and  $n$  is the integer value of  $t/t$ , assuming that the sequence begins at  $t=0$  and is uninterrupted.

Thus the load governed frequency transient on full load rejection is the instantaneous addition of the full load rejection component and the sum of the step load application components. A typical transient is shown in figure 57 which also shows the maximum frequency point,  $f_{max}$ , and the time for the frequency to return within the deadband, the 'return time'.

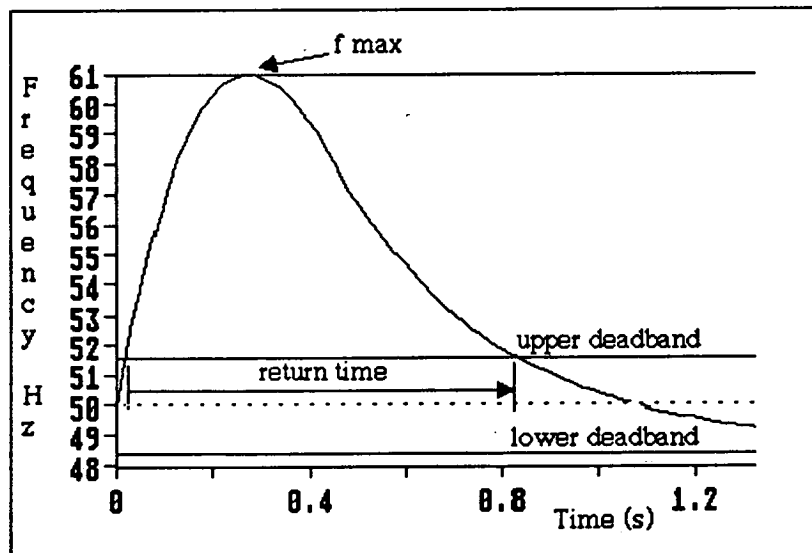


Figure 57 - Typical frequency transient

The rate of the application of the ballast load steps is *primarily* determined by the duration of the program loop when load changes are being effected. This is determined by the sum of the program cycle time, pc, and the added wait delay, wd. Given that pc is fixed ( 18 ms ) then wd has a direct affect on the rate of the ballast load application and hence the overall time for the governor to respond to the full load rejection.

A secondary effect on the rate of application of ballast load steps is the width of the preset deadband. There must be an initial delay in the application of the first ballast load step until the frequency rises out of the deadband and is detected by the ELG. For each of the test systems, the difference in the delay before the high frequency condition is detected proved to be negligible for selection of different deadbands.

#### 7.1.5. Resume

Subject to the assumptions stated in the above derivation, the complete expression for the frequency transient of the load governed system in response to a load rejection is,

$$f(t) = f_d \cdot [1 - \exp^{-t/\tau}] + \sum_{k=0}^n -0.0467 \cdot f_d \cdot [1 - \exp^{-(t-kt)/\tau}] \quad ( 7.9 )$$

The dominant parameters within this transient are as follows;

- i)  $f_d$  - the frequency change between the initial value and the final value on full load rejection. This is directly dependent on the runaway speed of the turbine, which, from Section 5.3.1., is determined by;

$$N_{ra} = (60/\pi).(C_v/D).\sqrt{(2gh)} \quad (\text{rev/min}) \quad (7.10)$$

The centre term,  $(C_v/D)$ , is a function of the particular design of the turbine and will remain constant once that design is selected, thereafter,  $f_d \propto f_{ra} \propto N_{ra} \propto \sqrt{h}$ . Assuming that the full load rejection occurs when the initial frequency is 50 Hz then the final, uncontrolled, frequency value depends on the square root of the head.

ii)  $\tau$  - the **mechanical time constant**. From equation 7.7, this term is proportional to the inertia,  $J$ , and the runaway frequency,  $f_{ra}$ , and is inversely proportional to the maximum turbine torque,  $T_{max}$ .

a) **The inertia** of the rotating components is usually a function of their design. It is possible for inertia to be increased through the addition of a flywheel to the shaft. Increasing the inertia in this way, or by customised design of the rotating plant, has the effect of increasing the time constant which reduces the *rate of rise* of the frequency and hence the value of  $f_{max}$  which can occur during the transient period.

b) **The runaway frequency** varies as described in i) above, ie  $f_{ra} \propto \sqrt{h}$ .

c) **The maximum torque** is given by equation 7.6. Again this will vary both in accordance with the turbine design,  $T_{max} \propto r.C_v$ , and with the hydraulic conditions prevailing,  $T_{max} \propto Q.\sqrt{h}$ . For a given design of turbine, as flow rises then  $T_{max}$  increases,  $\tau$  reduces and the *rate of rise* of frequency increases.



Combining b) and c) implies that  $\tau$  is independent of the head.

iii) **wd** - the wait delay added to the program cycle. This directly affects the duration of the transient, the greater the value of wd, the longer the return time. In addition, wd affects  $f_{\max}$ ; the rate of the application of the ballast load affects the sum of the load application components and hence the instantaneous frequency - refer equation 7.9.

For a given turbine design, with constant parameters and a fixed inertia, the general effects of variable hydraulic conditions on the frequency transient are as follows;

**Head.** The frequency at runaway is proportional to  $\sqrt{h}$  and this affects the final speed that the set would reach if it were not governed. In the load governed situation, the head therefore has a direct influence on  $f_{\max}$ , the maximum value of frequency that occurs during the transient period.

**Flow.** The time constant is inversely proportional to flow. If the flow increases then the rate of rise of frequency increases and, as a result,  $f_{\max}$  also rises.

To minimise  $f_{\max}$  for a given turbine design, the options available are;

- to increase artificially the inertia,  $J$ , of the rotating components of the plant. It is preferable that this is avoided.
-

- to minimise the added wait delay,  $w_d$ , which has the benefit of reducing the return time. This has to be traded off with the need to add a certain degree of wait delay to ensure stability on the occurrence of small-scale consumer load changes.

The reduction of the head and the flow would also achieve the same effect, but at the expense of reduced output power which is undesirable.

## **7.2. MEASURED TRANSIENT PERFORMANCE**

This Section presents the empirical data for the frequency transients against which the model has been validated. Following on from Section 6.3, the voltage during the transient period is also studied.

### **7.2.1. Frequency Transient**

Using the data acquisition system, refer Section 5.5, the frequency over the first second after instantaneous full load rejection was measured. The frequency transient during any one period depends not only on the variables discussed in Section 7.1 but also on the true conditions relating to the parameters which were 'assumed' in the derivation of that theory. For instance, the initial conditions may have differed, e.g. the frequency may not have been exactly 50 Hz; and the hydraulic conditions may have varied during the transient period. Consequently, no two measured transients are likely to be identical. An initial set of measurements were taken to assess the extent of such variation and the measured plots are estimated to be accurate to within  $\pm 0.5\text{Hz}$ .

---

For the Boving turbine, over 70 transient events were captured with variation of both head and/or flow by up to  $\pm 10\%$ . For each transient, a plot was made of frequency vs time which was stored on disc. The selection of deadband at either  $\pm 1.6$  Hz or  $\pm 1.92$  Hz made negligible difference to the outcome of the frequency transient and those presented below are all based on a deadband setting of  $\pm 1.6$  Hz. The operational deadband limits have been added to the plots in the process of their preparation.

The variation in the frequency transient for head values of 27, 29, 31 and 33m is shown in figures 58a to 58d respectively. The flow rate was 31 l/s and these tests were performed with no added wait delay. As predicted in Section 7.1, the trend is for  $f_{\max}$  to increase from 59.1 Hz to 62.1 Hz as the head increases.

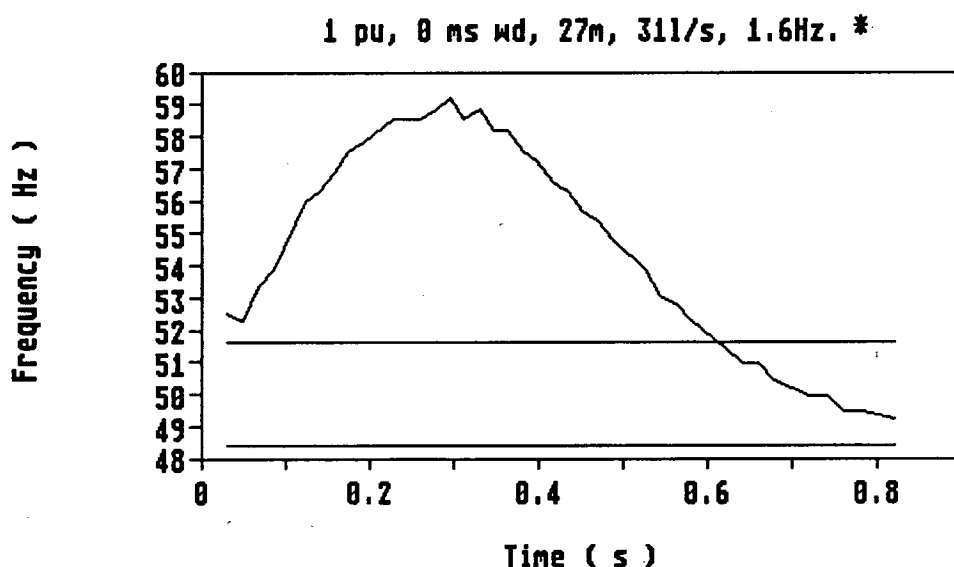


Figure 58a - Measured frequency transient for 27m head and 31l/s flow

\* Note : for a description of the notes at the head of these plots refer to Section 5.5.

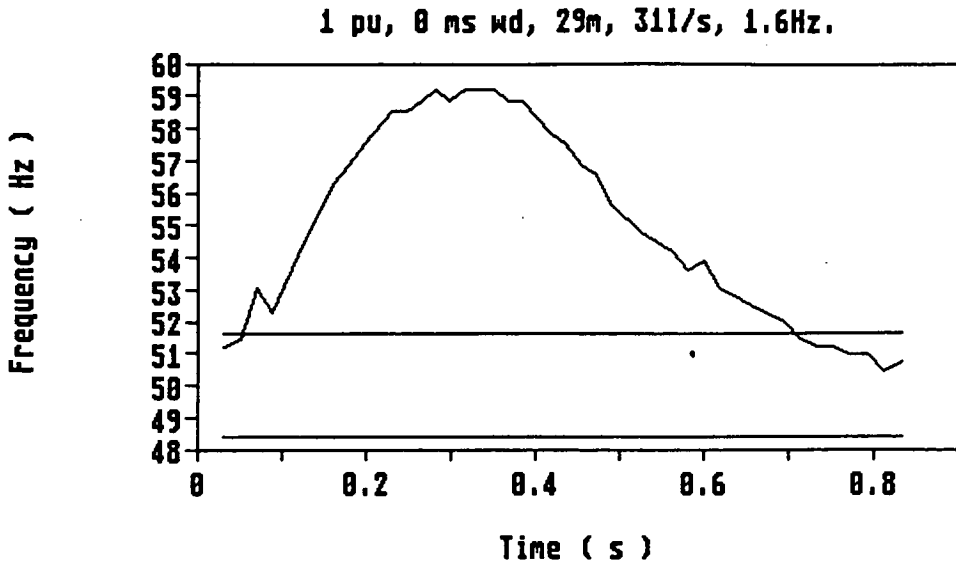


Figure 58b - Measured frequency transient for 29m head and 311/s flow

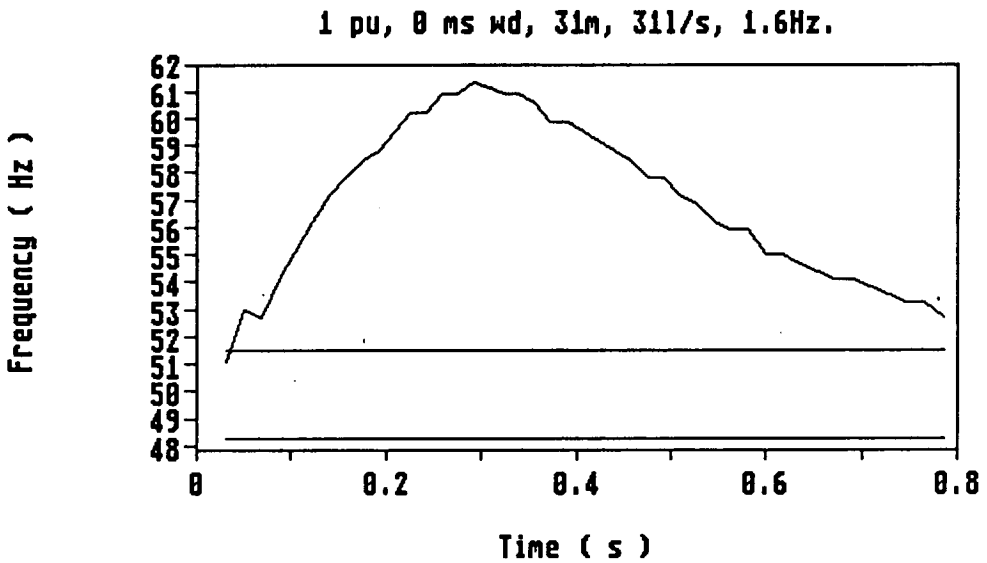


Figure 58c - Measured frequency transient for 31m head and 311/s flow

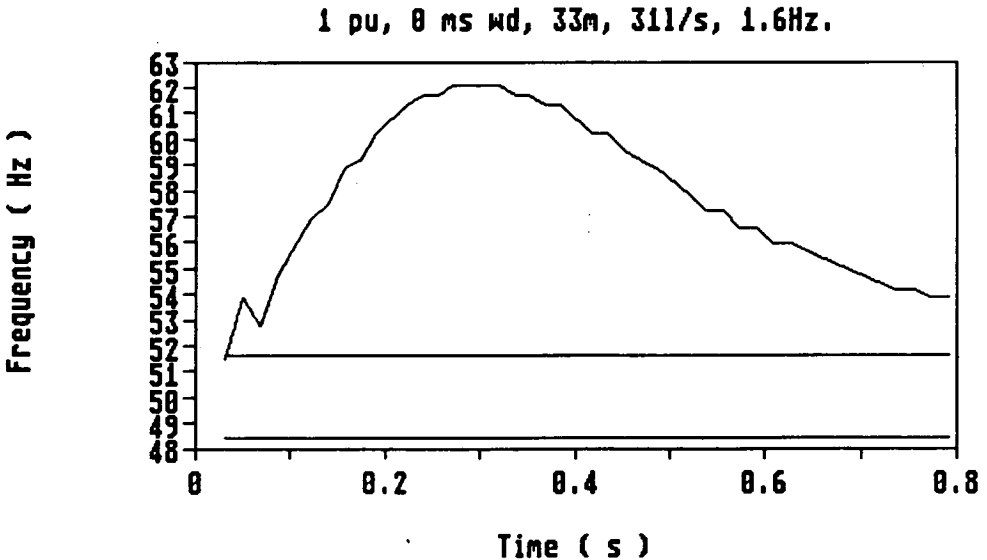


Figure 58d - Measured frequency transient for 33m head and 311/s flow

Figures 59a to 59d show the frequency transient for flow rates of 27, 29, 31 and 33l/s respectively. With the head constant at 30m and again with no added wait delay, the trend is also as predicted; as flow increases then the magnitude of  $f_{max}$  increases, from 58.8Hz to 61.7Hz.

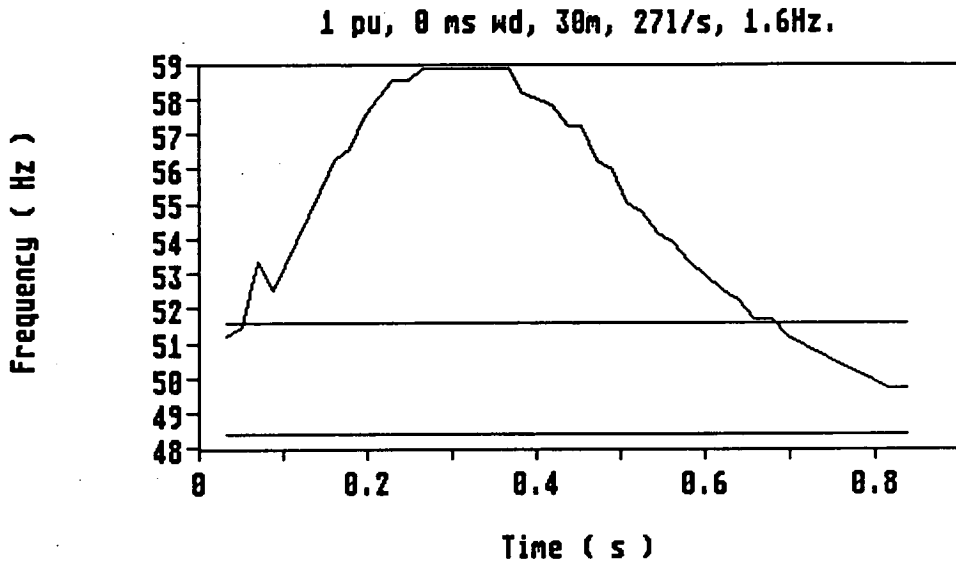


Figure 59a - Measured frequency transient for 30m head and 27l/s flow

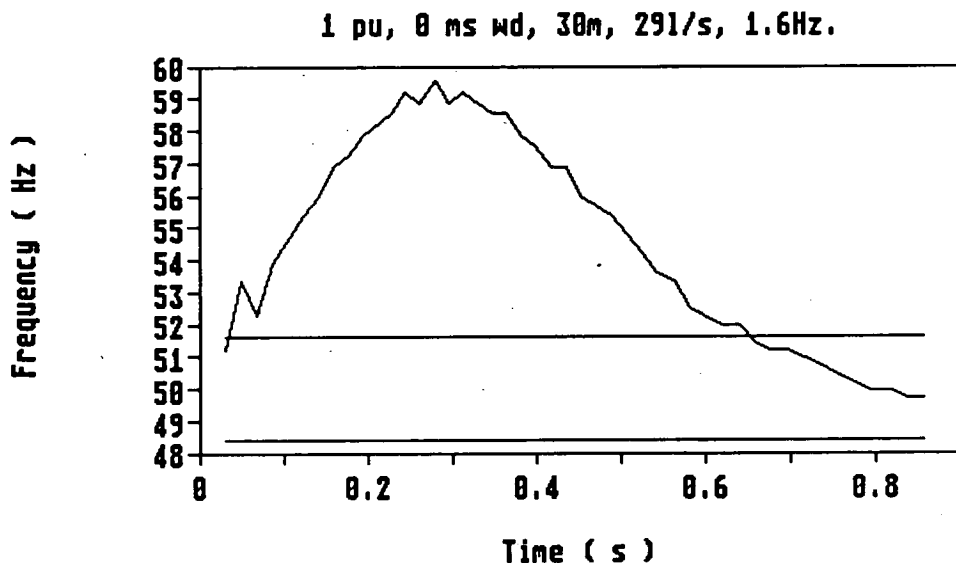
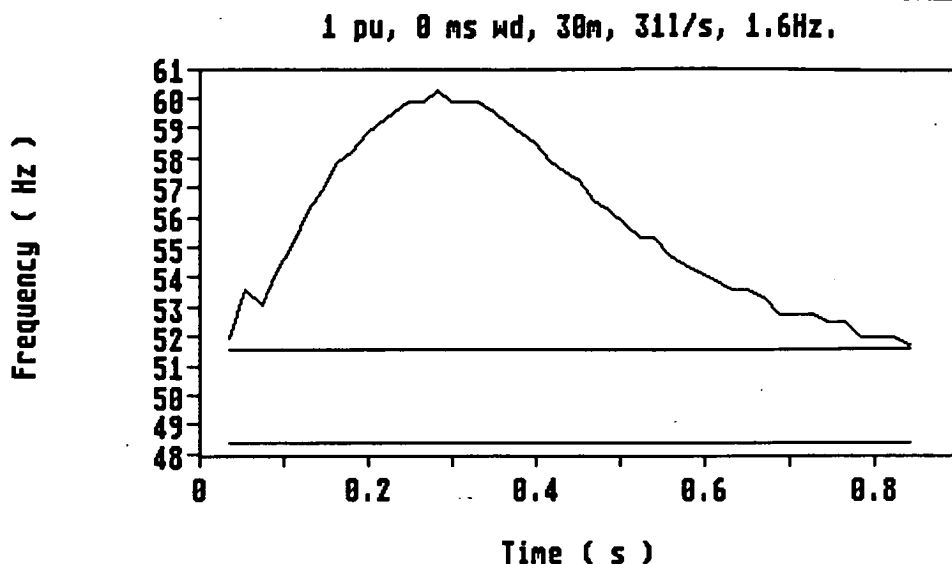
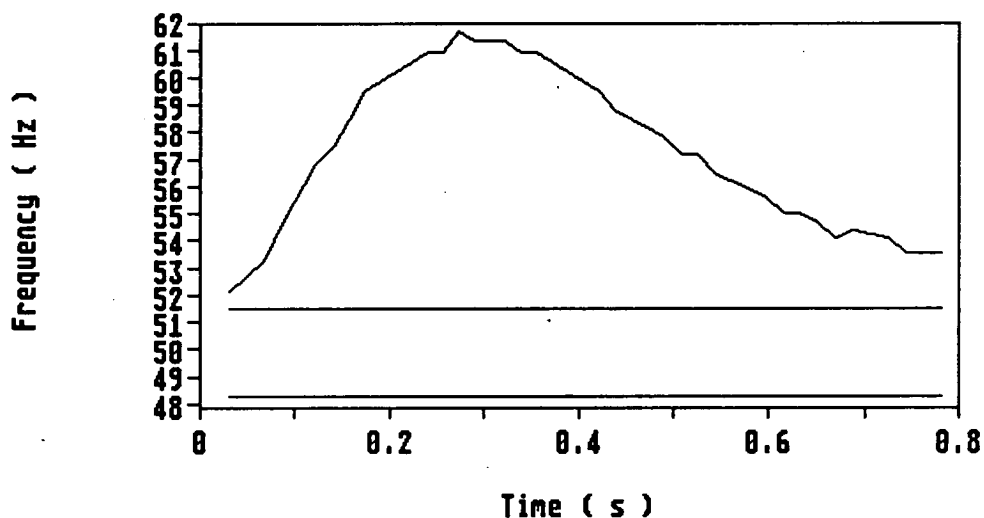


Figure 59b - Measured frequency transient for 30m head and 29l/s flow



**Figure 59c - Measured frequency transient for 30m head and 311/s flow  
1 pu, 0 ms wd, 30m, 311/s, 1.6Hz.**



**Figure 59d - Measured frequency transient for 30m head and 331/s flow**

The effect on the frequency transient through the addition of wait delay is shown in figures 60a to 60d, where the added delay is 0, 4, 8 and 12ms respectively. It is clear that as the wait delay is increased then the return time also increases. In addition, as predicted, the magnitude of  $f_{max}$  increases, from 60 Hz to 62.5 Hz, over the range of wait delay values. These tests were all performed at a head of 30m and a flow of 301/s.

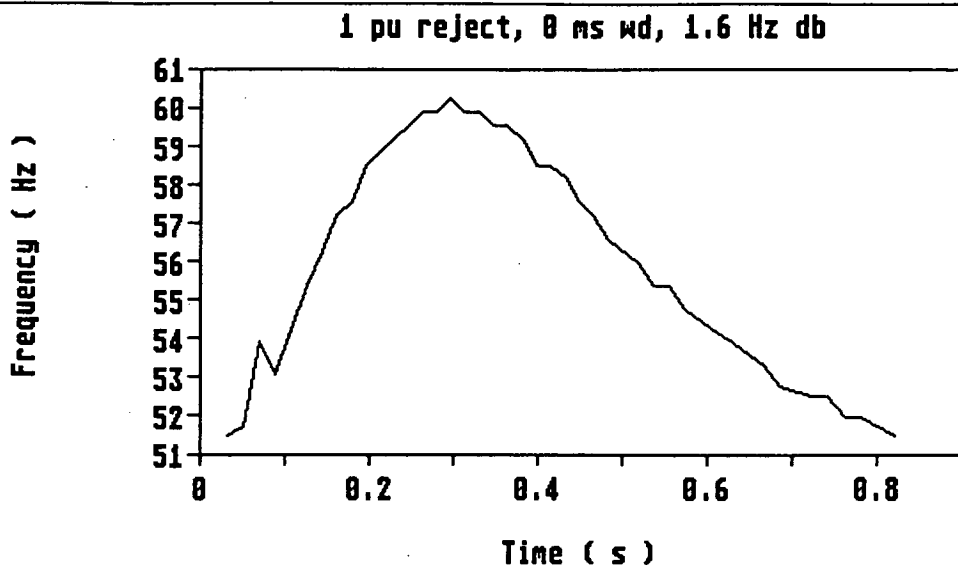


**Figure 60a - Measured frequency transient for zero wait delay  
1 pu reject, 4 ms wd, 1.6 Hz db**

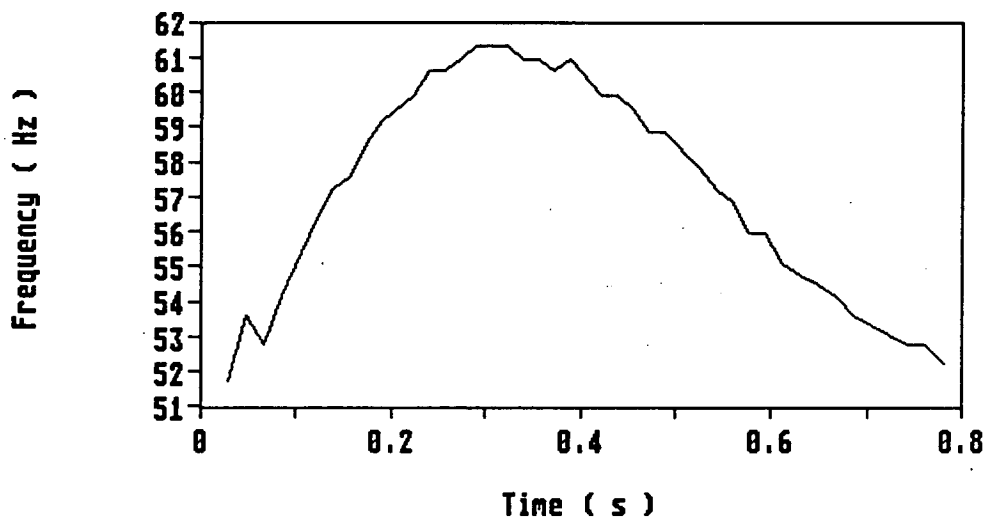


**Figure 60b - Measured frequency transient for 4ms wait delay  
1 pu reject, 1.6 Hz db, 8 ms wd**

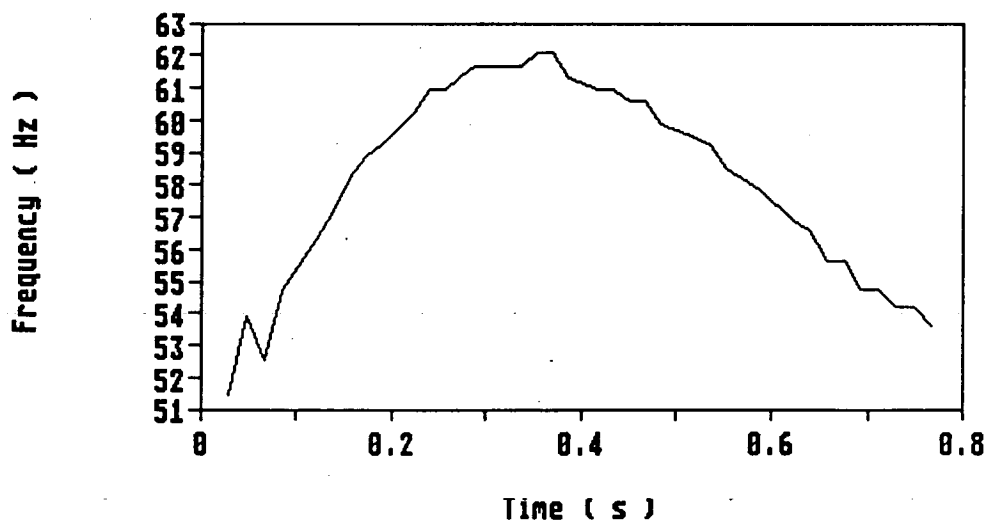


**Figure 60c - Measured frequency transient for 8ms wait delay**

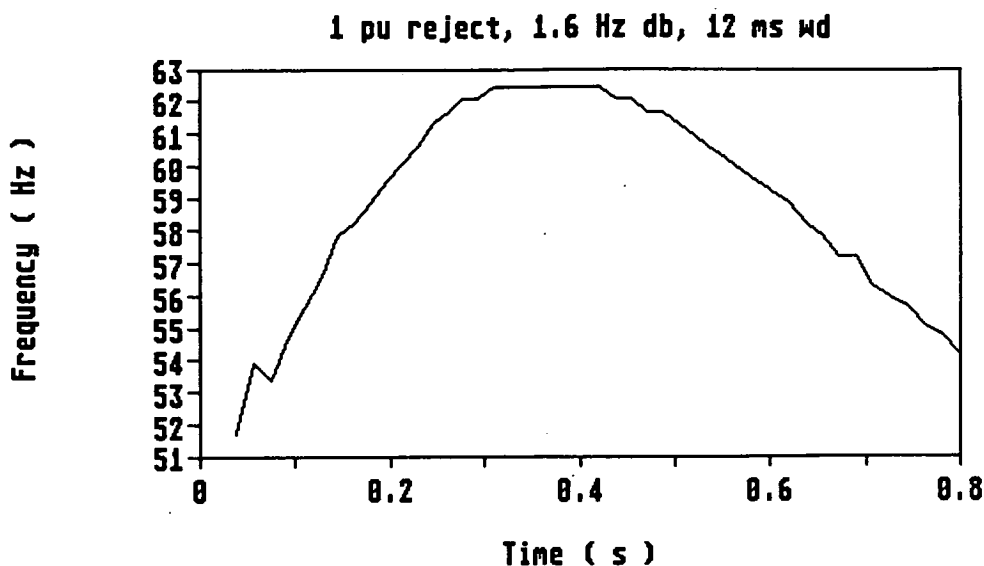


**Figure 60d - Measured frequency transient for 12ms wait delay**

### 7.2.2. Voltage Transient

Using the DSO to monitor the a.c. voltage waveform, as indicated in Section 5.4, the nature of the voltage variation during a transient period caused by a full load rejection was determined. The trace provides the envelope of the peak-to-peak voltage, and the rise in the peak voltage was measured using the cursors. This gives the rise in the r.m.s. voltage from the initial steady-state value to the maximum which occurs during the transient period.

Such measurements were done for a number of the operational conditions previously used when measuring the frequency transient data. It should be noted that the comparisons which result are therefore not based on the same specific event, rather they relate to two similar, but separate, events.



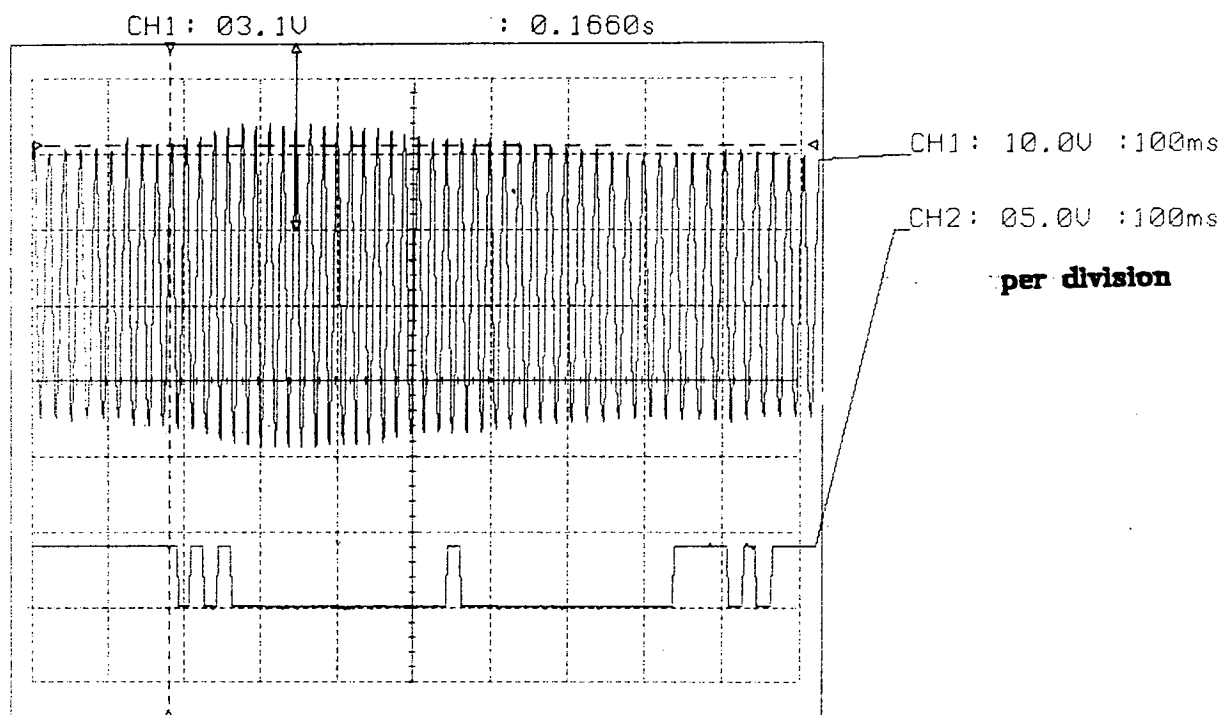


**Figure 61 - Voltage transient at 27m head**

Figures 61 and 62 present the voltage envelopes for variation in head at a constant flow of 31 l/s, with a deadband of  $\pm 1.6$  Hz and with no added wait delay. The former figure, for a head of 27 m, shows a rise in the r.m.s. voltage of 16.6% which compares with a rise in the frequency of 18.2%, refer figure 58a. Figure 62, for a head of 33 m, shows a rise in the r.m.s. voltage of 23.3% which compares with a frequency rise of 24.2%, refer figure 58d. As expected, the voltage rise is approximately proportional to the frequency rise.

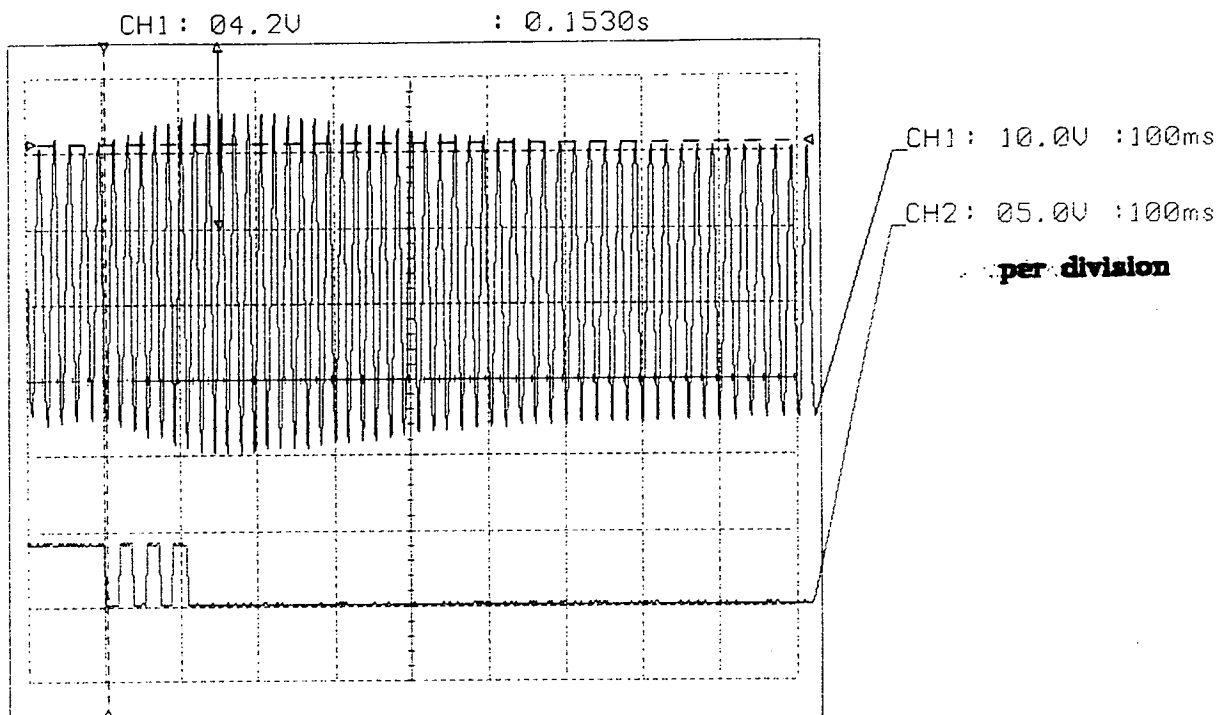


Figure 62 - Voltage transient at 33m head

### 7.3. TRANSFER FUNCTION

One approach to the preparation of a model is to determine the transfer function of the complete system. The general block diagram of the control system is given in figure 63. This is based on equation 7.1 and its component parts such that;

$$T_a = T_{\max} - T_v - (T_{cl} + T_{bl})$$

The *input* is a change in the consumer load torque  $T_{cl}$  and the *output* is the frequency of the generated waveform,  $f$ . The transfer functions for each of the blocks are derived in the following sub-sections.

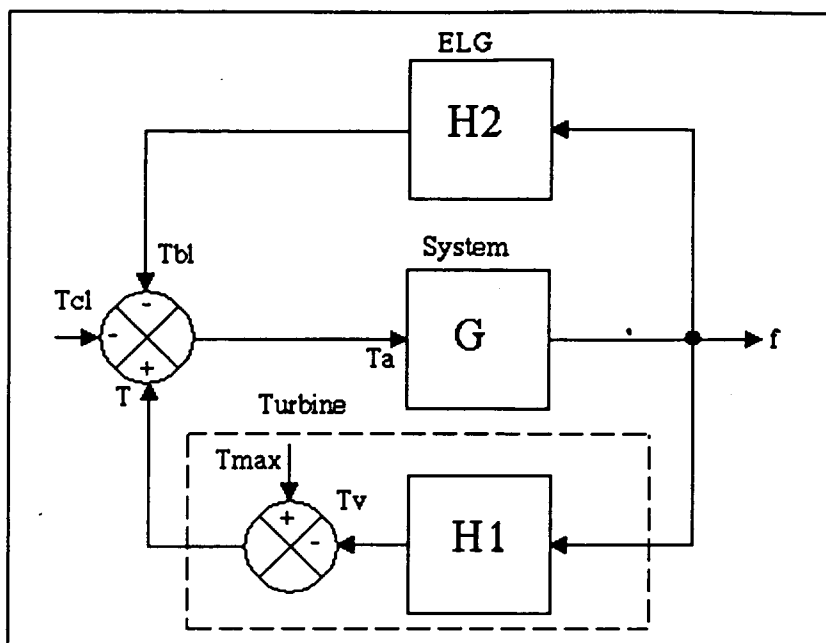


Figure 63 - Control system block diagram

### 7.3.1. The Rotating System Transfer Function

The input to the rotating system block, figure 64, is the accelerating torque and the output is the frequency. From equation 7.2, the relationship with respect to time between the net accelerating torque and the rate of change of frequency is given by;

$$T_a(t) = K_1 J \cdot df(t)/dt$$

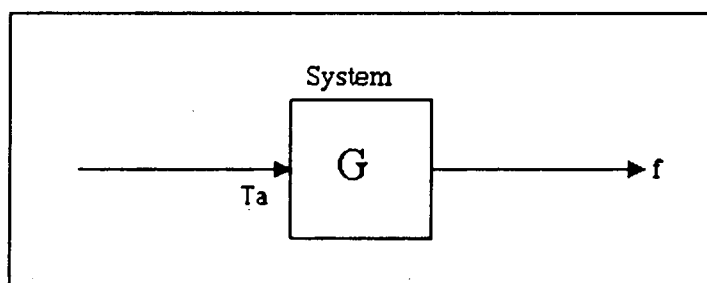


Figure 64 - Rotating system block diagram

Taking Laplace transforms<sup>62</sup> of both sides of this equation gives;

$$T_a(s) = K_1 J \cdot s \cdot F(s)$$

and the transfer function of this block is;

$$G = F(s)/T_a(s) = 1/(K_1 J.s)$$

### 7.3.2. The Turbine Transfer Function

From figure 65, the turbine torque can be considered as having a constant component and a frequency dependent component such that;

$$T = T_{\max} - K_2 f$$

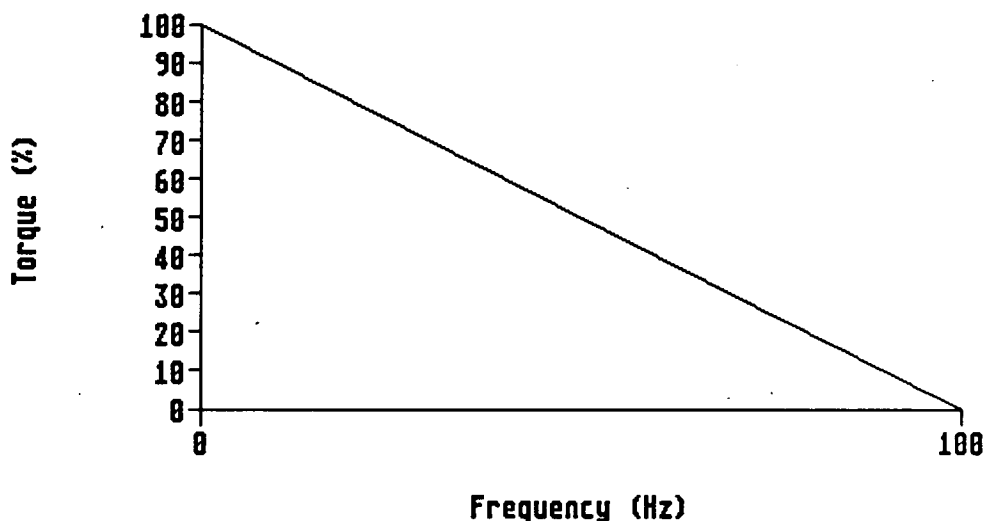


Figure 65 - Typical torque vs frequency curve

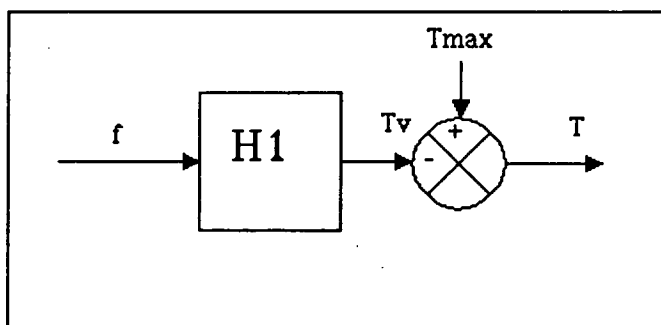


Figure 66 - Turbine block diagram

This can be represented in block diagram format as shown in figure 66 and the transfer function H1 can be derived from the frequency-dependent turbine torque component,  $T_v$ , expressed with

respect to time;

$$T_v(t) = -K_2.f(t)$$

Taking the Laplace transform<sup>62</sup> of both sides reveals H1 as;

$$H1 = T_v(s)/F(s) = -K_2$$

### 7.3.3. The ELG Transfer Function

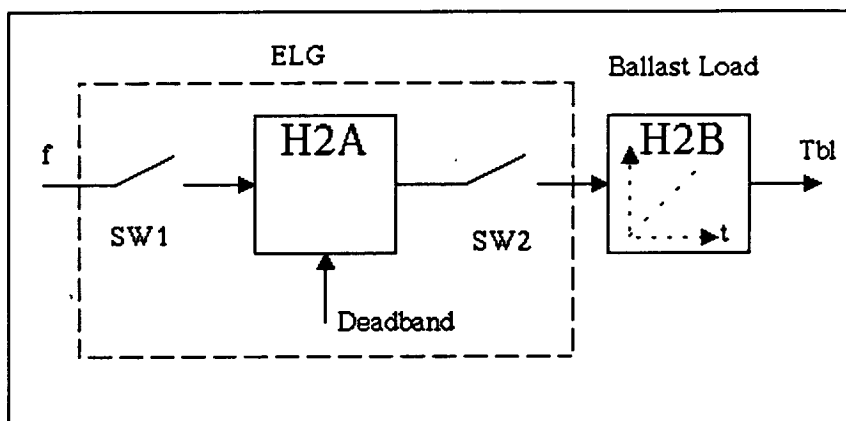


Figure 67 - ELG block diagram

The block diagram of the operation of the ELG and the ballast load which it controls is given in figure 67. The input is the system frequency,  $f$ , which is sampled, at a variable rate, and the switch SW1 is used to denote the sampling nature of the frequency measurement. The action of the ELG on sensing the frequency is to compare this with the preset frequency deadband. The output of this comparison is not an error signal, as is common in many control systems, but is a measured response to perform one of three options;

- i) do nothing - if the frequency is within the deadband.
- ii) add 1 step of ballast load if the frequency is above the deadband.

iii) remove 1 step of ballast load if the frequency is below the deadband.

In addition, options ii) and iii) are subject to a limit to the number of steps that can be added or removed respectively, i.e. there is a saturation effect possible. The block with response H2A on figure 67 represents the frequency comparison and the switch SW2 represents the digital '0' or '1' nature of the input to the next block.

The final block, H2B, represents the application of the ballast load. Assuming that the overall system is responding to an instantaneous full load rejection, then the reaction of the ELG is to apply ballast load steps continuously - at a switching rate determined by the program cycle and the added wait delay. As an approximation, the application of the ballast load torque will vary with time as shown in figure 68. In reality, the ballast load torque will be applied as a stepped function and is itself a function of the frequency;

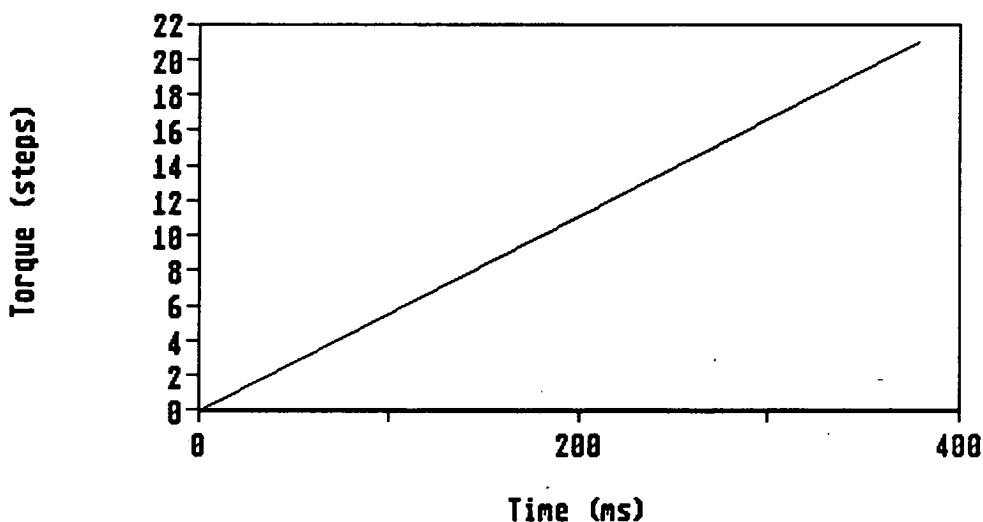


Figure 68 - Time varying application of ballast load

---

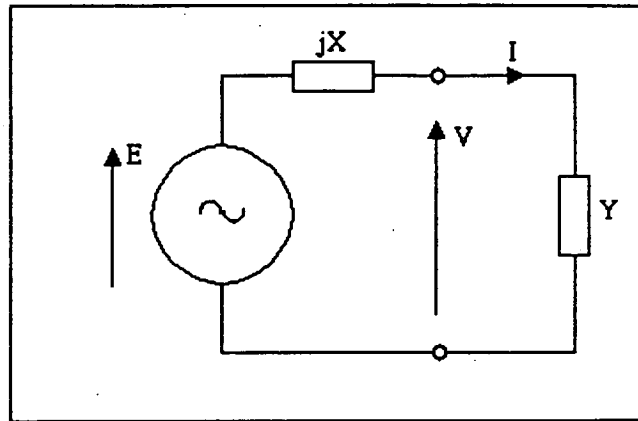


Figure 69 - Equivalent circuit of synchronous generator

From the general torque equation for a rotating machine<sup>63</sup>,

$$T_{bl} \propto I$$

ignoring the internal impedance of the synchronous generator, refer figure 69. As the admittance of the ballast load is increased in time, the generator output current,  $I$ , can be expressed with respect to time as,

$$I(t) = E.y.t$$

where  $y$  is the admittance of each step of ballast load and the saturation of the ballast load is ignored. The EMF is a function of the rotational speed ( and hence the frequency ) of the shaft, thus;

$$T_{bl}(t) = K_3.t.f(t) \quad ( 7.11 )$$

Taking the Laplace transform<sup>62</sup> of this expression gives;

$$T_{bl}(s) = K_3.F(s)/s^2 = H2B \quad ( 7.12 )$$

The output of this block is the ballast load torque and the input is either zero or is a constant. Hence equation 7.12 is the transfer function for this block, assuming that the input is not zero.

The solution for the additional effects of saturation, the deadband, the possibility of ballast load removal and the step effect of the ballast load application would require sophisticated analysis techniques which are beyond the scope of this study.

#### 7.3.4. Simplified Overall Block Diagram

Using standard block diagram reduction techniques<sup>64</sup>, the transfer functions for the rotating system and the turbine can be combined as shown in figure 70, where;

$$G' = G/(1 + GH1) = 1/(K_1 J.s - K_2)$$

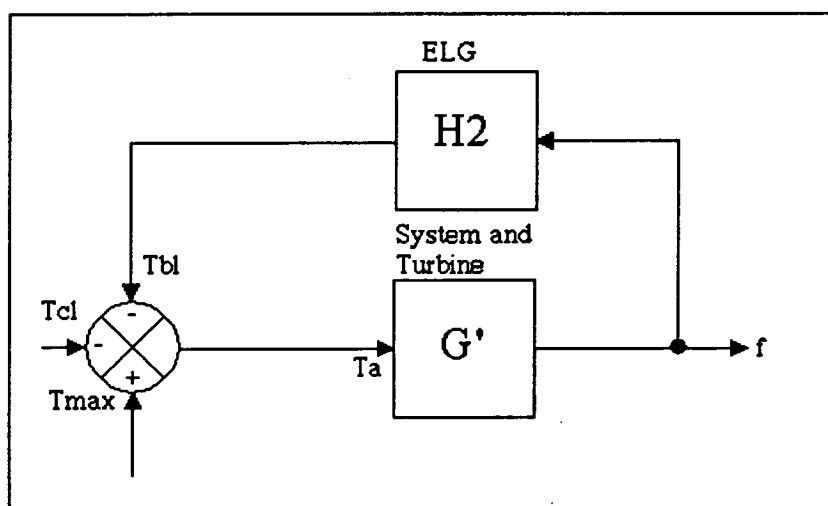


Figure 70 - Final block diagram of the control system

In the absence of the complete transfer function of the ELG it was not felt appropriate to reduce the overall diagram any further.



## 7.4. COMPUTER MODEL

Whilst the mathematical model of the control system proved complex, the logical operation of the ELG and the exponential nature of the frequency transient, equation 7.9, permitted the development of a computer program to model the frequency transient.

This Section of the thesis describes the development of the computer model and the testing of its validity against the measured frequency transient on the Boving turbine. The flexibility of the test facility permitted validation of the model over a range of operating conditions. The reliability of the model to predict the performance of the ELG on alternative installations is then assessed.

There are two variants of the program, STTURB4 which relates specifically to the Boving turbine and STTURB3 which permits modelling of any alternative Pelton turbine provided that design data is available. Both programs were written using ST BASIC on the Atari microcomputer.

### 7.4.1. STTURB4

This program is based on the theory developed in Section 7.1. and is designed to plot the frequency variation with time as the result of an instantaneous load rejection. The program assumes the same initial conditions apply as stated in Section 7.1, and the data pertaining to the Boving turbine, refer Section 5.3.1., is used within the program.

---

The operation of the program allows variation in the following input parameters;

- head, in metres,
- flow, in litres/sec,
- wait delay, either 0, 4, 8 or 12 ms, and,
- the p.u. value of load rejection from 0 p.u. to 1.0 p.u.

As the latter item of input data suggests, load rejections less than full load can be analysed, although it should be stressed that the program was primarily developed for analysis of full load rejections.

The program has an automatic deadband selection routine which is based on the deadband prediction theory developed in Section 5.3.1.3. and is essentially a function of the runaway speed ratio and the head. To provide flexibility in the use of the program, an operator over-ride facility is available for the deadband value that the program goes on to use.

The program plots two curves on the screen, the first is the ungoverned frequency transient to the load rejection based on equation 7.8. The second is the complete frequency transient of equation 7.9 for the ELG. The plots are both to an x-axis time scale of 1.5 seconds, sufficient to display the full transient period for a full load rejection. Also shown are broken horizontal lines which represent the deadband upper and lower limits. In addition to the title and the axes labels, the following data is output to the screen;

- the maximum frequency during the transient,  $f_{\max}$ ,
  - the time of the occurrence of  $f_{\max}$ ,
-

- the inertia of the rotating components,  $J$ ,
- the deadband value used,
- the power rating of the ballast load, 4700 W, and,
- the input data as above.

Finally the program permits saving of the x and y co-ordinates to disc for later use, typically to obtain a hardcopy of the plot other than by the computer "screen dump" facility. Figure 71 shows the screen output for a typical set of input conditions and the program is listed in Appendix 4.

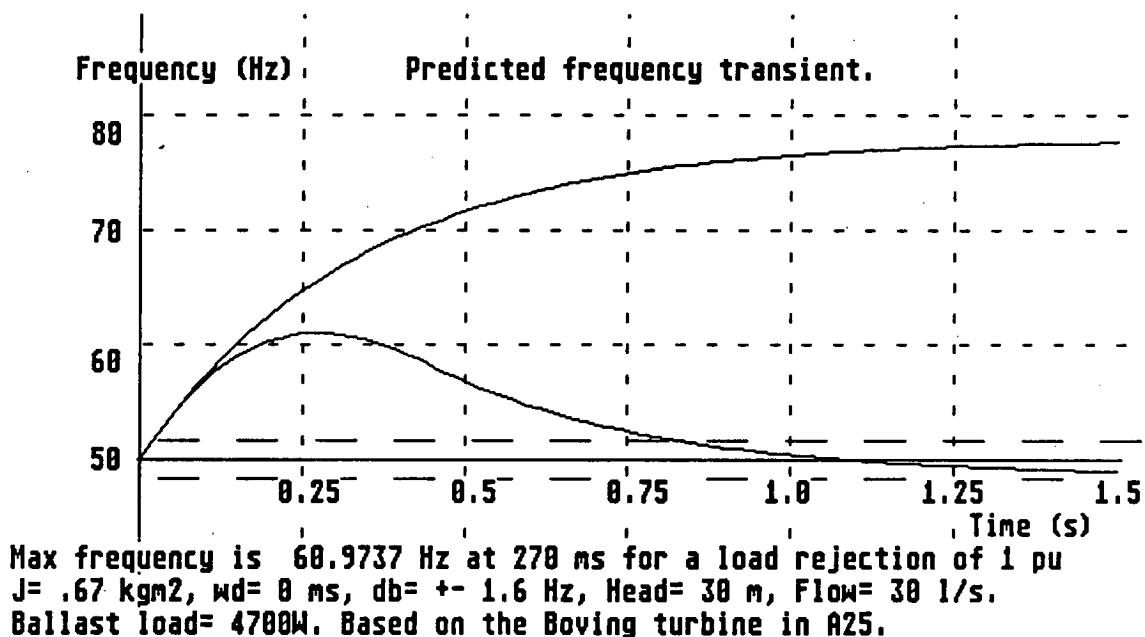


Figure 71 - Typical screen output of the STTURB4 model

A feature of this program is that the ballast load used is the one which is installed at the test facility in the Laboratory (A25), which is fixed in magnitude and is rated to suit the nominal operating conditions. Thus, if hydraulic data is input which does not match this ballast load, e.g. a higher head or a higher flow value, then the final frequency achieved in the steady-state will differ from the initial value.

### 7.4.2 STTURB3

This program provides the operator with the option of using the turbine data relating to the Boving turbine or to enter data for any alternative turbine installation. In this way, the model can be used to predict the transient frequency performance of the ELG on any installation, either existing or planned.

The additional input data required for an alternative turbine is as follows;

- the inertia of the rotating components,
- the normal running speed of the turbine which will provide a generated frequency of 50 Hz,
- the turbine runaway speed,
- the turbine radius, and,
- the value of  $C_v$ , the velocity coefficient.

The operation and the screen output of this program are identical to STTURB4 with the exception that the power rating of the ballast load is assumed to be matched to the hydraulic conditions prevailing, allowing for losses, and is not displayed. A program listing of STTURB3 is also given in Appendix 4.

### 7.4.3 Model Validity

A key application of the hydraulic test facility was its use to validate the computer model STTURB4, without which the model would be worthless. Having captured, plotted and stored the transient frequency

---

measurements for a wide variety of head and flow conditions applied to the Boving turbine, refer Section 7.2.1., it was possible to make comparison with the model output plots over the same range of hydraulic conditions. As for the measured transients, the predicted frequency transients produced by the model are based on full load rejections with a deadband setting of  $\pm 1.6$  Hz and a wait delay of 0 ms. Again, the deadband limits have been added to the plots in their preparation.

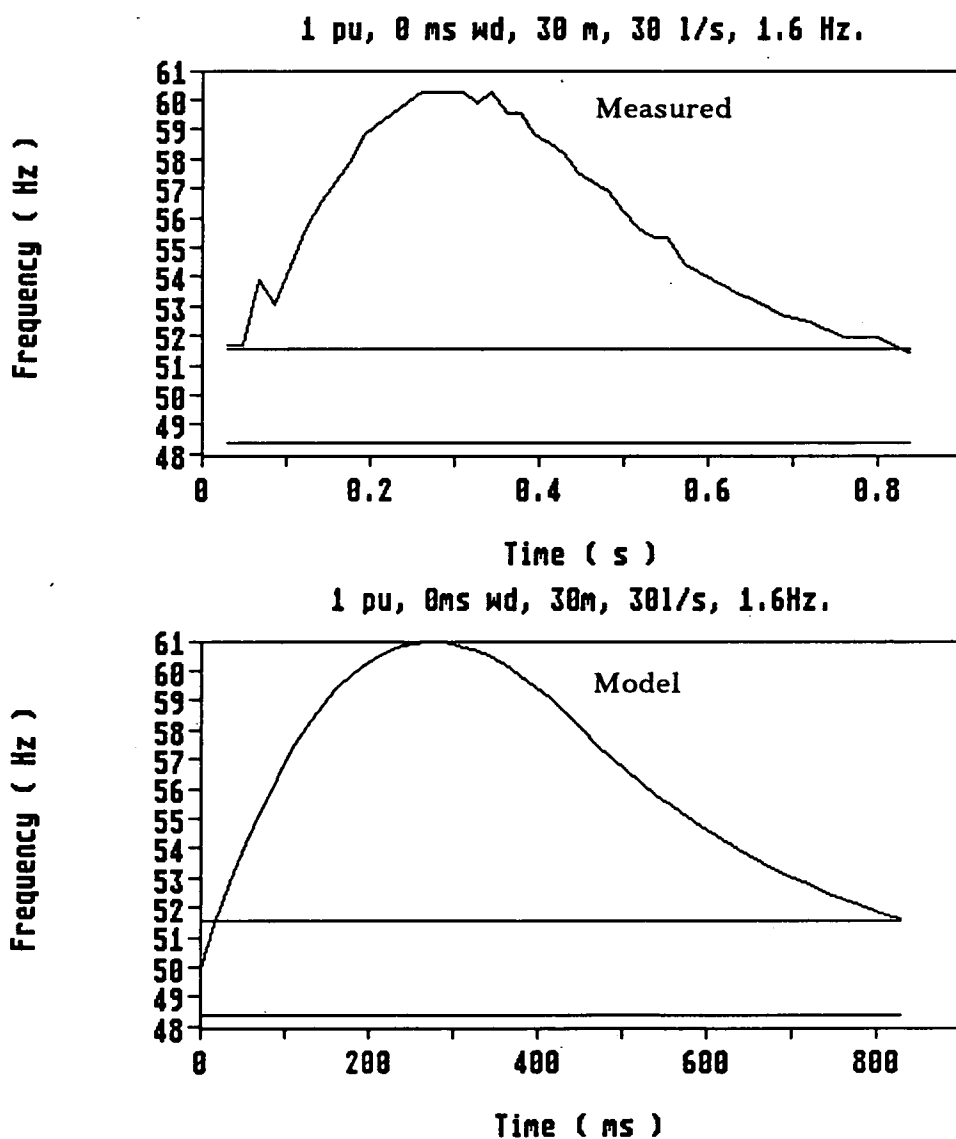


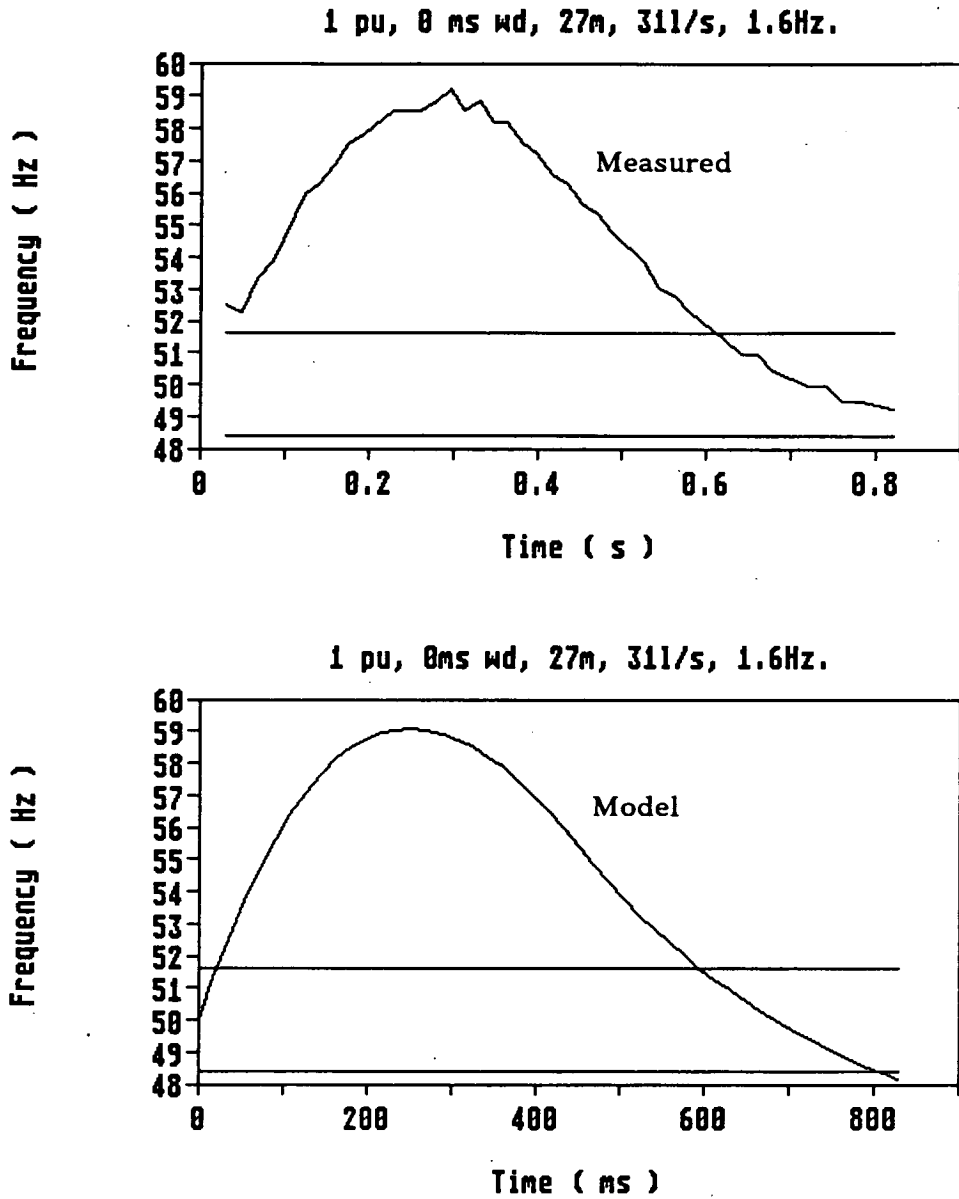
Figure 72 - Comparison of the measured and model frequency transients for the nominal operating conditions.

Figure 72 is a comparison between the measured trace and the model trace for a full load rejection at the nominal hydraulic operating conditions of 30m head and 30 l/s flow. Given that the accuracy of the measured transient is no better than  $\pm 0.5$  Hz, that aspects of the theory behind the model are based on assumptions, and that some of the parameters used by the model are subject to experimental error, then the model transient shows a reasonable similarity with the measured transient. The value of  $f_{\max}$  is within 0.75 Hz and the return time is almost identical.

To validate the model, comparisons are also presented for heads of 27m and 33m at constant flow, figures 73 and 74 respectively; and for flows of 27l/s and 33l/s at constant head, figures 75 and 76 respectively. Of these four comparisons, the largest difference in the value of  $f_{\max}$  is 1 Hz and, where determinable, the return times are within 0.07 second. On comparison of the model output with the measured frequency transients at other hydraulic conditions, these discrepancy values are considered to be typical.

As is expected, the model displays the trends in the frequency transient predicted by Section 7.1 in respect of head and flow variations. Figures 73 and 74 show the increase in  $f_{\max}$  for increasing head and are directly comparable with figures 58a and 58d. Figures 75 and 76 also display the expected increase in  $f_{\max}$  for increase in flow as shown previously in figures 59a and 59d.

---



**Figure 73 - Comparison of the measured and model frequency transients at 27m head and 311/s flow**

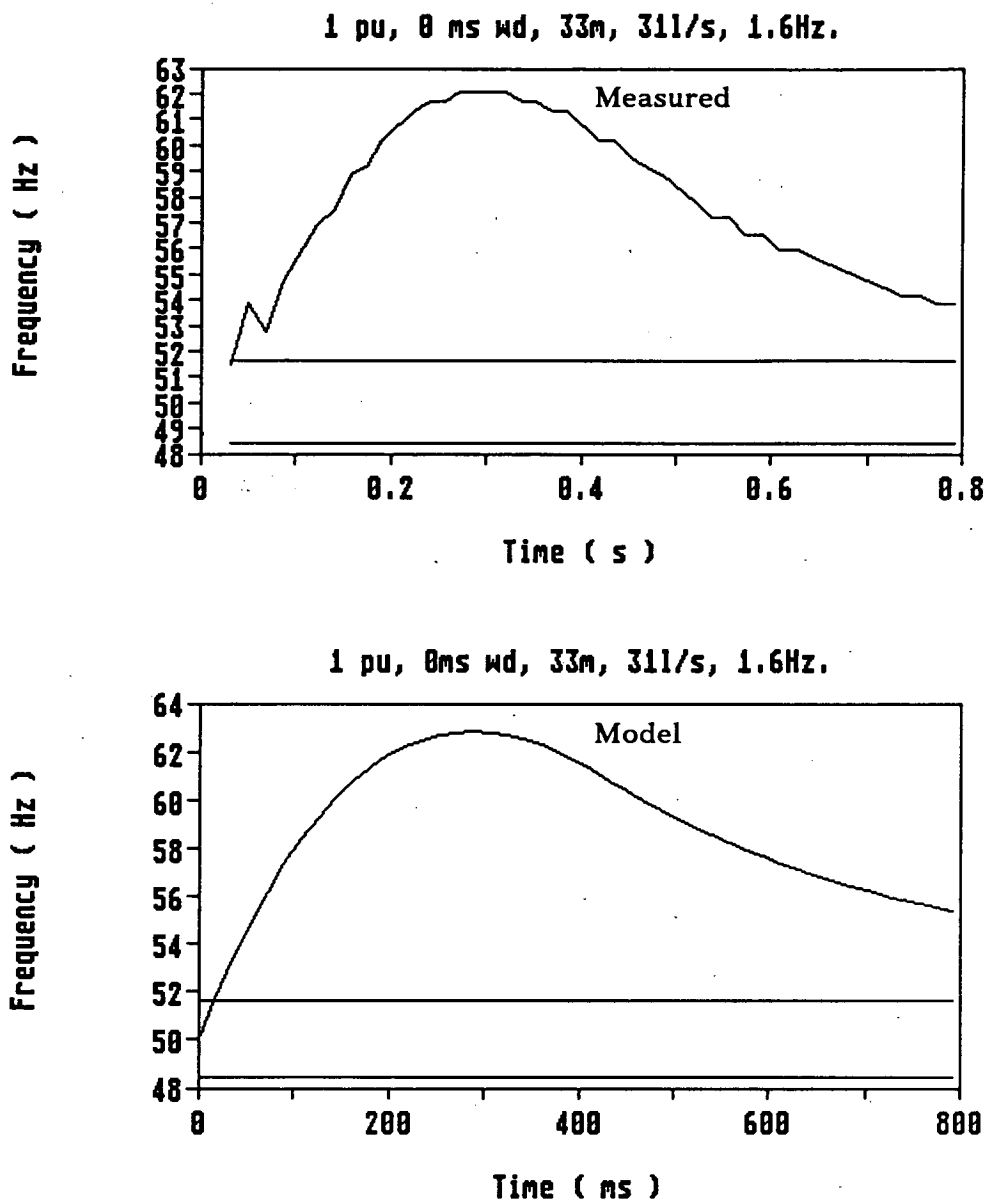


**Figure 74 - Comparison of the measured and model frequency transients at 33m head and 311/s flow**



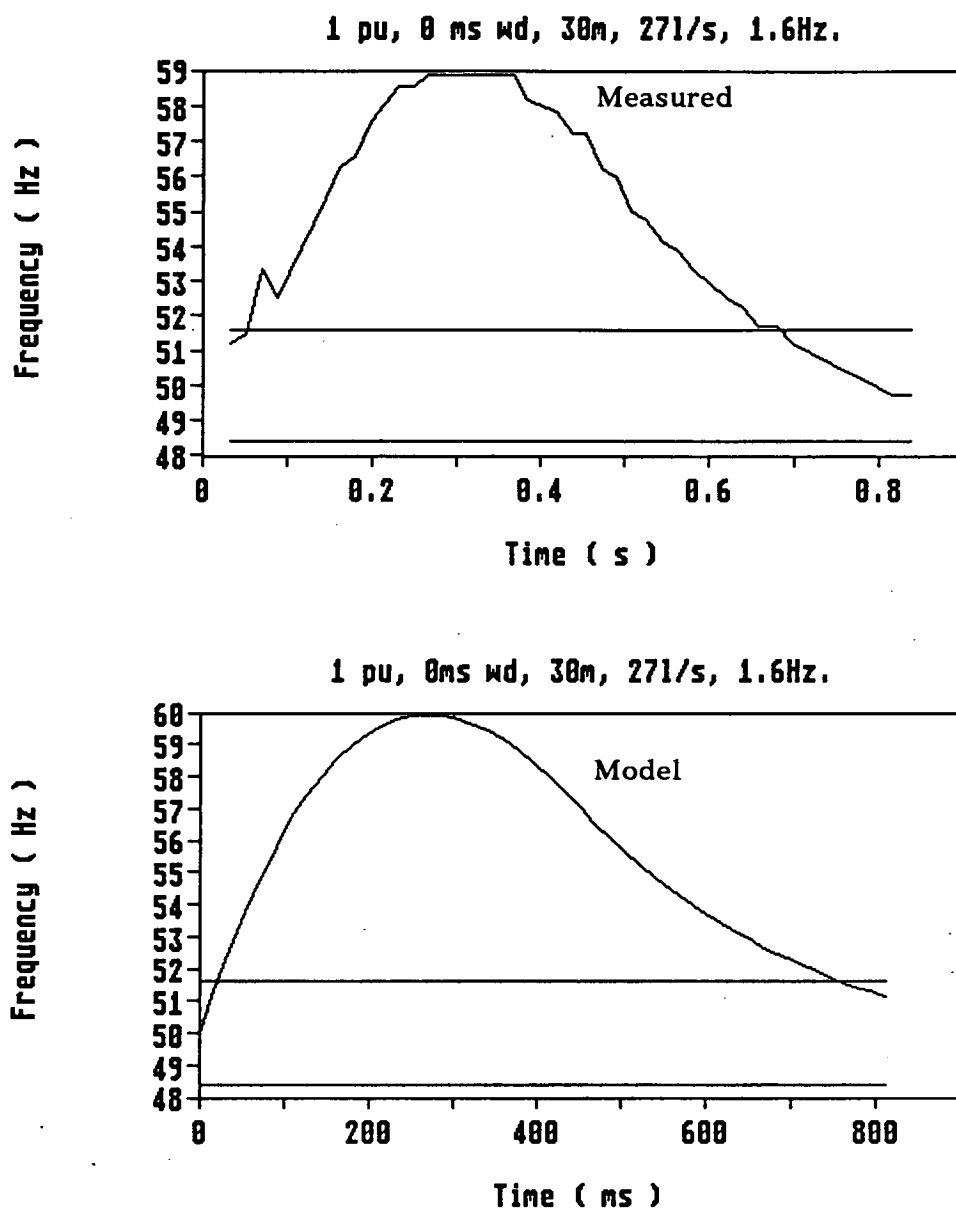


Figure 75 - Comparison of the measured and model frequency transient at 30m head and 271/s flow

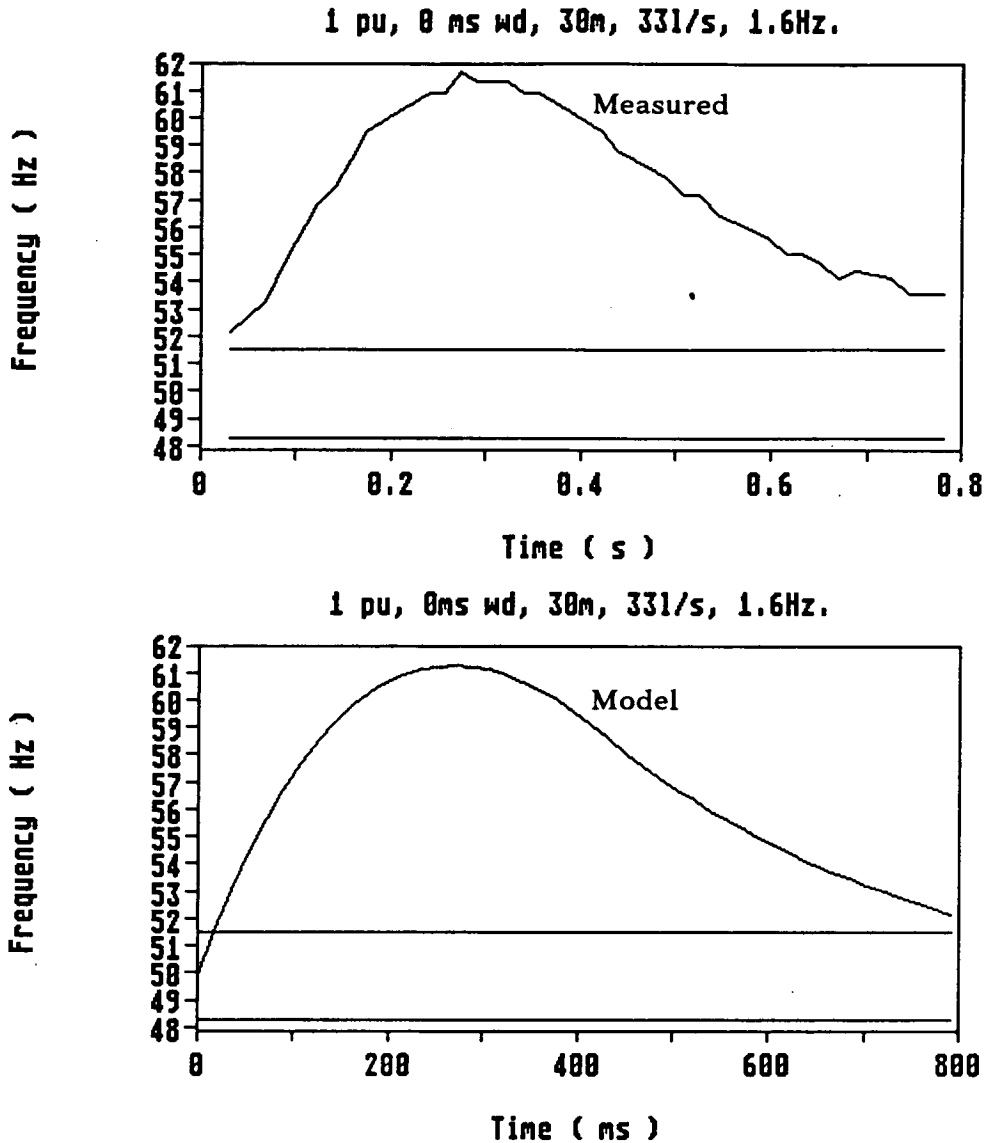


Figure 76 - Comparison of the measured and model frequency transient at 30m head and 331/s flow

#### 7.4.4. Model Use on Alternative Installations

The value of the model is in the prediction of ELG operation on any given installation. The opportunity to test the model against operation of the ELG on the Gilkes pelton turbine was taken. Using the data acquisition system, the frequency transient on full load rejection was

measured for the nominal operating conditions :- 19 m head, 11 l/s flow, +- 1.28 Hz deadband and 8 ms wait delay. The transient, refer figure 77, shows a maximum frequency of approximately 54 Hz.

Version STTURB3 of the model was used to input data relating to the Gilkes turbine. As for the Boving turbine, the item of data which was the subject of the least known accuracy was the inertia. Using comparisons with the Boving turbine and the known generator inertia<sup>63</sup>, the initial estimate of the inertia was  $0.91 \text{ kgm}^2$  as a  $WR^2$ . This value is known to be low, due to the presence of additional pulleys and a rope-brake drum on the shaft of indeterminate inertia.

For the model to produce the same maximum frequency as the measured transient, a value of  $2.4 \text{ kgm}^2$  is required for the inertia, refer figure 78. Allowing for the estimated accuracy of both the measurement and the model, an inertia of  $1.75 \text{ kgm}^2$  would produce a maximum frequency of higher magnitude but within tolerance. It is possible that the true inertia could be around this order but, presently, accurate data is not available to confirm this. The value for the runaway speed used in this instance is likely to be high, as the runaway speed test was performed without the belts connected. This too will have the effect of making the model predict a higher value for the maximum frequency than it would if the runaway speed were lower.

This result suggests that the model will be suitable for prediction of the ELG operation of Pelton turbine installations other than the Boving turbine against which it was originally written and tested. The result also highlights the need for accurate data for use with the model. It is

---

hoped that opportunity will arise for further validation of the model against ELG operation on other installations.

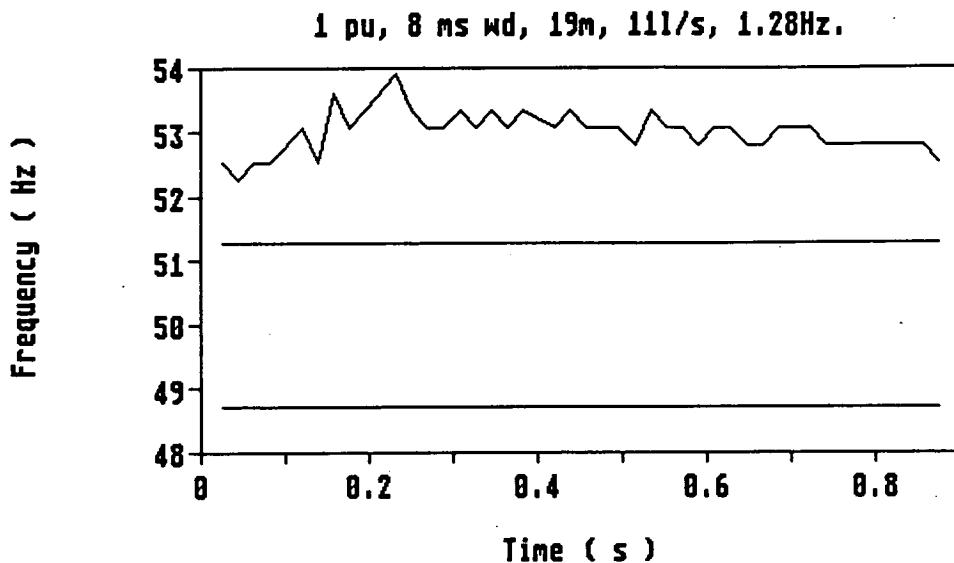


Figure 77 - Measured frequency transient for Gilkes turbine

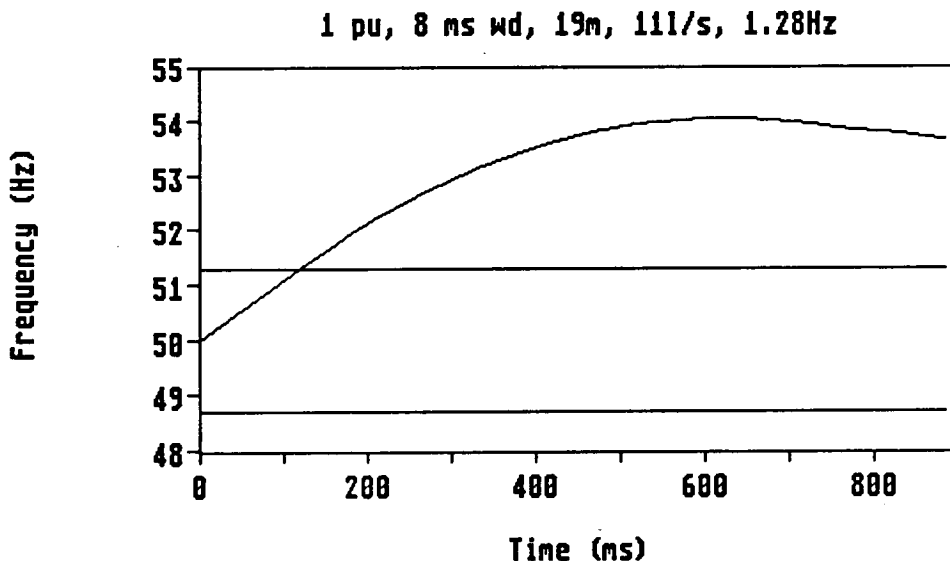


Figure 78 - Predicted frequency transient for Gilkes turbine \*

The model is based strictly on the theory relating to Pelton type turbines but it will be a relatively straightforward task to prepare alternative versions for application of the ELG to other turbine types.

\* Note. This trace is based on an inertia value of  $2.4 \text{ kgm}^2$ .

### 7.4.5. Model Applications

The application of the model can be;

- the prediction of the transient performance of an installation at the design and commissioning stages.

- the selection of inertia values for addition of flywheels, if necessary.

Figure 79 shows the comparison between the standard transient of figure 71 and that with  $2.0 \text{ kgm}^2$  added inertia, as if through the mounting of a flywheel on the shaft of the Boving turbine. As can be seen, the maximum frequency is significantly reduced as a result. The model could be used to determine the value of inertia required to limit the maximum frequency rise to a specified value.

- the future work on stability analysis, and the effect of the variation of the deadband and of the wait delay on stability. The duration of the period that the model covers would have to be extended in this instance.

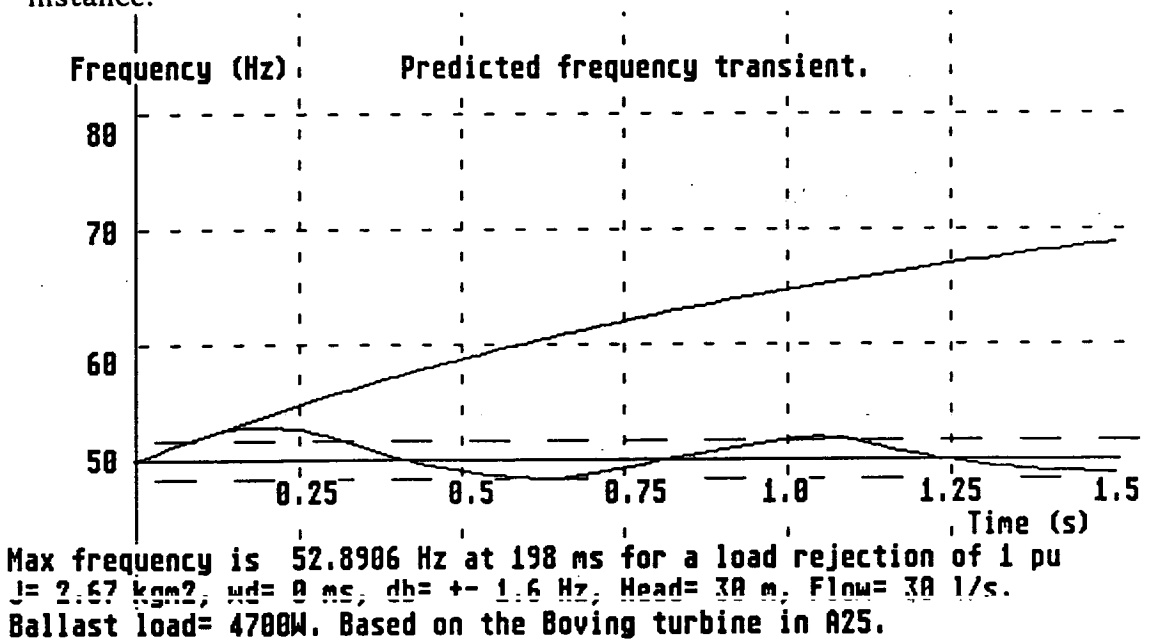


Figure 79 - Predicted frequency transient with added inertia

## 7.5 IMPROVING THE PERFORMANCE

The simple control action of the ELG, whereby only a single step of ballast load is added or subtracted on each switching operation, does result in relatively high variations in the frequency ( and hence the voltage ) during the transient period on full load rejection. In addition, the duration of the transient period is extended as result of the time required for step-by-step change from zero ballast load to full ballast load.

A further version of the program for the Boving turbine, PDCONT1, was written which introduced proportional and derivative control actions. Integral action is not necessary<sup>64</sup> as there is an acceptable steady-state error, arising from adopting the binary step - frequency deadband principle of operation. The result is that the model simulates a two-term controller through the determination of the initial rate of rise of frequency on load rejection which is then utilised in conjunction with a constant of proportionality. The program listing for this model is also given in Appendix 4.

The magnitude of the constant was determined using data from the original model. For a full load rejection, the initial rate of rise of frequency is typically 80 Hz/s and the response would be to apply the full ballast load in this event. Rounding the ballast load steps to 20 gave a magnitude for the constant of 4 Hz/s/step. The model calculates the number of steps to be added per switching by dividing the initial rate of frequency rise by the constant. The constant can presently be altered only by a change in the program, although for detailed study it

---

could be added to the data keyed in by the model operator. In practice the constant could be adjustable via the spare input microswitches.

The original model output, figure 80a, was compared with that from the two-term control model, figure 80b, for a full load rejection at the turbine nominal operating conditions. It may be seen that the latter offers a significant improvement in respect of the maximum frequency and the duration of the transient period. The frequency only rises by 8.4% instead of 22%, and the frequency returns within the deadband after 0.375s instead of 0.8s.

For a FLR the effect of increasing the magnitude of the constant of proportionality can be seen in figure 81, in comparison with figure 80b. The rate of application of the ballast load steps is decreased and hence the reaction is slower, increasing the magnitude of the maximum frequency during the transient period.

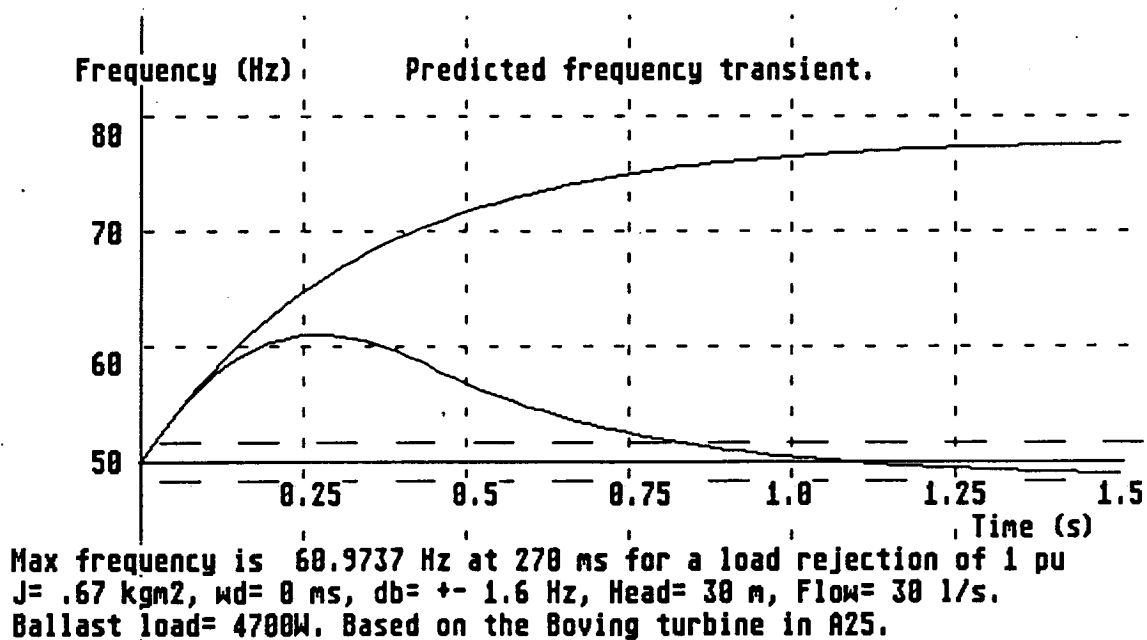
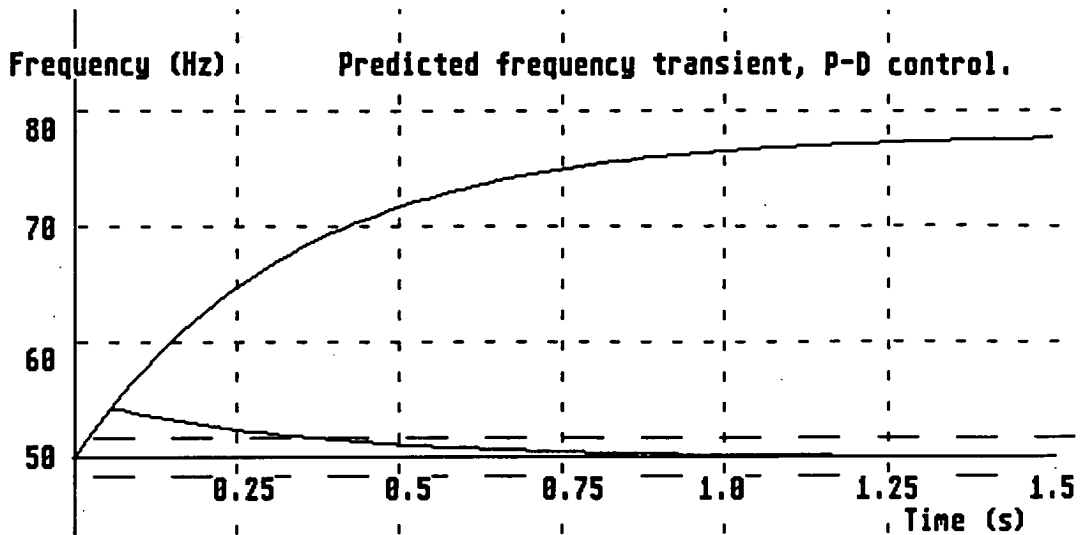
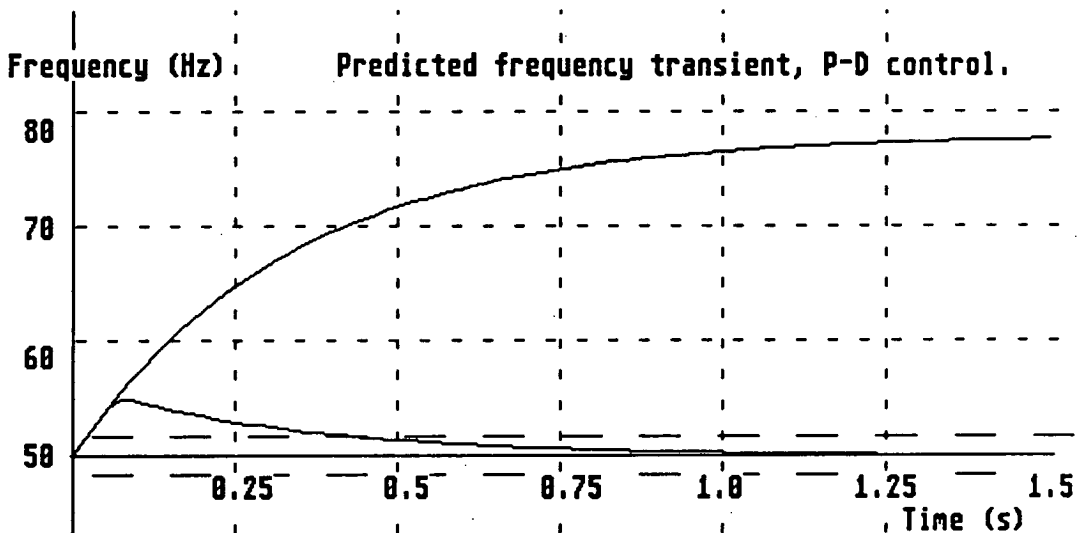


Figure 80a - Frequency transient for original control method



Max frequency is 54.1808 Hz at 54 ms for a load rejection of 1 pu  
 $J = .67 \text{ kgm}^2$ ,  $\omega_d = 0 \text{ ms}$ ,  $db = \pm 1.6 \text{ Hz}$ , Head = 30 m, Flow = 30 l/s.  
 Ballast load = 4700W. Based on the Boving turbine in A25. 1 step /4Hz/s

Figure 80b - Frequency transient with proportional-derivative actions



Max frequency is 54.7995 Hz at 72 ms for a load rejection of 1 pu  
 $J = .67 \text{ kgm}^2$ ,  $\omega_d = 0 \text{ ms}$ ,  $db = \pm 1.6 \text{ Hz}$ , Head = 30 m, Flow = 30 l/s.  
 Ballast load = 4700W. Based on the Boving turbine in A25. 1 step /8Hz/s

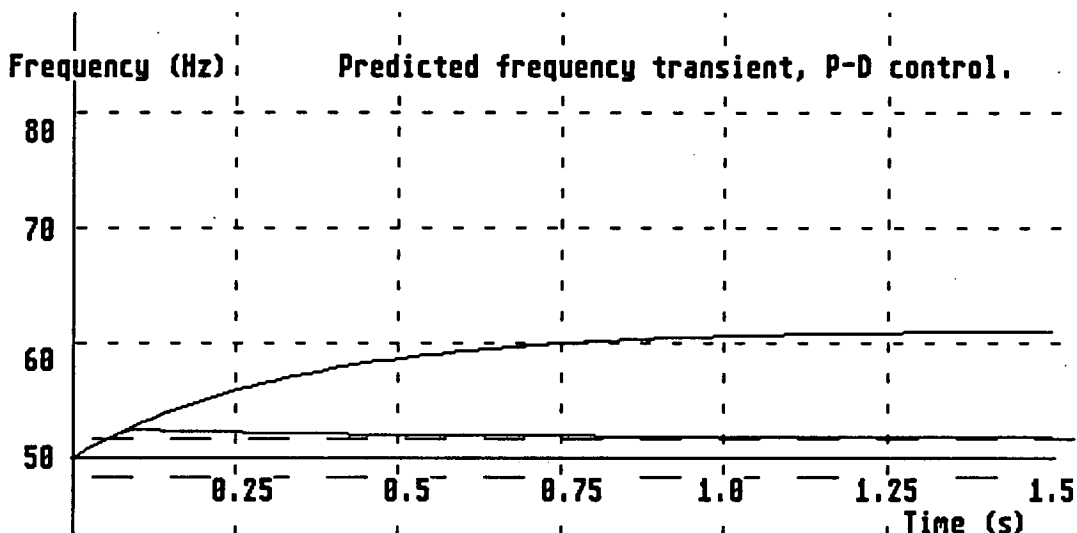
Figure 81 - Effect of increased constant of proportionality

For part-load rejections, the variation of the constant has an effect on the stability. Figures 82 a, b & c show the result of reducing the constant from 8 to 4 to 2 Hz/s/step respectively. With the higher value, the frequency does not in fact return to the deadband within the 1.5 second limit of the model study. At 4 Hz/s/step, the frequency



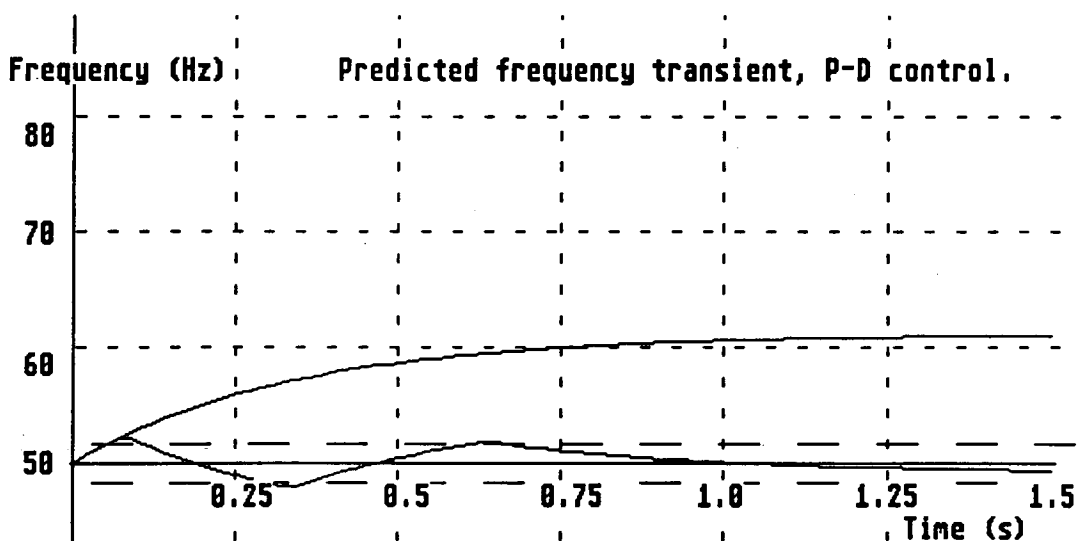
settles within 0.8 second, and the low constant value appears to cause the system to go unstable, the frequency rising latterly.

Allowing for the accuracy of the original model, the possible improvement in the performance of the ELG through the addition of proportional-derivative control actions appears to be very desirable.



Max frequency is 52.4745 Hz at 188 ms for a load rejection of .4 pu  
 $J = .67 \text{ kgm}^2$ ,  $\omega_d = 0 \text{ ms}$ ,  $db = \pm 1.6 \text{ Hz}$ , Head= 30 m, Flow= 30 l/s.  
 Ballast load= 4700W. Based on the Boving turbine in A25. 1 step /8Hz/s

Figure 82a - Part load rejection transient with constant = 8



Max frequency is 52.1721 Hz at 72 ms for a load rejection of .4 pu  
 $J = .67 \text{ kgm}^2$ ,  $\omega_d = 0 \text{ ms}$ ,  $db = \pm 1.6 \text{ Hz}$ , Head= 30 m, Flow= 30 l/s.  
 Ballast load= 4700W. Based on the Boving turbine in A25. 1 step /4Hz/s

Figure 82b - Part load rejection transient with constant = 4

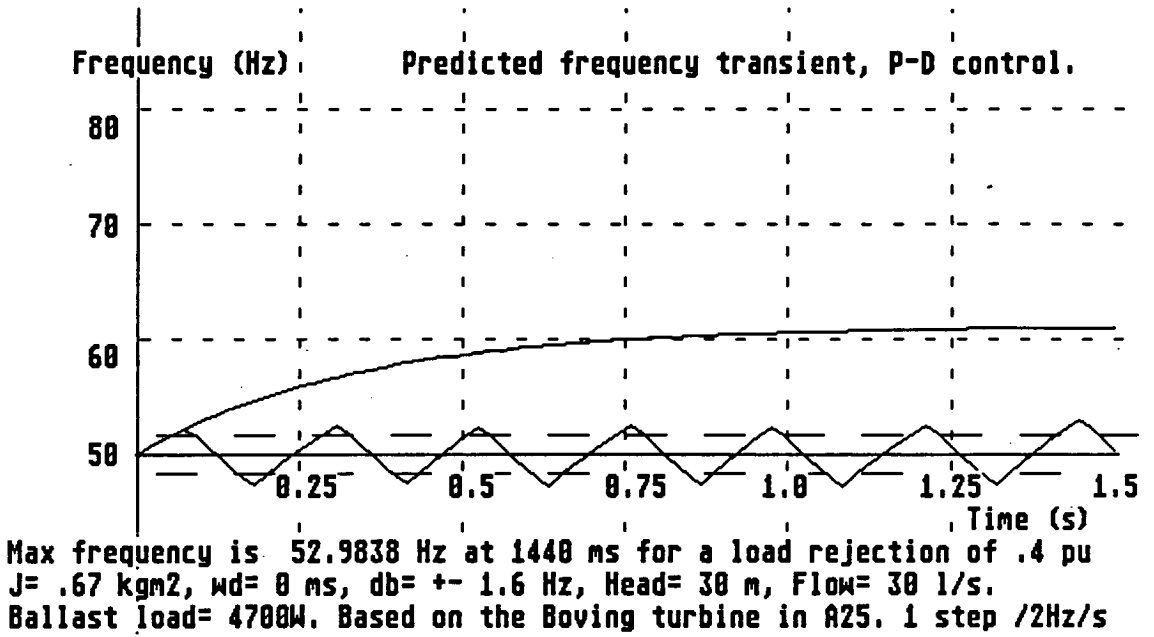


Figure 82c - Part load rejection transient with constant = 2

---

## **CHAPTER 8 CONCLUSIONS AND SUGGESTIONS FOR FURTHER WORK**

### **8.1 CONCLUSIONS AND OUTCOMES**

Most of the aims and objectives of the study have been achieved. The outcomes include;

1. The identification of the market for Electronic Load Governors.
2. The identification of the requirements for the ELG design.
3. The development of a functional and economic ELG.
4. The establishment of test facilities.
5. The prediction of deadband selection for steady-state operation.
6. The prediction of transient operation.

#### **8.1.1. The ELG Market**

It has been established that there is a market for Electronic Load Governors, wherever isolated micro hydro generating sets are to be installed. The response to the recent market survey highlighted an annual demand for over 100 units from only four ELG suppliers, it is estimated that the global market will be at least 5 times this figure.

It is recognised that the market is an international one, and that the demand will largely be from developing countries who are actively implementing micro hydro programmes. It is further recognised that presently there are a number of alternative designs of ELG on the market, and that to make an impact on this market a unit which can compete economically, as well as technically, will be required.

---

### 8.1.2. The Requirements of an ELG

Research determined that the requirements of an Electronic Load Governor are as follows;

- the ELG should aim to satisfy the specification of a rural electricity supply and hold the steady-state frequency within  $\pm 2\%$ , and the voltage within  $\pm 5\%$ .
  
  - it should be capable of balancing the currents of a three phase system to avoid excessive unbalanced situations, harmful to the generator.
  
  - it should minimise the harmonics that are produced by rapid switching of power electronic devices.
  
  - it should be suitable for stand-alone, black-start, operation.
  
  - it should avoid the use of analogue components for the control circuitry.
  
  - microprocessor operating systems should be straightforward and should be part of a single card microcomputer.
  
  - it should be simple to install and to operate.
  
  - it should have a target selling price of between £500 and £2000.
-

### 8.1.3. The Development of a Functional ELG

A prototype ELG was developed which met the majority of the requirements listed above, and which functioned successfully during trials on water turbine driven generators. On a typical Pelton turbine, the steady-state frequency variation is  $\pm 3.2\%$  and on the test generating systems, as the voltage is proportional to the frequency, the voltage variation is of the same order. The ELG has a built-in power supply which permits black-start operation; the unit powers up and begins operation as the generator terminal voltage builds up in response to the turbine accelerating from rest. Three phase current balancing is performed to  $\pm 14\%$  as a part of the load change routine. This was achieved through the use of a microprocessor and digital circuits. The hardware involved in obtaining knowledge of the currents can also be used for other functions.

The control functions are performed by digital electronic circuits using the FORTH Microcard, a single card microcomputer, based on the Rockwell RS65F12 single chip microprocessor. The application of a proprietary microcomputer was used to avoid the pitfalls of custom building a new system. During the course of the development, no disadvantages of this choice became apparent. Given that the ELG is based on this microcomputer, the future availability of the card, or at least its components, is a consideration.

The decision to program the microprocessor in the FORTH high level language also presented no major problems. The basic language proved simple to learn, the only significant difficulties experienced were those

---

of the detail of the interrupt handling procedures. Further minor problems arose when transferring the program to EPROM, but once resolved, replication proved straightforward.

The ELG is simple to install and as it is based on measurement of frequency rather than voltage, the unit can be sited at any part of the power system. Commissioning of the unit requires simple selection of microswitches and calibration of the current measuring potentiometers. It is expected that with use of the deadband prediction technique, and with further work on the estimation of the wait delay setting, the limit switches could be factory preset to avoid the need for on site adjustment. Once commissioned, the ELG requires no operator intervention.

The prototype ELG was developed at a cost which suggests that production versions **would be competitive** with the existing market, except at the lower end of the micro hydro rating category. This for a unit which is technically superior, as it reduces harmonics and performs three phase balancing. The usual problem of dis-economy of scale is applicable in this instance.

The prototype units presently assembled are reasonably rugged by virtue of the fact that they use properly designed and built PCBs, along with proprietary components such as transformers, solid state relays and current transformers. With only slight modification, a similar unit could be installed at a site which enjoys relatively good environmental conditions, as typically found in a weatherproof building in the UK.

---

For harsher environmental conditions, such as those described by Robinson<sup>65</sup>, close attention would be required to aspects such as PCB encapsulation, enclosure classification, heat dissipation, the ribbon cable interconnections and integrated circuit soldering. Techniques for improving the reliability for electronic components are described by Whittington<sup>66</sup>.

As it is likely that the repair policy appropriate to the unit would be one of repair by replacement of sub-assemblies, then the extent of the modularisation of the unit should be considered. The prototype unit has a semi-modular design at present; the main ELG enclosure contains only 3 separate assemblies, 1 transformer and 2 PCBs. It is recommended that unskilled personnel should not replace components on the PCBs and hence replacement of the complete PCB is all that would be required. The assumption here is that the investigating personnel have the skill in the first instance to pinpoint faults to this degree of accuracy. Other discrete modules which presently exist are the CTs and the solid state relays.

Further modularisation may be possible in respect of mounting of the PCBs on backplanes and the sub-division of the power supply circuit from the I/O board, however the increased cost of this should be weighed up against the perceived advantages. Given that there are different markets which the ELG could be applied to, in respect of their ability to afford, and to use, functions such as protection and data logging, these could be made available as options. The addition of an option simply through the insertion of an extra PCB clearly lends itself to a modular design.

---

Attention to the appropriate manufacturing and quality assurance standards would be the task of the Company who would ultimately produce the unit. Given that the largest market for the ELG is likely to be outwith the UK, then attention would also have to be given to the necessary import requirements, and the Standards applicable, in the recipient country. In addition, equipment of this nature will also be the subject of the latest CEC directive on Electromagnetic Compatibility<sup>67</sup> (EMC) which will require all equipment placed on the market to comply with the directive.

#### **8.1.4. The Establishment of Test Facilities**

The hydraulic test facility installed at the Merchiston Site of Napier University was converted through the replacement of the load pump with a three phase synchronous generator. This provided the unique opportunity to carry out laboratory based performance testing of the ELG on a Pelton turbine. In addition, a data acquisition system was established to enable computer based measurement of the transient frequency of the rotating plant during load changes.

In its present form, the hydraulic facility is now suitable for the testing of all major electro-mechanical components of a micro hydro scheme, i.e. turbines, generators and electronic load governors. Additional facilities have been established for functional testing of the ELG on the motor-generator set in the machines laboratory at the Craiglockhart Site of Napier University.

---



### 8.1.5. Prediction of Deadband Selection for Steady-State Operation

To avoid unstable operation arising due to small-scale changes in either the input hydraulic conditions or the consumer load, the ELG must operate within a selected deadband around the nominal frequency. A method for prediction of the necessary deadband was derived which requires knowledge only of the ratio of the turbine runaway speed to its nominal running speed. As this data is readily obtained from turbine manufacturers, a knowledge of the deadband selection required to give steady-state operation of the system is thus available at the initial design stage, as opposed to the site commissioning stage.

For the Pelton turbine, the theoretical runaway speed is twice the optimum running speed but is often less, typically 1.65 times the nominal speed. The associated droop requires a deadband setting of  $\pm 1.6$  Hz, giving the percentage frequency variation stated in Section 8.1.3. As it is currently designed, the ELG has the capability to govern the majority of common turbine types.

The concept of a "coefficient of stability" was developed as a measure of the probability of the frequency leaving the deadband due to small-scale torque disturbances. This is determined using the calculated deadband value and the selected deadband value. A unity value for the coefficient of stability represents the ideal deadband selection, a value less than unity implies a greater probability of frequency excursions.

---

### 8.1.6. Prediction of Transient Operation

The block diagram of the complete control system was established, with change in consumer-load torque as the input and the frequency of the generated waveform as the output. Transfer functions for the rotating system and the turbine were derived. The non-linear nature of the deadband, and of the saturation of the ballast load application, put the solution of the transfer function of the ELG beyond the scope of this study. The time varying nature of the ballast load application compounded the complexity of the model.

As an alternative, a computer program was written which models the frequency transient for a Pelton turbine during the period following a rejection of the consumer load. The initial validation of the model has been against the measured frequency transients of two different Pelton turbine installations; however, the absence of definitive inertia data gave rise to a small degree of uncertainty in respect of the accuracy of the model. The behaviour of the voltage during the transient period was studied and found to be largely in proportion to the frequency transient.

The original model program was modified to investigate the possible advantages accruing from the adoption of proportional-derivative control, based on the initial rate of rise of frequency. The outcome of this study suggested that it would be advantageous to modify the ELG program to two-term control.

---

## 8.2 FURTHER WORK

Arising out of the work have come several recommendations for extension of the subject area of the project; these are listed below.

A few minor problems were experienced during the testing of the ELG, and the suggestions for further work associated with this item are;

- the centering of the deadbands exactly on 50Hz.
- modification of the three phase balancing subroutine within the main ELG program.

A solution to the diseconomy of scale at ratings in the order of 5kW - 20kW is considered a suggestion for further work. In the event that the development proceeds towards production, then a more detailed estimate of the cost of a production-unit would also be required.

The data acquisition software had some minor operational problems and it is suggested that further work would be the improvement of the data acquisition system, in respect of both the software and the hardware.

Suggestions for further work associated with the transient operation and stability are;

- further validation of the model, preferably on additional Pelton installations.
  - preparation of alternative versions of the model for other turbine types, and the subsequent validation thereof.
-

- a more detailed study and analysis of the voltage transient.
  
  - prediction of the wait delay setting and consideration to the provision of longer wait delay periods, if required, for stability purposes.
  
  - a detailed stability analysis. It is known that the deadband and the wait delay are the significant parameters which affect the stability of the system, but their inter-relation and definitive values which ensure stability have not yet been established. The dependence on the magnitude of the initial load change which causes the frequency variation also needs investigation. It is expected that the foregoing will be achieved in conjunction with the improvement in either the solution of the transfer function or the accuracy of the model. The model should be extended and used for this purpose.
  
  - consideration of the need for wider deadbands, or to increase the number of ballast load sections, to ensure stability when applied to turbine types with runaway speed ratios greater than 2.93.
  
  - the implementation of proportional-derivative control to the main ELG program. The selection of the constant of proportionality may complicate matters in respect of the stability, however it is hoped that the nature of this control action will simplify the solution of the ELG transfer function and assist the stability analysis.
-

Key suggestions for further work are;

- the application of the ELG on a real hydro-electric installation to obtain feedback on its continuous performance under true operational conditions.
  
- the commercial production of the unit.

Other areas within the subject area which remain to be addressed are discussed in the following sections;

### **8.2.1. Reactive Power Control**

The work of this study has assumed that both the consumer load and the ballast load are purely resistive. In the latter case, this is a reasonable assumption as the use for the ballast load is predominately for heating of one form or another. In the case of the consumer load, it is possible that variable reactive loads such as motors will form part of the load.

For a load with resistance and inductance, the current is considered as having two components, the active component,  $I \cos \phi$ , and the reactive component,  $I \sin \phi$ . The power is a function only of  $I \cos \phi$ , and hence the electrical torque which the consumer load applies to the generator shaft,  $T_{cl}$ , is more accurately defined as being proportional to  $G$ , the conductance, not  $Y$ , the admittance.

When a reactive load is connected to a generator, a problem can arise for the generator - and the cabling - when the reactive power increases

---

without a subsequent decrease in the active power. A given generator should not be operated outwith the limits of its capability chart, and as an approximation, in the over-excited state, this is bounded by the apparent power rating of the machine. If the apparent power increases beyond the limit, then dangerous stator overheating can occur.

The operation of the ELG is based presently solely on frequency variation. When operating with inductive loads, it is envisaged that problems may occur unless additional measures are taken by the ELG. For example, consider a circuit where the magnitude of the current is held constant at rated level, but  $R$  and  $X_l$  can vary such that  $I \cos \phi$ , and hence the generator shaft torque,  $T_{cl}$ , can change. If  $T_{cl}$  decreases, then from the torque balance, equation 7.1, the speed will rise and the ELG will add ballast load, hence increasing the current to potentially harmful levels. Another problem is that of voltage regulation. Mackintosh<sup>52</sup> observed that cage induction type motors, supplied from the generator, stalled as the current increased due to added inductive load. This was due to the torque output of the motor reducing with the square of the applied voltage, which was decreasing as the current rose.

It is suggested that computer simulation of complex loads be initiated which will study the effect of varying the reactive component of the load, and the reaction of the ELG. On the strength of this, suggestions for improvements to the ELG program should arise. For instance, the ELC could also perform automatic power factor correction, but the added complexity of this would need to be studied carefully. As the magnitude of the current is fundamental to this problem, it likely that this will impinge on the unit protection function, refer Section 8.2.2.

---

Another area which will require investigation is the interaction of the ELG in the event that the generator is fitted with an automatic voltage regulator, (AVR). It is known that the two separate control systems associated with the ELG and the AVR may cause oscillations to occur. Research and experimentation should be performed to establish the extent of the problems that may occur and determine solutions to avoid adverse interaction between the two controllers.

### **8.2.2. Protection Functions**

A hydro-electric generating unit must be provided with a reasonable degree of electrical and mechanical protection to prevent fault or abnormal conditions from causing damage to the unit. Protection for the electrical distribution system would normally be provided separately.

The extent of electrical protection considered appropriate for a micro hydro-electric generator is as follows<sup>38</sup>;

- overcurrent,
- overvoltage,
- underfrequency and overfrequency.

In addition, the minimum mechanical protection required would be prevention of continuous running at overspeed beyond the design capability of the turbine and generator.

The ELG operation is such that it normally provides corrective action in the event that the frequency deviates outwith preset frequency limits. Hence, additional frequency *protection* would operate at wider limits,

---

say  $\pm 15$  Hz, which would indicate that an abnormal condition was present. In addition, based on the existing ELG control action, relatively high frequency and voltage swings would be expected to occur under normal transient conditions, and so any protection function would need to recognise the possible existence of such swings for short periods of time.

In its present form, the ELG monitors the frequency and the program recognises wide frequency values, but takes no action. The ELG also presently reads the relative values of the three line currents as part of the load balancing routine. In addition, the I/O PCB has provision for a fourth ADC circuit which could be used to determine the magnitude of the voltage. Thus with only minor addition of components to the I/O PCB, and with relatively straightforward software modifications, it will be possible to implement detection of the fault conditions listed above.

Of equal importance is the action taken by the ELG in the event of detection of a fault, and the action must be appropriate for the anticipated installation. Raising alarms which may not be understood, or which rely on operator action, may not be suitable. For instance, in the event that overcurrent is detected, automatic load shedding may be more applicable, followed if necessary by the opening of the line circuit breaker. The likely cause of high voltage swings will largely depend on the nature of the load and the relative proportion of reactive load to resistive load. As mentioned above, this aspect requires further study in conjunction with the reactive power control work. As a minimum, the generator field circuit should be opened to avoid damage to the winding insulation. Sustained over- or underfrequency operation should initiate a

---



shutdown of the set. This could be achieved by automatic closure of the main inlet valve, however this would imply that such automation was economically and technically feasible.

The addition of the protection functions begins the conversion of the ELG into an Electronic Load Controller and is clearly an important development for the unit. It is recommended that this work is pursued as soon as possible to maximise the appeal of the unit.

### **8.2.3. Data Logging / Condition Monitoring**

Both of these topics are vast in their own right and whilst their addition to the ELG as further conversion to an ELC may seem desirable at first sight, they should only be implemented if appropriate. It is certain that implementation would be possible technically, what is less certain is the nett advantage that would accrue as a result.

#### ***Data Logging***

This term conveys the concept that pertinent data will be read, and will either instantly be printed out on paper, or will be stored over a predetermined time in some standard form. The addition of this function to the ELG implies that use will be made of the stored data, and this itself will require careful research, in respect of the method of data interrogation and the resultant feedback. This may be best performed in the intended market territories.

---

The data to be stored will typically be the 3 line currents, the voltage, the frequency, and perhaps the historical sequence of load changes. Given the implementation of the protection functions listed above, access to this data will be inherent. The additional facilities required would be;

- non-volatile memory devices or mass storage media.
- interrogation means, either via a plug/socket or by chip removal.

The logistics of the interrogation would require to be researched in terms of the availability and use of skilled personnel, or the training of unskilled personnel. The specific location of the interrogation also requires consideration, e.g. on-site or elsewhere.

### ***Condition Monitoring***

This function is essentially an intelligence which can diagnose and predict fault conditions before they occur, rather than simply detect a fault as it occurs. Monitoring of vibration, stator temperature and cavitation are performed on small and large hydro plant but are rarely applied to micro hydro installations because of their cost.

The further work which is suggested here is the research into the existing techniques in data logging and condition monitoring to determine which, if any, would be appropriate for this application. Thereafter, these functions could be added to the ELG, provided that this can be done without adversely affecting the economics of the unit.

---

#### 8.2.4. Additional Control Functions

Each of the following control functions merit research as further work in the development of the ELC.

Presently, the selection of the sections of ballast load which are energised is a function of the binary nature of the ballast load. Additional intelligence could be added to the selection procedure in order to perform **load management**, allowing a more strategic selection of ballast load. Such an option would erode the general nature of the ELC design as it would incur the cost penalty of being site-specific and therefore requires additional research.

In the event that the consumer load remains at a low per-unit level for a significant time, and that the use of the compensatory ballast load is not of particular importance, then it is possible that **water economising** could be applied. This function would require a more sophisticated water regulating device, hence increasing the cost, and again requires additional research before implementation.

For applications where the generating set is normally connected to a grid system but also runs isolated for periods of time, then the ability to use the ELC to **synchronise the generator** to the grid would be an advantage. Research should be carried out to determine the feasibility of using the ELC as an automatic synchroniser.

---

### **8.2.5. Market Penetration**

As a result of the market survey undertaken, all of the existing suppliers of ELGs who responded to the survey were from developed countries. It is considered that a substantial portion of the total market will be in the developing countries. It may be that penetration of that market would require some form of Technology Transfer where the manufacture and assembly of the ELG is performed in the territory in a factory with the requisite electronic assembly skills. The topic of Technology Transfer is also vast in its own right, and is the subject of several postgraduate studies within the Department of Electrical Engineering at the University of Edinburgh. It is suggested that research is done to apply the lessons learnt in these studies to this particular application, or to make this the subject of a separate study.

### **8.3 POSTSCRIPT**

The performance of this research has exposed the author to many new experiences, in not only an academic sense but also a cultural sense. The logistics of performing the study over a five and a half year period on a part-time basis has been an experience in its own right. The completion of this thesis is considered a major personal achievement and has been thoroughly rewarding. It is the author's intention to continue with as much of the suggested further work as is possible, either personally or on a supervisory basis.

---

APPENDIX 1 PRINTED CIRCUIT BOARD DETAIL

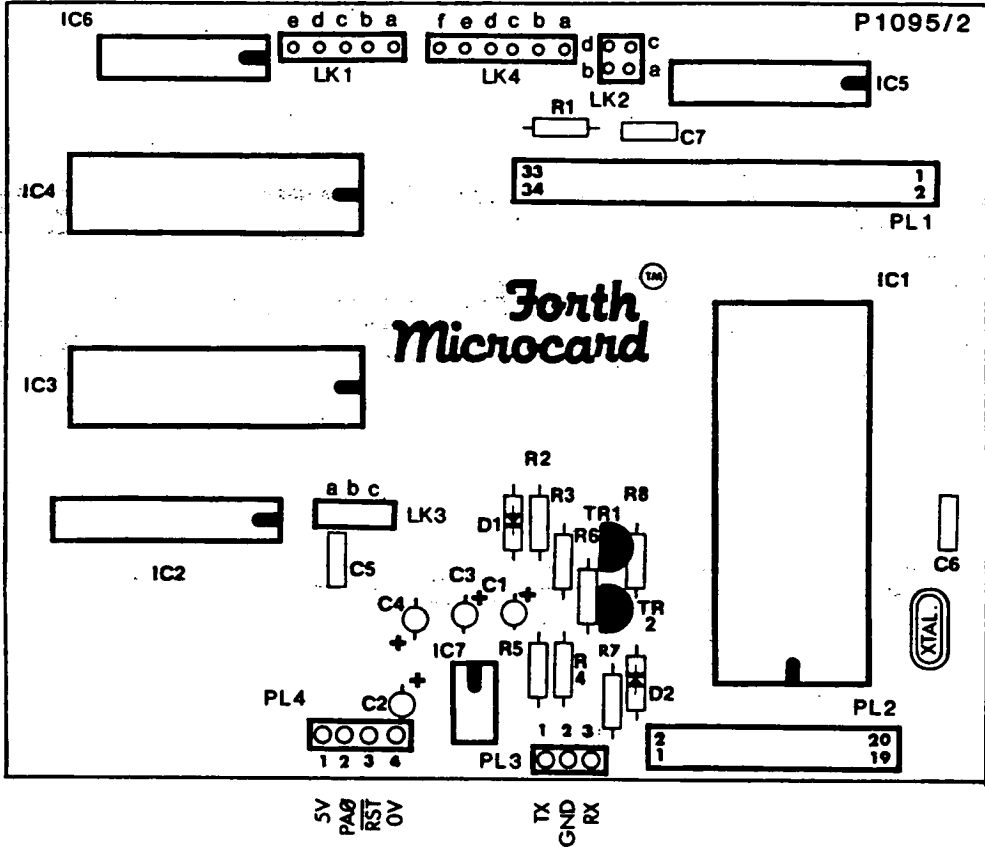


Figure A1.1 - Essex FORTH Microcard PCB layout

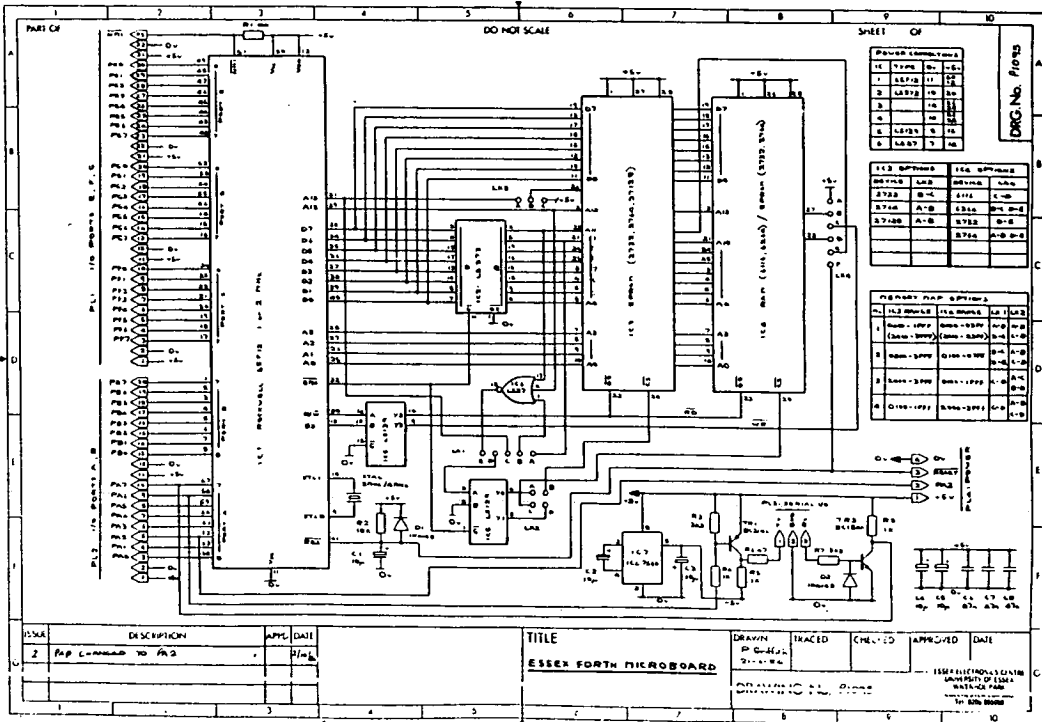


Figure A1.2 - Essex FORTH Microcard circuit diagram

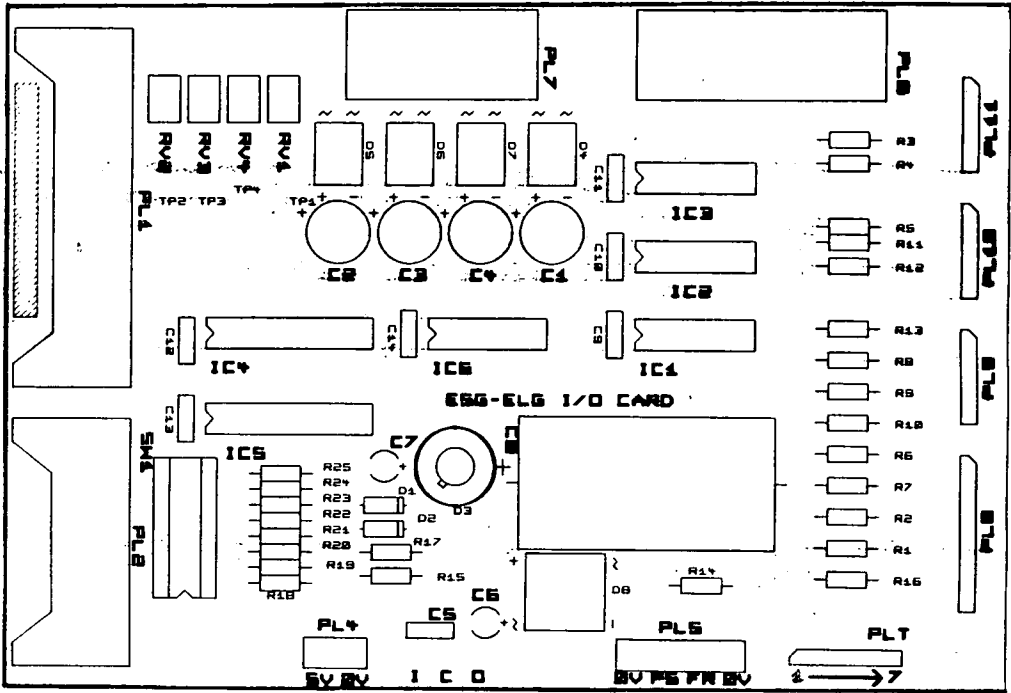
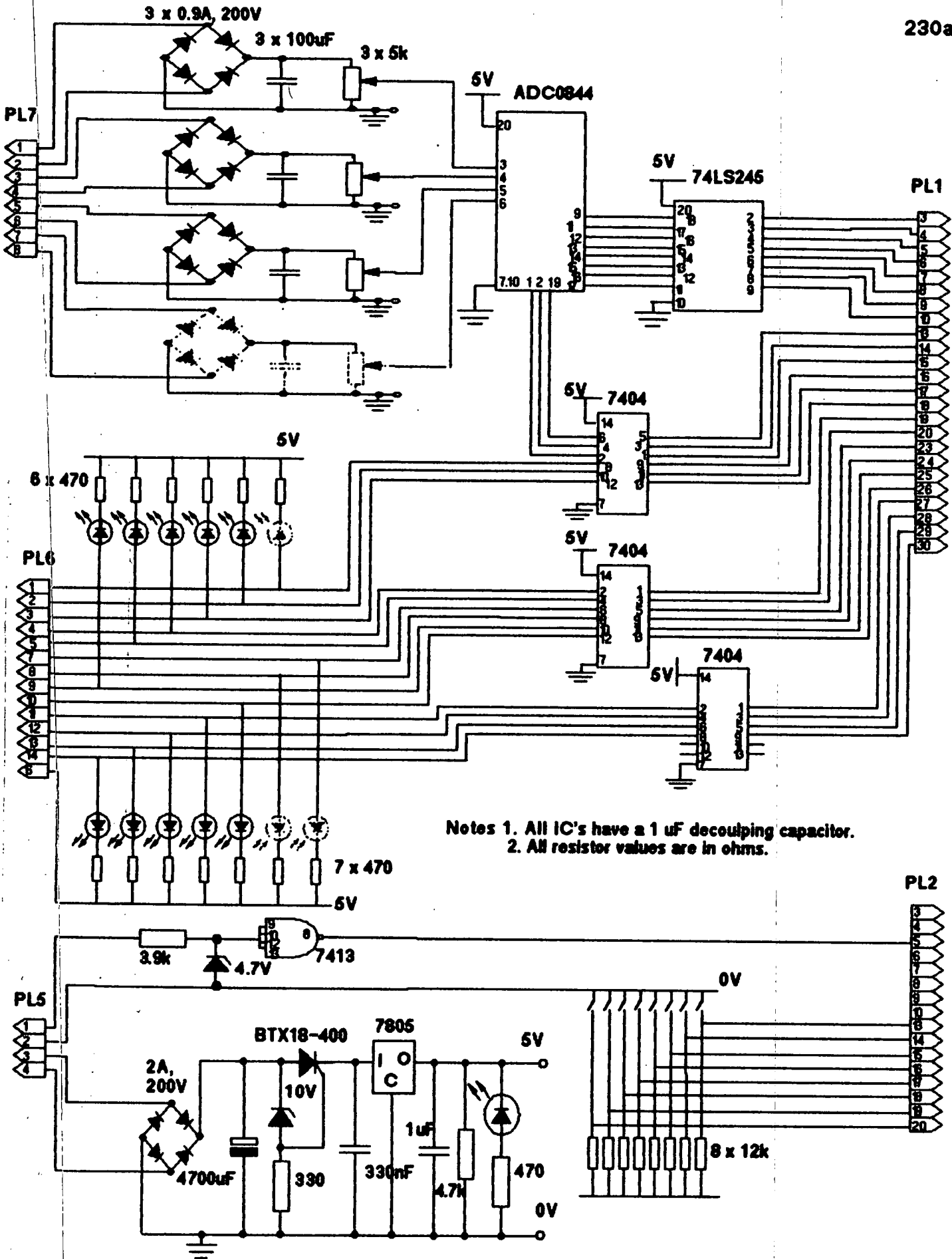


Figure A1.3 - I/O PCB layout



Notes 1. All IC's have a 1 µF decoupling capacitor.  
2. All resistor values are in ohms.

Figure A1.4 - I/O PCB circuit diagram

---

**APPENDIX 2 THE FORTH LOAD GOVERNING PROGRAM**
**A2.1 LG9**

( FILENAME :- LG9. START WORD :- RUN. DATE 12/7/90)

( FINAL VERSION FOR EPROM PROG TG6 BASED ON 50HZ, 3 PHASE)  
 ( OPERATION. PROG TO MEASURE FREQUENCY BY NEG EDGE)  
 ( DETECTION AND CODE DEF IRQ, READ DEADBAND SETTING,)  
 ( COMPARE THE TWO THEN PERFORM THREE PHASE BALANCING)  
 ( LOAD CHANGES. PA2 NOT DISABLED. READS FDB EVERY 255)  
 ( CYCLES. VARIABLE WAIT DELAY AFTER LOAD CHANGE ONLY. INC)  
 ( UFF TO INHIBIT LOW FREQ OP)

HEX

CODE SERV	( IRQ SERV RTN)
PHA,	
TYA,	
PHA,	
1D LDA,	( READ UCB)
200 STA,	( STORE UCB)
11 LDA,	
202 STA,	
FF * LDA,	( LOAD ACC)
1E STA,	( START TIMER)
FB * LDA,	( RE-ENABLE IRQ)
10 AND,	
10 STA,	
PLA,	
TAY,	
PLA,	
RTI,	
END-CODE	

@ SERV @ 0040 !	( SAVE IRQVEC)
-----------------	----------------

FORTH

220 CONSTANT FDBTAB	( BASE MEMORY FOR DB TABLE)
3C CONSTANT FPLOLIM	( 40 HZ LIMIT)
87 CONSTANT FPUPLIM	( 65 HZ LIMIT)
54 USER DBC	( DEADBAND COUNT)
56 USER RED	( RED BU STATUS)
58 USER YELLOW	( YELL BU STATUS)
5A USER BLUE	( BLUE BU STATUS)
5C USER FMLOLIM	( INIT FREQ LOWER LIM)
5E USER FMUPLIM	( INIT FREQ UPPER LIM)
60 USER DSH	( FOR TOGGLE)

---



---

```

62 USER WD          ( WAIT DELAY)
64 USER RCUR        ( RED CURRENT)
66 USER YCUR        ( YELL CURRENT)
68 USER BCUR        ( BLUE CURRENT)
6A USER LEAST       ( MIN CURRENT)
6C USER MOST        ( MAX CURENT)

: INITIALISE        ( INITIALISES THE VARIABLES)
FF DBC !
0 RED !
0 YELLOW !
0 BLUE !
0 FMLOLIM !
0 FMUPLIM !
0 WD !
0 RCUR !
0 YCUR !
0 BCUR !
0 LEAST !
0 MOST !
0 DSH !
6364 220 !          ( STORE D'BAND TABLE FOR 50 HZ)
6265 222 !
6166 224 !
6067 226 !
5F68 228 !
5E69 22A !
5D6A 22C !
5C6B 22E ! ;

: ZERO              ( ZERO PE/PG)
0 PE C! 0 PG C! ;

: WAIT1             ( 1s DELAY)
80 0 DO 80 0 DO LOOP LOOP ;

: WAIT20            ( 20 ms DELAY)
140 0 DO LOOP ;

: WAIT4             ( 4 ms DELAY)
40 0 DO LOOP ;

: WAITVAR           ( VARIABLE WAIT DELAY)
0 DO WAIT4 LOOP ;

: READWD            ( READS PB3&4)
PB C@ 8 / 3 AND WD ! ;

: WAIT              ( WAIT DELAY AFTER CHLOAD)
READWD WD @
.1 < NOT IF WD @ WAITVAR THEN ;

```

---

---

```

: BITSH3L                ( SHIFT TO LEFT BY 3 BITS)
8 * ;

: TOG                    ( TO TOGGLE PG3 AT END OF SEQU)
DSH @ NOT DUP DSH !
BITSH3L BLUE @ + PG C! ;

: INCTEST                ( TEST FOR FULL LOAD AND INC BY 1)
DUP 7 =                  ( TEST FOR FULLY LOADED)
IF ELSE 1 + THEN        ( IF FALSE, ADD 1, IF TRUE ADD 0)
DUP ;                    ( DUPS STACK FOR FUTURE USE)

: DECTEST                ( DEC BY 1 AND TEST FOR ZERO LOAD)
DUP 0 =                  ( TESTS FOR ZERO LOAD)
IF ELSE 1 - THEN        ( IF FALSE, SUB 1, IF TRUE SUB 0)
DUP ;                    ( DUPS STACK FOR FUTURE USE)

: PG@ PG C@ ;

: PG! PG C! ;

: ADCGO                  ( ADC OPERATION ROUTINE)
PG@ DUP DUP DUP DUP DUP
40 OR PG!
C0 OR PG!
40 OR PG!
0 OR PG!
1 0 DO LOOP
60 OR PG! ;

: READIR                 ( READ RED CURRENT)
4 PF C! ADCGO PF C@ RCUR !
0 OR PG! ;

: READIY                 ( READ YELL CURRENT)
5 PF C! ADCGO PF C@ YCUR !
0 OR PG! ;

: READIB                 ( READ BLUE CURRENT)
6 PF C! ADCGO PF C@ BCUR !
0 OR PG! ;

: READI
READIR READIY READIB ;

: INCR                   ( RTN TO INC RED BY 1)
RED @                    ( READS LAST VALUE FOR RED)
INCTEST
RED !                    ( STORES NEW VALUE OF RED)
BITSH3L                 ( 3 BIT SHIFT TO LEFT)

```

---

---

```

YELLOW @ +                ( ADDS PRESENT Y VALUE)
PE C! ;                   ( OUTPUTS TO SSR'S)

: INCY                    ( RTN TO INC YELL BY 1)
YELLOW @
INCTEST
YELLOW !
RED @ BITSH3L +
PE C! ;

: INCB                    ( RTN TO INC BLUE BY 1)
BLUE @
INCTEST
BLUE !
DSH @ BITSH3L +
PG! ;

: DECR                    ( RTN TO DEC RED BY 1)
RED @
DECTEST
RED !
BITSH3L
YELLOW @ +
PE C! ;

: DECY                    ( RTN TO DEC YELL BY 1)
YELLOW @
DECTEST
YELLOW !
RED @ BITSH3L +
PE C! ;

: DECB                    ( RTN TO DEC BLUE BY 1)
BLUE @
DECTEST
BLUE !
DSH @ BITSH3L +
PG! ;

: INCLOAD                ( 3 PH BALANCING LOADING)
READI
RCUR @ YCUR @
< IF RCUR @ LEAST ! ELSE YCUR @ LEAST ! THEN
LEAST @ BCUR @
< IF ELSE BCUR @ LEAST ! THEN
RCUR @ LEAST @ =
IF INCR ELSE BCUR @ LEAST @ =
  IF INCB ELSE YCUR @ LEAST @ =
  IF INCY THEN
  THEN

```

---

```

THEN
WAIT ;

: DECLOAD          ( 3 PH BALANCING UNLOADING)
READI
RCUR @ YCUR @
> IF RCUR @ MOST ! ELSE YCUR @ MOST ! THEN
MOST @ BCUR @
> IF ELSE BCUR @ MOST ! THEN
RCUR @ MOST @ =
  IF DECR ELSE BCUR @ MOST @ =
  IF DECB ELSE YCUR @ MOST @ =
  IF DECY THEN
    THEN
    THEN
  WAIT ;

: READFDB          ( READ FRQ D'BAND SETTING)
PB C@ 7 AND        ( READS DB)
2 * FDBTAB + DUP   ( CREATES CORRECT MEMORY LOCAT'S)
C@ FMUPLIM !       ( ASSIGNS UPPER LIM VARIABLE)
1 + C@ FMLOLIM ! ; ( ASSIGNS LOWER LIM VARIABLE)

: DBCW             ( DEADBAND COUNT WORD)
DBC @
FF = IF READFDB 0 DBC ! THEN
DBC @ 1 + DBC ! ;

: SETCB            ( SEL/IMIT CB)
EO MCR C!          ( SEL TIMER MODE)
FF 1C C!           ( IMIT LLB)
FF 1D C! ;         ( INIT ULB)

: ENABLE           ( ENABLE IRQ FROM PA2)
4 IER C! ;

: LOOK 202 C@ 20 AND 20 = ;

: CHLOAD
200 C@             ( READS MEM LOC WITH UCB STORED)
FMLOLIM @ <       ( COMP WITH LOWER LIM)
IF DECLOAD        ( IF LESS, PERFORM DECLOAD)
ELSE 200 C@
FMUPLIM @ >       ( COMP WITH UPPER LIM)
IF INCLOAD THEN   ( IF MORE, PERFORM INCLOAD)
THEN ;

: COMPFM           ( COMP WITH DB AND CHLOAD IF NESS)
LOOK NOT
IF CHLOAD ELSE WAIT! THEN ;

```

---

```

: COMPFP                ( COMP WITH LIMITS)
200 C@ DUP
FPLOLIM <
IF 0 ELSE 1 THEN
SWAP
FPUPLIM >
IF 0 ELSE 1 THEN
AND
IF COMPFM THEN ;

: SEQU                  ( SEQU TO MEAS/COMPARE/CHANGE)
DBCW                    ( READS FREQ DEADBAND)
COMPFP TOG ;           ( FREQ COMP FOR MEAS, TOGS PG3)

: RUN
081C 40 !
ZERO                    ( RESETS PORTS)
INITIALISE
SETCB ENABLE WAIT20    ( ENABLES PA2-IRQ THEN WAITS 20ms)
BEGIN SEQU AGAIN ;    ( PERFORMS SEQU INDEFINITELY)

```

---

## A2.2 STANDARD RSC-FORTH WORDS IN LG9

CODE, END-CODE, PHA,, TYA,, LDA,, STA,, AND,, PLA,, TAY,, RTI,, '. @,  
 !, CONSTANT, USER, PE, PF, PG, C!, C@, DO, LOOP, AND, OR, <, >,  
 NOT, IF, THEN, ELSE, \*, +, -, /, DUP, =, MCR, IER, BEGIN, AGAIN.

## A2.3 USER DEFINED WORDS IN LG9

SERV, INITIALISE, ZERO, WAIT1, WAIT20, WAIT4, WAITVAR, READWD,  
 WAIT, BITSH3L, TOG, INCTEST, DECTEST, PG@, PG!, ADCGO, READIR,  
 READIY, READIB, READI, INCR, INCY, INCB, DECR, DECY, DECB,  
 INCLOAD, DECLOAD, READFDB, DBCW, SETCB, ENABLE, LOOK,  
 CHLOAD, COMPFM, COMPFP, SEQU, RUN.

---

### APPENDIX 3 D.C. MOTOR MODEL

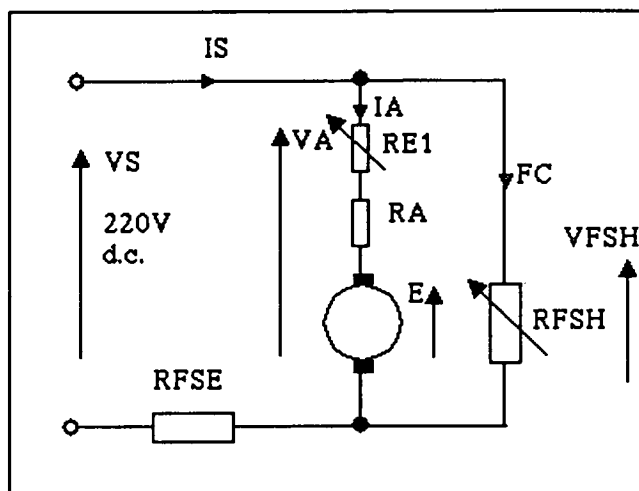


Figure A3.1 - D.C. motor circuit diagram for model

#### PROGRAM MODEL4.BAS

```

10  dim f(20)
20  dim fp(20)
30  dim is(20)
40  fullw 2
50  clearw 2
60  ' prog MODEL4 ( 9.12.91 ) for plotting the dc motor results
70  ? "Program to model the dc shunt motor in LB14":?
80  vs=230
90  ' Inputting instructions
100 ??:? "Select option":?
110 ? "1. Add external armature resistance ":?
120 ? "2. Vary shunt field resistance from 540 ohm":?
130 ? "3. Quit program. ":?
140 input m
150 ??:?
160 if m=1 then goto 190
170 if m=2 then goto 230
180 if m=3 then goto 920
190 rt2=0:drf=0
200 Input "Enter value of added armature resistance from 0 to
    1.7 ohm ",re1
210 if re1>1.7 or re1<0 then ?:goto 200
220 goto 250
230 rt2=0:re1=0
240 input "Enter difference + or - from 540 ohm ",drf
250 rfsh=540+drf
260 clearw 2
270 ' axes plot
280 linef 65,40,65,320
290 linef 55,240,565,240

```

```

300 ' horizontal lines
310 for yc=80 to 280 step 40
320 for xc=67 to 565 step 16
330 linef xc,yc,(xc+4),yc
340 next xc
350 next yc
360 ' vertical lines
370 for xc2=135 to 565 step 70
380 for yc2=40 to 320 step 16
390 linef xc2,yc2,xc2,(yc2+4)
400 next yc2
410 next xc2
420 ' calculations and plot
430 ' j represents the load current
440 for j=3 to 14
450 if j>8 then rfsh=rfsh+2
460 gosub 760
470 ' calcs coords first
480 is(j)=(j*35)+65-105:fp(j)=240-(fr*40)
490 ' skips first point
500 if j=3 then goto 520
510 linef is(j),fp(j),is(j-1),fp(j-1)
520 next j
530 droop=(f(3)-f(14))/2.13
540 db=droop*0.12
550 rfsh=540+drf
560 ' labels plot
570 gotoxy 4,4:? 54:gotoxy 4,9:? 52:gotoxy 4,13:? 50
580 gotoxy 10,14:? 0.18:gotoxy 18,14:? 0.57:gotoxy 27,14:? 0.96
590 gotoxy 35,14:? 1.35:gotoxy 44,14:? 1.75:gotoxy 53,14:? 2.13
600 gotoxy 4,2:? "Frequency (Hz)":gotoxy 25,1:? "DC Motor frequency
v load"
610 gotoxy 46,15:? "Generator output power (kW)"
620 gotoxy 10,17:? "Droop is";droop;"Hz/kW. Min deadband is";db;"Hz."
630 gotoxy 4,18:? 48:gotoxy 10,18:? "Shunt field R is";rfsh;"ohm. Added
Ra is";rel;"ohm."
640 input "Press return to continue",h
650 clearw 2
660 ' Saves coordinates to disc for VIP plot later
670 input "Do you want these coords saved to disc, 1 for y, 0 for n ",
disc
680 if disc=1 then ? :input "enter filename ",name$:filename$=name$+
".prn"
690 if disc=0 then goto 740
700 open "o",#1,filename$
710 for j=3 to 14
720 print#1,j,f(j)
730 next j
740 close 1:clearw 2
750 goto 90

```

```
760 ' calculation subroutine
770 ra=2
780 g=3.02
790 va=vs-(j*rt2)
800 vfsh=va
810 fc=vfsh/rfsh
820 ia=j-fc
830 rt1=ra+rel
840 e=va-(rt1*ia)
850 wr=e/(g*fc)
860 nr=wr*9.55
870 ' actual frequency
880 f(j)=nr/30
890 ' frequency rise above 50 Hz
900 fr=f(j)-50
910 return
920 end
```

---



---

**APPENDIX 4      MODEL PROGRAM LISTINGS****A4.1   PROGRAM STTURB4.BAS**

```
10 ' Program name " STTURB4 "9.12.91 - saves f&t to disc/turbine
    variations
20 ' includes auto selection of deadband
30 ' ARRAY DIMENSIONING
40 DIM MY(125)
50 DIM Y(125)
60 DIM TLC(125)
70 DIM F(125)
80 DIM G(125)
86 dim freq(125)
90 ' MAKES OUTPUT WINDOW FULL SIZE
100 FULLW 2
110 ' CLEARS OUTPUT WINDOW
120 CLEARW 2
130 ?? " This program graphs the load governed performance of a
    pelton wheel"
140 ?? " water turbine to a load rejection":?
150 ?? " The turbine is the Boving machine in A2S at Merchiston"
160 ?? " as currently configured for ELC testing."
170 ' PROMPTS AND INPUTS FOR VARIABLE DATA
200 ' CONSTANTS FOR BOVING TURBINE IN A2S
210 j=.67:rs=1200:fhs=770:rad=.133:Cv=.81
220 ?:input "Enter nett operating head in metres ",H?:input "Enter flow
    in l/s ",flow
230 RS=SQR(H/30)*RS
240 ' FREQ DEVIATION AND TIME CONSTANT CALCS
250 fr=((rs/fhs)-1)*50:fmax=50+fr
260 Tmax=2*flow*rad*cv*sqr(19.62*H)
270 K2=fmax/Tmax:TC=j*K2*1000:TA=1/TC
280 ?:input "select p.u. value of load rejection ",PU
290 if pu>1 then goto 280
300 ?:INPUT "Select multiplier for Wait Delay, WD, 0,1,2 or 3 ",WD1
310 if wd1>3 then goto 300
320 ' CONVERT WAIT DELAY TO ms AND PRODUCE PROG CYCLE
330 wd=wd1*4:pc=18+wd
340 H1=H*.726:FLOW1=1.43*FLOW
350 ' CALCS FOR DEADBAND AUTO SELECTION
360 dbc=fr/21
370 if dbc <.32 then db=.32
380 if dbc >=.32 and dbc <.64 then db=.64
390 if dbc >=.64 and dbc <.96 then db=.96
400 if dbc >=.96 and dbc <1.28 then db=1.28
410 if dbc >=1.28 and dbc <1.6 then db=1.6
420 if dbc >=1.6 and dbc <1.92 then db=1.92
430 if dbc >=1.92 and dbc <2.24 then db=2.24
440 if dbc >=2.24 and dbc <2.56 then db=2.56
```

---

```
450 if dbc >=2.56 then db=2.56:? "Deadband too wide for ELC."
460 ?:? "The auto db selector has calculated a value of +-";db;"Hz."
470 ?:input "Enter (1) if you accept this, or (0) if you wish to overrule
      ",ovr
480 if ovr=1 then goto 490 else goto 1590
490 ' LOAD REJECTION FREQ RISE
500 FD=fr*pu
510 clearw 2
520 ' DRAWS AXES
530 linef 65,0,65,340
540 linef 55,300,565,300
550 ' DRAWS HORIZONTAL DOTTED LINES
560 for yc=60 to 240 step 60
570 for xc=67 to 565 step 16
580 linef xc,yc,(xc+4),yc
590 next xc
600 next yc
610 ' CALC FOR DEADBAND LINES
620 P=DB*6:P1=300-P:P2=300+P
630 ' DRAWS VERTICAL DOTTED LINES
640 for xc2=148 to 480 step 83
650 for yc2=0 to 340 step 16
660 linef xc2,yc2,xc2,(yc2+4)
670 next yc2
680 next xc2
690 ' DRAWS UPPER DEADBAND LINE
700 for xc3=75 to 565 step 40
710 linef xc3,p1,(xc3+20),p1
720 next xc3
730 ' DRAWS LOWER DEADBAND LINE
740 for xc4=75 to 565 step 40
750 linef xc4,p2,(xc4+20),p2
760 next xc4
770 ' PLOTS UNGOVERNED TRANSIENT
780 FOR T=PC TO 1500 STEP PC
790 ' FREQUENCY DEVIATION AT TIME T
800 X2=FD*(1-(EXP(-T*TA)))
810 ' SCALE AND OFFSET FOR Y-AXIS
820 W2=X2*6
830 V2=300-W2
840 ' SCALE AND OFFSET FOR X-AXIS
850 Z2=(T/3)+65
860 ' FREQUENCY DEVIATION AT TIME T-PC
870 X1=FD*(1-(EXP(-(T-PC)*TA)))
880 W1=X1*6
890 V1=300-W1
900 Z1=((T-PC)/3)+65
910 ' DRAW LINE FROM T-PC TO T
920 LINEF Z1,V1,Z2,V2
930 NEXT T
```

```
940 ' INITIAL CONDITIONS
950 Q=0
960 MX=28/21
970 ' 28=((1200/770)-1)*50
980 TB=0.003
990 ' tb is 1/time constant for 30 H, 30 Q
1000 X=0
1010 FTA=0
1020 N=1
1030 BU=0:P=0:L=1
1040 freqmax=50
1060 FOR T=0 TO 1500 STEP PC
1070 ' DELAYED START ON LOAD APPLICATION UNTIL F>DB
1080 IF X<DB THEN FTA=0:N=1 ELSE FTA=FTA+PC
1090 ' LOAD REJECTION COMPONENT
1100 X=FD*(1-(EXP(-T*TA)))
1110 ' LOGIC TO SET THE LOAD MAGNITUDE/SIGN OF A GIVEN STEP
    AND LIMITS ON BU
1120 IF Q>DB AND BU<22 THEN MY(N)=MX:BU=BU+1 ELSE IF Q<-DB
    AND BU>-1 THEN MY(N)=-MX:BU=BU-1 ELSE MY(N)=0
1130 ' K IS NUMBER OF ACTIVE STEPS SINCE DELAYED START
1140 FOR K=1 TO N
1150 ' CURRENT TIME FOR EACH STEP
1160 TLC(K)=(FTA+PC)-(K*PC)
1170 ' CURRENT LOAD APPLICATION COMPONENT FOR EACH STEP
1180 Y(K)= MY(K)*(1-(EXP(-TLC(K)*TB)))
1190 ' SUM OF THE APPLICATION COMPONENTS OF FREQUENCY
1200 P=P+Y(K)
1210 NEXT K
1220 ' DIFFERENCE BETWEEN REJECTION AND APPLICATION
    COMPONENTS
1230 Q=X-P
1240 ' ACTUAL FREQUENCY VALUE
1250 freq(l)=50+q
1270 ' DETERMINES AND RETAINS MAX FREQUENCY
1280 if freq(l)>freqmax then freqmax=freq(l):tfm=t
1290 ' SCALE AND OFFSET FOR Y-AXIS
1300 W=Q*6
1310 F(L)=300-W
1320 ' SCALE AND OFFSET FOR X-AXIS
1330 G(L)=(T/3)+65
1340 ' DRAWS FIRST SECTION OF THE GOVERNED CURVE
1350 IF T=0 THEN DRAW 65,300,G(L),F(L):GOTO 1390
1360 ' DRAWS THE REMAINDER OF THE CURVE
1370 DRAW G(L-1),F(L-1),G(L),F(L)
1380 ' RESETS VALUES
1390 N=N+1
1400 P=0
1410 L=L+1
1420 NEXT T
```

---

```

1430 ' ANNOTATES GRAPH
1440 gotoxy 4,3:790
1450 gotoxy 4,7:? 80:gotoxy 4,10:? 70:gotoxy 4,14:? 60:gotoxy 4,17:? 50
1460 gotoxy 17,18:? "0.25":gotoxy 28,18:? "0.5":gotoxy 38,18:? "0.75"
1470 gotoxy 48,18:? "1.0":gotoxy 58,18:? "1.25":gotoxy 69,18:? "1.5"
1480 gotoxy 4,5:? "Frequency (Hz)"
1490 gotoxy 25,5:? "Predicted frequency transient."
1500 gotoxy 61,19:? "Time (s)"
1510 ' OUTPUTS DATA TO SCREEN
1520 ? "Max frequency is ";freqmax;"Hz at";tfm;"ms for a load rejection
of";pu ;"pu"
1530 ? "J=";j;"kgm2, wd=";wd;"ms, db= +-";db;"Hz, Head=";H;"m,
Flow=";flow;"l/s.
1540 ? "Ballast load= 4700W.":? " Based on the Boving turbine in A25."
1550 ' RETURNS TO BEGIN AGAIN
1560 if disc=1 then close 1
1561 input "Do you want these coords saved on disc, 1 for y, 0 for n
",disc
1562 if disc=0 then goto 1570
1563 if disc=1 then gosub 2050
1570 input "Do you want to go again, 1 for yes, 0 for no ",answ
1580 if answ=1 then goto 200 else end
1590 ' SUBROUTINE FOR DEADBAND SELECTION WHEN AUTO SELECT
OVERRULED
1600 ?:? "Select multiplier for deadband from 1 to 8."
1610 ?:? "DBM DB+--"
1620 ?" 1 0.32":?" 2 0.64":? " 3 0.96":? " 4 1.28"
1630 ?" 5 1.60":?" 6 1.92":?" 7 2.24":?" 8 2.56"
1640 ?:input dbm
1650 db=dbm*.32
1660 goto 490
2050 ' subroutine for disc save coords for VIP plot later
2060 clearw 2
2070 input "enter filename ",name$:filename$=name$+".prn"
2080 open "o",#1,filename$
2085 l=1
2090 for t=0 to 1500 step pc
2100 print#1,t,freq(l),50+db,50-db
2105 l=l+1
2110 next t
2120 close 1
2125 ?
2130 return

```

**A4.2 PROGRAM STTURB3.BAS**

```

10 ' Program name " STTURB3 "5.03.92 - saves f&t to disc/turbine
    variations
20 ' includes auto selection of deadband
30 ' ARRAY DIMENSIONING
40 DIM MY(125)
50 DIM Y(125)
60 DIM TLC(125)
70 DIM F(125)
80 DIM G(125)
90 ' MAKES OUTPUT WINDOW FULL SIZE
100 FULLW 2
110 ' CLEARS OUTPUT WINDOW
120 CLEARW 2
130 ?? " This program graphs the load governed performance of a
    pelton wheel"
140 ?? " water turbine to a load rejection":?
150 ' PROMPTS AND INPUTS FOR VARIABLE DATA
160 ? :input "Do you want next set of co-ords saved on disc, 1 for y, 0
    for n ",disc
170 if disc=1 then ? :input "enter filename ",name$:filename$=name$+".prn"
180 ? :input "Select Boving A25 turbine (1) or any alternative turbine (0)
    ",TUR
190 If TUR>1 or TUR<0 then goto 180
200 ' CONSTANTS FOR BOVING TURBINE IN A25
210 If TUR=1 then j=.67:rs=1200:fhs=770:rad=.133:cv=.81 else goto 1570
220 ? :input "Enter nett operating head in metres ",H?:input "Enter flow
    in l/s ",flow
230 IF TUR=1 THEN RS=SQR(H/30)*RS
240 ' FREQ DEVIATION AND TIME CONSTANT CALCS
250 fr=((rs/fhs)-1)*50:fmax=50+fr
260 Tmax=2*flow*rad*cv*sqr(19.62*H)
270 K2=fmax/Tmax:TC=j*K2*1000:TA=1/TC
280 ? :input "select p.u. value of load rejection ",PU
290 if pu>1 then goto 280
300 ? :INPUT "Select multiplier for Wait Delay, WD, 0,1,2 or 3 ",WD1
310 if wd1>3 then goto 300
320 ' CONVERT WAIT DELAY TO ms AND PRODUCE PROG CYCLE
330 wd=wd1*4:pc=18+wd
340 IF TUR=1 THEN H1=H*.726:FLOW1=1.43*FLOW ELSE
    H1=H:FLOW1=FLOW
350 ' CALCS FOR DEADBAND AUTO SELECTION
360 dbc=fr/21
370 if dbc < .32 then db=0.32
380 if dbc >=.32 and dbc<.64 then db=.64
390 if dbc >=.64 and dbc<.96 then db=.96
400 if dbc >=.96 and dbc<1.28 then db=1.28
410 if dbc >=1.28 and dbc<1.6 then db=1.6
420 if dbc >=1.6 and dbc<1.92 then db=1.92

```

---

```

430 if dbc >=1.92 and dbc<2.24 then db=2.24
440 if dbc >=2.24 and dbc<2.56 then db=2.56
450 if dbc >=2.56 then db=2.56:? "Deadband too wide for ELC."
460 ?? "The auto db selector has calculated a value of +-";db;"Hz."
470 ?input "Enter (1) if you accept this, or (0) if you wish to overrule
      ",ovr
480 if ovr=1 then goto 490 else goto 1690
490 ' LOAD REJECTION FREQ RISE
500 FD=fr*pu
510 clearw 2
520 ' DRAWS AXES
530 linef 65,0,65,340
540 linef 55,300,565,300
550 ' DRAWS HORIZONTAL DOTTED LINES
560 for yc=60 to 240 step 60
570 for xc=67 to 565 step 16
580 linef xc,yc,(xc+4),yc
590 next xc
600 next yc
610 ' CALC FOR DEADBAND LINES
620 P=DB*6:P1=300-P:P2=300+P
630 ' DRAWS VERTICAL DOTTED LINES
640 for xc2=148 to 480 step 83
650 for yc2=0 to 340 step 16
660 linef xc2,yc2,xc2,(yc2+4)
670 next yc2
680 next xc2
690 ' DRAWS UPPER DEADBAND LINE
700 for xc3=75 to 565 step 40
710 linef xc3,p1,(xc3+20),p1
720 next xc3
730 ' DRAWS LOWER DEADBAND LINE
740 for xc4=75 to 565 step 40
750 linef xc4,p2,(xc4+20),p2
760 next xc4
770 ' PLOTS UNGOVERNED TRANSIENT
780 FOR T=PC TO 1500 STEP PC
790 ' FREQUENCY DEVIATION AT TIME T
800 X2=FD*(1-(EXP(-T*TA)))
810 ' SCALE AND OFFSET FOR Y-AXIS
820 W2=X2*6
830 V2=300-W2
840 ' SCALE AND OFFSET FOR X-AXIS
850 Z2=(T/3)+65
860 ' FREQUENCY DEVIATION AT TIME T-PC
870 X1=FD*(1-(EXP(-(T-PC)*TA)))
880 W1=X1*6
890 V1=300-W1
900 Z1=((T-PC)/3)+65
910 ' DRAW LINE FROM T-PC TO T

```

---

```
920 LINEF Z1,V1,Z2,V2
930 NEXT T
940 ' INITIAL CONDITIONS
950 Q=0
960 MX=fr/21
970 X=0
980 FTA=0
990 N=1
1000 BU=0:P=0:L=1
1010 freqmax=50
1020 if disc=1 then open "o",#1,filename$
1030 FOR T=0 TO 1500 STEP PC
1040 ' DELAYED START ON LOAD APPLICATION UNTIL F>DB
1050 IF X<DB THEN FTA=0:N=1 ELSE FTA=FTA+PC
1060 ' LOAD REJECTION COMPONENT
1070 X=FD*(1-(EXP(-T*TA)))
1080 ' LOGIC TO SET THE LOAD MAGNITUDE/SIGN OF A GIVEN STEP
    AND LIMITS ON BU
1090 IF Q>DB AND BU<22 THEN MY(N)=MX:BU=BU+1 ELSE IF Q<-DB
    AND BU>-1 THEN MY(N)=-MX:BU=BU-1 ELSE MY(N)=0
1100 ' K IS NUMBER OF ACTIVE STEPS SINCE DELAYED START
1110 FOR K=1 TO N
1120 ' CURRENT TIME FOR EACH STEP
1130 TLC(K)=(FTA+PC)-(K*PC)
1140 ' CURRENT LOAD APPLICATION COMPONENT FOR EACH STEP
1150 Y(K)= MY(K)*(1-(EXP(-TLC(K)*TA)))
1160 ' SUM OF THE APPLICATION COMPONENTS OF FREQUENCY
1170 P=P+Y(K)
1180 NEXT K
1190 ' DIFFERENCE BETWEEN REJECTION AND APPLICATION
    COMPONENTS
1200 Q=X-P
1210 ' ACTUAL FREQUENCY VALUE
1220 freq=50+q
1230 if disc=1 then print#1,T,freq,50+db,50-db
1240 ' DETERMINES AND RETAINS MAX FREQUENCY
1250 if freq>freqmax then freqmax=freq:tfm=t
1260 ' SCALE AND OFFSET FOR Y-AXIS
1270 W=Q*6
1280 F(L)=300-W
1290 ' SCALE AND OFFSET FOR X-AXIS
1300 G(L)=(T/3)+65
1310 ' DRAWS FIRST SECTION OF THE GOVERNED CURVE
1320 IF T=0 THEN DRAW 65,300,G(L),F(L):GOTO 1360
1330 ' DRAWS THE REMAINDER OF THE CURVE
1340 DRAW G(L-1),F(L-1),G(L),F(L)
1350 ' RESETS VALUES
1360 N=N+1
1370 P=0
1380 L=L+1
```

```

1390 NEXT T
1400 ' ANNOTATES GRAPH
1410 gotoxy 4,3:??90
1420 gotoxy 4,7:? 80:gotoxy 4,10:? 70:gotoxy 4,14:? 60:gotoxy 4,17:? 50
1430 gotoxy 17,18:? "0.25":gotoxy 28,18:? "0.5":gotoxy 38,18:? "0.75"
1440 gotoxy 48,18:? "1.0":gotoxy 58,18:? "1.25":gotoxy 69,18:? "1.5"
1450 gotoxy 4,5:? "Frequency (Hz)"
1460 gotoxy 25,5:? "Predicted frequency transient."
1470 gotoxy 61,19:? "Time (s)"
1480 ' OUTPUTS DATA TO SCREEN
1490 ? "Max frequency is ";freqmax;"Hz at";tfm;"ms for a load rejection
of";pu ;"pu"
1500 ? "J=";j;"kgm2, wd=";wd;"ms, db= +-";db;"Hz, Head=";H;"m,
Flow=";flow;"l/s.
1510 if tur=1 then ? "Based on the Boving turbine."
1520 ' RETURNS TO BEGIN AGAIN
1530 if disc=1 then close 1
1540 input "Do you want to go again, 1 for yes, 0 for no ",answ
1550 if answ=1 then goto 160 else end
1560 ' INPUTS DATA FOR ALTERNATIVE TURBINE
1570 ?:"The following data is required for the alternative turbine;"
1580 ?:"Enter data in response to the prompts"
1590 ?:input "Inertia in kgm2 ",j
1600 ?:input "50 Hz speed in rev/min ",fhs
1610 if fhs>3600 then goto 1600
1620 ?:input "Runaway speed in rev/min ",rs
1630 if fhs>rs then goto 1600
1640 if rs>(2*fhs) then ?"Runaway speed excessive":goto 1600
1650 ?:input "Pelton wheel radius in metres ",rad
1660 ?:input "Nozzle coefficient, Cv, ( typically 0.7 to 0.96 ) ",Cv
1670 if Cv>0.98 or Cv <0.7 then goto 1660
1680 goto 220
1690 ' SUBROUTINE FOR DEADBAND SELECTION WHEN AUTO SELECT
OVERRULED
1700 ?:"Select multiplier for deadband from 1 to 8."
1710 ?:"DBM DB+-"
1720 ?" 1 0.32":?" 2 0.64":?" 3 0.96":?" 4 1.28"
1730 ?" 5 1.60":?" 6 1.92":?" 7 2.24":?" 8 2.56"
1740 ?:input dbm
1750 db=dbm*.32
1760 goto 490

```



**A4.3 PROGRAM PDCONT1.BAS**

```

10  ' Program name "PDCONT1 "20.03.92 - saves f&t to disc/
    turbine variations
20  ' includes auto selection of deadband AND PROP- DERIV CONTROL
30  ' ARRAY DIMENSIONING
40  DIM MY(125)
50  DIM Y(125)
60  DIM TLC(125)
70  DIM F(125)
80  DIM G(125)
85  dim q(125)
86  dim freq(125)
90  ' MAKES OUTPUT WINDOW FULL SIZE
100 FULLW 2
110 ' CLEARS OUTPUT WINDOW
120 CLEARW 2
130 ?? " This program graphs the load governed performance of a
    pelton wheel"
140 ?? " water turbine to a load rejection - including P-D actions":?
150 ?? " The turbine is the Boving machine in A25 at Merchiston"
160 ?? " as currently configured for ELC testing."
170 ' PROMPTS AND INPUTS FOR VARIABLE DATA
200 ' CONSTANTS FOR BOVING TURBINE IN A25
210 j=.67:rs=1200:fhs=770:rad=.133:Cv=.81
220 ?:input "Enter nett operating head in metres ",H:?:input "Enter
    flow in l/s ",flow
230 RS=SQR(H/30)*RS
240 ' FREQ DEVIATION AND TIME CONSTANT CALCS
250 fr=((rs/fhs)-1)*50:fmax=50+fr
260 Tmax=2*flow*rad*cv*sqr(19.62*H)
270 K2=fmax/Tmax:TC=j*K2*1000:TA=1/TC
280 ?:input "select p.u. value of load rejection ",PU
290 if pu>1 then goto 280
300 ?:INPUT "Select multiplier for Wait Delay, WD, 0,1,2 or 3 ",WD1
310 if wd1>3 then goto 300
320 ' CONVERT WAIT DELAY TO ms AND PRODUCE PROG CYCLE
330 wd=wd1*4:pc=18+wd
340 H1=H*.726:FLOW1=1.43*FLOW
350 ' CALCS FOR DEADBAND AUTO SELECTION
360 dbc=fr/21
370 if dbc <.32 then db=.32
380 if dbc >=.32 and dbc <.64 then db=.64
390 if dbc >=.64 and dbc <.96 then db=.96
400 if dbc >=.96 and dbc <1.28 then db=1.28
410 if dbc >=1.28 and dbc <1.6 then db=1.6
420 if dbc >=1.6 and dbc <1.92 then db=1.92
430 if dbc >=1.92 and dbc <2.24 then db=2.24
440 if dbc >=2.24 and dbc <2.56 then db=2.56
450 if dbc >=2.56 then db=2.56:?"Deadband too wide for ELC."

```

---

```

460  ?? "The auto db selector has calculated a value of +-" ;db;"Hz."
470  ? :input "Enter (1) if you accept this, or (0) if you wish to overrule
    ",ovr
480  if ovr=1 then goto 490 else goto 1590
490  ' LOAD REJECTION FREQ RISE
500  FD=fr*pu
510  clearw 2
520  ' DRAWS AXES
530  linef 65,0,65,340
540  linef 55,300,565,300
550  ' DRAWS HORIZONTAL DOTTED LINES
560  for yc=60 to 240 step 60
570  for xc=67 to 565 step 16
580  linef xc,yc,(xc+4),yc
590  next xc
600  next yc
610  ' CALC FOR DEADBAND LINES
620  P=DB*6:P1=300-P:P2=300+P
630  ' DRAWS VERTICAL DOTTED LINES
640  for xc2=148 to 480 step 83
650  for yc2=0 to 340 step 16
660  linef xc2,yc2,xc2,(yc2+4)
670  next yc2
680  next xc2
690  ' DRAWS UPPER DEADBAND LINE
700  for xc3=75 to 565 step 40
710  linef xc3,p1,(xc3+20),p1
720  next xc3
730  ' DRAWS LOWER DEADBAND LINE
740  for xc4=75 to 565 step 40
750  linef xc4,p2,(xc4+20),p2
760  next xc4
770  ' PLOTS UNGOVERNED TRANSIENT
780  FOR T=PC TO 1500 STEP PC
790  ' FREQUENCY DEVIATION AT TIME T
800  X2=FD*(1-(EXP(-T*TA)))
810  ' SCALE AND OFFSET FOR Y-AXIS
820  W2=X2*6
830  V2=300-W2
840  ' SCALE AND OFFSET FOR X-AXIS
850  Z2=(T/3)+65
860  ' FREQUENCY DEVIATION AT TIME T-PC
870  X1=FD*(1-(EXP(-(T-PC)*TA)))
880  W1=X1*6
890  V1=300-W1
900  Z1=((T-PC)/3)+65
910  ' DRAW LINE FROM T-PC TO T
920  LINEF Z1,V1,Z2,V2
930  NEXT T
940  ' INITIAL CONDITIONS

```

---

```

960  MX=28/21
970  ' 28=((1200/770)-1)*50
980  TB=0.003
990  ' tb is 1/time constant for 30 H, 30 Q
1000 X=0
1010 FTA=0
1020 mt=1
1025 buav=21
1030 BU=0:P=0:L=1
1035 q(l)=0
1040 freqmax=50
1060 FOR T=0 TO 1500 STEP PC
1070 ' DELAYED START ON LOAD APPLICATION UNTIL F>DB
1080 IF X<DB THEN FTA=0:N=1 ELSE FTA=FTA+PC
1090 ' LOAD REJECTION COMPONENT
1100 X=FD*(1-(EXP(-T*TA)))
1110 if q(l-1) >db and bu<=21 and mt>=0 then buav=21-bu: if buav>
    mt then gosub 2000 else mt=buav:gosub 2000 else if q(l-1)<-db
    and bu>=0 and mt<=0 th en buav=bu-0:if buav>=mt then
    gosub 2000 else mt=buav:gosub 2000 else my(n)=0
1130 ' K IS NUMBER OF ACTIVE STEPS SINCE DELAYED START
1140 FOR K=1 TO N
1150 ' CURRENT TIME FOR EACH STEP
1160 TLC(K)=(FTA+PC)-(K*PC)
1170 ' CURRENT LOAD APPLICATION COMPONENT FOR EACH STEP
1180 Y(K)= MY(K)*(1-(EXP(-TLC(K)*TB)))
1190 ' SUM OF THE APPLICATION COMPONENTS OF FREQUENCY
1200 P=P+Y(K)
1210 NEXT K
1220 ' DIFFERENCE BETWEEN REJECTION AND APPLICATION
    COMPONENTS
1230 Q(l)=X-P
1240 ' ACTUAL FREQUENCY VALUE
1250 freq(l)=50+q(l)
1270 ' DETERMINES AND RETAINS MAX FREQUENCY
1280 if freq(l)>freqmax then freqmax=freq(l):tfm=t
1290 ' SCALE AND OFFSET FOR Y-AXIS
1300 W=Q(l)*6
1310 F(L)=300-W
1320 ' SCALE AND OFFSET FOR X-AXIS
1330 G(L)=(T/3)+65
1340 ' DRAWS FIRST SECTION OF THE GOVERNED CURVE
1350 IF T=0 THEN DRAW 65,300,G(L),F(L):GOTO 1390
1360 ' DRAWS THE REMAINDER OF THE CURVE
1370 DRAW G(L-1),F(L-1),G(L),F(L)
1380 ' RESETS VALUES
1390 N=N+1
1400 P=0
1405 if t>=pc then gosub 1800
1410 L=L+1

```

```

1420 NEXT T
1430 ' ANNOTATES GRAPH
1440 gotoxy 4,3:790
1450 gotoxy 4,7:? 80:gotoxy 4,10:? 70:gotoxy 4,14:? 60:gotoxy 4,17:? 50
1460 gotoxy 17,18:? "0.25":gotoxy 28,18:? "0.5":gotoxy 38,18:? "0.75"
1470 gotoxy 48,18:? "1.0":gotoxy 58,18:? "1.25":gotoxy 69,18:? "1.5"
1480 gotoxy 4,5:? "Frequency (Hz)"
1490 gotoxy 25,5:? "Predicted frequency transient, P-D control."
1500 gotoxy 61,19:? "Time (s)"
1510 ' OUTPUTS DATA TO SCREEN
1520 ? "Max frequency is ";freqmax;"Hz at";tfm;"ms for a load rejection
of";pu ;"pu"
1530 ? "J=";j;"kgm2, wd=";wd;"ms, db= +-";db;"Hz, Head=";H;"m, Flow="
;flow;"l/s.
1540 ? "Ballast load= 4700W.":? " Based on the Boving turbine in A25.
1 step /4Hz/s"
1550 ' RETURNS TO BEGIN AGAIN
1560 if disc=1 then close 1
1561 input "Do you want to save these coords on disc, 1 for y, 0 for n
",disc
1562 if disc=0 then goto 1570
1563 if disc=1 then gosub 2050
1570 input "Do you want to go again, 1 for yes, 0 for no ",answ
1580 if answ=1 then goto 200 else end
1590 ' SUBROUTINE FOR DEADBAND SELECTION WHEN AUTO SELECT
OVERRULED
1600 ?? "Select multiplier for deadband from 1 to 8."
1610 ?? "DBM DB+-"
1620 ?" 1 0.32":?" 2 0.64":? " 3 0.96":? " 4 1.28"
1630 ?" 5 1.60":?" 6 1.92":?" 7 2.24":?" 8 2.56"
1640 ?:input dbm
1650 db=dbm*.32
1660 goto 490
1800 ' subroutine to calc proportional constant
1810 rfr=(q(l)-q(l-1))/pc
1820 mt=int(rfr/.004)
1830 return
2000 my(n)=mt*mx:bu=bu+mt
2010 return
2050 ' subroutine for disc save of coords for VIP plot later
2060 clearw 2
2070 input "enter filename ",name$:filename$=name$+".prn"
2080 open "o",#1,filename$
2085 l=1
2090 for t = 0 to 1500 step pc
2100 print#1,t,freq(l),50+db,50-db
2105 l=l+1
2110 next t
2120 close 1
2125 ?
2130 return

```

---

**APPENDIX 5 PUBLICATIONS LIST**

1. GAIR, S., HENDERSON, D.S., MACPHERSON, D.E., WALLACE, A.R., and WHITTINGTON, H.W. 1987. "An integrated design approach for micro hydro generating equipment". Proceedings of the 22nd UPEC, Sunderland Polytechnic, UK.
  2. GAIR, S., HENDERSON, D.S., and WALLACE, A.R. 1987. "Technical and economic considerations for small scale hydro-electric plant". Rural Energy Planning and Technology Assessment in Asian Countries, Beijing, China.
  3. HENDERSON, D.S., MACPHERSON, D.E., and WHITTAKER, K. 1987. "Experiences with rural electrification in Papua New Guinea". Ibid.
  4. HENDERSON, D.S., WALLACE, A.R., and WHITTINGTON, H.W. 1987. "Rural electricity supplies". Ibid.
  5. HENDERSON, D.S., GAIR, S., and MACPHERSON, D.E. 1988. "Electronic Load Governing for small scale wind energy generating units". Proceedings of BWEA 10, London, UK.
  6. WHITTINGTON, H.W., WALLACE, A.R., and HENDERSON, D.S. 1988. "An economic analysis of capital costs in micro-hydro". Third International Conference on Small Hydro, Cancun, Mexico.
  7. MACPHERSON, D.E., WHITTINGTON, H.W., WALLACE, A.R., GAIR, S., and HENDERSON, D.S. 1988. "Development of a prototype integrated generating unit for micro-hydro". Ibid.
  8. HENDERSON, D.S., and MACPHERSON, D.E. 1988. "Electronic load governing for micro-hydro generating units". Proceedings of 23rd UPEC, Trent Polytechnic, UK.
  9. GAIR, S., HENDERSON, D.S., and WALLACE, A.R. 1988. "A micro-hydro generating unit test cell". Ibid.
  10. WALLACE, A.R., MACPHERSON, D.E., and HENDERSON, D.S. 1988. "An integrated generating unit for micro-hydro electrification". Power India '88, New Delhi, India.
  11. WALLACE, A.R., HENDERSON, D.S., and RENTON, M.W. 1988. "A review of small scale hydro power in Europe". Seminar on Small Hydro-electric Power Stations, Lisbon, Portugal.
-

12. WALLACE, A.R., HENDERSON, D.S., and WHITTINGTON, H.W. 1989. "Capital cost modelling for micro-hydro appraisal". Waterpower '89, USA.
  13. WALLACE, A.R., HENDERSON, D.S., and RENTON, M.W. 1989. "A review of small scale hydro power in Europe". Proceedings 24th UPEC, Belfast, UK.
  14. WALLACE, A.R., HENDERSON, D.S., and WHITTINGTON, H.W. 1989. "Capital cost modelling of small scale hydro schemes". Ibid.
  15. HENDERSON, D.S., and MACPHERSON, D.E. 1990. "Development of a three phase, microprocessor based electronic load governor for micro-hydro generation". Proceedings 25th UPEC, Aberdeen, UK.
  16. HENDERSON, D.S. 1990. "Development of a three phase, microprocessor based electronic load governor for micro-hydro generation". World Renewable Energy Congress, Reading, UK.
  17. HENDERSON, D.S., and MACPHERSON, D.E. 1990. "Development of a three phase, microprocessor based electronic load governor for micro-hydro generation". Fourth International Conference on Small Hydro, Kuala Lumpur, Malaysia.
-

---

**LIST OF REFERENCES**

1. BUTERA, F. M., 1989, "Renewable Energy Sources in Developing Countries: Successes and Failures in Technology Transfer and Diffusion", PFE, Rome, Italy, LB-18.
  2. FRITZ, J. J., 1984, "Small and Mini Hydropower Systems", McGraw Hill, ISBN 0-07-022470-6.
  3. "Handbook 1992", 1992, International Water Power & Dam Construction, ISBN 0-617-01235-0.
  4. RAABE, J., 1985, "Hydro Power", VDI-Verlag GmbH, ISBN 3-18-400616-6.
  5. "Small Scale Hydro-electric Generation Potential in the UK", 1989, Department of Energy, ETSU, SSH-4063-P1, Vols I, II & III, UK.
  6. "Small Hydro Power", 1990, Water Power & Dam Construction, Supplement to Vol 42, No 4.
  7. WILLIAMS, D. A., 1990, "Water Turbines and Associated Items", IEE, Proceedings of Small Scale Hydro - Opportunities for Development in Scotland, UK.
  8. PARRY, G. E., 1990, "Hydro Generation and Control", IEE, Proceedings of Small Scale Hydro - Opportunities for Development in Scotland, UK.
-

9. SMITH, N. P. A. *et al*, 1990, "Stand Alone Induction Generators for Reliable, Low-cost Micro Hydro Installations", Energy and the Environment, Vol 5, Proceedings of the 1st World Renewable Energy Congress, UK, 2904-2908, ISBN 0-08037541-3.
  
  10. WOODWARD, J. L., BOYS, J. T., and ELDER, J. M., 1983. "Philosophy, Theory and Practice of Low Cost Micro Hydro", Proceedings of Waterpower '83 International Conference.
  
  11. WALLACE, A. R., 1990, "Mini Hydro Power Plant for Developing Countries", Energy and the Environment, Vol 5, Proceedings of the 1st World Renewable Energy Congress, UK, 2909-2913, ISBN 0-08037541-3.
  
  12. WICKE, P. W., 1984, "Experience of Planning Small Scale Hydro Stations for Peru", Proceedings of 1st International Conference on Small Hydro, Singapore.
  
  13. HISLOP, D., 1985, "Upgrading Micro Hydro in Sri Lanka", Intermediate Technology, ISBN 0-946688-62-1.
  
  14. MACKAY, L., 1990, IEE Power Engineering Journal, Vol 4, No 5, 223-231.
  
  15. WALLACE, A. R. and HENDERSON, D. S., 1987, "Report to Intermediate Technology Development Group on visit to Laurieston Hall Micro Hydro Installation", Energy Systems Group, UK.
-



16. HOLLAND, R. E., "Economics of Micro Hydro Power Plants", Intermediate Technology, UK.
  17. WOODWARD, J. L., 1986, "Appropriate Speed and Frequency Control of Micro Hydro Plants", Proceedings of Workshop on Micro Hydro Installations, Papua New Guinea.
  18. MAUJEAN, J-M., JOUVE, J. and FERME, J-M., 1990, Water Power & Dam Construction, Vol 42, No 1, 8-11.
  19. KORNEGAY, D. L., 1989, Water Power & Dam Construction, Vol 41, No 10, 36-38.
  20. "G.P. Electronic Load Controllers for Small Hydro", G.P. Electronics.
  21. BARNES, R., 1989, IEE Power Engineering Journal, Vol 3, No 1, 11-15.
  22. JOHNSON, F. G., 1990, "Hydro Generation in Scotland - Past Development and Future Potential", IEE, Proceedings of Small Scale Hydro - Opportunities for Development in Scotland, UK.
  23. "Review", 1990, Department of Energy, Issue 13, UK.
  24. "Review, Supplement - The Non-Fossil Fuel Obligation", 1991, Department of Energy, with Issue 17, UK.
  25. WHITTINGTON, H. W., RANDELL, J., and WALLACE, A. R., 1989, "Electrical Power in South-East Asia", Proceedings of UPEC '89, UK.
-

26. ANDERSON, T. M. and WHITTINGTON, H. W., 1990, "Micro Hydro Scheme Design for Nepal", Energy and the Environment, Vol 5, Proceedings of 1st World Renewable Energy Congress, UK.
27. MEIER, U. and ARTER, A., 1989, Water Power & Dam Construction, Vol 41, No 6, 9-11.
28. HISLOP, D., 1987, World Water, Vol 10, No 9, 39-41.
29. KORMILO, S. and ROBINSON, P., 1984, IEE Proceedings, Vol 131, Pt E, No 4, 132-136.
30. WATSON, C., 1986, "A Three Phase Electronic Load Governor for Micro Hydro Installations", University of Edinburgh, Honours Project Report HSP536.
31. EVES, S., 1987, "A Three Phase Microprocessor Based Load Governor for Small Hydro Schemes", University of Edinburgh, Honours Project Report HSP566.
32. LANDER, C. W., 1987, "Power Electronics", McGraw Hill, 2nd Edition, ISBN 0-07-084162-4, p279.
33. ELDER, J. M., BOYS, J. T. and WOODWARD, J. L., 1985, IEE Proceedings, Vol 132, Pt C, No 2, 57-66.
34. "Instruction Manual for Delphi Electronic Load Governor", Delphi Industries Ltd.
-

35. ROBINSON, P. and KORMILO, S., 1984, "Recent Advances in the Development of Microprocessor Based Load Controllers", Proceedings of 1st International Conference on Small Hydro, Singapore.
36. WOODWARD, J. L. and BOYS J. T., 1980, Water Power & Dam Construction, Vol 32, No 7, 37-39.
37. MACPHERSON, D. E. *et al*, 1988, "Development of a Prototype Integrated Generating Unit for Micro Hydro", Proceedings of 3rd International Conference on Small Hydro, Cancun, Mexico.
38. HOLLAND, R. E., 1986, Water Power & Dam Construction, Vol 38, No 11, 17-19.
39. ARTWICK, B. A., 1980, "Microprocessor Interfacing", Prentice Hall, ISBN 0-13-580902-9.
40. "Essex FORTH Microcard, Technical Manual", 1984, Essex Electronics Centre, Rev 1.0.
41. "Fixed Series Regulators", 1986, RS Components Ltd, Data Sheet 6610.
42. "Essex FORTH Writer, Technical Manual", 1985, Essex Electronics Centre.
43. "RSC-FORTH Users Manual", 1983, Rockwell International.
-

44. "Operating Instructions for Jay-Jay Fan-cooled Loading Resistor".  
Jay-Jay Instruments.
45. BROWN, A., 1990, "Micro Hydro in Developing Countries: Cost Effective Power and Local Participation", IEE, Proceedings of Small Scale Hydro - Opportunities for Development in Scotland, UK.
46. "Protective Relays Application Guide", 1975, GEC Measurements, 2nd Edition.
47. "Motor Protection Relay and Accessories", 1985, RS Components Ltd, Data Sheet 5948.
48. SEN, P. C., 1989, "Principles of Electric Machines and Power Electronics", John Wiley & Sons, ISBN 0-471-61717-2.
49. WALLACE, A. R., 1990, "Small-Scale Hydro Power Generation", University of Edinburgh.
50. DAUGHERTY, R. L., FRANZINI, J. B. and FINNEMORE, E. J., 1989, "Fluid Mechanics with Engineering Applications", McGraw Hill.
51. DUNCAN, W. J., THOM, A. S., and YOUNG, A. D., 1962, "An Elementary Treatise on the Mechanics of Fluids", E Arnold Ltd, p650.
52. MACKINTOSH, R. L., 1992, "Application of Electronic Load Governing to a Francis Turbine and to Inductive Loading", Napier University, Honours Project Report.
-

53. BURGHEES, D., and GRAHAM, A., 1986, "Introduction to Control Theory Including Optimal Control", Ellis Horwood Ltd, ISBN 0-85312-181-8.

54. FAZALARE, R. W., 1991, Water Power & Dam Construction, Vol 43, No 8, 18-20.

55. "Operation & Maintenance Instructions, Type LC & LCS 19-32 AC Generator", Markon Engineering, UK, Ref No 93-022.

56. "Operation & Maintenance Instructions, Type SCN21 AC Generator", Markon Engineering, UK, Ref No 93-054.

57. SAY, M. G., 1976, "Alternating Current Machines", Pitman Publishing Ltd, 4th Edition, ISBN 0-273361-97-X.

58. SAY, M. G. and TAYLOR, E. O., 1986, "Direct Current Machines", Pitman Publishing Ltd, 2nd Edition, ISBN 0-273-02457-4, p163.

59. WEIDNER, R. T. and SELLS, R. L., 1973, "Elementary Classical Physics", Allyn & Bacon, Vol 1, 2nd Edition, LCCC No 72-90870, p210.

60. Private fax communication from Newage International, 27th August 1991.

61. HUGHES, A., 1990, "Electric Motors and Drives", Heinemann Newnes, ISBN 0-434-90795-2.

---

62. JACOBS, O. L. R., 1974, "Introduction to Control Theory", Oxford University Press, ISBN 0-19-856148-2, p16.
63. McLAREN, P. G., 1984, "Elementary Electric Power and Machines", Ellis Horwood Ltd, ISBN 0-85312-269-5.
64. McDONALD, A. C. and LOWE, H., 1981, "Feedback and Control Systems", Reston Publishing Co Ltd, ISBN 0-8359-1898-X, p55.
65. ROBINSON, P., 1988, IEE Power Engineering Journal, Vol 2, No 5, p273-280.
66. WHITTINGTON, H. W. and SPENCER, D., 1987, J.Phys.E. : Sci Instrum. Vol 20. p246-253.
67. CHRISTOPOULOS, C., 1992, IEE Power Engineering Journal, Vol 6, No 2, p89-94.
-

---

**BIBLIOGRAPHY**

1. TOCCI, R. J. and LASKOWSKI, L. P., 1987, "Microprocessors and Microcomputers, Hardware and Software", Prentice Hall, 3rd Edition, ISBN 0-13-581844-3.
  2. MONEY, S. A., 1982, "Microprocessor Data Book", Granada, ISBN 0-246-11531-9.
  3. SCANLON, L.J., 1982, "FORTH Programming", Howard W Sams, ISBN 0-672-22007-5.
  4. BRODIE, L., 1987, "Starting FORTH", Prentice Hall, 2nd Edition, ISBN 0-13-843079-9.
  5. KATZAN JR, H., 1981, "Invitation to FORTH", Petrocelli, ISBN 0-89433-173-6.
  6. BRODIE, L., 1984, "Thinking FORTH", Prentice Hall, ISBN 0-13-917568-7.
  7. SEN GUPTA, D. P. and LYNNE, J. W., 1980, "Electrical Machine Dynamics", Macmillan Press Ltd, 1st Edition, ISBN 0-333-13884-8.
  8. "Small Hydro '88", Proceedings of the 3rd International Conference on Small Hydro, Cancun, Mexico.
-

9. "Waterpower '89", Proceedings of the Waterpower '89 Conference, Vol 3, Niagara Falls, USA.

10. "Small Hydro '90", Proceedings of the 4th International Conference on Small Hydro, Kuala Lumpur, Malaysia.

11. BS4821 : 1990. "Recommendations for the Presentation of Theses".  
British Standards Institution.

12. "Instructions for Preparation of Final Typescript". IEE.

---